

TARGETING *PLASMODIUM FALCIPARUM* HEAT
SHOCK PROTEIN 90 (PFHSP90): A STRATEGY TO
REVERSE ANTIMALARIAL RESISTANCE

by

Dea Shahinas

A thesis submitted in conformity with the requirements
for the degree of Doctor of Philosophy

Department of Laboratory Medicine and Pathobiology
University of Toronto

© Copyright by Dea Shahinas (2012)

TARGETING *PLASMODIUM FALCIPARUM* HEAT SHOCK PROTEIN 90 (PFHSP90): A STRATEGY TO REVERSE ANTIMALARIAL RESISTANCE

Dea Shahinas

Doctor of Philosophy

Department of Laboratory Medicine and Pathobiology
University of Toronto

2012

Abstract

Drug resistance is one of the major impediments to control *Plasmodium falciparum* malaria worldwide. Heat shock protein 90 (Hsp90) is an essential component of the buffering capacity of eukaryotic cells as a part of the stress response. *P. falciparum* is no different and requires Hsp90 to chaperone proteins essential for cell cycle progression and drug resistance. Inhibition of *P. falciparum* Hsp90 (PfHsp90) may be able to not only cripple the parasite but also serve as an adjunctive antimalarial by circumventing drug resistance. The results presented in this thesis identify novel Hsp90 inhibitors that synergize with conventional antimicrobials, such as chloroquine (CQ), when used in combination. The objectives were to identify specific malaria Hsp90 inhibitors, the mechanism of the synergistic phenotype, and whether the strategy translates *in vivo*. To this end, the antimalarial activity of the purine analog PU-H71, and novel PfHsp90 inhibitors was tested. PU-H71 and the novel inhibitors APPA, harmine, and acrisorcin exhibited antimalarial activity in the nanomolar range and displayed synergistic activity with CQ. PU-H71 was able to reverse CQ resistance in a cell-based assay using the CQ-resistant strain W2. PU-H71 caused ring-stage arrest during the intra-erythrocytic cycle. Co-immunoprecipitation studies revealed that PfHsp90 interacts directly with the CQ resistance

transporter (PfCRT). In the *P. berghei* mouse model of malaria, PU-H71 and harmine were able to reduce parasitemia and synergize with CQ. The interaction of PfHsp90 with PfCRT may underlie the synergistic phenotype. We conclude that PU-H71 and harmine are effective adjunctive antimalarial drugs that may be useful in combination therapies.

Acknowledgments

I would like to take this opportunity to show my gratitude for the support that I have received during this degree. First and foremost, I am immensely thankful to my co-supervisors Dr. Dylan R. Pillai and Dr. Donald E. Low for giving me the opportunity, resources and support to work on this project as well as other side projects at the Public Health Labs. Dr. Dylan R. Pillai has provided extensive input in the development of ideas and the progress of this project.

My PhD has been a rewarding professional journey. Many thanks go to my committee members Dr. Leah E. Cowen, Dr. Cyril Guyard and Dr. Ian Crandall for their prompt support, insight, and expertise. Dr. Ian Crandall has provided indispensable support for the testing of the antimalarial combinations in mouse models of malaria. His company at the Division of Comparative Medicine facilitated the progress of the mouse experiments. I would like to offer special thanks to Dr. Harry Elsholtz and Ferzeen Dharas at the Department of Laboratory Medicine and Pathobiology for prompt administrative support and advice.

I am also grateful to the parasitology clinical laboratory staff, the molecular research staff and all the blood donors at the Public Health Labs that made it possible to culture malaria parasites. In particular, I would like to acknowledge Rachel Lau for optimizing the conditions of growing malaria parasites and also for helping me with the optimization of the flow cytometry protocols. I would also like to acknowledge the support of two summer students Michael Liang and Christan Benedict, the research assistant Gregory MacMullin and the two post-doctoral fellows: Dr. Krishna Khairnar and Dr. Gitanjali Arya. Special thanks also to Dr. Walid A. Houry, Dr. John Glover and Elisa Leung for providing me access to the Biophysics facility at the Department of Biochemistry and for sharing their protocols in order to achieve biochemical characterization of PfHsp90.

The work presented here has been possible as a result of collaborations with: Dr. Alessandro Datti at the SMART high throughput screening facility at Mount Sinai Hospital, Dr. Gabriella Chiosis and Dr. Tony Taldone at the Memorial Sloan Kettering Cancer Centre and Dr. David Fidock, Dr. Jerome Clain who provided us with insight for the drug interaction analysis.

Last, but not least, thanks go to my husband Peter Siegler, our parents and my brother for the support, patience and love that they have shown throughout the years as well as for the appreciation that they have for my career.

Table of Contents

Chapter 1: Introduction	1
1 HISTORY OF MALARIA	1
2 AN OVERVIEW OF THE DISEASE.....	5
3 THE MALARIA LIFE CYCLE	7
4 ANTIMALARIALS AND THE EMERGENCE OF RESISTANCE.....	11
5 HEAT SHOCK PROTEIN 90.....	14
6 HEAT SHOCK PROTEIN 90 INHIBITORS	19
7 <i>PLASMODIUM FALCIPARUM</i> HEAT SHOCK PROTEIN 90	20
References.....	22
Chapter 2: ARTESUNATE MISUSE BY RETURNING TRAVELLER WITH <i>PLASMODIUM FALCIPARUM</i> INFECTION	28
1 THE PATIENT.....	28
References.....	34
Chapter 3: IDENTIFICATION OF NOVEL AND SELECTIVE PFHSP90 INHIBITORS WITH DRUG POTENTIAL.....	35
1 INTRODUCTION.....	35
2 MATERIALS AND METHODS	38
2.1 Cloning and Protein Purification.....	38
2.2 4,40-dianalino-1,10-binaphthyl-5,50-disulfonic acid Dipotassium salt (bis-ANS) Binding Assay with the PfHsp90 ATP-Binding Domain.....	38
2.3 <i>P. falciparum</i> Culture Methods.....	39
2.4 Antimalarial Drug Screening Cell Assay and <i>in vitro</i> susceptibility testing.....	39
2.5 <i>Entamoeba histolytica</i> cultures	40
3 RESULTS.....	41
3.1 Robotic High Throughput Screen with Recombinant Hsp90 ATP-Binding Domains	41
3.2 EhHsp90 and PfHsp90 inhibitor effect on cell culture.....	44

3.3 APPA, Harmine and Acrisorcin show Antimalarial Potency in <i>P. falciparum</i> Drug Resistant Strains	49
3.4 APPA, harmine and acrisorcin act synergistically with chloroquine	53
3.5 Harmine displays synergistic activity with known antimalarials <i>in vitro</i>	56
4 DISCUSSION	58
References.....	64

Chapter 4: BIOCHEMICAL CHARACTERIZATION OF

***PLASMODIUM FALCIPARUM* HEAT SHOCK PROTEIN 90..... 71**

1 INTRODUCTION.....	71
2 MATERIALS AND METHODS	81
2.1 Multiple sequence alignment.....	81
2.2 Sequencing of the PfHsp90 ATP-Binding Domain	81
2.3 PU-H71 and Geldanamycin (GA) docking in the PfHsp90 GHKL domain structure .	81
2.4 Cloning and Protein Purification.....	81
2.5 Site-directed mutagenesis.....	82
2.6 Surface Plasmon Resonance (SPR) Measurements.....	82
2.7 ATPase Activity Assay	83
2.8 <i>P. falciparum</i> culture methods and preparation of protein extracts	83
3 RESULTS.....	84
3.1 The PfHsp90 ATP binding domain is structurally conserved.....	84
3.2 Sequencing of the PfHsp90 ATP-Binding Domain from <i>P. falciparum</i> Malaria Patient Isolates.....	84
3.3 Homology modeling reveals that PU-H71 fits well in the PfHsp90 ATP binding domain	88
3.4 Homology modeling reveals ortholog specific interactions with harmine and harmalol.....	90
3.5 PU-H71 binds the PfHsp90 ATP-binding domain with high affinity	92
3.6 Harmine has affinity for the PfHsp90 ATP-binding domain	95
3.7 PU-H71 and harmine inhibit PfHsp90 ATPase activity.....	97
3.8 Anti-PfHsp90 antibody displays antigenic specificity against PfHsp90.....	102
4 DISCUSSION	104

References.....	107
-----------------	-----

Chapter 5: THE ATP MIMETIC PU-H71 REVERSES

ANTIMALARIAL RESISTANCE – INSIGHTS ON CELLULAR

MECHANISMS 108

1 INTRODUCTION.....	108
2 MATERIALS AND METHODS	109
2.1 <i>P. falciparum</i> Culture Methods and Antimalarial Cell Assay.....	109
2.2 In vitro PU-H71 and chloroquine drug interactions.....	109
2.3 Parasite protein extraction.....	110
2.4 Co-immunoprecipitation of PfHsp90 and PfCRT.....	110
2.5 LC-MS/MS Analysis.....	111
3 RESULTS.....	113
3.1 PU-H71 exhibits anti-malarial activity in <i>P.falciparum</i> cell culture, acts synergistically with chloroquine, and can reverse chloroquine resistance.....	113
3.2 Immunoprecipitation studies demonstrate a direct association between PfHsp90 and PfCRT.....	118
3.3 LC-MS/MS analysis of co-immunoprecipitated proteins confirms the association of PfCRT and PfHsp90	123
3.4 Resistance selection results in an ATP binding domain mutant with elevated PU-H71 IC50	127
3.5 PU-H71 arrests growth at the ring stage in the erythrocytic cycle.....	131
4 DISCUSSION	134
References.....	137

Chapter 6: THE *PLASMODIUM FALCIPARUM* HEAT SHOCK

PROTEIN 90 INHIBITORS HARMINE AND PU-H71 ARE

SYNERGISTIC *IN VIVO* – The *P.berghei* model..... 141

1 INTRODUCTION.....	141
2 MATERIALS AND METHODS	143
2.1 <i>Plasmodium berghei</i> mouse model studies and drug administration	143
3 RESULTS.....	144

3.1 PU-H71 shows a significant antimalarial effect in mouse models of malaria without significant toxicity	144
3.2 Harmine potentiated chloroquine in mouse models of malaria without significant toxicity	150
4 DISCUSSION	155
References	157
Chapter 7: DISCUSSION AND CONCLUSIONS	159
References	164
Appendices.....	166
APPENDIX 1: LIST OF THE WIDE RANGE OF HSP90 TARGETING PROJECTS...	166
APPENDIX 2: SAFETY AND TOLERABILITY OF AVAILABLE ANTIMALARIAL DRUGS	169
APPENDIX 3: A DETAILED OVERVIEW OF THE INTERACTORS IDENTIFIED THROUGH CO-IMMUNOPRECIPITATION AND LC-MS/MS ANALYSIS	170

List of Tables

Table 2-1: Results of sequencing single-nucleotide polymorphisms of *Plasmodium falciparum* isolates.

Table 3-1: Summary of inhibition results for the EhHsp90 protein screen and the effect of the inhibitors on *E.histolytica* culture.

Table 3-2: *In vitro* susceptibility of PfHsp90 high-throughput screen hits. The drugs were tested on intra-erythrocytic cell culture of *P.falciparum* 3D7.

Table 3-3: Summary of Antimalarial Assay IC₅₀ Values for the Inhibitors Identified in This Study When Compared to Known Antimalarials

Table 3-4: Summary of the results of the effect of harmine and its combinations on *Plasmodium falciparum* cell culture. CQ: chloroquine; ART: artemisinin; ACR: acrisorcin.

Table 4-1: Surface plasmon resonance (SPR) measurements for harmalol and harmine binding of the ATP-binding domains of PfHsp90 and HsHsp90. Where possible, the steady state responses were fit using non-linear regression to a single class of binding site model to obtain the K_d value indicated. The number in parentheses represents standard error.

Table 6-1: Summary of the drug combinations tested in the *Plasmodium berghei* mouse model trials.

List of Figures

Figure 1-1: *Laveran's drawings of Plasmodium falciparum in blood.* This figure has been copied from Sherman (1).

Figure 1-2: *Illustrated summary of the major discoveries that paved the way to a molecular understanding of the malaria pathogen Plasmodium falciparum.*

Figure 1-3: *An illustration of the intra-erythrocytic cycle of Plasmodium falciparum.* The inset pictures have been taken under a light microscope and show the appearance of the parasites at the different stages upon Giemsa staining. One cycle in *P. falciparum* typically takes 48 h to complete.

Figure 1-4: *Illustration of the localization of human and malaria Hsp90 paralogs inside an RBC infected with P.falciparum.* The focus of this thesis will be on PfHsp90 (PF07_0029), which is the cytosolic isoform with a conserved EEVD motif.

Figure 2-1: *In vitro drug susceptibility of representative patient isolates from returning travelers who visited friends and relatives in Africa.* The mean 50% inhibitory concentrations (IC₅₀) of chloroquine, mefloquine, artemisinin, artesunate, dihydroartemisinin, and artemether are plotted in nmol/L for each isolate, performed in triplicate (error bars indicate SD; n = 3). Nigeria A denotes the patient described in this report. The black horizontal line represents the median value.

Figure 3-1: *Competitive binding assay using the fluorescent probe bis-ANS for the identification of PfHsp90 specific inhibitors at a screening final concentration of 2.5 μM.* (a) *Plasmodium falciparum* (Pf) Hsp90 ATP-binding domain; (b) human (Hs) Hsp90 ATP-binding domain. (c) *Entamoeba histolytica* (Eh) Hsp90. The asterisk identifies compounds that did not compete with HsHsp90 ATP-binding domain binding. The error bars represent standard deviation of duplicate readings. Inhibition is defined as >70% reduction of fluorescence in this assay.

Figure 3-2: *Chemical structures of harmine and harmaline.* Harmaline contains two extra hydrogen atoms in the heterocyclic amine ring. As a result, harmine has a markedly lower pKa. Harmalol is a commercially available analog of harmine and harmaline. The affinity of harmalol

for the Hsp90 ATP-binding domain is described in chapter 4. These chemical drawings were generated from ChemDB (24).

Figure 3-3: *Antimalarial activity of APPA (blue), harmine (red), and acrisorcin (pink) using a standard cell-based fluorescence assay.* (a) The chemical structure of each of the three selective PfHsp90 inhibitors and the corresponding IC₅₀ value in the 3D7 (drug sensitive) parasite line. (b) Representative IC₅₀ curves are shown for the three specific inhibitors for laboratory strain 3D7. Actual IC₅₀ values in 3D7 and drug resistant parasite lines are summarized in Table 3-3.

Figure 3-4: *Synergistic activity of APPA (a), harmine (b), and acrisorcin (c) in combination with the known antimalarial chloroquine for laboratory strain 3D7.* The light blue, red and pink lines represent the activity of APPA, harmine and acrisorcin alone. The dark blue line represents the IC₅₀ curve of chloroquine when tested alone. The green line depicts the IC₅₀ curve for the PfHsp90 inhibitor in combination with 0.125pM chloroquine. The orange line depicts the IC₅₀ curve for chloroquine in combination with 1.25pM novel PfHsp90 inhibitor. APPA, harmine and acrisorcin exhibited FIC ratios of 0.11, 0.08, and 0.01, respectively, in combination with chloroquine. FIC ratios of <0.5 indicate synergistic activity (19, 25). A single representative experiment in the 3D7 parasite line is shown.

Figure 4-1: *An illustration of the differences between a conventional GHKL domain and the ATP-binding Bergerat fold domain.* The nucleotide binding site in this domain is located at the interface between the N- and C- terminals. (a) Bergerat fold unique features. The most representative feature of this domain is the ATP-lid loop (L4). The purple boxes represent the conserved motifs that are characteristic of the Bergerat fold. The blue triangles represent regions of structural variation among different members of the Bergerat fold family. (b) An illustration of the topology of a conventional nucleotide binding fold found in kinases and other ATPase domain containing proteins. The breaks indicate points in the surface loops where extra peptide segments may be inserted. The illustration has been adapted and redrawn from Dutta and Inouye (7).

Figure 4-2: *Illustration of the topology features that distinguish different members of the Bergerat fold family of GHKL ATPases.* (a) The composition and conformation of the ATP-lid domain is the most unique feature. This domain is a long loop in GyrB that folds to close the ATP binding domain. The insertion of a short helix in the loop domain of MutL does not allow

for complete closure of the lid leaving the bound nucleotide partially exposed. Hsp90 has two helices inserted in the ATP-lid loop. The bound nucleotide is therefore, completely exposed to solution. Even though, EnvZ and Hsp90 have the same degree of openness of the lid domain, they can be distinguished by the insertion of a histidine kinase domain known as the F-box in EnvZ. (b) An illustration of the different conformations and degree of openness of the ATP-lid among the different members of the Bergerat fold protein family. This figure has been adapted and redrawn from Dutta and Inouye (7).

Figure 4-3: *Model of PfHsp90 dimerization.* The model coordinates were generated with Phyre (9) and SymmDock (10) using the structure template 2IOQ (Protein Databank). The cartoon illustration was generated with PyMOL (11).

Figure 4-4: *Superposition of the human and P.falciparum Hsp90 ATP binding domains.* The domains show conservation of the domain architecture, but display some amino acid substitutions in the pocket where ATP binds (described in the text). ATP is colored yellow in this figure. This image has been reproduced from Corbett and Berger, 2010 (15).

Figure 4-5: *Multiple sequence alignment of the ATP binding domains of Hsp90 orthologs in different taxa.* Positions of variation are highlighted in grey. The green arrow represents beta-sheets and the orange rectangle represents the positions of the alpha-helices. The multiple sequence alignment was generated using the MUSCLE algorithm (17).

Figure 4-6: *Sequencing of the PfHsp90 ATP-binding domain from 102 globally distributed patient isolates.* (a) WebLogo representation of the multiple sequence alignment. Asterisks indicate two low frequency mutations that were identified as Ile41Thr and Ser106Leu. The WebLogo representation was generated using version3 (23). (b) Homology modeling of the domain revealed that Ile41 is outside the ATP-binding domain. (c) Substitution of Ser106 by leucine (blue) does not affect substrate binding in the ATP-binding domain. The homology model diagrams were generated using PyMOL (11).

Figure 4-7: *Illustration of docking PU-H71 (a) and geldanamycin (GA) (b) within the ATP-binding site of PfHsp90.* The models were generated using the PfHsp90 crystal structure (PDB ID: 3K60). By convention, the electrostatic potential surface in the background denotes acidic

residues in red and basic residues in blue. It has been included only in this figure to depict the architecture of the pocket.

Figure 4-8: (a): Docking of harmalol in the ATP-binding site of HsHsp90 (PDB ID: 2FWZ). The residues highlighted in orange represent positions of variation among the Hsp90 ATP-binding pockets in different taxa. (b) Docking of harmine in the PfHsp90 crystal structure (PDB ID: 3K60).

Figure 4-9: SPR measurements for PU-H71 binding of the ATP-binding domain of PfHsp90. The colors on the sensorgrams represent varying concentrations of the respective drug injected over the surface with the immobilized PfHsp90. The steady state responses were fit using non-linear regression to a single class of binding site model (as shown on the right) to obtain the K_d value indicated. The number in parentheses represents standard error. (a) SPR measurements for PU-H71 binding of the ATP-binding domain of PfHsp90 (b) 17-AAG was used as a positive control drug. (c) SPR measurements for PU-H71 binding of the site directed R98K mutant ATP-binding domain of PfHsp90.

Figure 4-10: The effect of each of PU-H71 (a) and harmine (b) on the ATPase activity of full length recombinant PfHsp90. The positive control drugs 17-AAG (c) and radicicol (d) were also tested for inhibition of the activity. The IC_{50} of PfHsp90 ATPase activity was determined by plotting percent activity remaining (relative to no drug control) versus inhibitor concentration (MATLAB R2009). The inset shows the logarithmic curve of the reduction of ATPase activity with increasing concentrations of each drug.

Figure 4-11: Anti-PfHsp90 antibody displays antigenic specificity. Blotting with anti-PfHsp90 antibody shows that only the PfHsp90 N-terminal ATP binding domain can be recognized but not the HsHsp90 N-terminal ATP binding domain (a). This antigen specificity extends to recognition of the native protein from protein extracts (b). The chemiluminescence signal was only present in the lanes with the parasite protein extracts.

Figure 5-1: Antimalarial activity of PU-H71 using a standard SYBR Green cell based flow cytometry assay. The activity was tested in the laboratory strain 3D7 obtaining an IC_{50} of 111 ± 8 nM (single experiment performed in duplicate).

Figure 5-2: *PU-H71 acts synergistically with chloroquine (CQ) in the laboratory P.falciparum 3D7 strain (a) and can reverse CQ resistance in the resistant strain W2 (b).* Synergistic activity was defined by calculations of the average sum fractional inhibitory concentration ratio FIC_{50} and by the FIC_{50} ratios lying under the line of additivity in the diagrams shown here. The lines joining the points in the isobologram denote replicates. (a) Mean ΣFIC_{50} : 0.27 ± 0.19 (b) Mean ΣFIC_{50} : 0.40 ± 0.36

Figure 5-3: *PU-H71 potentiates chloroquine and reverses chloroquine resistance.* The PU-H71 resistance reversal and CQ potentiation activity was determined by a response modification index (RMI) $\ll 1$ (9, 10). The corresponding RMI is shown for each of the doses tested in both the CQ sensitive parasite line 3D7 and the CQ resistant line W2.

Figure 5-4: *PfHsp90 interacts with PfCRT based on co-immunoprecipitation studies.* (A) Under non-denaturing conditions, immunoprecipitation with anti-PfHsp90 pulled down both itself and the *P. falciparum*. Chloroquine resistance transporter (PfCRT), and the converse experiment with anti-PfCRT resulted in both itself and PfHsp90 being pulled down as compared to mock (beads alone plus extract).

Figure 5-5: *Co-immunoprecipitation of PfHsp90 and PfCRT under denaturing conditions.* (a) Anti-PfCRT and Anti-PfHsp90 western blots of the immunoprecipitation proteins. Controls include from left to right: empty beads incubated with the extract, rabbit antiserum conjugated beads incubated with extract, denatured anti-PfHsp90 beads with no extract, denatured anti-PfCRT beads with no extract and denatured antiserum beads with no extract. (b) PfHsp90 and PfCRT are present in *P.falciparum* culture extracts. (c) Anti-hemoglobin western blot of stripped blots from (a) to determine the identity of the secondary band. (d) Anti-PfCRT western blot of pulled down proteins from histidine tagged full length PfHsp90 bound Ni-NTA beads. GSH Beads: Glutathione beads.

Figure 5-6: *Treatment with PU-H71 lowers the level of PfCRT protein.* Extracts from *P.falciparum* strain W2 treated and untreated with 111 nM PU-H71 (24 h) and immunoblotted with anti-PfCRT and anti-PfHsp90 antibody to determine the level of PfCRT. The Coomassie stained gel has been included to show equal loading (24 μ g/lane).

Figure 5-7: *Unweighted protein-protein interaction network of LC-MS/MS analyzed PfHsp90 and PfCRT co-immunoprecipitated proteins.* (a) The image was generated using Cytoscape v2.8. For the list of the members of each cluster, please see Appendix 3. (b) An enlarged excerpt of the interaction network that depicts the interaction between PfHsp90 and PfCRT.

Figure 5-8: *A simplified model of the PfHsp90 interactome as witnessed from the LC-MS/MS analysis and verified by published literature.* The interactors shown with a black outline have been included for completion. They were not present in the list of identified interactors from the LC-MS/MS analysis. Client refers to any protein that requires the chaperone activity of PfHsp90 for folding. CRT and MDR1 are introduced in this study as novel clients.

Figure 5-9: *A step-wise selection method was used to generate the PfHsp90 Thr163Pro mutant in strain Dd2.* (a) An illustration of the selection method. (b) The mutation is depicted in the model structure of the ATP-binding domain. (c) The presence of this mutation resulted in doubling of the PU-H71 IC₅₀ in the cell-based assay. (d) Synergy between PU-H71 and CQ in the Thr163Pro mutant was observed. The inset provides a magnified view of the FIC₅₀ ratios for the different PU-H71 and CQ drug combinations.

Figure 5-10: *PU-H71 slows down transition of rings to matures: a feature of Hsp90 inhibitors in malaria.* (a) Scheme of heat shock stress (HSC) was followed as previously published to simulate malaria febrile episodes. (b) This sample experiment depicts separation of rings and mature parasites using flow cytometry during a normal 48 hour life cycle of *P. falciparum* in culture. The red circle gate captures rings and the yellow circle, the mature parasites. The gradient of green-blue-yellow-red of the dots in the background represents the intensity of counted events in that particular area of the plot. (c) Quantification of rings and matures in the presence and absence of HSC or drug (after the full 22 hr period shown in (a) using flow cytometry. *Significance relative to no drug controls. (Unpaired two-tailed Student's t-test $p < 0.05$) $n = 2$. A representative replicate is shown in (c). No significant difference was observed with CQ in the progression of rings to matures.

Figure 6-1: *Plasmodium berghei mouse model results of intra-peritoneal injection treatment with PU-H71.* Mice were infected on day 0 and treatment was started on day 5 at parasitemia of 1%. (a) Average parasitemia levels in response to drug treatments alone as indicated ($n = 4$).

* denotes significant differences in parasitemia relative to the vehicle control (Student's t-test $p \leq 0.05$). (b) Kaplan-Meier survival plot for PU H71 alone versus placebo.

Figure 6-2: *Plasmodium berghei* mouse model results of intra-peritoneal injection treatment with 25 mg/kg PU-H71 and 0.25 mg/kg CQ. Mice were infected on day 0 and treatment was started on day 5 at parasitemia of 1%. (a) Average parasitemia levels in response to drug treatments as indicated (n = 4). * denotes significant differences in parasitemia relative to PU-H71 treatment alone. ** denotes significant differences in parasitemia relative to the CQ treatment alone (Student's t-test $p \leq 0.05$). (b) Kaplan-Meier survival plot for this combination treatment.

Figure 6-3: *Plasmodium berghei* mouse model results of intra-peritoneal injection treatment with 25 mg/kg PU-H71 and 0.5 mg/kg CQ. Mice were infected on day 0 and treatment was started on day 5 at parasitemia of 1%. (a) Average parasitemia levels in response to drug treatments as indicated (n = 4). * denotes significant differences in parasitemia relative to PU-H71 treatment alone. ** denotes significant differences in parasitemia relative to the CQ treatment alone (Student's t-test $p \leq 0.05$). (b) Kaplan-Meier survival plot for this combination treatment.

Figure 6-4: *Plasmodium berghei* mouse model results of intra-peritoneal injection treatment with 75 mg/kg PU-H71 and 0.5 mg/kg CQ. Mice were infected on day 0 and treatment was started on day 5 at parasitemia of 1%. (a) Average parasitemia levels in response to drug treatments as indicated (n = 4). * denotes significant differences in parasitemia relative to PU-H71 treatment alone. ** denotes significant differences in parasitemia relative to the CQ treatment alone (Student's t-test $p \leq 0.05$). (b) Kaplan-Meier survival plot for this combination treatment.

Figure 6-5: *Plasmodium berghei* parasitemia changes in response to intra-peritoneal injection treatment with harmine and its combinations. Mice were infected on day 0 and treatment was started on day 3 at parasitemia of 1%. The first graph shows average parasitemia levels in response to drug treatments alone (n = 4). * denotes significant differences in parasitemia relative to the vehicle control (Student's t-test $p \leq 0.05$). In the combination treatment graphs, * denotes significant differences in parasitemia relative to harmine treatment alone. ** denotes significant differences in parasitemia relative to the CQ treatment alone (n = 4) (Student's t-test $p \leq 0.05$).

Figure 6-6: *Plasmodium berghei* mouse model weight changes in response to intra-peritoneal injection treatment with harmine. No significant changes in weight were observed (Student's t-test $p \leq 0.05$).

Figure 7-1: *Illustration of the emerging cellular model of PfHsp90 inhibitors and CQ in CQS and CQR P.falciparum infected RBCs.* Drug application introduces pharmacological stress which may result in activation of the PfHsp90 chaperone machinery. CQ accumulation in the digestive vacuole inhibits the detoxification of hemoglobin byproducts in CQS, but not CQR parasites. Inhibition of PfHsp90 chemosensitizes the cells by an arrest of folding clients involved in detoxification, multiple drug resistance and virulence factors. CQS: CQ sensitive CQR: CQ resistant.

List of Appendices

APPENDIX 1: LIST OF THE WIDE RANGE OF HSP90 TARGETING PROJECTS

APPENDIX 2: SAFETY AND TOLERABILITY OF AVAILABLE ANTIMALARIAL DRUGS

APPENDIX 3: A DETAILED OVERVIEW OF THE INTERACTORS IDENTIFIED
THROUGH CO-IMMUNOPRECIPITATION AND LC-MS/MS ANALYSIS

List of Abbreviations

Hsp90: Heat shock protein 90

PfHsp90: *Plasmodium falciparum* Hsp90

HsHsp90: *Homo sapiens* Hsp90

CQ: Chloroquine

PfCRT: *Plasmodium falciparum* chloroquine resistance transporter

RBC: Red blood cell

EMP1: Erythrocyte membrane binding protein 1

ACT: Artemisinin-based combination therapy

SP: Sulfadoxine-pyrimethamine

CQR: CQ resistant

CQS: CQ sensitive

PfMDR1: *Plasmodium falciparum* multidrug resistance transporter 1

PfATP6: Calcium transporting ATPase 6 with homology to mammalian SERCA

HSP: Heat shock protein

HSP70: Heat shock protein 70

HSP60: Heat shock protein 60

TRAP1: TNF receptor-associated protein 1

Grp94: ER localized paralog of Hsp90

DV: Digestive vacuole

ER: Endoplasmic reticulum

MT: Mitochondrion

GA: Geldanamycin

17-AAG: 17-allylamino geldanamycin

Rad: Radicicol

LD₅₀: Lethal dose causing 50% death

ATP: Adenosine triphosphate

ATPase: ATP hydrolysis domain

MQ: mefloquine

ART: artemisinin

IC₅₀: 50% minimum inhibitory concentration

FIC₅₀: Fractional IC₅₀

\sum FIC₅₀: Sum FIC₅₀

WARN: World Antimalarial Resistance Network

EhHsp90: *Entamoeba histolytica* heat shock protein 90

FDA: Food and Drug Administration

APPA: \pm 2-amino-3-phosphono propionic acid

ACR: Acrisorcin

DMSO: Dimethyl sulfoxide

bis-ANS: 4,4'-Dianilino-1,1'-Binaphthyl-5,5'-Disulfonic Acid, Dipotassium Salt

AhR: Androgen hydrocarbon receptor

PAH: Polycyclic aromatic hydrocarbons

THP1: Human acute monocytic leukemia cell line

LC₅₀: Lethal concentration causing 50% death

GHKL: Gyrase, Hsp, Kinase and MutL

gyrB: DNA gyrase B

MutL: DNA mismatch repair protein

EnvZ: histidine kinase protein

PDB: Protein Databank

K_d: dissociation constant

GO: Gene Ontology

AMA-1: apical membrane antigen 1

EBA-165: erythrocyte binding antigen 165

MSP1: Merozoite surface protein 1

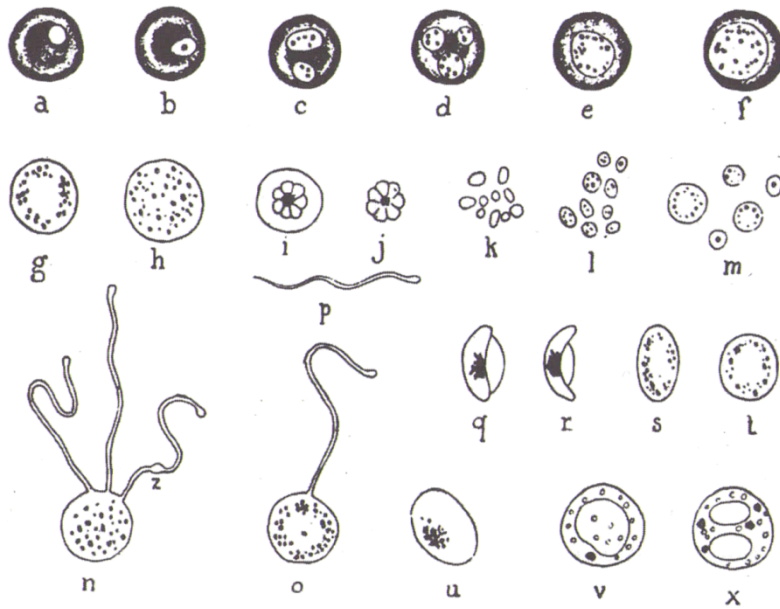
MSP7: Merozoite surface protein 7

Chapter 1 INTRODUCTION

1 HISTORY OF MALARIA

Malaria, historically known as “ague”, is associated with an enlarged spleen, periodic fevers, headaches, chills, and weakness (1, 2). The disease was recognized by the presence of periodic fevers in ancient times and was thought to be transmitted via “bad air”. Therefore, it received its name from “bad air” (Italian). In October 1880, Alphonse Laveran first showed that protozoa, which looked like telltale crescents (malaria gametocytes), were the causative agent of malaria. He found these organisms in 70% of the microscope slides prepared with blood from the soldiers that he examined in Algeria. The soldiers that did not have the crescent bodies had no symptoms (1-3). Laveran microscopically examined the development of malaria parasites and provided the first detailed drawings of the intra-erythrocytic life cycle (Figure 1-1) (1-3).

In 1886, Camillo Golgi discovered that the malaria parasite reproduces asexually by fission and showed that fever coincides with erythrocyte lysis and parasite release (1). In 1897, Ronald Ross (surgeon-major in the Indian medical service), observed cysts on the stomach lining of *Anopheles* mosquitoes that had fed on infected patients. The Italian scientists Grassi and Bignami demonstrated unequivocally that anopheline mosquitoes transmit human malaria (1). All human malarial agents are transferred via the female anopheline mosquito, which inoculates less than 25 sporozoites in the blood upon receiving its blood meal (1).



MÉMOIRES PRÉSENTÉS.

PHYSIOLOGIE PATHOLOGIQUE. — *De la nature parasitaire des accidents de l'impaludisme.* Note de M. A. LAVERAN.

« Il existe, dans le sang des malades atteints d'impaludisme, des éléments parasitaires qui se présentent sous les aspects suivants :

• 1° Eléments cylindriques, effilés à leurs extrémités, presque toujours incurvés en croissant. La longueur de ces corps est de $0^{\text{mm}},008$ à $0^{\text{mm}},009$; leur largeur, de $0^{\text{mm}},003$ en moyenne. Les contours sont indiqués par une ligne très fine; le corps est transparent, incolore, sauf à la partie moyenne,

Figure 1-1: Laveran's drawings of *Plasmodium falciparum* in blood. This figure has been copied from Sherman (1).

In 1948, H.E. Shortt and P.C.C Garnham discovered the missing link of the exo-erythrocytic phase of the malarial life cycle by inoculating rhesus monkeys with sporozoites obtained from the salivary glands of mosquitoes carrying *Plasmodium cynomolgi*. They found that the parasites replicated in the liver of the monkeys after 1 week (1). After the mosquitoes fed on human volunteers, the liver stage was discovered in patients infected with tertian malaria caused by *P. vivax* and *P. falciparum*. The malaria sporozoites travel to the liver in less than 1 h. Asexual reproduction in the liver produces more than 10,000 infectious merozoites (2).

An important contribution to malaria drug research was the discovery in 1948 by the Belgian parasitologist Ignace Vincke of a malaria parasite (*P. berghei*) in thicket rats of the Katanga region of Zaire. This parasite has been widely used for the clinical assessment of several antimalarial drugs (1, 2). In addition, the discovery of an *in vitro* culturing system for *P. falciparum* facilitated future studies with this parasite, which causes the most severe form of malaria. The “taming” of *P. falciparum* took place in the Rockefeller University laboratory of William Trager, who discovered that *P. falciparum* needs 7% CO₂ and 5% O₂ in order to grow in human red blood cell (RBC) culture (4, 5). Trager established the candle jar method in 1975. Using this method, it has been possible to grow malaria cultures by modifying the ratio of O₂ and CO₂ in a closed jar using a candle (5). The ability to culture malaria parasites opened the door to a molecular understanding of the pathogen, the disease, the vector, and the host. In 2002, an international consortium sequenced the genomes of *P. falciparum* and *A. gambiae* (6, 7). The entry of malaria into the genomics era raised hopes for the eradication of this so-called “neglected disease”. The timeline of the historical events described here is illustrated in Figure 1-2. To date, the hopes for its eradication have reached an impasse, but efforts are mainly focusing on vaccine and drug development as well as vector control.

TIMELINE OF MONUMENTAL DISCOVERIES IN THE HISTORY OF MALARIA RESEARCH

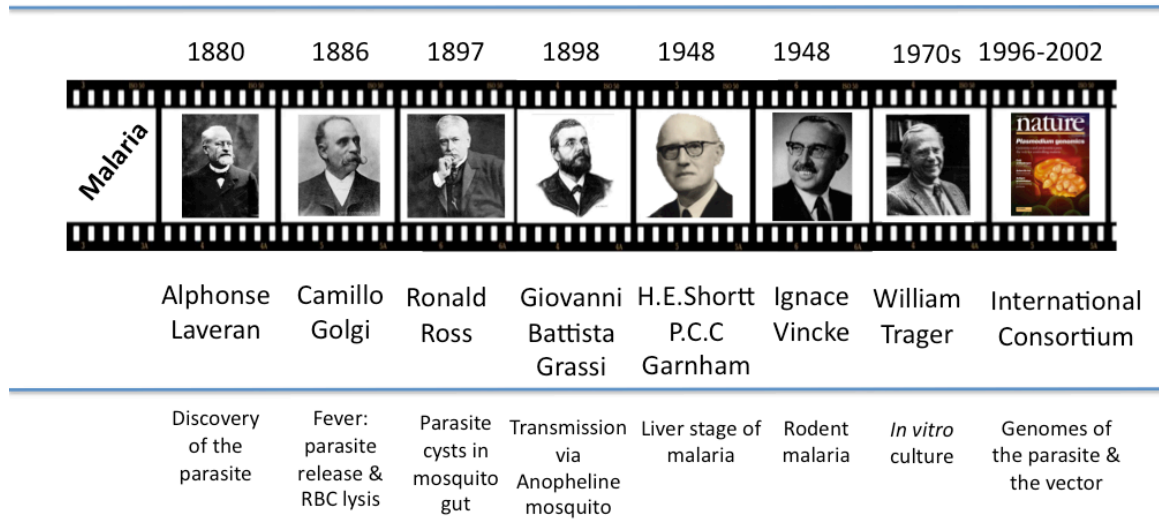


Figure 1-2: *Illustrated summary of the major discoveries that paved the way to a molecular understanding of the malaria pathogen Plasmodium falciparum.*

2 AN OVERVIEW OF THE DISEASE

The protozoan parasite *P. falciparum* is responsible for the most severe form of human malaria and causes a tremendous economic burden (8), leading to at least 1 million deaths per year, particularly in developing countries where failure to eradicate the anopheline mosquito vector leads to occasional epidemics (9, 10). Approximately 250 million people are infected with malaria worldwide every year, mainly consisting of pregnant women and children under the age of 5 years old (10). Other species of malaria that infect humans include *P. ovale*, *P. vivax*, *P. malariae*, and *P. knowlesi*. The onset of symptoms takes place at 10–15 days after being bitten, resulting in fevers of up to 41.5°C, chills, headaches, and vomiting (1, 2, 11-13). If these symptoms are not addressed with chemotherapeutic treatment, the disease may progress to severe malaria (12, 13), which consists of severe anemia, acute respiratory failure, hypoglycemia, renal failure, pulmonary edema, seizures, and unarousable coma (13).

Naturally acquired immunity to malaria is slow to develop, is not sterile, and is mostly lost in the absence of continual antigenic exposure (14-16). Individuals raised in malaria-endemic regions eventually become immune to severe malaria and are protected from death (16). How this immunity is acquired and the duration of the immune memory are not understood. Young children, returning immigrants who have lost previous immunity, and pregnant women are more susceptible to developing severe anemia (13). Treatment of severe disease with intravenous artemisinin or quinine is an option, but even with this treatment more than 20% of adults, 15% of children, and 50% of pregnant women still die (12).

There is no commercially available vaccine to protect against malaria (14, 15). The most promising candidate is the RTS,S vaccine, which consists of the parasite circumsporozoite protein and the hepatitis B surface antigen (17). It does not provide complete protection, but has demonstrated efficacy against complicated and uncomplicated malaria in children (18-20). This vaccine minimizes the morbidity and mortality of the disease, but does not eliminate the parasite (14).

Endeavors to eliminate malaria have raised global interest ever since the 1950s, but have failed because of the resistance of mosquito vectors to insecticides, resistance of the parasites to drugs, socioeconomic problems, and the lack of effective vaccines. Transmission control is one of the

main goals of global efforts by focusing on increased access to insecticide nets, diagnostic tests, vaccines to prevent disease, and novel therapies (3, 14).

Apart from the complexity of the disease, malaria faces a continuous abandonment of drug research and development by the greater part of the pharmaceutical industry due to a lack of profit, which has resulted in a serious shortage in the antimalarial armamentarium (2, 8). A wake-up call for the development of antimalarial strategies was the war in Vietnam, in which large numbers of non-immune soldiers were exposed to chloroquine (CQ)-resistant *P. falciparum* malaria in the 1960s. This allowed the United States Army Research and Development Command and the Walter Reed Army Institute of Research to re-assess valuable old leads for their antimalarial effects (2). These efforts led to the discovery of two powerful antimalarial drugs: mefloquine and halofantrine (21).

3 THE MALARIA LIFE CYCLE

Before receiving a blood meal, the *Anopheles* mosquito releases anticoagulants into the host blood; simultaneously, the injection of malaria sporozoites takes place (22). The sporozoites travel in the blood until they reach hepatocytes by binding to negatively charged sugars (23). This is the environment under which the sporozoites grow and replicate their DNA to become multinucleated schizonts that give rise to tens of thousands of merozoites (1). Merozoites are of minimal size ($0.9 \times 1.3 \mu\text{M}$) and ellipsoidal with a flat-ended apex. They contain an irregularly shaped hemispherical nucleus and a group of secretory vesicles at the apical prominence that are known as rhoptries, micronemes, and dense granules. These vesicles contain the proteins required for invasion (1).

When the merozoites are released from the hepatocytes into the bloodstream, the intra-erythrocytic cycle starts (23). The erythrocytic cycle is the stage of the parasite life cycle that is responsible for the clinical symptoms of malaria (1), and this cycle can be recapitulated *in vitro*. The stages of the intra-erythrocytic cycle are depicted in Figure 1-3. For *P. vivax* and *P. ovale* infections, some of the sporozoites develop into dormant parasites called hypnozoites. Their switch into sporozoites and their replication result in relapses that can occur years after the initial infection (12).

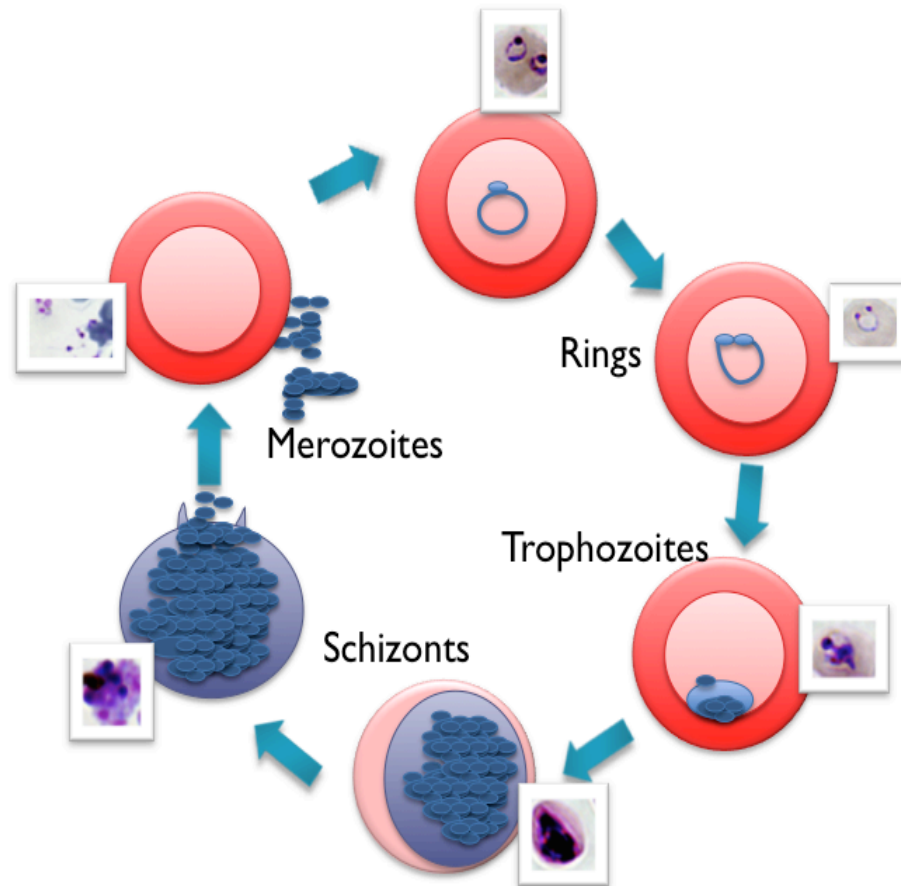


Figure 1-3: An illustration of the intra-erythrocytic cycle of *Plasmodium falciparum*. The inset pictures have been taken under a light microscope and show the appearance of the parasites at the different stages upon Giemsa staining. One cycle in *P. falciparum* typically takes 48 h to complete.

The different *Plasmodium* species take different times to complete one full asexual replication cycle in blood, e.g., *P. falciparum*, *P. vivax*, and *P. ovale* cycles take 48 h, the *P. malariae* life cycle is 72 h, and the *P. knowlesi* life cycle is 24 h (24, 25). The mouse and rat parasite *P. berghei* has a life cycle that is essentially the same as that of the *P. falciparum* parasite that infects humans, but with differences in the duration of the different stages of the life cycle. The pre-erythrocytic cycle, for example, requires between 42 and 72 h, while the asexual, intra-erythrocytic cycle takes between 22 and 25 h (1). During *P. falciparum* infection, the addition of the parasite's erythrocyte membrane binding protein 1 (EMP1) to the surface of the RBC causes parasitized RBCs to stick to the endothelial cells of blood vessels, avoiding the clearance of these infected cells by the spleen (26) and causing vascular blockage and reduced O₂ delivery to other organs. The hemolysis leads to anemia and intermittent fever (26).

Once *P. falciparum* has successfully invaded a RBC, it spends the first 20–24 h in what is known as the “ring stage” due to the ring-shape appearance of Giemsa-stained parasites under the microscope. During this stage, the parasite feeds on hemoglobin and plasma nutrients, synthesizes ring-stage molecules, and modifies the RBC membrane (1, 26). The ring shaped parasites are 2–3.7 μM in diameter and discoidal with a biconcave shape. The thicker periphery of the ring contains most of the organelles, including the nucleus (1).

The next stage is the trophozoite stage that appears at 24–36 h after RBC invasion by *P. falciparum* (27). At this point in its development, the parasite is feeding, growing, and modifying the RBC membrane more than at any other stage (26). Trophozoites are rounded forms of the parasite that possess a single pigment vacuole with increased basophilia. At this stage, the parasite has lost its biconcave form and rolls into an ellipsoidal or spheroidal shape. The infected RBC starts to develop “knobs”, which consist of dense material from the RBC cytoskeleton (26). Knobs are first seen in the trophozoite stage, but increase over time and reach a maximum size at the beginning of the schizont period (1). The trophozoite stage is also characterized by the appearance of 2 or 3 cytostomes, which are involved in the formation of many hemoglobin-containing food vacuoles near them. These food vacuoles are internalized and further processing of hemoglobin takes place (1, 28). As the parasite feeds on hemoglobin, it produces toxic heme by-products that it polymerizes into non-toxic hemozoin (28). As the parasite continues to grow

and differentiate, it exports membranes, clefts, small vesicles, and proteins to the surrounding RBC. The molecular details of this export are not well understood (29, 30).

Trophozoites replicate their DNA to grow into schizonts (31). In the schizont stage, the parasite transitions from its trophic activities and cytochalasin feeding to maturation. A spindle pole body appears from the nuclear envelope; this is the onset of nuclear division and merozoite formation, and all of the organelles multiply during this phase (31). The nucleus undergoes 4 mitotic divisions, resulting in 8–32 nuclei for *P. falciparum*. Synthesized and organized organelles take over the entire area of the RBC. This process of organelle replication continues as the merozoites bud off from the cytoplasm (1, 31, 32).

Once the RBCs infected with schizonts burst, they release as many as 16–32 new merozoites that have the potential to invade fresh RBCs and repeat the intra-erythrocytic cycle (32). In some cases, the merozoites enter RBCs and do not divide, but differentiate into female and male gametocytes (the crescents that Laveran initially observed). The trigger of this differentiation process is not well understood. When ingested by the mosquito, the male gamete divides into 8 flagellated microgametes that escape from the ingested RBC (1). One microgamete fertilizes the female macrogamete. The resultant zygote is motile and is called an ookinete, and has the ability to move through the cells of the stomach wall to form an oocyst. In the oocyst, many threadlike sporozoites are produced through asexual reproduction until the oocyst bursts and the sporozoites are released into the body cavity of the mosquito. They then find their way to the salivary glands so that when the mosquito receives a blood meal, the transmission cycle is complete (1).

4 ANTIMALARIALS AND THE EMERGENCE OF RESISTANCE

Most of the currently available antimalarials have been identified from natural products that exhibited antimalarial activity. The identification of antimalarials such as quinine and artemisinin was serendipitous and involved no rationally identified molecular targets (3, 33). The rest of the antimalarials such as CQ, artesunate, antifolates, and tetracyclines were identified either by their chemical relationship to natural products or from their activity against other infectious organisms.

In fact, most of the existing antimalarials have similar modes of action: 1) 4-aminoquinolines (e.g., CQ and amodiaquine) and aryl amino alcohols (e.g., mefloquine, lumefantrine, and quinine) interfere with the formation of the hemozoin crystal and, therefore, the parasite's ability to deal with toxic heme by-products (3, 33); 2) antifolates (e.g., sulfadoxine, pyrimethamine, and proguanil) disrupt folate metabolism in the parasite (34); 3) artemisinin and its active derivatives (e.g., artemether, artesunate, artemotil, and dihydroartemisinin) are endoperoxides that interact with reduced heme and modify the parasite's enzymes and lipids (35); and 4) antibiotics that interfere with parasite RNA and inhibit protein synthesis (e.g., tetracycline, doxycycline, and clindamycin) (3, 33).

Antifolates are among the very few antimalarials with well-defined targets and mechanism of action in the folate biosynthesis pathway, but resistance to these inhibitors, including pyrimethamine and cycloguanil, arose soon after their deployment as antimalarials (3, 33). The mutations in dihydrofolate reductase that generate resistance first appeared in Asia and spread to Africa (3, 36). Apart from encountered resistance, other issues associated with current antimalarials are their access and severe side effects. Mefloquine is effective in most countries (apart from Southeast Asia), but it causes severe side effects such as seizures, acute psychosis, and anxiety neurosis (12). Artemisinin is extracted from *Artemisia annua* for the semi-synthetic production of artemisinin derivatives (35). The content of artemisinin in each plant is between 0.01–0.8% of the dry weight, making it one of the most expensive treatments (3).

Resistance has emerged to all existing drugs in Southeast Asia (3). Multidrug resistance (defined as resistance to >3 drugs) is also common (3). Causes of antimalarial resistance include incorrect

dosing, non-adherence to dosing regimens, poor drug quality, including the dispensing of fraudulent drugs, poor absorption, and misdiagnosis. Resistance develops when parasites undergo point mutations or gene amplification events that provide a fitness advantage, especially under repeated drug exposure (3). The World Health Organization recommends that cases of uncomplicated *P. falciparum* malaria be treated using artemisinin-based combination therapy (ACT). However, resistance has emerged recently to ACT at the Thai-Cambodia border and may soon be widespread. The two most widely used and cheapest antimalarial drugs, CQ and sulfadoxine-pyrimethamine (SP), have failed at an unprecedented rate in most malaria-endemic regions (3). Antimalarial resistance has consequently resulted in increased morbidity and mortality from malaria (37).

The use of CQ began worldwide in the 1940s. This drug remained the gold standard for the prevention and treatment of uncomplicated malaria for several decades. It was characterized by its rapid parasitocidal action, low cost (\$0.2 for a 3-day treatment), safety, and widespread availability (1, 3). CQ is active only at the parasite stages that degrade hemoglobin. CQ acts by binding to the heme moieties produced from proteolytically processed hemoglobin and, as such, it interferes with heme detoxification, which takes place inside the digestive vacuole. Once inside the acidic vacuole environment, CQ becomes diprotonated and membrane impermeant (1, 3). Resistance to CQ was first documented in the 1950s in Colombia and Thailand. By the 1970s, CQ resistance was widespread in Africa, South America, and Asia (1, 3). In 1987, Krogstad *et al.* showed that CQ-resistant (CQR) parasites released pre-accumulated CQ almost 50 times faster than CQ-sensitive (CQS) parasites (38). In the early 1990s, Wellems *et al.* identified the CQ resistance transporter (PfCRT) by genetic crosses of Dd2 and HB3 clones (CQR and CQS, respectively) (39). The CQR allele differs by 6–8 point mutations from the canonical CQS HB3 *pfCRT* allele (40, 41).

Analogous to mammalian cells, the gene for the multidrug transporter, *pfmdr1*, was amplified in some CQR strains. The PfMDR1 protein is also localized on the membrane of the digestive vacuole (1, 3). Point mutations in PfMDR1 are also linked to CQ resistance (1, 3). In spite of the prevalence of CQR *P. falciparum*, CQ is still widely used in sub-Saharan Africa for symptom alleviation due to its low cost (1, 3).

For quinine, the first reports of decreased *P. falciparum* susceptibility date back to 1908 in Brazil (34). In 1984, mefloquine was introduced as monotherapy in Thailand. Five years later, in 1989, the cure rates with mefloquine dropped by >50%, leading to the development of multidrug resistance (3). Variance in artemisinin susceptibility sometimes correlates with *pfmdr1* copy number (25-fold 50% inhibitory concentrations (IC₅₀s)) (42). Even though the target of artemisinin derivatives has been postulated to be PfATP6, a calcium transporting ATPase with homology to mammalian SERCA (42, 43), polymorphisms in this gene do not always correlate with resistance (3). These vicious cycles of antimalarial resistance development are perpetuated by the fact that the only affordable treatment options are rapidly losing their therapeutic efficacy.

However, the widespread resistance to CQ and SP, the two lowest cost antimalarials, provides a great incentive for the development of new therapeutic approaches with novel mechanisms of action, particularly in this era in which the understanding of the biochemistry and genome of malaria may aid in the identification of new rationales and mechanistic approaches. White *et al.* (37) argued that the loss of cheap and effective antimalarials to resistance may represent the single most important threat to the health of people in tropical countries. The life of antimalarials such as CQ can be resurrected by combining them with resistance-reversing or sensitizing agents (44-46).

The ideal antimalarial should be cheap, kill the parasite quickly, be safe, and address the problem of resistance (3, 33). Fast treatment (3-day antimalarial regimen) ensures compliance, avoids resistance, and allows for the rapid clearance of parasites before severe malaria develops. The discovery of antimalarials with new mechanisms of action avoids the development of cross-resistance and provides the option of synergy with existing antimalarials. Many of the newly discovered inhibitors have very short half-lives (3, 33), which necessitates their use in combination with a longer-acting drug such as amodiaquine or CQ.

5 HEAT SHOCK PROTEIN 90

Heat shock proteins (HSPs) are a class of highly conserved molecular chaperones that facilitate protein folding (47, 48). HSPs function in partnerships in which protein substrates are partially folded by one group of HSPs and then handed over to another group of chaperones before they reach their full functional conformation (47, 48). For example, Hsp70 and Hsp90 play independent chaperone roles, but they exist in a functional partnership ensuring that some peptide substrates are passed from Hsp70 to Hsp90 (49). An adaptor called Hop (Hsp70-Hsp90 organizing protein) functionally links Hsp70 to Hsp90 (50).

Hsp90 is one of the best-studied members of the HSP family, and it is important for normal eukaryotic growth and development. Cytosolic Hsp90 exists in the form of a multichaperone complex and, together with Hsp70 and Hsp60, helps newly synthesized proteins to fold and to modulate the activities of transcription factors and protein kinases (48, 50). It is postulated that Hsp90 serves as a buffer by preventing cellular toxicity caused by misfolded and aggregated proteins in response to stress (51-53). Hsp90 is not involved in primary protein-folding events, but rather in conformationally labile client protein maturation (54-57). It provides a compensatory regulatory mechanism that maintains the functional conformation of regulatory proteins, including many that are involved in drug resistance (51, 52, 58, 59). Inhibition of the broad spectrum of Hsp90 interactions and signaling pathways provides a wide range of anti-disease effects and a decreased likelihood for developing resistance. Several Hsp90 inhibitors are in clinical evaluation for the treatment of various cancers (53, 55, 60-63).

Pharmacologic inhibition of Hsp90 effectively results in lethality in abnormal cells (64, 65). Infection, transformation, and neurodegeneration are all characterized by abnormal cell signaling, altered expression levels, and different protein interactions in the cell. In particular, the ATPase activity of Hsp90 is essential for driving the chaperone cycle and directing binding, induction of the active conformation, and release of its client proteins. Inhibition of this ATPase activity at the N-terminal ATP-binding domain is an effective approach for inhibiting its function and interaction with client proteins (64, 65). Significant similarity exists at the ATP-binding domain between other eukaryotic stress-inducible Hsp90s and *P. falciparum* Hsp90 (PfHsp90) (11, 59, 66-69).

Human and malaria genomes encode four paralogs of Hsp90 (Figure 1-4). Hsp90 α (MIM: 140571) is the human inducible homolog that is over-expressed in cancer cells. Hsp90 β (MIM: 140572) is the constitutive form. An additional two paralogs of Hsp90 exist, but unlike Hsp90 α and Hsp90 β that are cytosolic, the Hsp90 paralog known as TRAP1 (MIM: 606219) is confined to the mitochondria, while Grp94 (MIM: 191175) is localized in the endoplasmic reticulum. These organellar variants are derived separately from the prokaryotic form of Hsp90, known as HTPG. Each of the Hsp90 paralogs folds a distinct set of client proteins (48). In the human host, Hsp90 α and Hsp90 β contain an EEVD interaction motif, but for malaria, only one of the cytosolic Hsp90s (PF07_0029) contains the EEVD motif and is known to be induced by stress and highly expressed during the erythrocytic life cycle of the parasite (69). The focus of this project is to outline a combination therapy strategy that targets this stress-inducible Hsp90 isoform for antimalarial chemotherapy.

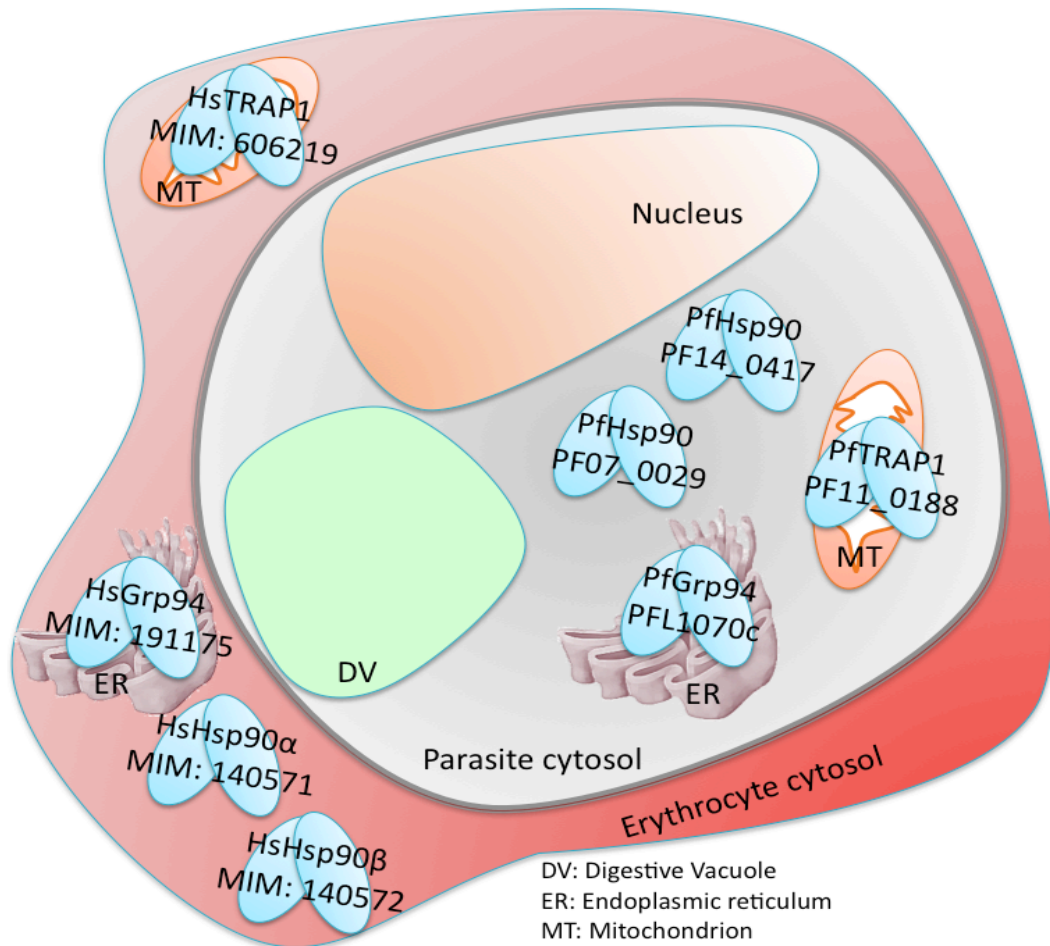


Figure 1-4: Illustration of the localization of human and malaria Hsp90 paralogs inside an RBC infected with *P. falciparum*. The focus of this thesis will be on PfHsp90 (PF07_0029), which is the cytosolic isoform with a conserved EEVD motif.

Hsp90 has been exploited as a successful drug target in many cancers, neurodegenerative diseases, as well as viral and fungal infections (Appendix 1) due to its activation and mediation of stress-induced interactions in abnormal cells. Hsp90 has a unique Bergerat fold of its ATP binding pocket with an open “lid” domain in the N-terminal domain, which can be inhibited competitively and selectively by several small molecules (70). Since Hsp90 regulates the cell cycle, potentiates drug resistance, and buffers phenotypic variation, many clients of Hsp90 are essential cellular proteins with pathogenic functions that render the inhibition of the Hsp90 pathway lethal to stressed cells, but not to normal cells.

Crystal structures have revealed paralog-specific conformational differences in response to ATP or geldanamycin (GA) binding in fungi. For example, while the ATP binding pocket is acidic in Grp94 and yeast Hsp82, the neighboring phosphate-binding regions differ (71-74). In yeast Hsp82, this neighboring region is basic and better complements the charge of the nucleotide, while in Grp94, this region is acidic and strongly repels the ligand. Unique differences in the ATPase domains of Hsp90 paralogs account for the specificity of cytosolic Hsp90-targeted inhibitors (71-74). Targeting of cytosolic inducible PfHsp90 may result in higher efficacy and therapeutic control.

Cowen *et al.* have shown that Hsp90 inhibitors synergize with known antifungals to which the microbe would otherwise be resistant. In fungi (51, 75), Hsp90 governs the antimicrobial resistance of agents with different mechanisms of action (e.g., ergosterol and cell wall biosynthesis) (51, 75). Cowen and Lindquist used a titratable (51) Cre-Lox system to examine the role of Hsp90 in potentiating fluconazole resistance. Fluconazole-resistant colonies were present only in strains with high levels of Hsp90. Fluconazole resistance disappeared in strains where Hsp90 expression was reduced by Cre-mediated recombination. The mechanism of resistance could be both acquired and maintained independent of Hsp90 (through mutations in a drug resistance transporter), despite the fact that Hsp90 is crucial for resistance acquisition. The Hsp90 inhibitors, GA and radicicol, reduced fluconazole resistance in *Saccharomyces cerevisiae* strains with mutations in the ergosterol biosynthesis pathway (51). Thus, this work laid the foundations by showing that Hsp90 mediates the mechanisms that allow cells to cope with abnormal conditions such as drug-induced stress. The most important implication of these

findings is that Hsp90 inhibitors have the ability to counter independently evolved drug resistance (51).

6 HEAT SHOCK PROTEIN 90 INHIBITORS

A range of Hsp90 inhibitors that target the N-terminal domain have been developed including natural product inhibitors such as GA and radicicol, and synthetic inhibitors comprised of purines, pyrazoles, isoxazoles, and other scaffolds (63, 64, 76). GA, an ansamycin antibiotic, was the first selective Hsp90 inhibitor shown to bind to Hsp90 and interfere with heterocomplex formation (48, 77). On inhibition, Hsp90 client proteins cannot attain their active conformation and are degraded by the proteasome (48, 77). Degradation of these proteins leads to growth arrest and apoptosis. Inhibition of *Brugia pahangi* Hsp90 from endogenous protein extracts showed that Hsp90 is a selective target in parasites and supports the identification of novel chemotypes with enhanced potency and selectivity (78).

The broad spectrum of Hsp90 interactions and signaling pathways provides a potentially wide range of anti-disease effects and a decreased likelihood for developing resistance. GA and its analog 17-AAG are potent Hsp90 inhibitors, but their clinical use has been precluded by severe hepatotoxicity, strict dosing limitations, and metabolic and chemical instability (48, 74, 76). Radicicol (Rad) is a macrocyclic lactone with anti-Hsp90 activity in cell culture, but it is not stable in serum and, therefore, has no activity *in vivo*. Due to the toxicity caused by GA and its derivatives in animal and human studies, alternative small molecule inhibitors have been sought (48, 73, 74, 76).

Efforts in identifying alternative drugs that inhibit Hsp90 have resulted in the discovery of numerous inhibitors from a variety of scaffolds, which take advantage of the unique shape that ATP assumes when it binds to the Hsp90 ATP binding domain and that show specificity for Hsp90 (76, 79, 80). The first members of this ATP-mimetic group were composed of a purine scaffold tethered by a linker to an aryl moiety consisting of the first scaffold drug PU3, which had lower anti-Hsp90 activity than GA and Rad. However, the structure of PU3 was used for extensive chemical modifications in order to enhance its potency, including the introduction of a fluorine at C2 and a sulfide linker (76, 79-81). The most potent and orally bioavailable representative of this group with an attractive pharmacokinetic profile is PU-H71 (MeSH:C526550) (76, 79-81).

7 PLASMODIUM FALCIPARUM HEAT SHOCK PROTEIN 90

In *P. falciparum*, 1 cytosolic Hsp90 (PF07_0029, PfHsp90) is known to be induced by stress (48, 59) and highly expressed during the erythrocytic life cycle (82). PfHsp90 is essential for the development of the parasite (11, 66, 69, 83). In a recent study, Pallavi *et al.* also implicated Hsp90 as a drug target against malaria and *Trypanosoma* infections in animal models (68). Biochemical characterization of full-length PfHsp90 in this study showed that PfHsp90 retains a high level of ATPase activity that was inhibited successfully using 17-AAG. 17-AAG reduced parasite infection load in the *P. berghei* model at the tested dose (50 mg/kg) (68).

The crystal structures of the ATP-binding domains of PfHsp90 and human Hsp90 (HsHsp90) reveal a unique Bergerat fold with an open “lid” domain in comparison to other ATPase domains and several unique residues at the drug binding site that can be exploited for drug binding specificity (70, 73, 74, 84, 85). In particular, Val186 of human Hsp90 is replaced by Ile173; PfHsp90 contains Ala38 instead of Ser52 (human Hsp90) and at Lys112, PfHsp90 contains Arg98 (85). In general, these substitutions result in a more constricted, basic, and hydrophobic pocket in PfHsp90.

PfHsp90 may play a role in the development of drug resistance in the malaria parasite because of its interaction with the CQ resistance-associated protein Cg4 (59). Hence, PfHsp90 has the potential to not only serve as a drug target but also circumvent drug resistance to conventional antimalarials when used in combination through synergy. Indeed, GA synergizes with calcineurin and cyclosporine A, which target Hsp90-interacting proteins, when tested in tandem for antimalarial activity (66, 69). Furthermore, the parasite interaction network exhibits functional differences with that of *S. cerevisiae* and the human host (59), highlighting the potential of this protein target for the design of specific antimalarial inhibitors.

Heat shock is part of the parasite life cycle when it changes hosts and during the febrile episodes of malaria. Chaperones are very important in responding to this stress and in buffering mechanisms that ensure parasite survival and growth. The increase in temperature activates the PfHsp90 stress response pathway and may facilitate the arousal of new phenotypes by chaperoning mutant client proteins that develop drug resistance, enhance virulence, or

cytoadherence properties (66, 69). GA was shown to inhibit growth at an LD₅₀ of 200 nM and cause a transition block at the ring stage, suggesting an important role for PfHsp90 in parasite growth. GA inhibition of PfHsp90 disrupted the PfHsp90 complex consisting of PfHsp70, PfPP5, and tubulin, among other proteins (66). Inhibition of PfHsp90 function in combination with other antimalarials may circumvent the development of drug resistance.

Taken together, the following key factors suggest that PfHsp90 represents a promising target: 1) the antimalarial activity of known cross-species Hsp90 inhibitors such as GA; 2) the essential and multifaceted chaperone function of Hsp90; 3) its potential cross-talk with pathways involved in drug resistance; and 4) the unique structural features in the ATP-binding domain between human and *P. falciparum* Hsp90.

Malaria prophylaxis and treatment is challenged by the difficulty to prevent the evolution of antimalarial resistance due to the complex parasite life cycle. This problem is further compounded by the absence of a defined target for most of the available antimalarials. Broad-spectrum effects of most of the antimalarial drugs and failure to detect post-treatment remnant parasites create the perfect ground for nurturing antimalarial resistance. The development of new drugs with a known mechanism and target as well as their combination with current antimalarials is the only way to meet this challenge. The aim of this thesis is to propose an effective strategy that makes use of the capacity of PfHsp90 to cross-talk with multiple pathways to identify synergistic combinations of drugs that have the potential to reverse antimalarial resistance and are synergistic in mouse models of malaria.

References

1. Sherman IW (2005) The life of Plasmodium: an overview. *Molecular approaches to malaria*, ed Sherman IW (ASM Press, Washington, D.C), pp 3-23.
2. Robinson WPaBL (1999) Malaria. *Handbook of mouse models of infection*, ed M.Sandy OZa (Academic, London), pp 757-773.
3. Fidock DA, Rosenthal PJ, Croft SL, Brun R, & Nwaka S (2004) Antimalarial drug discovery: efficacy models for compound screening. *Nature reviews. Drug discovery* 3(6):509-520.
4. Trager W (1979) Plasmodium falciparum in culture: improved continuous flow method. *The Journal of protozoology* 26(1):125-129.
5. Jensen JB & Trager W (1977) Plasmodium falciparum in culture: use of outdated erythrocytes and description of the candle jar method. *The Journal of parasitology* 63(5):883-886.
6. Gardner MJ, *et al.* (2002) Genome sequence of the human malaria parasite Plasmodium falciparum. *Nature* 419(6906):498-511.
7. Holt RA, *et al.* (2002) The genome sequence of the malaria mosquito Anopheles gambiae. *Science* 298(5591):129-149.
8. Sachs J & Malaney P (2002) The economic and social burden of malaria. *Nature* 415(6872):680-685.
9. Snow RW, Guerra CA, Noor AM, Myint HY, & Hay SI (2005) The global distribution of clinical episodes of Plasmodium falciparum malaria. *Nature* 434(7030):214-217.
10. Hay SI, Guerra CA, Tatem AJ, Noor AM, & Snow RW (2004) The global distribution and population at risk of malaria: past, present, and future. *The Lancet infectious diseases* 4(6):327-336.
11. Acharya P, Kumar R, & Tatu U (2007) Chaperoning a cellular upheaval in malaria: heat shock proteins in Plasmodium falciparum. *Molecular and biochemical parasitology* 153(2):85-94.
12. Ashley E, *et al.* (2006) In vivo sensitivity monitoring of mefloquine monotherapy and artesunate-mefloquine combinations for the treatment of uncomplicated falciparum malaria in Thailand in 2003. *Tropical medicine & international health : TM & IH* 11(12):1898-1899; author reply 1899.
13. Ndam NT & Deloron P (2007) Molecular aspects of Plasmodium falciparum Infection during pregnancy. *Journal of biomedicine & biotechnology* 2007(5):43785.
14. Douradinha B & Doolan DL (2011) Harnessing immune responses against Plasmodium for rational vaccine design. *Trends in parasitology* 27(6):274-283.
15. Doolan DL, Dobano C, & Baird JK (2009) Acquired immunity to malaria. *Clinical microbiology reviews* 22(1):13-36, Table of Contents.
16. Langhorne J, Ndungu FM, Sponaas AM, & Marsh K (2008) Immunity to malaria: more questions than answers. *Nature immunology* 9(7):725-732.

17. Casares S, Brumeanu TD, & Richie TL (2010) The RTS,S malaria vaccine. *Vaccine* 28(31):4880-4894.
18. Alonso PL, *et al.* (2004) Efficacy of the RTS,S/AS02A vaccine against *Plasmodium falciparum* infection and disease in young African children: randomised controlled trial. *Lancet* 364(9443):1411-1420.
19. Alonso PL, *et al.* (2005) Duration of protection with RTS,S/AS02A malaria vaccine in prevention of *Plasmodium falciparum* disease in Mozambican children: single-blind extended follow-up of a randomised controlled trial. *Lancet* 366(9502):2012-2018.
20. Bejon P, *et al.* (2008) Efficacy of RTS,S/AS01E vaccine against malaria in children 5 to 17 months of age. *The New England journal of medicine* 359(24):2521-2532.
21. Peters W, Robinson BL, & Ellis DS (1987) The chemotherapy of rodent malaria. XLII. Halofantrine and halofantrine resistance. *Annals of tropical medicine and parasitology* 81(5):639-646.
22. Tuteja R (2007) Malaria - an overview. *The FEBS journal* 274(18):4670-4679.
23. Cowman AF & Crabb BS (2006) Invasion of red blood cells by malaria parasites. *Cell* 124(4):755-766.
24. Bray RS & Garnham PC (1982) The life-cycle of primate malaria parasites. *British medical bulletin* 38(2):117-122.
25. Chin W, Contacos PG, Coatney GR, & Kimball HR (1965) A Naturally Acquired Quotidian-Type Malaria in Man Transferable to Monkeys. *Science* 149(3686):865.
26. Bannister L & Mitchell G (2003) The ins, outs and roundabouts of malaria. *Trends in parasitology* 19(5):209-213.
27. Baumeister S, Winterberg M, Przyborski JM, & Lingelbach K (2010) The malaria parasite *Plasmodium falciparum*: cell biological peculiarities and nutritional consequences. *Protoplasma* 240(1-4):3-12.
28. Francis SE, Sullivan DJ, Jr., & Goldberg DE (1997) Hemoglobin metabolism in the malaria parasite *Plasmodium falciparum*. *Annual review of microbiology* 51:97-123.
29. Przyborski JM, Wickert H, Krohne G, & Lanzer M (2003) Maurer's clefts--a novel secretory organelle? *Molecular and biochemical parasitology* 132(1):17-26.
30. Cooke BM, Mohandas N, & Coppel RL (2004) Malaria and the red blood cell membrane. *Seminars in hematology* 41(2):173-188.
31. Ben Mamoun C, *et al.* (2001) Co-ordinated programme of gene expression during asexual intraerythrocytic development of the human malaria parasite *Plasmodium falciparum* revealed by microarray analysis. *Molecular microbiology* 39(1):26-36.
32. Koussis K, *et al.* (2009) A multifunctional serine protease primes the malaria parasite for red blood cell invasion. *The EMBO journal* 28(6):725-735.
33. Fidock DA (2010) Drug discovery: Priming the antimalarial pipeline. *Nature* 465(7296):297-298.
34. Gregson A & Plowe CV (2005) Mechanisms of resistance of malaria parasites to antifolates. *Pharmacological reviews* 57(1):117-145.

35. Taylor DK, *et al.* (2004) Novel endoperoxide antimalarials: synthesis, heme binding, and antimalarial activity. *Journal of medicinal chemistry* 47(7):1833-1839.
36. Imwong M, *et al.* (2001) Association of genetic mutations in *Plasmodium vivax* dhfr with resistance to sulfadoxine-pyrimethamine: geographical and clinical correlates. *Antimicrobial agents and chemotherapy* 45(11):3122-3127.
37. White NJ, *et al.* (1999) Averting a malaria disaster. *Lancet* 353(9168):1965-1967.
38. Krogstad DJ, *et al.* (1987) Efflux of chloroquine from *Plasmodium falciparum*: mechanism of chloroquine resistance. *Science* 238(4831):1283-1285.
39. Wellems TE, Walker-Jonah A, & Panton LJ (1991) Genetic mapping of the chloroquine-resistance locus on *Plasmodium falciparum* chromosome 7. *Proceedings of the National Academy of Sciences of the United States of America* 88(8):3382-3386.
40. Djimde A, Doumbo OK, Steketee RW, & Plowe CV (2001) Application of a molecular marker for surveillance of chloroquine-resistant *falciparum* malaria. *Lancet* 358(9285):890-891.
41. Djimde A, *et al.* (2001) A molecular marker for chloroquine-resistant *falciparum* malaria. *The New England journal of medicine* 344(4):257-263.
42. Eckstein-Ludwig U, *et al.* (2003) Artemisinins target the SERCA of *Plasmodium falciparum*. *Nature* 424(6951):957-961.
43. Uhlemann AC & Krishna S (2005) Antimalarial multi-drug resistance in Asia: mechanisms and assessment. *Current topics in microbiology and immunology* 295:39-53.
44. White NJ (1998) Preventing antimalarial drug resistance through combinations. *Drug resistance updates : reviews and commentaries in antimicrobial and anticancer chemotherapy* 1(1):3-9.
45. Crandall I, Charuk J, & Kain KC (2000) Nonylphenoethoxylates as malarial chloroquine resistance reversal agents. *Antimicrobial agents and chemotherapy* 44(9):2431-2434.
46. Pereira MR, *et al.* (2011) In vivo and in vitro antimalarial properties of azithromycin-chloroquine combinations that include the resistance reversal agent amlodipine. *Antimicrobial agents and chemotherapy* 55(7):3115-3124.
47. Pesce ER, Cockburn IL, Goble JL, Stephens LL, & Blatch GL (2010) Malaria heat shock proteins: drug targets that chaperone other drug targets. *Infectious disorders drug targets* 10(3):147-157.
48. Shonhai A (2010) Plasmodial heat shock proteins: targets for chemotherapy. *FEMS immunology and medical microbiology* 58(1):61-74.
49. Wegele H, Muller L, & Buchner J (2004) Hsp70 and Hsp90--a relay team for protein folding. *Reviews of physiology, biochemistry and pharmacology* 151:1-44.
50. Smith DF, *et al.* (1993) Identification of a 60-kilodalton stress-related protein, p60, which interacts with hsp90 and hsp70. *Molecular and cellular biology* 13(2):869-876.
51. Cowen LE & Lindquist S (2005) Hsp90 potentiates the rapid evolution of new traits: drug resistance in diverse fungi. *Science* 309(5744):2185-2189.

52. Cowen LE, *et al.* (2009) Harnessing Hsp90 function as a powerful, broadly effective therapeutic strategy for fungal infectious disease. *Proceedings of the National Academy of Sciences of the United States of America* 106(8):2818-2823.
53. Marubayashi S, *et al.* (2010) HSP90 is a therapeutic target in JAK2-dependent myeloproliferative neoplasms in mice and humans. *The Journal of clinical investigation* 120(10):3578-3593.
54. Mollapour M & Neckers L (2011) Post-translational modifications of Hsp90 and their contributions to chaperone regulation. *Biochimica et biophysica acta*.
55. Moulick K, *et al.* (2011) Affinity-based proteomics reveal cancer-specific networks coordinated by Hsp90. *Nature chemical biology* 7(11):818-826.
56. Tatokoro M, *et al.* (2011) Potential role of Hsp90 inhibitors in overcoming cisplatin resistance of bladder cancer-initiating cells. *International journal of cancer. Journal international du cancer*.
57. Wang Y, Trepel JB, Neckers LM, & Giaccone G (2010) STA-9090, a small-molecule Hsp90 inhibitor for the potential treatment of cancer. *Curr Opin Investig Drugs* 11(12):1466-1476.
58. Cowen LE, Carpenter AE, Matangkasombut O, Fink GR, & Lindquist S (2006) Genetic architecture of Hsp90-dependent drug resistance. *Eukaryot Cell* 5(12):2184-2188.
59. Pavithra SR, Kumar R, & Tatu U (2007) Systems analysis of chaperone networks in the malarial parasite *Plasmodium falciparum*. *PLoS computational biology* 3(9):1701-1715.
60. Cerchiatti LC, *et al.* (2010) BCL6 repression of EP300 in human diffuse large B cell lymphoma cells provides a basis for rational combinatorial therapy. *The Journal of clinical investigation*.
61. Taldone T, *et al.* (2010) Assay strategies for the discovery and validation of therapeutics targeting *Brugia pahangi* Hsp90. *PLoS neglected tropical diseases* 4(6):e714.
62. Taldone T, *et al.* (2011) Synthesis of purine-scaffold fluorescent probes for heat shock protein 90 with use in flow cytometry and fluorescence microscopy. *Bioorganic & medicinal chemistry letters* 21(18):5347-5352.
63. Taldone T, *et al.* (2011) Design, synthesis, and evaluation of small molecule Hsp90 probes. *Bioorganic & medicinal chemistry* 19(8):2603-2614.
64. Jhaveri K, Taldone T, Modi S, & Chiosis G (2011) Advances in the clinical development of heat shock protein 90 (Hsp90) inhibitors in cancers. *Biochimica et biophysica acta*.
65. Usmani SZ & Chiosis G (2011) HSP90 inhibitors as therapy for multiple myeloma. *Clinical lymphoma, myeloma & leukemia* 11 Suppl 1:S77-81.
66. Banumathy G, Singh V, Pavithra SR, & Tatu U (2003) Heat shock protein 90 function is essential for *Plasmodium falciparum* growth in human erythrocytes. *The Journal of biological chemistry* 278(20):18336-18345.
67. Kumar R, Pavithra SR, & Tatu U (2007) Three-dimensional structure of heat shock protein 90 from *Plasmodium falciparum*: molecular modelling approach to rational drug design against malaria. *Journal of biosciences* 32(3):531-536.

68. Pallavi R, *et al.* (2010) Heat shock protein 90 as a drug target against protozoan infections: biochemical characterization of HSP90 from *Plasmodium falciparum* and *Trypanosoma evansi* and evaluation of its inhibitor as a candidate drug. *The Journal of biological chemistry* 285(49):37964-37975.
69. Pavithra SR, Banumathy G, Joy O, Singh V, & Tatu U (2004) Recurrent fever promotes *Plasmodium falciparum* development in human erythrocytes. *The Journal of biological chemistry* 279(45):46692-46699.
70. Dutta R & Inouye M (2000) GHKL, an emergent ATPase/kinase superfamily. *Trends in biochemical sciences* 25(1):24-28.
71. Dollins DE, Immormino RM, & Gewirth DT (2005) Structure of unliganded GRP94, the endoplasmic reticulum Hsp90. Basis for nucleotide-induced conformational change. *The Journal of biological chemistry* 280(34):30438-30447.
72. Dollins DE, Warren JJ, Immormino RM, & Gewirth DT (2007) Structures of GRP94-nucleotide complexes reveal mechanistic differences between the hsp90 chaperones. *Molecular cell* 28(1):41-56.
73. Immormino RM, *et al.* (2004) Ligand-induced conformational shift in the N-terminal domain of GRP94, an Hsp90 chaperone. *The Journal of biological chemistry* 279(44):46162-46171.
74. Immormino RM, *et al.* (2009) Different poses for ligand and chaperone in inhibitor-bound Hsp90 and GRP94: implications for paralog-specific drug design. *Journal of molecular biology* 388(5):1033-1042.
75. Singh SD, *et al.* (2009) Hsp90 governs echinocandin resistance in the pathogenic yeast *Candida albicans* via calcineurin. *PLoS pathogens* 5(7):e1000532.
76. Chiosis G, Caldas Lopes E, & Solit D (2006) Heat shock protein-90 inhibitors: a chronicle from geldanamycin to today's agents. *Curr Opin Investig Drugs* 7(6):534-541.
77. Chiosis G, Vilenchik M, Kim J, & Solit D (2004) Hsp90: the vulnerable chaperone. *Drug discovery today* 9(20):881-888.
78. Taldone T, *et al.* (Assay strategies for the discovery and validation of therapeutics targeting *Brugia pahangi* Hsp90. *PLoS Negl Trop Dis* 4(6):e714.
79. Taldone T & Chiosis G (2009) Purine-scaffold Hsp90 inhibitors. *Current topics in medicinal chemistry* 9(15):1436-1446.
80. Taldone T, Gozman A, Maharaj R, & Chiosis G (2008) Targeting Hsp90: small-molecule inhibitors and their clinical development. *Curr Opin Pharmacol* 8(4):370-374.
81. Caldas-Lopes E, *et al.* (2009) Hsp90 inhibitor PU-H71, a multimodal inhibitor of malignancy, induces complete responses in triple-negative breast cancer models. *Proc Natl Acad Sci U S A* 106(20):8368-8373.
82. Su XZ & Wellems TE (1994) Sequence, transcript characterization and polymorphisms of a *Plasmodium falciparum* gene belonging to the heat-shock protein (HSP) 90 family. *Gene* 151(1-2):225-230.
83. Banumathy G (2004) Functional insights into heat shock protein 90 multichaperone complex in *Plasmodium falciparum*. *A Thesis submitted for the Degree of Doctor of*

Philosophy in the Faculty of Science. Department of Biochemistry(Indian Institute of Science).

84. Immormino RM, Kang Y, Chiosis G, & Gewirth DT (2006) Structural and quantum chemical studies of 8-aryl-sulfanyl adenine class Hsp90 inhibitors. *Journal of medicinal chemistry* 49(16):4953-4960.
85. Corbett KD & Berger JM (2010) Structure of the ATP-binding domain of Plasmodium falciparum Hsp90. *Proteins* 78(13):2738-2744.

Chapter 2

ARTESUNATE MISUSE BY RETURNING TRAVELLER WITH *PLASMODIUM FALCIPARUM* INFECTION

This chapter has been published under the following citation:

Shahinas D, Lau R, Khairnar K, Hancock D, Pillai DR.
Emerg Infect Dis. 2010 Oct;16(10):1608-10.

Artemisinin derivatives were recently approved by the Food and Drug Administration for the treatment of *Plasmodium falciparum* malaria in North America and are available through the US Centers for Disease Control and Prevention and through Health Canada (1). Artemisinin based combination therapy (ACT) remains the most effective therapy for *P. falciparum* malaria throughout the world, with the possible exception of the Thailand–Cambodia border (2). Because of the large numbers in the Toronto area of returning travelers and recent immigrants who have returned to countries of origin and visited friends and relatives, the Public Health Laboratory (Toronto) identifies ≈ 200 positive malaria smears annually; most *P. falciparum* isolates have come from sub-Saharan Africa. Evidence has indicated that such travelers tend not to seek medical advice before travel and are therefore at high risk of acquiring malaria (3).

1 THE PATIENT

A 38-year-old Nigerian-born woman, who lived in the Toronto area (and has a good ability to recount her experiences), returned to Lagos, Nigeria, for a visit in January 2009. She did not seek pre-travel advice. On arrival in Lagos, the woman purchased artesunate locally and began taking two 50-mg tablets weekly for the 4 weeks of her visit. Immediately on her return to Toronto, the patient experienced myalgia, nausea with vomiting, and chills, ≈ 7 days after she had taken her last dose of oral artesunate. She sought treatment at the emergency department of a community hospital. Physical examination showed that her temperature was 39.1°C and that she was dehydrated. Laboratory tests showed the following: leukocyte count 3,700 cells/ μ L, thrombocyte

count 72×10^3 cells/ μL , haemoglobin level 12.7 g/dL. Her chest radiograph showed that her lungs were clear. An examination of peripheral blood by thick and thin blood films showed a 0.7% parasitemia with *P. falciparum*. Her condition was treated with 1,250 mg of oral mefloquine as a single dose. She was treated as an outpatient, and she reported that symptoms promptly resolved over the next 48 hours without side effects.

A blood specimen was placed into culture in our lab, and the *P. falciparum* isolate was tested for drug susceptibility (4). The 50% inhibitory concentration (IC_{50}) was the following for certain antimicrobial agents (tested in triplicate): chloroquine 170.5 ± 7.8 nmol/L, mefloquine 16.6 ± 0.7 nmol/L, artemisinin 20.1 ± 0.6 nmol/L, artesunate 6.2 ± 1.4 nmol/L, dihydroartemisinin 1.8 ± 0.9 nmol/L, and artemether 21.4 ± 5.3 nmol/L.

For this *P. falciparum* isolate, IC_{50} was significantly higher for artemisinin, artesunate, and artemether than for other representative *P. falciparum* isolates imported from Africa (Figure 2-1). Because of the short half-life of artesunate, the weekly doses of the oral drug may have led to development of a resistant strain when the patient was in Nigeria. Artesunate-containing drugs therefore should not be used for prophylaxis or single drug therapy. The purchased artesunate may also have been counterfeit and may have contained lower levels of active drug. Although these data suggest that this isolate has reduced susceptibility to artemisinin derivatives, the correlation between *in vitro* susceptibility and treatment outcomes does not appear to be consistent (2).

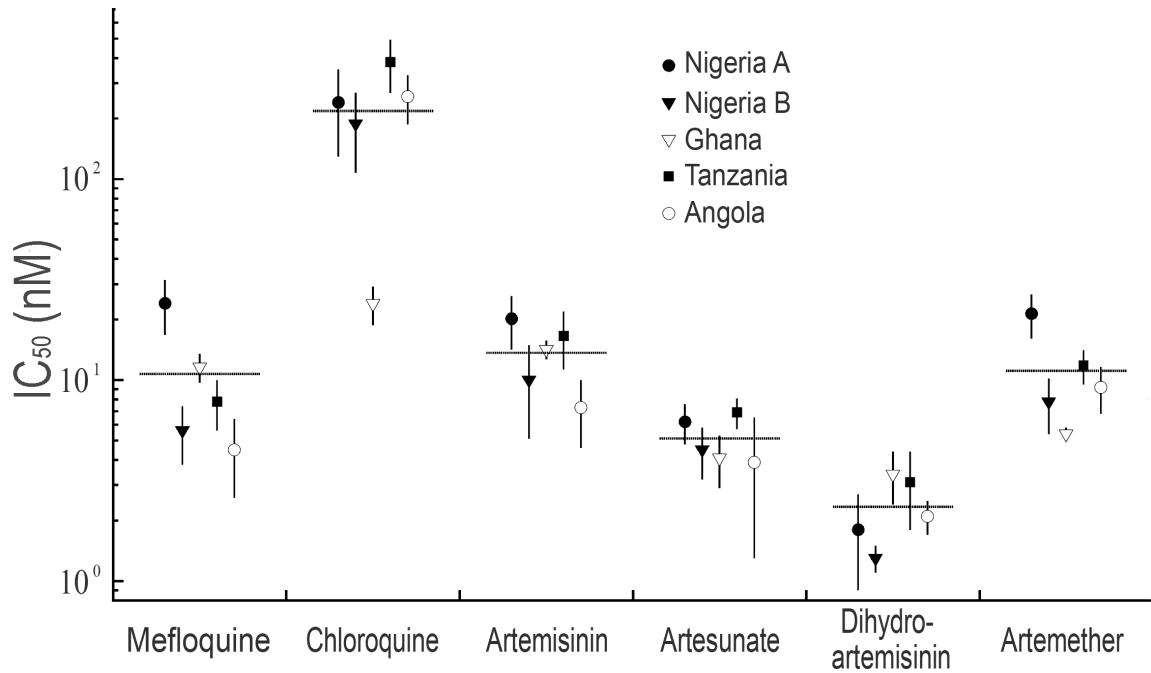


Figure 2-1: *In vitro* drug susceptibility of representative patient isolates from returning travelers who visited friends and relatives in Africa. The mean 50% inhibitory concentrations (IC₅₀) of chloroquine, mefloquine, artemisinin, artesunate, dihydroartemisinin, and artemether are plotted in nmol/L for each isolate, performed in triplicate (error bars indicate SD; n = 3). Nigeria A denotes the patient described in this report. The black horizontal line represents the median value.

Previous studies have reported that resistance to artemisinin is mediated by an increase in gene copy number, mutations within the efflux pump of the *P. falciparum* multidrug resistance 1 (*pfmdr1*) gene, or mutations in the calcium transporter *pfATP6* (5, 6). When we examined each gene, using a combination of real-time PCR and DNA sequencing, we found that *pfmdr1* copy number was elevated in this isolate relative to that of the susceptible control strain 3D7. We also observed non-synonymous mutations in both *pfmdr1* (Y184F) and *pfATP6* (A623E, S769N), whereas other implicated residues remained in the wild-type form (7) (Table 2-1). Similar molecular analysis of other representative imported African clinical isolates demonstrated variable mutations for *pfmdr1* and *pfATP6* and copy number in relation to IC₅₀ values for key drugs (Table 2-1). A trend, albeit weak, was observed in which increased *pfmdr1* copy number was correlated with an elevated IC₅₀ to mefloquine ($r = 0.52$) and artemisinin ($r = 0.42$). The presence of an asparagine (N) at position 86 of PfMDR1, when coupled to an elevated *pfmdr1* copy number, appeared to correlate well with reduced susceptibility to artemisinin (Table 2-1). Chavchich *et al.* recently demonstrated that increased *pfmdr1* copy number occurred in a laboratory strain placed under drug selection pressure with artemisinin derivatives (8). However, Imwong *et al.* have indicated that genetic polymorphisms and copy number in *pfmdr1* do not predict treatment outcome with ACT (9).

Table 2-1: Results of sequencing single-nucleotide polymorphisms of *Plasmodium falciparum* isolates.

Strain	Pfmdr1					PfATPase		<i>pfmdr1</i> copy no.	CQ IC ₅₀ , nmol/L	MQ IC ₅₀ , nmol/L	ART IC ₅₀ , nmol/L
	86	184	1034	1042	1246	623	769				
3D7	N	Y	S	N	D	A	S	1.00	6.1	2.1	6.1
W2	Y	Y	S	N	D	A	S	0.97	252	3.2	7.3
Cameroon	Y	F	S	N	D	E	N	1.85	163	7.7	8.07
Congo	Y	F	S	N	D	E	N	1.51	355	10.7	10.9
Kenya	Y	F	S	N	D	E	N	1.75	282	11.7	10.1
Liberia	N	F	S	N	D	E	N	1.65	109	16.2	16.5
Nigeria C	Y	F	S	N	D	E	N	1.06	222	8.7	8.1
Nigeria A	N	F	S	N	D	E	N	1.52	171	16.6	20.1
Nigeria B	Y	F	S	N	D	E	N	1.09	188	5.6	10.0
Ghana	N	F	S	N	D	E	N	0.96	24.0	11.6	14.2
Tanzania	Y	F	S	N	Y	E	N	1.88	381	7.8	16.6
Angola	Y	F	S	N	D	E	N	0.81	258	4.5	7.3

PfMDR1 and PfATP6 residues previously implicated in artemisinin resistance and gene copy number of *pfmdr1* by quantitative real-time PCR in relation to mean IC₅₀ (n = 3) data for key drugs (5, 6, 9). *pfmdr1*, *P. falciparum* multidrug resistance 1; CQ, chloroquine; MQ, mefloquine; ART, artemisinin; IC₅₀, 50% minimum inhibitory concentration; N, asparagine; Y, tyrosine; S, serine; D, aspartic acid; A, alanine; E, glutamic acid; 3D7, chloroquine-sensitive laboratory strain; W2, chloroquine-resistant laboratory strain; Nigeria A, clinical isolate described here. Nigeria B and C, other unrelated clinical isolates from Nigeria.

Findings in the published literature vary in terms of use of artemisinin derivatives for *in vitro* drug susceptibility testing. Jambou *et al.* reported treatment failures with ACT in Cambodia, French Guiana, and Senegal (5). These authors used artemether for testing and showed IC₅₀ values of \approx 30 nmol/L in their “resistant” isolates from Senegal. Noedl *et al.* described treatment failures with ACT in Cambodia, for which IC₅₀ values to dihydroartemisinin were \approx 10 nmol/L (10). Dondorp *et al.* showed IC₅₀ values of 4–6 nmol/L to dihydroartemisinin and 6–8 nmol/L to artesunate in a region of Cambodia and Thailand where ACT treatment failures have occurred (2). Systematic molecular surveillance and standardized drug-testing methods with clinical isolates are required to establish the molecular correlates of reduced susceptibility to antimalarial drugs. In this regard, efforts are ongoing under the auspices of the Worldwide Antimalarial Research Network (11).

The patient’s infection responded to mefloquine when she was back in Canada, possibly because of the high oral dose of mefloquine. Current guidelines from the US Centers for Disease Control and Prevention recommend quinine sulfate plus doxycycline, tetracycline, or clindamycin; or atovaquone-proguanil (Malarone; GlaxoSmithKline, Mississauga, Ontario, Canada) as first- and second-line treatment for uncomplicated *P. falciparum* malaria. Reduced susceptibility to artesunate is more likely to occur when it is associated with inappropriate use of artemisinin derivatives than because of circulating artemisinin-resistant *P. falciparum* in sub-Saharan Africa.

In an effort to achieve consensus that artesunate oral monotherapies should not be marketed, the World Health Organization convened the international pharmaceutical sector in April 2006. At that time, 15 companies agreed to cease manufacturing artesunate monotherapies. However, oral artesunate monotherapies may still be purchased over the counter in malaria-endemic countries, as this report shows. Thus, strains of *P. falciparum* malaria are currently at risk of developing reduced susceptibility to artesunate derivatives.

References

1. Watts G (2011) Use artesunate not quinine to treat severe malaria, say experts. *BMJ* 342:d2590.
2. Dondorp AM, *et al.* (2009) Artemisinin resistance in *Plasmodium falciparum* malaria. *The New England journal of medicine* 361(5):455-467.
3. Bacaner N, Stauffer B, Boulware DR, Walker PF, & Keystone JS (2004) Travel medicine considerations for North American immigrants visiting friends and relatives. *JAMA : the journal of the American Medical Association* 291(23):2856-2864.
4. Johnson JD, *et al.* (2007) Assessment and continued validation of the malaria SYBR green I-based fluorescence assay for use in malaria drug screening. *Antimicrobial agents and chemotherapy* 51(6):1926-1933.
5. Jambou R, *et al.* (2005) Resistance of *Plasmodium falciparum* field isolates to in-vitro artemether and point mutations of the SERCA-type PfATPase6. *Lancet* 366(9501):1960-1963.
6. Price RN, *et al.* (1999) The *pfmdr1* gene is associated with a multidrug-resistant phenotype in *Plasmodium falciparum* from the western border of Thailand. *Antimicrobial agents and chemotherapy* 43(12):2943-2949.
7. Livak KJ & Schmittgen TD (2001) Analysis of relative gene expression data using real-time quantitative PCR and the 2⁻(-Delta Delta C(T)) Method. *Methods* 25(4):402-408.
8. Chavchich M, *et al.* (2010) Role of *pfmdr1* amplification and expression in induction of resistance to artemisinin derivatives in *Plasmodium falciparum*. *Antimicrobial agents and chemotherapy* 54(6):2455-2464.
9. Imwong M, *et al.* (2010) Exploring the contribution of candidate genes to artemisinin resistance in *Plasmodium falciparum*. *Antimicrobial agents and chemotherapy* 54(7):2886-2892.
10. Noedl H, *et al.* (2010) Artemisinin resistance in Cambodia: a clinical trial designed to address an emerging problem in Southeast Asia. *Clinical infectious diseases : an official publication of the Infectious Diseases Society of America* 51(11):e82-89.
11. Plowe CV, *et al.* (2007) World Antimalarial Resistance Network (WARN) III: molecular markers for drug resistant malaria. *Malaria journal* 6:121.

Chapter 3

IDENTIFICATION OF NOVEL AND SELECTIVE PFHSP90 INHIBITORS WITH DRUG POTENTIAL

A major part of this chapter has been published. Reprinted and adapted with permission from:

Shahinas D, Liang M, Datti A, Pillai DR.
J Med Chem. 2010 May 13;53(9):3552-7.
© 2010 American Chemical Society

1 INTRODUCTION

Despite an increased understanding of the pathogenesis and drug targets for malaria, developing new antimalarials remains an expensive, laborious and long process. Different models have been proposed and employed for the discovery of novel antimalarials and chemotherapeutic tools to study malaria (1, 2). The urgent need of developing efficacious, inexpensive and safe drugs has been historically neglected due to lack of profit from the industry and the inexperience of academia for antimalarial drug translation to the clinic. An attractive approach of identifying novel antimalarials is the repurposing approach. First, repurposing approved and abandoned drugs against malaria represents an opportunity to capitalize on existing safety and pharmacokinetic data and experience in order to bypass the initial evaluation of drug bioavailability, metabolic stability, adsorption and excretion. Secondly, regulatory agencies have recently opened new and more rapid paths to approval of repurposed drug therapies (3).

Due to these two incentives, many researchers have adopted the drug repurposing approach and have strategically selected antimalarial targets. One model of drug repurposing is to select drug targets that are present in the host, but sufficient differences are present between the host and the malaria target to account for selectivity. A major advantage of this model is that in most cases, the human host target has been considered as a therapeutic target for other diseases, and a wide spectrum of chemicals are available for repurposing. Studies that have successfully utilized this model have identified targets such as the parasite cysteine proteases and protein farnesyl

transferases. Inhibitors against these parasite targets were repurposed from human cysteine protease cathepsin K treatments for osteoporosis (4, 5) and human farnesyl transferases as treatments for cancer (6).

An alternative model involves the selection of targets from enzymes or pathways that are present in the malaria parasite, but not in humans. The complexity of understanding brand-new proteins as targets is offset by the selectivity of inhibitors to such targets (1, 2). This model is very attractive in cases when the parasite target is found in other microbial organisms for which inhibitors have been generated and are readily available for further development as antiparasitic agents. For example tetracyclines and clindamycin act selectively against prokaryotes and malaria parasites because they target prokaryotic protein synthesis; in malaria, they target the apicoplasts, which are known to have a cyanobacterial origin (7). Another example of important antimalarials that have been identified using this model are the dihydrofolate reductase inhibitors pyrimethamine and proguanil, which are characterized by their high selectivity, but have encountered widespread resistance due to extended periods of monotherapy (8, 9).

An additional model aims to identify the molecular targets for either existing antimalarial drugs that can be chemically modified or the targets of new chemicals that inhibit malarial growth (1, 2). For example, the discovery of the CQ mechanism of action has led to efforts to modify the structure of CQ to generate new antimalarials that inhibit the formation of hemozoin crystals (1, 2). The advantage of this model is the focus on chemoprobes that are known to have antimalarial activity. However, this strategy faces two major challenges: 1) the modification of existing antimalarials with the same mechanism of action facilitates the evolution of resistance due to an existing pool of polymorphisms and mechanism of subversion; and 2) because the inhibitors were not discovered with a specific target in mind, they often have multiple targets or off-site effects. In this case, screening for resistance and elucidating the drug target is extremely difficult.

This study focused on PfHsp90 as a target, not only for the repurposing of inhibitors that have antimalarial activity but also the identification of inhibitors that afford the possibility of developing a synergistic adjunctive therapy with the potential of reversing CQ resistance. Dual targeting of PfHsp90 and one of its clients should provide an effective strategy for the identification of synergistic drug combinations with the potential to circumvent drug resistance. This goal fits with the drug repurposing principles of identifying antimalarial compounds with an

established target by using a pool of existing drugs and inhibitors with characterized safety and bioavailability profiles. Stress-inducible PfHsp90 is unique as a target because Hsp90 regulates the cell cycle, potentiation of drug resistance, and buffering of phenotypic variation; therefore, many Hsp90 clients are essential cellular proteins with pathogenic functions that render the inhibition of the Hsp90 pathway lethal in stressed cells, but not in normal cells (10-15).

Therefore, PfHsp90 inhibitors are expected to target infected cells even though they may target HsHsp90 non-specifically. In the pursuit of PfHsp90 inhibitors in this work, their effect was also tested on HsHsp90, so that parasite specific inhibitors could be identified. The inhibitors were also tested on *Entamoeba histolytica* Hsp90 (EhHsp90), as a target for another prevalent neglected tropical disease.

A robotic high-throughput screen (HTS) was performed using 4000 small molecules from natural compound (Spectrum), pharmacologically active (Lopac), and Food and Drug Administration (FDA)-approved (Prestwick) drug libraries for the competitive inhibition of the ATP-binding (GHKL) domain of PfHsp90. Hits were further screened for specificity according to the differential inhibition of PfHsp90 in comparison to HsHsp90 and EhHsp90. The top EhHsp90 inhibitors showed 30–100% inhibition of *E. histolytica* in culture. PfHsp90-specific inhibitors showed IC₅₀s in the nanomolar range when tested using a cell-based antimalarial validation assay. Three hits, identified as selective PfHsp90 inhibitors in the HTS, also demonstrated synergistic activity in the presence of CQ. These data support PfHsp90 as a specific antimalarial target with the potential for synergy with known antimalarials.

2 MATERIALS AND METHODS

2.1 Cloning and Protein Purification

A *P. falciparum* Hsp90 ATP-binding domain construct was amplified from genomic DNA harvested from the intra-erythrocytic life cycle of *P. falciparum* strain 3D7 (Forward primer: 5' CGCCGGCGCCATATGAGTTTTCCAAG 3' Reverse primer 5' CGCCGGCGCGGATCCTAAATTCATTAATAACT 3') and was cloned into the pET28b vector. The *E. histolytica* Hsp90 ATP-binding domain was also amplified from genomic DNA extracted from a frozen *E. histolytica* culture (Forward primer: 5'CCGGGATCCATGGGAAATAGAAAA3') (Reverse primer: 5'GCGCGGTTTCGAAATATTGAATAAATTC 3') and was cloned into the pET28a vector.

The clones were expressed in BL21 (DE3) CodonPlus cells grown in terrific broth, and induced with 0.4 mM IPTG overnight at 24°C. Cells were harvested by centrifugation, resuspended in lysis buffer (20 mM HEPES, pH 7.5, 10% glycerol, 20 mM imidazole, 500 mM NaCl, 0.5% NP-40) and supplemented with 100x bacterial protease inhibitor cocktail (Sigma). Cells were lysed by sonication. The cell debris was removed by centrifugation, and the protein was purified using Ni-NTA resin (QIAGEN). TEV protease was added at a ratio of 1:50 TEV protease in dialysis buffer (20 mM HEPES, pH 7.5, 100 mM NaCl, 5 mM MgCl₂, and 0.01 mM bis-ANS) and incubated overnight at 4°C. This mixture was washed over a nickel column to remove the TEV protease and cleaved His-tags from the purified protein. The proteins were concentrated to ~10 mg/mL. The same conditions were used for the expression and purification of the HsHsp90 ATP-binding domain. The HsHsp90 ATP binding domain pET15b clone was kindly provided by Dr. Daniel Gewirth (Hauptman-Woodward Medical Research Institute).

2.2 4,40-dianalino-1,10-binaphthyl-5,50-disulfonic acid Dipotassium salt (bis-ANS) Binding Assay with the PfHsp90 ATP-Binding Domain

By optimization of a previously established technique (16), the fluorescent probe 4,40-dianalino-1,10-binaphthyl-5,50-disulfonicacid dipotassium salt (bis-ANS, Sigma-Aldrich) was used to demonstrate nucleotide binding to the GHKL domain of PfHsp90. Recombinant purified protein (final protein concentration 1 μM) was pre-incubated for 45 min at 37°C with no drug or in the

presence of 200 nL of drug to a final concentration of 100 nM (Spectrum and Lopac libraries) and 50 nM (Prestwick library). bis-ANS was then added to a final concentration of 5 μ M in binding buffer (20 mM Tris pH 7.5, 10 mM MgCl₂, 50 mM KCl) in a final volume of 20 μ L and incubated at 37°C for 30 min. In order to facilitate the high throughput screening of 4000 compounds, all these volumes were optimized for robotic handling. The drug distribution was handled using a pintoole that can accurately dispense 200nL volumes, in order to obtain the results at an economical cost of the drug libraries. Fluorescence emission data were collected on an EnVision fluorescent monochromator spectrophotometer (Perkin-Elmer Life Sciences). Excitation wavelength for bis-ANS was set at 372 nm, and emission was captured at 490 nm. All chemical compounds had 99% purity by high performance liquid chromatography (HPLC).

2.3 *P. falciparum* Culture Methods

P. falciparum strains 3D7 and W2 and clinical isolate 208432 (Nigerian isolate described in chapter 2) were grown in RPMI 1640 medium supplemented with 0.25% Albumax II, 2 g/L sodium bicarbonate, 0.1 mM hypoxanthine, 25 mM HEPES (pH 7.5), 50 g/L gentamycin, and human erythrocytes at 37°C, 5% O₂, and 6% CO₂.

2.4 Antimalarial Drug Screening Cell Assay and *in vitro* susceptibility testing

Growth inhibition of *P. falciparum* cultures was quantified using a flow cytometric assay (17). The cultures were synchronized to 0.8% rings and 0.5% hematocrit and cultured in the presence of each of the inhibitors. After a 48 h growth period in the presence or absence of inhibitor, cultures were stained for 1 h at room temperature (RT) with 1 \times SYBR Green in phosphate buffered saline (PBS) solution pH 7.4. Samples were analyzed with a Cytomics FC500 MPL flow cytometer (Beckman Coulter). Uninfected erythrocytes background autofluorescence was minimal. Parasite growth in each sample was determined relative to infected erythrocytes without drug treatment (DMSO vehicle alone). Chloroquine, mefloquine, and artemisinin were used as standardization controls with each assay run. IC₅₀s and fractional IC₅₀s (FIC₅₀) were determined by fitting dose-response curves from duplicates. FIC₅₀ was determined using the formula $IC_{50} (A + \text{fixed } [B]) / IC_{50} \text{ of } A \text{ alone}$, where A and B represent each of the drugs. Average sum FIC₅₀ was determined by the sum of the ratio of the IC₅₀ of each drug in

combination treatments over the IC_{50} of each of the drug administered alone. Synergistic activity was defined by a sum FIC ratio ≤ 0.5 according to previously published definitions (18, 19).

2.5 *Entamoeba histolytica* cultures

Dr. Anjan Debnath at the University of California in San Francisco conducted the *Entamoeba histolytica* culture inhibitor susceptibility experiments. *E. histolytica* trophozoites from the HM1:IMSS strain were maintained in TYI-S-33 medium that was supplemented with penicillin (100 U/mL), streptomycin (100 μ g/mL), and 15% adult bovine serum, under axenic conditions according to the methods of Diamond (20-22). All of the experiments were conducted with trophozoites that had been harvested during the logarithmic phase of growth. Parasite count was monitored to assess the effect of the drugs.

3 RESULTS

3.1 Robotic High Throughput Screen with Recombinant Hsp90 ATP-Binding Domains

The initial screen was based on competitive inhibition of bis-ANS binding with 4000 compounds consisting of natural compounds [Spectrum], FDA approved drugs [Prestwick], and pharmacologically active compounds [Lopac]. 46 compounds were identified that caused a reduction of >70% in fluorescence, suggesting competitive inhibition of PfHsp90 ATP-binding (Figure 3-1a). This threshold was set based on PfHsp90 inhibition by radicicol, a well-known cross-species Hsp90 inhibitor. The 46 small molecules were also screened for competitive inhibition of ATP-binding by the homologous region of HsHsp90 in order to identify compounds that cause selective inhibition of PfHsp90. Differential binding, defined as reduction of 70% in fluorescence for PfHsp90 but no significant reduction for HsHsp90 based on Student's t-test ($p < 0.01$), was observed for three compounds: 2-amino-3-phosphonopropionic acid (Figure 3-1b, compound 1, Pubchem ID 44291306) (APPA) from LOPAC, harmine (harmaline) (Figure 3-1b, compound 2, Pubchem ID 5280953), and acrisorcin (Figure 3-1b, compound 3, Pubchem ID 24144) from SPECTRUM. Of note, no inhibition of fluorescence was observed in the presence of vehicle (DMSO) alone. Screening of the top 46 inhibitors against the EhHsp90 ATP-binding domain showed that 19 of them competitively inhibit this domain by >70% (Table 3-1).

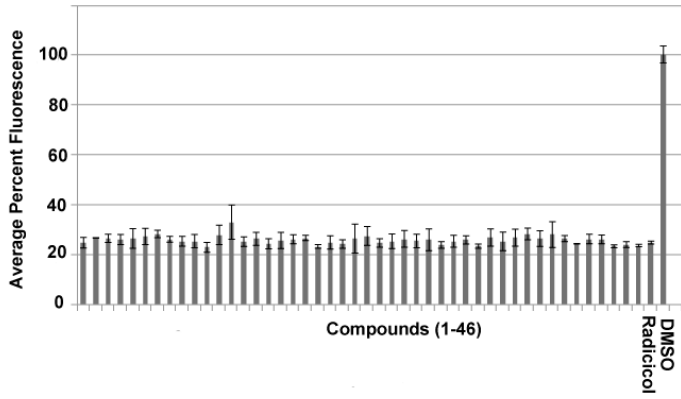
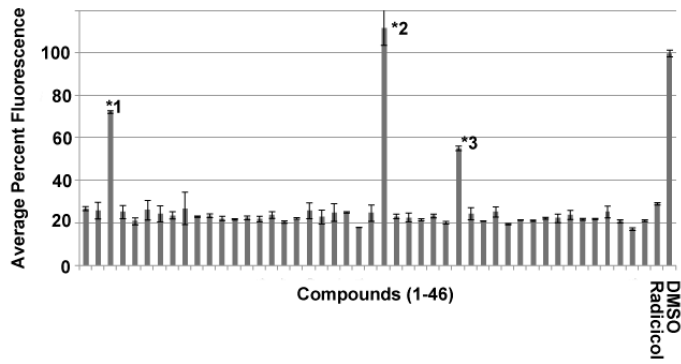
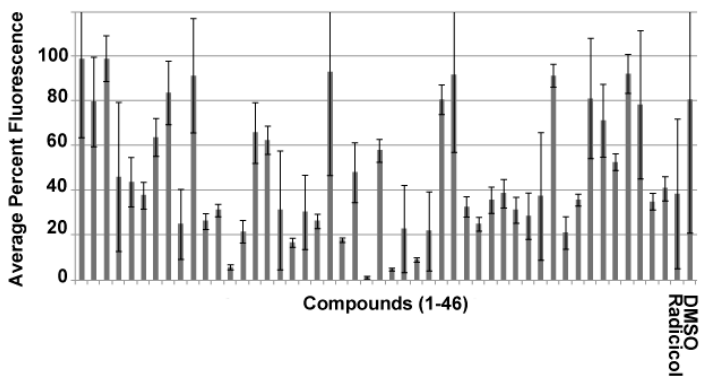
(a)**(b)****(c)**

Figure 3-1: Competitive binding assay using the fluorescent probe bis-ANS for the identification of PfHsp90 specific inhibitors at a screening final concentration of 2.5 μ M. (a) *Plasmodium falciparum* (Pf) Hsp90 ATP-binding domain; (b) human (Hs) Hsp90 ATP-binding domain. (c) *Entamoeba histolytica* (Eh) Hsp90. The asterisk identifies compounds that did not compete with HsHsp90 ATP-binding domain binding. The error bars represent standard deviation of duplicate readings. Inhibition is defined as >70% reduction of fluorescence in this assay.

3.2 EhHsp90 and PfHsp90 inhibitor effect on cell culture

The hits of the protein screen were further tested on standard lab strains of *E. histolytica* and *P. falciparum* cultures. *E. histolytica in vitro* susceptibility testing was performed by Dr. Anjan Debnath at the University of San Francisco in California. 5 out of the 19 EhHsp90 protein hits had activity in culture (Table 3-1) and inhibited *E. histolytica* growth in the range of 30-100%. These five compounds were: rifabutin, rutilantinone, cetylpyridinium chloride, pararosaniline pamoate, and gentian violet.

All 46 hits of the PfHsp90 ATP binding domain screen were tested for susceptibility on the 3D7 strain of *P. falciparum*. Three different concentrations of each drug were tested (Table 3-2): 1.5, 3 and 6 μM . All the inhibitors showed inhibition of malaria growth in infected erythrocytes. The top hits of cell culture inhibition were: karanjin, 1,4-naphthoquinone and quinacrine. The use of the three different concentrations for each of the drugs allowed to determine if a dose-dependent effect of the drugs was present in this concentration range. For these three top hits, comparable high inhibition was observed in all three concentrations suggesting that the IC_{50} lies in the sub-micromolar range. Among the three selective inhibitors of the protein screen, harmaline exhibited the highest growth inhibition potency in this initial *in vitro* screen.

Table 3-1: Summary of inhibition results for the EhHsp90 protein screen and the effect of the inhibitors on *E.histolytica* culture.

Compound	Percent inhibition of fluorescence in protein screen at 2.5μM (%)	Percent inhibition of <i>E.histolytica</i> growth at 25μM (%)
GW5074	70.5	-
Sanguinarine sulfate	71.3	-
Rifabutin	73.7	30
Bilirubin	73.7	-
Clofazimine	73.7	-
Purpurin	75.0	-
Tyrphostin AG 538	75.0	-
Rutilantinone	77.1	100
Rifaximin	78.2	-
Berberine chloride	78.3	-
Chlorophyllide	78.9	-
Amodiaquindihydrochloridedihydrate	82.1	-
Daunorubicin hydrochloride	83.2	-
WB 64 (Malachite Green)	84.9	-
Hycanthone	90.9	-
Mitoxantronedihydrochloride	95.3	-
Cetylpyridinium chloride	95.9	42
Pararosaninepamoate	99.0	81
Gentian Violet	99.3	35

Table 3-2: *In vitro* susceptibility of PfHsp90 high-throughput screen hits. The drugs were tested on intraerythrocytic cell culture of *P.falciparum* 3D7.

Compound	Percent inhibition of <i>P.falciparum</i> growth at 1.5μM (%)	Percent inhibition of <i>P.falciparum</i> growth at 3μM (%)	Percent inhibition of <i>P.falciparum</i> growth at 6μM (%)
Apigenin	24.1	32.9	40.3
3-Amino-1-propanesulfonate	19.1	12.1	40.0
2-Amino-3-phosphonopropionate	21.5	21.8	12.1
Amsacrine hydrochloride	44.4	62.1	66.8
GW5074	0.9	9.1	23.5
Nicardipine hydrochloride	12.9	1.2	1.2
SU4312	0.3	2.6	8.8
WB64	10.9	17.1	11.2
Amodiaquin dihydrochloride	6.2	17.4	27.1
Clofazimine	17.1	14.1	26.8
Quinacrine	74.7	84.4	82.9
Palmatine chloride	73.2	79.1	74.7
Berberine chloride	78.8	77.1	77.4
Methoxy-6-harmalan	18.2	15.6	45.9
Phenazopyridine hydrochloride	32.9	57.6	55.3
Ethaverine hydrochloride	74.1	77.1	77.9

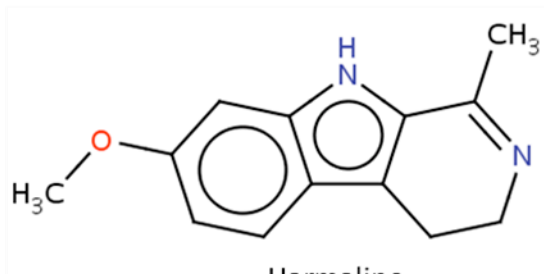
Verteporfin	72.9	70.9	77.1
Rifabutin	15.9	17.4	31.5
N-methyl anthranilate	5.6	25.0	22.6
4,4.-Dimethoxydalbergione	21.8	2.7	20.9
Tyramine	21	2.36	30.6
12a-Hydroxy-9-demethylmunderone-8-carboxylate	23.2	15.6	8.2
Retusoquinone	35.3	17.6	12.1
Xylocarpus A	12.6	11.8	12.3
Harmaline	30	19.4	25.3
1,4-Naphthoquinone	83.5	81.2	76.8
Quinalizarin	28.8	25.6	21.8
Palmatine chloride	73.8	64.1	24.7
Astaxanthin	82.1	77.4	72.1
Rutilantinone	29.4	16.2	14.1
Acrisorcin	26.5	12.9	5.3
4'-Methoxyflavone	76.2	74.7	73.5
Karanjin	99.7	97.1	86.5
Hycanthone	79.1	46.8	28.2
Pararosaniline pamoate	36.8	20.6	7.7
Mitoxantrone dihydrochloride	70.9	72.9	52.9
Rhetsinine	60.3	28.2	4.4
Chloranil	42.6	2.1	2.1
Gingketin	15.3	11.8	17.1

Tetrachloroisophthalonitrile	14.1	12.4	10.6
Rifaximin	10.6	2.9	2.6
Purpurin	65.6	35.3	40.9
Dibenzoylmethane	45.3	36.2	11.8
Chlorophyllide	6.5	3.2	0
Curcumin	2.4	5.0	6.2
Chlormadinone acetate	35.9	6.2	0.3

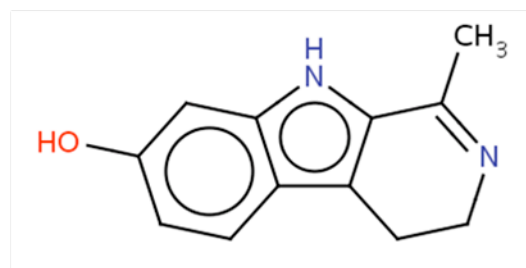
3.3 APPA, Harmine and Acrisorcin show Antimalarial Potency in *P. falciparum* Drug Resistant Strains

The cell-based antimalarial assay relies on fluorescence staining of parasitized erythrocytes. The three small molecules that showed PfHsp90-specific activity were further pursued for antimalarial susceptibility testing in different lines of *P. falciparum* malaria. Because harmaline was not commercially available, the very closely related derivative (harmine) was used. Harmaline contains two extra hydrogen atoms in the heterocyclic amine ring (Figure 3-2).

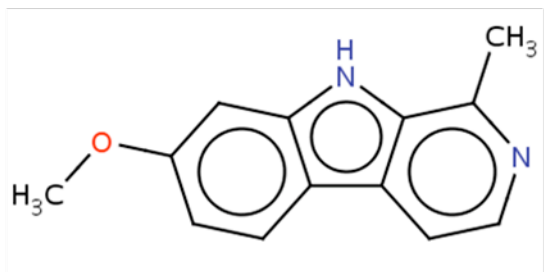
APPA, Harmaline and Acrisorcin demonstrated 50% inhibitory concentrations (IC_{50}) in the nanomolar range (Figure 3-3 and Table 3-3). These compounds also showed similar potency against the chloroquine-resistant strain W2 and the multidrug resistant clinical isolate 208432, which was described in chapter 2 (23).



Harmaline



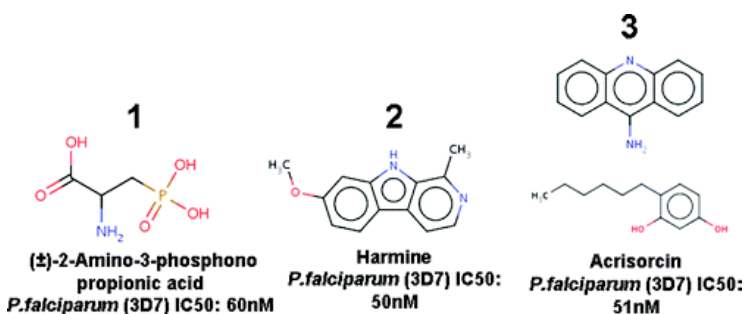
Harmalol



Harmine

Figure 3-2: *Chemical structures of harmine and harmaline.* Harmaline contains two extra hydrogen atoms in the heterocyclic amine ring. As a result, harmine has a markedly lower pKa. Harmalol is a commercially available analog of harmine and harmaline. The affinity of harmalol for the Hsp90 ATP-binding domain is described in chapter 4. These chemical drawings were generated from ChemDB (24).

(a)



(b)

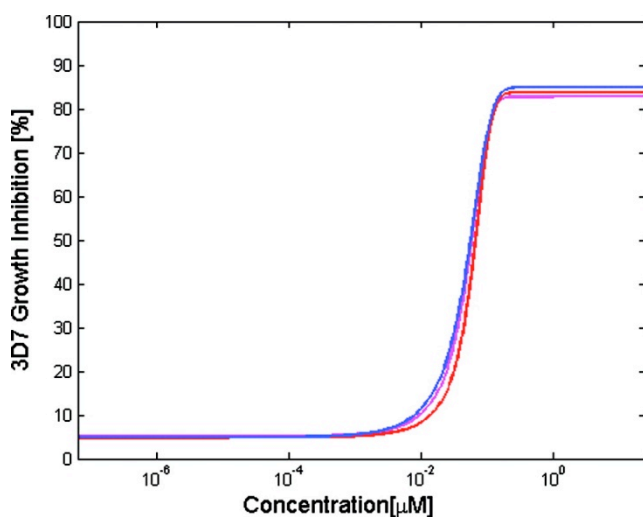


Figure 3-3: Antimalarial activity of APPA (blue), harmine (red), and acrisorcin (pink) using a standard cell-based fluorescence assay. (a) The chemical structure of each of the three selective PfHsp90 inhibitors and the corresponding IC₅₀ value in the 3D7 (drug sensitive) parasite line. (b) Representative IC₅₀ curves are shown for the three specific inhibitors for laboratory strain 3D7. Actual IC₅₀ values in 3D7 and drug resistant parasite lines are summarized in Table 3-3.

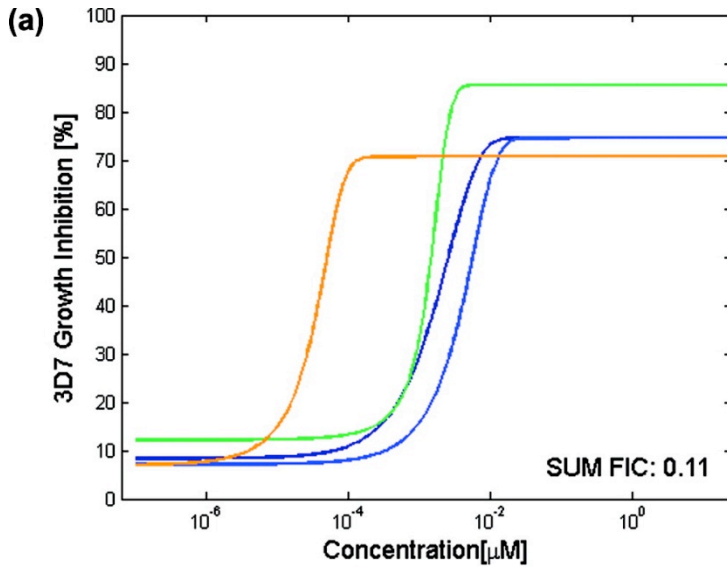
Table 3-3: Summary of Antimalarial Assay IC₅₀ Values for the Inhibitors Identified in This Study When Compared to Known Antimalarials

Compound	IC ₅₀ (μM)		
	3D7	W2	208432
Acrisorcin	0.0513 ± 0.0237	0.3124 ± 0.0156	0.0544 ± 0.0071
APPA	0.0603 ± 0.0145	0.0844 ± 0.0137	0.0471 ± 0.0069
Harmine	0.0501 ± 0.0098	0.0280 ± 0.0054	0.1824 ± 0.0293
Artemisinin	0.0061 ± 0.0014	0.0073 ± 0.0021	0.0683 ± 0.0091
Mefloquine	0.0021 ± 0.0019	0.0032 ± 0.0011	0.0894 ± 0.0134
Chloroquine	0.0046 ± 0.0015	0.2524 ± 0.0542	0.4514 ± 0.0463

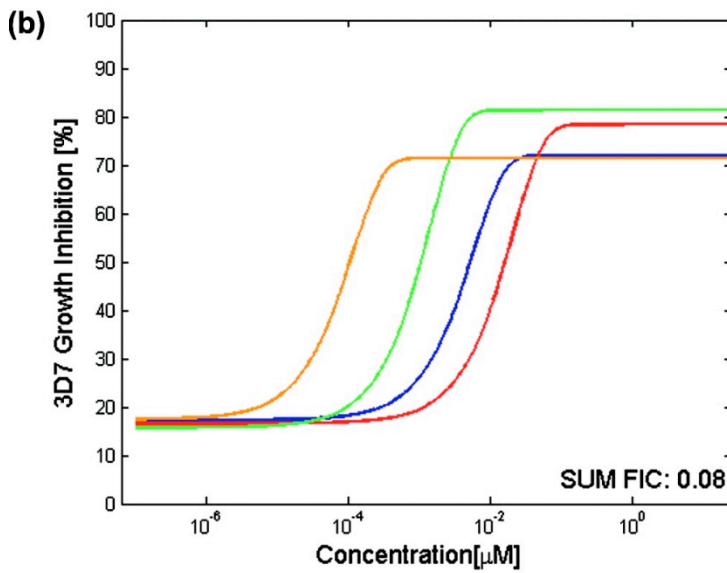
3D7 is a fully susceptible laboratory strain. W2 is a chloroquine-resistant laboratory strain. 208432 is a clinical isolate from a patient with multidrug resistant malaria from West Africa (23). This clinical isolate was described in chapter 2.

3.4 APPA, harmine and acrisorcin act synergistically with chloroquine

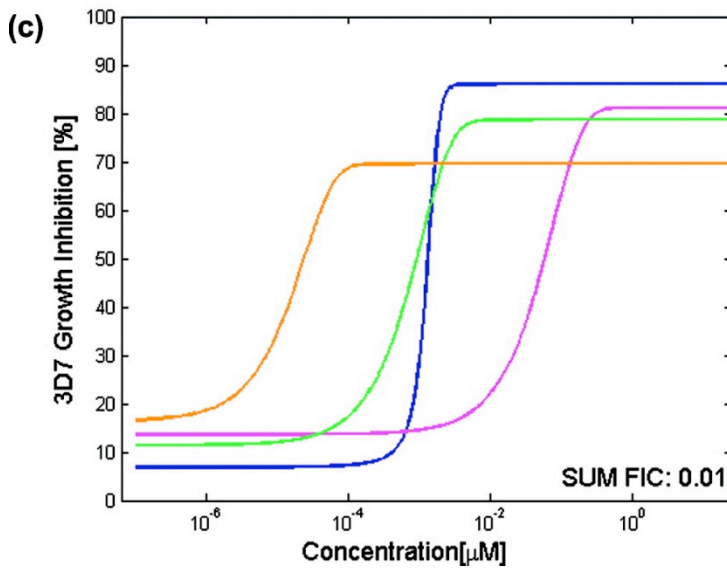
The selective PfHsp90 hits were evaluated for synergy in combination with chloroquine against *P. falciparum* 3D7. Inhibition of growth curves were generated for the synergistic combination of each drug as shown (Figure 3-4). Fractional inhibitory concentration (FIC) ratios were calculated as previously described. APPA, harmine and acrisorcin exhibited FIC ratios of 0.11, 0.08, and 0.01, respectively, in combination with chloroquine. FIC ratios of <0.5 indicate synergistic activity (19, 25).



APPA



Harmine



Acrisorcin

Figure 3-4: *Synergistic activity of APPA (a), harmine (b), and acrisorcin (c) in combination with the known antimalarial chloroquine for laboratory strain 3D7.* The light blue, red and pink lines represent the activity of APPA, harmine and acrisorcin alone. The dark blue line represents the IC₅₀ curve of chloroquine when tested alone. The green line depicts the IC₅₀ curve for the PfHsp90 inhibitor in combination with 0.125pM chloroquine. The orange line depicts the IC₅₀ curve for chloroquine in combination with 1.25pM novel PfHsp90 inhibitor. APPA, harmine and acrisorcin exhibited FIC ratios of 0.11, 0.08, and 0.01, respectively, in combination with chloroquine. FIC ratios of <0.5 indicate synergistic activity (19, 25). A single representative experiment in the 3D7 parasite line is shown.

3.5 Harmine displays synergistic activity with known antimalarials in vitro

The antimalarial potency of harmine, its synergistic activity with chloroquine and previously reported studies showing that harmine and other closely related derivatives are the active ingredients of several traditional herbs used to treat malaria in Mali served as major incentives for further experimentation with this compound to understand its synergistic activity (26, 27). The susceptibility profile of harmine on the *P. falciparum* strains 3D7 and W2 has been summarized in table 3-4. To determine if the synergistic activity of harmine extends to more antimalarials other than chloroquine, several combinations of harmine and artemisinin were tested. Synergistic activity was observed with an average sum FIC of 0.1. To test the hypothesis that harmine is displaying synergistic activity by targeting PfHsp90, the combination of harmine with acrisorcin was tested. As expected, synergistic activity was not observed between harmine and acrisorcin ($\sum\text{FIC}_{50} = 0.75$) (Table 3-4).

Table 3-4: Summary of the results of the effect of harmine and its combinations on *Plasmodium falciparum* cell culture. CQ: chloroquine; ART: artemisinin; ACR: acrisorcin.

3D7 IC50	W2 IC50	SUM FIC with CQ	SUM FIC with ART	SUM FIC with ACR
0.0501±0.0098	0.0280±0.0054	0.08	0.1	0.75

* Concentration of the drugs used to assess SUM FIC: 1.2nM Harmine; 123pM each of the combination drugs. The combination treatments were all tested on the 3D7 line of *P.falciparum*.

4 DISCUSSION

Multidrug resistance is an issue of great concern in malaria. Recent reports demonstrate the emergence of artemisinin-resistant parasites in South East Asia, the last line of pharmacotherapy against this disease (28-30). To identify novel antimalarials, three libraries consisting of natural compounds, FDA-approved drugs, and pharmacologically active compounds consisting of approximately 4000 small molecules were screened using a robotic, protein-based high-throughput screen. Malaria hits were validated using a standard cell-based antimalarial assay and malaria-specific compounds were pursued for susceptibility testing in different lines of *P. falciparum* malaria. Our findings suggest that PfHsp90-specific inhibitors can be identified using this repurposing strategy and the identified inhibitors demonstrate synergistic activity with known antimalarials.

Hsp90 is a hub in several intracellular pathways required for cell survival under stress conditions such as heat shock (31-33). Experiments performed in yeast (13, 34), plants (35), and animal systems (36) support the idea that Hsp90 regulates cell cycle, development, potentiation of drug resistance and buffering of phenotypic variation (37). In fungi, inhibitors of Hsp90 have been able to reverse resistance to existing antifungals (13). Malaria PfHsp90 appears to be induced and translocated to the nucleus upon heat stress at 41°C (31, 38). Indeed, heat shock during hallmark febrile episodes of malaria infection implies that heat shock stress may not only be clinically relevant but also essential to *P. falciparum* growth and survival (31, 32, 38).

The 46 inhibitors of PfHsp90 that were identified from the high throughput screen were structurally diverse and displayed antimalarial activity of varying potencies. Our recombinant Hsp90 ATP-binding domain assay relies on competitive inhibition of bis-ANS which is known to compete with ATP for ATPase domain binding and which emits fluorescence upon hydrophobic pocket binding (16). This suggests that the hit compounds identified here compete for the ATP-binding domain. While the full binding mode has not been fully elucidated for these hits, the Hsp90 ATP-binding domain contains several basic and hydrophobic residues that are characteristic of protein binding pockets that bind structurally diverse compounds (39).

Only 19 out of the 46 compounds inhibited bis-ANS binding of the EhHsp90 ATP binding domain and 43 of the 46 compounds inhibited the HsHsp90 ATP binding domain. This result

suggests that there is sufficient biochemical diversity in this pocket to allow for ortholog selectivity of some of these compounds. The 19 EhHsp90 hits were tested against cultures of *E. histolytica* and 5 of the 19 compounds exhibited inhibitory activity *in vitro*. The other 14 compounds may not have been able to penetrate the surface coat of the trophozoites *in vitro*.

The discovery of five compounds that inhibit *E. histolytica* growth has significant implications for antiparasitic development against amebiasis. Amebiasis caused by *E. histolytica* is responsible for 35-50 million cases of symptomatic disease and about 100,000 deaths per year (40). Parasite cysts are transmitted through contaminated food and water. Currently, nitroimidazoles (metronidazole) are prescribed for treatment, but despite toxic side effects, cure is not reached in 40-60% of the patients (40). Infection occurs after ingestion of cysts and may lead to liver abscess (40, 41). Parasite excystation in the small intestine produces eight trophozoites per cyst, which colonize the large intestine, existing both in the lumen and attached to mucus and epithelial cells (42). Children bear an enormous amount of developmental consequences from infection. An understanding has emerged that not all strains have the same virulence and are capable of causing liver abscess (40). Therefore chaperoning of virulence factors by stress-inducible Hsp90 must be important in this parasite.

The five inhibitors of EhHsp90 with promising activity against the parasite were rifabutin, rutilantinone, cetylpyridinium chloride, pararosanine pamoate, and gentian violet. Rifabutin is a rifamycin-class antibiotic with an ansamycin moiety (43, 44). Ansamycin inhibitors such as GA are well characterized inhibitors of the chaperone activity of Hsp90 (45-47). Both rifamycin and rifabutin have been used widely against mycobacteria (43, 44), but there is no report of their use against amebiasis. Other studies have suggested that rifabutin is effective against cryptosporidiosis (48, 49), another parasitic infectious disease. Rutilantinone is the crystalline form of the antibiotic rutilantin, which has antiphage and antiviral activity (50, 51). Cetylpyridinium chloride is an antiseptic compound that is used in mouthwash and other mouth/throat care products (52-56). Its potent activity has also been reported against the fungal pathogen: *Candida albicans* (57). Pararosanine pamoate has already been used as an antiparasitic drug against schistosomiasis in the Philippines (58). This compound has shown anti-Hsp90 activity in another high throughput screen as well (United States Patent Application 20110263693). Gentian violet is also known as crystal violet and is one of the constituents of the Gram stain used to visualize bacteria (59, 60). 1% solution of gentian violet is reported as an

excellent treatment for *Candida albicans* infections (61). Gentian violet and pararosaniline pamoate are structurally related molecules. In fact, gentian violet is known in the chemical literature as hexamethyl pararosaniline chloride (PubChem).

Three of the 46 compounds, APPA, harmaline (harmine), and acrisorcin, specifically inhibit the PfHsp90 ATP-binding domain when compared to the HsHsp90 ATP-binding domain. Harmine has been used to treat breast cancer cells (62) and has shown effectiveness and low toxicity in single therapy in mice against lung carcinoma (63, 64) and depression (65). APPA is a normal human metabolite found in diverse tissues, such as liver, intestine, and spleen. It has shown pharmacologic activity as a metabotropic glutamate receptor agonist. It is able to block the amyloid precursor protein release evoked by glutamate receptor stimulation in neurons of the cortex and hippocampus, a condition that is believed to produce nerve damage in Alzheimer's disease (66-68). APPA was tested in the Alzheimer's mouse model in which it showed effectivity at 60 nmol (69). Acrisorcin consists of a combination of 9-aminoacridine and 4-hexylresorcinol and has been used for over 40 years as an antifungal agent for the treatment of tinea versicolor, a skin infection that causes discolored patches of skin in humans (70). The active component of acrisorcin, 9-aminoacridine, has previously shown activity in malaria mouse models infected with the mouse pathogens *Plasmodium berghei* and *Plasmodium chabaudi* (71). This class of compounds is recently shown to be effective against the liver stage of malaria, even though the mechanism of action has not been elucidated (Personal communication: Dr. Jane X. Kelly). These three compounds exhibit nanomolar range antimalarial potency against the drug sensitive strain 3D7 and, importantly, to the drug resistant strain W2 and multidrug resistant clinical isolate 208432.

It is important to mention that two of the 46 hits against PfHsp90 are known antimalarials: quinacrine and amodiaquin (a.k.a amodiaquine). Quinacrine is an old antimalarial drug with an unknown mechanism. Extended use of quinacrine in the 1950s and 1960s was associated with a high incidence of female sterility and its use was therefore, discontinued (72). Currently, quinacrine was repurposed against cancer and implicated in Hsp90 targeting (73). Using the screening approach presented here, other non-specific targets of the compounds such as quinacrine cannot be ruled out, particularly in cases where side effects of the compounds exist. However, this approach has been effective in both the identification of PfHsp90 inhibitors that can be further pursued for antimalarial development, as well as in the identification of

compounds with known antimalarial activity, but unknown mechanism of action. Another such compound among the hits is curcumin. Curcumin is a major component of turmeric. It has been recently reported to enhance the activity of histone deacetylase (HDAC) inhibitors by Hsp90 inhibition (74). Curcumin is also thought to inhibit nuclear localization of telomerase by interrupting association of Hsp90 with the co-chaperone p23 (75). Curcumin is synergistic with artemisinin *in vivo* (76, 77). Identification of curcumin in our screen confirms Hsp90 as a target and it also serves as an internal control for the identification of PfHsp90 inhibitors with antimalarial potential.

The need for synergistic antimalarials is paramount, as the parasite inexorably develops resistance to single drug therapy (78). Combination therapy has been widely used for the first line antimalarial artemisinin because single therapy with artemisinins has encountered drug resistance (79-82). The three malaria-specific inhibitors identified in this study exhibited synergistic activity based on sum FIC ratios with the drug combination IC_{50} in the picomolar range. The potential synergy of PfHsp90 inhibitors will serve as a strong basis for combination therapy in human disease. A potential limitation of this study is that our protein-based assay relied on competitive inhibition of ATP-binding rather than inhibition of ATPase activity. Nevertheless, the significant antimalarial effect and the prior use of the candidates identified in this repurposing study for other human conditions taken together make these compounds attractive for further clinical development.

The ideal drugs against malaria should be inexpensive, orally bioavailable, quickly efficacious against drug-resistant malaria and safe to administer in children and pregnant women. Most of the drugs in development require trade-offs among these desired drug features. Most available antimalarials have multiple side effects (Appendix 2), but their use is driven by cost, especially in Africa, where most people must survive on less than USD \$15 per month (1, 2). In fact, in Africa, 75% of the population do not have access to chemical treatments, but have access to traditional medicine for treating fevers (27). Harmine and other closely related derivatives are the active ingredients of several traditional herbs used to treat malaria in Mali (26, 27, 83).

One of these medicinal plants, *Guiera senegalensis*, is a shrub found in the savannah region of West and Central Africa. Its leaves are commonly used in traditional medicine to treat gastrointestinal disorders, respiratory infections, rheumatism and malaria via the preparation of

febrifugal decoctions (83). A synergistic effect was observed between total alkaloids extracted from leaves of *Guiera senegalensis* and the extracts of three other herbal plants. These studies have shown potent *in vitro* antimalarial activity of pure compounds or methanolic fractions isolated from these plants (26, 84). It is often argued that the efficacy of herbal medicines is a result of the combined action of multiple constituents that work synergistically or additively (85). However, the desired effect of the preparations of botanical medicines faces the challenge that the identity and concentration of the chemical components may vary from one preparation to the next (85).

In addition, the use of pure natural compounds instead of crude metabolic extracts is advantageous for more efficacious therapy and to reduce unwanted side effects from other metabolites of no therapeutic benefit. Apart from harman and its derivative beta-carboline alkaloids, the leaf extracts of *G. senegalensis* contain flavonoids, naphthopyrans, tannins, and a naphthyl butanone (guieranone A) (86). Unlike the beta-carboline alkaloids, guieranone A presented high cytotoxicity towards two cancer cell lines and against normal skin fibroblasts (83). Traditionally, *G. senegalensis* is used in synergistic combination with *Mitragyna inermis* to avoid the severity of these side effects (83). The natural selection of these potent synergistic antimalarial metabolites provides an untapped resource for establishing efficacious therapeutic regimens with the pure, natural and low-cost antimalarial compounds coming from herbal medicine.

Although we cannot rule out alternate targets for harmine such as androgen receptors (87), topoisomerase I (88) and DNA excision-repair (89), our data support PfHsp90 as a target for harmine. For example, as shown in Table 3-3, harmine is not synergistic with the other PfHsp90 inhibitor acrisorcin. Harmol (a closely related derivative) is synergistic with pyrvinium pamoate, which has been implicated in androgen receptor inhibition (87) suggesting that harmol and pyrvinium pamoate may have alternate targets. The targeting of PfHsp90 may explain the synergistic effects observed between these beta-carboline analogs and chloroquine. However, it is not clear with the existing body of molecular evidence how the targeting of PfHsp90 may explain the synergistic activity between harmine and chloroquine in both drug sensitive and drug resistant strains of *P. falciparum*. Further efforts to address this question are described in chapter 5.

Additional evidence that suggests that harmine is targeting PfHsp90 comes from the fact that all plant extracts that contain harman and its derivatives inhibit the transition of the early ring stage parasites into trophozoites (27). This is a hallmark phenotype observed with the conventional Hsp90 inhibitor geldanamycin (31, 32). Even though, harman was shown to induce the mRNA, protein and activity levels of the carcinogen-activating enzyme by androgen hydrocarbon receptor (AhR) mediated signaling, it was a weak ligand of AhR (90). In fact, it is quite likely that inhibition of Hsp90 by harman perturbs the regulation of AhR signaling, because harman is reported to decrease the mutagenicity of several polycyclic aromatic hydrocarbons (PAHs) which are known to mediate carcinogenesis using AhR mediated signaling (90, 91). In the inactive form, AhR is bound to Hsp90 and the co-chaperone p23. Upon ligand binding (such as binding by PAHs), AhR gets activated and translocated to the nucleus (91).

Genotoxic, mutagenic and cytotoxic activities of the closely related derivatives harman, harmine and harmalol as evaluated by the Salmonella Ames test, SOS chromotest and micronucleus test suggest that harman induced SOS functions, but the dihydrobeta-carbolines (harmine and harmalol) were not genotoxic in any microorganisms (89). Evaluation of the cytotoxicity of these alkaloids on THP1 cells showed that the LC_{50} was 20-40 \times higher than the IC_{50} observed for antimalarial activity (26).

Local access to alleviating treatments is important in Africa, in particular if the combination of chloroquine with traditional medicine is an option, especially if harmine can be purified from local extracts as suggested by Ancolio *et al* (26). Indeed in Mali, sometimes patients empirically combine chloroquine with traditional medicines (27). Treatment options are limited in endemic regions and novel therapeutic strategies are required. In traditional societies, the combination of a natural product from the native environment with the known antimalarial chloroquine may be more widely accepted than a novel chemical therapy.

References

1. Fidock DA (2010) Drug discovery: Priming the antimalarial pipeline. *Nature* 465(7296):297-298.
2. Fidock DA, Rosenthal PJ, Croft SL, Brun R, & Nwaka S (2004) Antimalarial drug discovery: efficacy models for compound screening. *Nature reviews. Drug discovery* 3(6):509-520.
3. Weir SJ, Degennaro LJ, & Austin CP (2012) Repurposing Approved and Abandoned Drugs for the Treatment and Prevention of Cancer through Public-Private Partnerships. *Cancer research*.
4. Rosenthal PJ (2004) Cysteine proteases of malaria parasites. *International journal for parasitology* 34(13-14):1489-1499.
5. Rosenthal PJ, Sijwali PS, Singh A, & Shenai BR (2002) Cysteine proteases of malaria parasites: targets for chemotherapy. *Current pharmaceutical design* 8(18):1659-1672.
6. Chakrabarti D, *et al.* (2002) Protein farnesyltransferase and protein prenylation in *Plasmodium falciparum*. *The Journal of biological chemistry* 277(44):42066-42073.
7. Ralph SA, D'Ombrain MC, & McFadden GI (2001) The apicoplast as an antimalarial drug target. *Drug resistance updates : reviews and commentaries in antimicrobial and anticancer chemotherapy* 4(3):145-151.
8. Sridaran S, *et al.* (2010) Anti-folate drug resistance in Africa: meta-analysis of reported dihydrofolate reductase (dhfr) and dihydropteroate synthase (dhps) mutant genotype frequencies in African *Plasmodium falciparum* parasite populations. *Malaria journal* 9:247.
9. Barnadas C, *et al.* (2009) High prevalence and fixation of *Plasmodium vivax* dhfr/dhps mutations related to sulfadoxine/pyrimethamine resistance in French Guiana. *The American journal of tropical medicine and hygiene* 81(1):19-22.
10. Cerchiatti LC, *et al.* (2010) BCL6 repression of EP300 in human diffuse large B cell lymphoma cells provides a basis for rational combinatorial therapy. *The Journal of clinical investigation*.
11. Cerchiatti LC, *et al.* (2009) A purine scaffold Hsp90 inhibitor destabilizes BCL-6 and has specific antitumor activity in BCL-6-dependent B cell lymphomas. *Nature medicine* 15(12):1369-1376.
12. Chiosis G, Caldas Lopes E, & Solit D (2006) Heat shock protein-90 inhibitors: a chronicle from geldanamycin to today's agents. *Curr Opin Investig Drugs* 7(6):534-541.
13. Cowen LE & Lindquist S (2005) Hsp90 potentiates the rapid evolution of new traits: drug resistance in diverse fungi. *Science* 309(5744):2185-2189.
14. Cowen LE, *et al.* (2009) Harnessing Hsp90 function as a powerful, broadly effective therapeutic strategy for fungal infectious disease. *Proceedings of the National Academy of Sciences of the United States of America* 106(8):2818-2823.
15. Taldone T, *et al.* (2010) Assay strategies for the discovery and validation of therapeutics targeting *Brugia pahangi* Hsp90. *PLoS neglected tropical diseases* 4(6):e714.

16. Wassenberg JJ, Reed RC, & Nicchitta CV (2000) Ligand interactions in the adenosine nucleotide-binding domain of the Hsp90 chaperone, GRP94. II. Ligand-mediated activation of GRP94 molecular chaperone and peptide binding activity. *The Journal of biological chemistry* 275(30):22806-22814.
17. Johnson JD, *et al.* (2007) Assessment and continued validation of the malaria SYBR green I-based fluorescence assay for use in malaria drug screening. *Antimicrobial agents and chemotherapy* 51(6):1926-1933.
18. Mishra LC, Bhattacharya A, & Bhasin VK (2007) Antiplasmodial interactions between artemisinin and triclosan or ketoconazole combinations against blood stages of *Plasmodium falciparum* in vitro. *The American journal of tropical medicine and hygiene* 76(3):497-501.
19. Pereira MR, *et al.* (2011) In vivo and in vitro antimalarial properties of azithromycin-chloroquine combinations that include the resistance reversal agent amlodipine. *Antimicrobial agents and chemotherapy* 55(7):3115-3124.
20. Debnath A, Akbar MA, Mazumder A, Kumar S, & Das P (2005) *Entamoeba histolytica*: Characterization of human collagen type I and Ca²⁺ activated differentially expressed genes. *Experimental parasitology* 110(3):214-219.
21. Debnath A, Das P, Sajid M, & McKerrow JH (2004) Identification of genomic responses to collagen binding by trophozoites of *Entamoeba histolytica*. *The Journal of infectious diseases* 190(3):448-457.
22. Diamond LS, Harlow DR, & Cunnick CC (1978) A new medium for the axenic cultivation of *Entamoeba histolytica* and other *Entamoeba*. *Transactions of the Royal Society of Tropical Medicine and Hygiene* 72(4):431-432.
23. Shahinas D, Lau R, Khairnar K, Hancock D, & Pillai DR (2010) Artesunate misuse and *Plasmodium falciparum* malaria in traveler returning from Africa. *Emerging infectious diseases* 16(10):1608-1610.
24. Chen J, Swamidass SJ, Dou Y, Bruand J, & Baldi P (2005) ChemDB: a public database of small molecules and related chemoinformatics resources. *Bioinformatics* 21(22):4133-4139.
25. Mishra S, Karmodiya K, Parasuraman P, Surolia A, & Surolia N (2008) Design, synthesis, and application of novel triclosan prodrugs as potential antimalarial and antibacterial agents. *Bioorganic & medicinal chemistry* 16(10):5536-5546.
26. Ancolio C, *et al.* (2002) Antimalarial activity of extracts and alkaloids isolated from six plants used in traditional medicine in Mali and Sao Tome. *Phytotherapy research : PTR* 16(7):646-649.
27. Azas N, *et al.* (2002) Synergistic in vitro antimalarial activity of plant extracts used as traditional herbal remedies in Mali. *Parasitology research* 88(2):165-171.
28. Mok S, *et al.* (2011) Artemisinin resistance in *Plasmodium falciparum* is associated with an altered temporal pattern of transcription. *BMC genomics* 12:391.
29. Dondorp AM, *et al.* (2010) Artemisinin resistance: current status and scenarios for containment. *Nature reviews. Microbiology* 8(4):272-280.

30. Dondorp AM, *et al.* (2009) Artemisinin resistance in *Plasmodium falciparum* malaria. *The New England journal of medicine* 361(5):455-467.
31. Banumathy G, Singh V, Pavithra SR, & Tatu U (2003) Heat shock protein 90 function is essential for *Plasmodium falciparum* growth in human erythrocytes. *The Journal of biological chemistry* 278(20):18336-18345.
32. Pavithra SR, Banumathy G, Joy O, Singh V, & Tatu U (2004) Recurrent fever promotes *Plasmodium falciparum* development in human erythrocytes. *The Journal of biological chemistry* 279(45):46692-46699.
33. Pavithra SR, Kumar R, & Tatu U (2007) Systems analysis of chaperone networks in the malarial parasite *Plasmodium falciparum*. *PLoS computational biology* 3(9):1701-1715.
34. Chang HC & Lindquist S (1994) Conservation of Hsp90 macromolecular complexes in *Saccharomyces cerevisiae*. *The Journal of biological chemistry* 269(40):24983-24988.
35. Queitsch C, Sangster TA, & Lindquist S (2002) Hsp90 as a capacitor of phenotypic variation. *Nature* 417(6889):618-624.
36. Birnby DA, *et al.* (2000) A transmembrane guanylyl cyclase (DAF-11) and Hsp90 (DAF-21) regulate a common set of chemosensory behaviors in *Caenorhabditis elegans*. *Genetics* 155(1):85-104.
37. Rutherford SL & Lindquist S (1998) Hsp90 as a capacitor for morphological evolution. *Nature* 396(6709):336-342.
38. Acharya P, Kumar R, & Tatu U (2007) Chaperoning a cellular upheaval in malaria: heat shock proteins in *Plasmodium falciparum*. *Molecular and biochemical parasitology* 153(2):85-94.
39. Dutta R & Inouye M (2000) GHKL, an emergent ATPase/kinase superfamily. *Trends in biochemical sciences* 25(1):24-28.
40. Ralston KS & Petri WA, Jr. (2011) Tissue destruction and invasion by *Entamoeba histolytica*. *Trends in parasitology* 27(6):254-263.
41. Ralston KS & Petri WA (2011) The ways of a killer: how does *Entamoeba histolytica* elicit host cell death? *Essays in biochemistry* 51:193-210.
42. Petri WA, Jr., Haque R, & Mann BJ (2002) The bittersweet interface of parasite and host: lectin-carbohydrate interactions during human invasion by the parasite *Entamoeba histolytica*. *Annual review of microbiology* 56:39-64.
43. O'Brien RJ, Geiter LJ, & Lyle MA (1990) Rifabutin (ansamycin LM427) for the treatment of pulmonary *Mycobacterium avium* complex. *The American review of respiratory disease* 141(4 Pt 1):821-826.
44. O'Brien RJ, Lyle MA, & Snider DE, Jr. (1987) Rifabutin (ansamycin LM 427): a new rifamycin-S derivative for the treatment of mycobacterial diseases. *Reviews of infectious diseases* 9(3):519-530.
45. Porter JR, Ge J, Lee J, Normant E, & West K (2009) Ansamycin inhibitors of Hsp90: nature's prototype for anti-chaperone therapy. *Current topics in medicinal chemistry* 9(15):1386-1418.

46. Onuoha SC, *et al.* (2007) Mechanistic studies on Hsp90 inhibition by ansamycin derivatives. *Journal of molecular biology* 372(2):287-297.
47. Bohlen SP (1998) Genetic and biochemical analysis of p23 and ansamycin antibiotics in the function of Hsp90-dependent signaling proteins. *Molecular and cellular biology* 18(6):3330-3339.
48. Fichtenbaum CJ, Zackin R, Feinberg J, Benson C, & Griffiths JK (2000) Rifabutin but not clarithromycin prevents cryptosporidiosis in persons with advanced HIV infection. *AIDS* 14(18):2889-2893.
49. Holmberg SD, *et al.* (1998) Possible effectiveness of clarithromycin and rifabutin for cryptosporidiosis chemoprophylaxis in HIV disease. HIV Outpatient Study (HOPS) Investigators. *JAMA : the journal of the American Medical Association* 279(5):384-386.
50. Hume V, Westwood JC, & Appleyard G (1965) The Anti-Viral Action of Rutilantin A. *Journal of general microbiology* 38:143-151.
51. Asheshov IN & Gordon JJ (1961) Rutilantin: an antibiotic substance with antiphage activity. *The Biochemical journal* 81:101-104.
52. Rioboo M, *et al.* (2011) Clinical and microbiological efficacy of an antimicrobial mouth rinse containing 0.05% cetylpyridinium chloride in patients with gingivitis. *International journal of dental hygiene*.
53. Herrera D (2009) Cetylpyridinium chloride-containing mouth rinses and plaque control. *Evidence-based dentistry* 10(2):44.
54. Gunsolley JC (2008) Uncontrolled randomized clinical trial demonstrates similar long-term (6 months) antigingivitis and antiplaque efficacy for 2 mouth rinses: one that uses cetylpyridinium chloride (CPC) as an active agent and the other that uses essential oils (EO) as an active agent. *The journal of evidence-based dental practice* 8(2):85-86.
55. Herrera D, *et al.* (2005) Efficacy of a 0.15% benzydamine hydrochloride and 0.05% cetylpyridinium chloride mouth rinse on 4-day de novo plaque formation. *Journal of clinical periodontology* 32(6):595-603.
56. Sheen S, Eisenburger M, & Addy M (2003) Effect of toothpaste on the plaque inhibitory properties of a cetylpyridinium chloride mouth rinse. *Journal of clinical periodontology* 30(3):255-260.
57. Jones DS, Schep LJ, & Shepherd MG (1995) The effect of cetylpyridinium chloride (CPC) on the cell surface hydrophobicity and adherence of *Candida albicans* to human buccal epithelial cells in vitro. *Pharmaceutical research* 12(12):1896-1900.
58. Pesigan TP, Banzon TC, Santos AT, Nosenas J, & Zabala RG (1967) Pararosanine pamoate (CI-403-A) in the treatment of *Schistosoma japonicum* infection in the Philippines. *Bulletin of the World Health Organization* 36(2):263-274.
59. Saji M, Taguchi S, Shikida R, & Ohkuni H (1994) [Bactericidal effects of gentian violet (Gv) and acrinol (Ac) against methicillin-resistant *Staphylococcus aureus* (MRSA) and gram-negative bacteria isolated from clinical materials]. *Kansenshogaku zasshi. The Journal of the Japanese Association for Infectious Diseases* 68(10):1287-1289.

60. Berberovic M (1953) [Triphenyl methane dyes (brilliant green and crystal violet) as substitution for gentian violet in bacterial staining according to Gram]. *Higijena; casopis za higijenu, mikrobiologiju, epidemiologiju i sanitarnu tehniku* 5(6):415-418.
61. Traboulsi RS, *et al.* (2011) Gentian violet exhibits activity against biofilms formed by oral *Candida* isolates obtained from HIV-infected patients. *Antimicrobial agents and chemotherapy* 55(6):3043-3045.
62. Ma Y & Wink M (2010) The beta-carboline alkaloid harmine inhibits BCRP and can reverse resistance to the anticancer drugs mitoxantrone and camptothecin in breast cancer cells. *Phytotherapy research : PTR* 24(1):146-149.
63. Abe A, Yamada H, Moriya S, & Miyazawa K (2011) The beta-carboline alkaloid harmol induces cell death via autophagy but not apoptosis in human non-small cell lung cancer A549 cells. *Biological & pharmaceutical bulletin* 34(8):1264-1272.
64. Abe A & Yamada H (2009) Harmol induces apoptosis by caspase-8 activation independently of Fas/Fas ligand interaction in human lung carcinoma H596 cells. *Anti-cancer drugs* 20(5):373-381.
65. Fortunato JJ, *et al.* (2009) Acute harmine administration induces antidepressive-like effects and increases BDNF levels in the rat hippocampus. *Progress in neuro-psychopharmacology & biological psychiatry* 33(8):1425-1430.
66. Wishart DS, *et al.* (2009) HMDB: a knowledgebase for the human metabolome. *Nucleic acids research* 37(Database issue):D603-610.
67. Wishart DS (2007) Human Metabolome Database: completing the 'human parts list'. *Pharmacogenomics* 8(7):683-686.
68. Wishart DS, *et al.* (2007) HMDB: the Human Metabolome Database. *Nucleic acids research* 35(Database issue):D521-526.
69. Cahusac PM & Mavulati SC (2009) Non-competitive metabotropic glutamate 1 receptor antagonists block activity of slowly adapting type I mechanoreceptor units in the rat sinus hair follicle. *Neuroscience* 163(3):933-941.
70. Nierman MM (1961) Akrinol, a new topical anti-infective agent. *The Journal of the Indiana State Medical Association* 54:614-617.
71. Gemma S, *et al.* (2009) Combining 4-aminoquinoline- and clotrimazole-based pharmacophores toward innovative and potent hybrid antimalarials. *Journal of medicinal chemistry* 52(2):502-513.
72. Bhatt RV, Aparicio A, Laufe LE, Parmley T, & King TM (1980) Quinacrine-induced pathologic changes in the fallopian tube. *Fertility and sterility* 33(6):666-667.
73. Neznanov N, *et al.* (2009) Anti-malaria drug blocks proteotoxic stress response: anti-cancer implications. *Cell Cycle* 8(23):3960-3970.
74. Giommarelli C, *et al.* (2010) The enhancement of antiproliferative and proapoptotic activity of HDAC inhibitors by curcumin is mediated by Hsp90 inhibition. *Cellular and molecular life sciences : CMLS* 67(6):995-1004.
75. Lee JH & Chung IK (2010) Curcumin inhibits nuclear localization of telomerase by dissociating the Hsp90 co-chaperone p23 from hTERT. *Cancer letters* 290(1):76-86.

76. Martinelli A, Rodrigues LA, & Cravo P (2008) Plasmodium chabaudi: efficacy of artemisinin + curcumin combination treatment on a clone selected for artemisinin resistance in mice. *Experimental parasitology* 119(2):304-307.
77. Nandakumar DN, Nagaraj VA, Vathsala PG, Rangarajan P, & Padmanaban G (2006) Curcumin-artemisinin combination therapy for malaria. *Antimicrobial agents and chemotherapy* 50(5):1859-1860.
78. Fidock DA, Eastman RT, Ward SA, & Meshnick SR (2008) Recent highlights in antimalarial drug resistance and chemotherapy research. *Trends in parasitology* 24(12):537-544.
79. Noedl H, Socheat D, & Satimai W (2009) Artemisinin-resistant malaria in Asia. *The New England journal of medicine* 361(5):540-541.
80. Noedl H, *et al.* (2008) Evidence of artemisinin-resistant malaria in western Cambodia. *The New England journal of medicine* 359(24):2619-2620.
81. Price RN & Douglas NM (2009) Artemisinin combination therapy for malaria: beyond good efficacy. *Clinical infectious diseases : an official publication of the Infectious Diseases Society of America* 49(11):1638-1640.
82. Dahlstrom S, *et al.* (2009) Plasmodium falciparum multidrug resistance protein 1 and artemisinin-based combination therapy in Africa. *The Journal of infectious diseases* 200(9):1456-1464.
83. Fiot J, *et al.* (2006) Phytochemical and pharmacological study of roots and leaves of Guiera senegalensis J.F. Gmel (Combretaceae). *Journal of ethnopharmacology* 106(2):173-178.
84. Traore-Keita F, *et al.* (2000) Antimalarial activity of four plants used in traditional medicine in Mali. *Phytotherapy research : PTR* 14(1):45-47.
85. Junio HA, *et al.* (2011) Synergy-directed fractionation of botanical medicines: a case study with goldenseal (Hydrastis canadensis). *Journal of natural products* 74(7):1621-1629.
86. Benoit F, *et al.* (1996) In vitro antimalarial activity of vegetal extracts used in West African traditional medicine. *The American journal of tropical medicine and hygiene* 54(1):67-71.
87. Jones JO, *et al.* (2009) Non-competitive androgen receptor inhibition in vitro and in vivo. *Proceedings of the National Academy of Sciences of the United States of America* 106(17):7233-7238.
88. Funayama Y, *et al.* (1996) Effects of beta- and gamma-carboline derivatives of DNA topoisomerase activities. *Mutation research* 349(2):183-191.
89. Picada JN, da Silva KV, Erdtmann B, Henriques AT, & Henriques JA (1997) Genotoxic effects of structurally related beta-carboline alkaloids. *Mutation research* 379(2):135-149.
90. El Gendy MA & El-Kadi AO (2010) Harman induces CYP1A1 enzyme through an aryl hydrocarbon receptor mechanism. *Toxicology and applied pharmacology* 249(1):55-64.

91. Denison MS & Nagy SR (2003) Activation of the aryl hydrocarbon receptor by structurally diverse exogenous and endogenous chemicals. *Annual review of pharmacology and toxicology* 43:309-334.

Chapter 4

BIOCHEMICAL CHARACTERIZATION OF *PLASMODIUM FALCIPARUM* HEAT SHOCK PROTEIN 90

1 INTRODUCTION

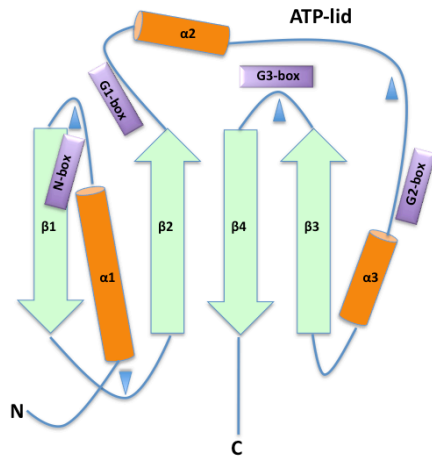
As mentioned in the first chapter, PfHsp90 (or PfHsp86 PF07_0029) is essential for the development of the parasite during the intra-erythrocytic cycle and is the only cytosolic paralog with an EEVD motif at the C-terminus (1-3). Significant similarities exist at the NH₂-terminal nucleotide-binding domain (also known as the GHKL domain) in the central acidic hinge region as well as at the COOH-terminal substrate-binding domain between other eukaryotic Hsp90 and PfHsp90 molecules (4). PfHsp90 complexes play an important role in the life cycle of the parasite (2, 5, 6). Inhibition of the function of PfHsp90 using GA arrests parasite development between the ring and trophozoite stages during the intra-erythrocytic cycle (3). Analysis of PfHsp90 function in the parasite has revealed its essential role in the regulation of parasite development following heat shock (3). The focus of this chapter is on the further characterization of PfHsp90 as a selective drug target against malaria. The emphasis is, in particular, on the N-terminal ATP binding domain, which is classified as a GHKL ATPase domain.

The conventional core structure of the GHKL ATPase domain consists of 4 open parallel β sheets surrounded by 2 α -helices on each side (7) (Figure 4-1). Proteins such as adenylate kinase, elongation factor Tu, and p21 contain a conventional GHKL ATPase domain (7). Proteins such as Hsp90, DNA gyrase B, and the DNA mismatch repair protein MutL are characterized by a unique Bergerat fold at the ATP-binding domain, which consists of an α/β sandwich structure and a unique long flexible ATP lid (L4) (Figure 4-1) (7, 8). The residues make contact with the ATP cluster in the highly conserved surface loops that connect the Bergerat fold elements. The only exception is the N-box because the ATP contact residues lie in the α 1 helix in this motif. The conserved asparagine residue of the N-box coordinates a bound Mg²⁺ ion that connects all the phosphates of ATP to the protein through solvent-mediated hydrogen bonds. A conserved aspartate residue in box G1 interacts directly with ATP and forms a hydrogen bond. Conserved

glycines in the G1 and G2 boxes form the 2 hinges that confer flexibility of movement to the ATP lid domain (7, 8).

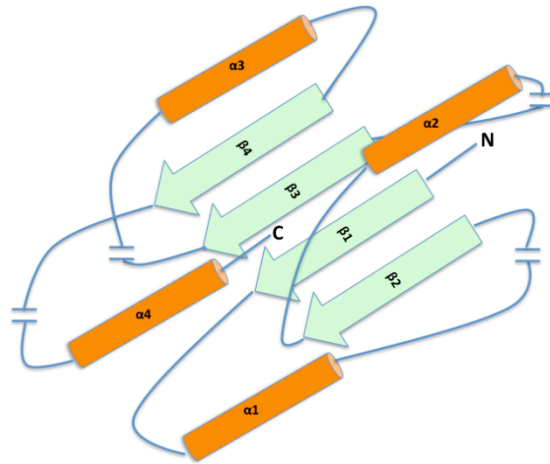
Even though a high degree of resemblance exists in topology among the nucleotide-binding domains of Bergerat fold family members, there are several features of the ATP lid domain that distinguish them (Figure 4-2) (7). In GyrB, the ATP lid is very long and completely encloses the bound nucleotide. In MutL, the loop is broken in the middle by a short α -helix, which leaves the bound adenine partially exposed to the solvent. Hsp90 has 2 short α -helices in the loop structure that do not allow the ATP lid domain to close. The histidine kinase EnvZ also has an ATP lid that is extended away from the rest of the molecule, completely exposing the bound nucleotide; however, it contains a conserved histidine kinase F-box domain in the loop region instead of the 2 short α -helices present in Hsp90 (7). In conjunction with these differences, the ATP lid of Hsp90 is considerably longer, consisting of 25 residues compared to the average of 17 (7).

(a)



BERGERAT FOLD

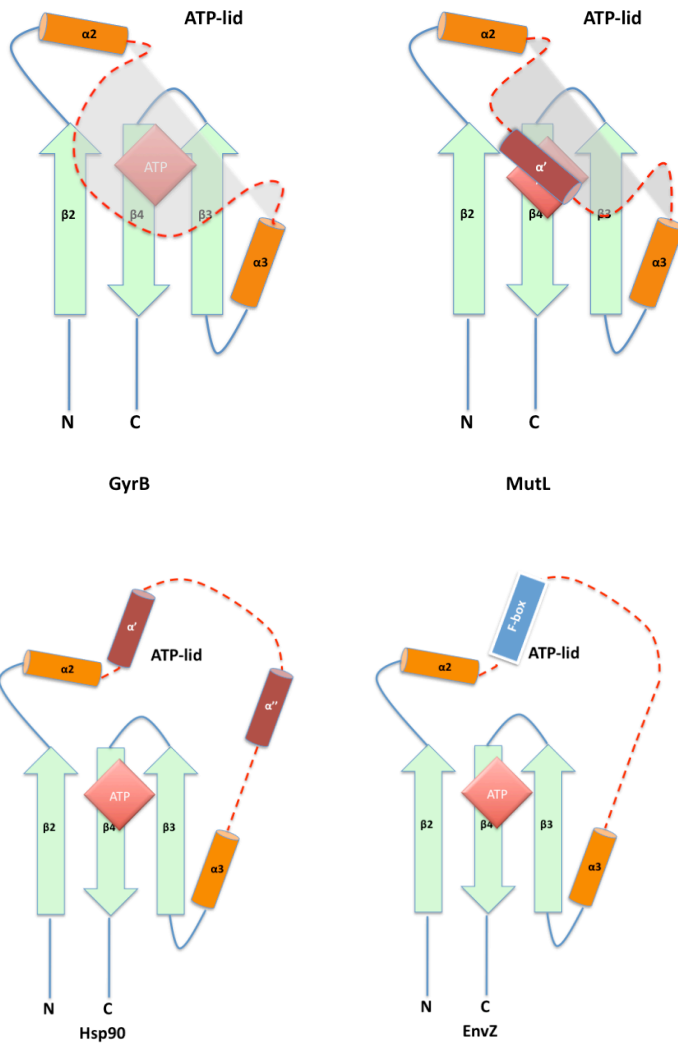
(b)



CONVENTIONAL FOLD

Figure 4-1: An illustration of the differences between a conventional GHKL domain and the ATP-binding Bergerat fold domain. The nucleotide binding site in this domain is located at the interface between the N- and C- terminals. (a) Bergerat fold unique features. The most representative feature of this domain is the ATP-lid loop (L4). The purple boxes represent the conserved motifs that are characteristic of the Bergerat fold. The blue triangles represent regions of structural variation among different members of the Bergerat fold family. (b) An illustration of the topology of a conventional nucleotide binding fold found in kinases and other ATPase domain containing proteins. The breaks indicate points in the surface loops where extra peptide segments may be inserted. The illustration has been adapted and redrawn from Dutta and Inouye (7).

(a)



(b)

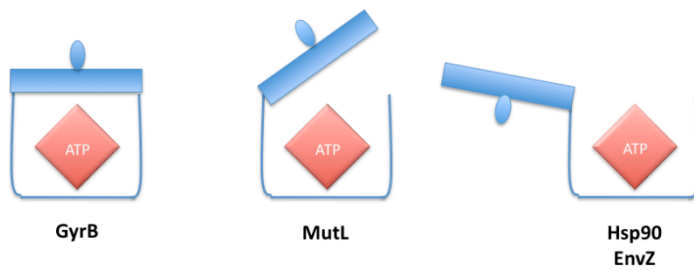


Figure 4-2: *Illustration of the topology features that distinguish different members of the Bergerat fold family of GHKL ATPases.* (a) The composition and conformation of the ATP-lid domain is the most unique feature. This domain is a long loop in GyrB that folds to close the ATP binding domain. The insertion of a short helix in the loop domain of MutL does not allow for complete closure of the lid leaving the bound nucleotide partially exposed. Hsp90 has two helices inserted in the ATP-lid loop. The bound nucleotide is therefore, completely exposed to solution. Even though, EnvZ and Hsp90 have the same degree of openness of the lid domain, they can be distinguished by the insertion of a histidine kinase domain known as the F-box in EnvZ. (b) An illustration of the different conformations and degree of openness of the ATP-lid among the different members of the Bergerat fold protein family. This figure has been adapted and redrawn from Dutta and Inouye (7).

MutL, Hsp90, and EnvZ exist as homodimers in solution, while GyrB exists as a tetramer. Nucleotide binding induces an intermolecular interaction causing the ATP-binding domains of these proteins to dimerize (Figure 4-3). The pocket created within the clamp has been proposed to accommodate the length of double-stranded DNA in the case of GyrB and MutL or the unfolded peptide in Hsp90 (7). Differences in the ATP lid domain have functional implications for the different substrates that these Bergerat fold family proteins accept (e.g., DNA versus unfolded peptides); therefore, selective inhibitors of each target molecule potentially exist.

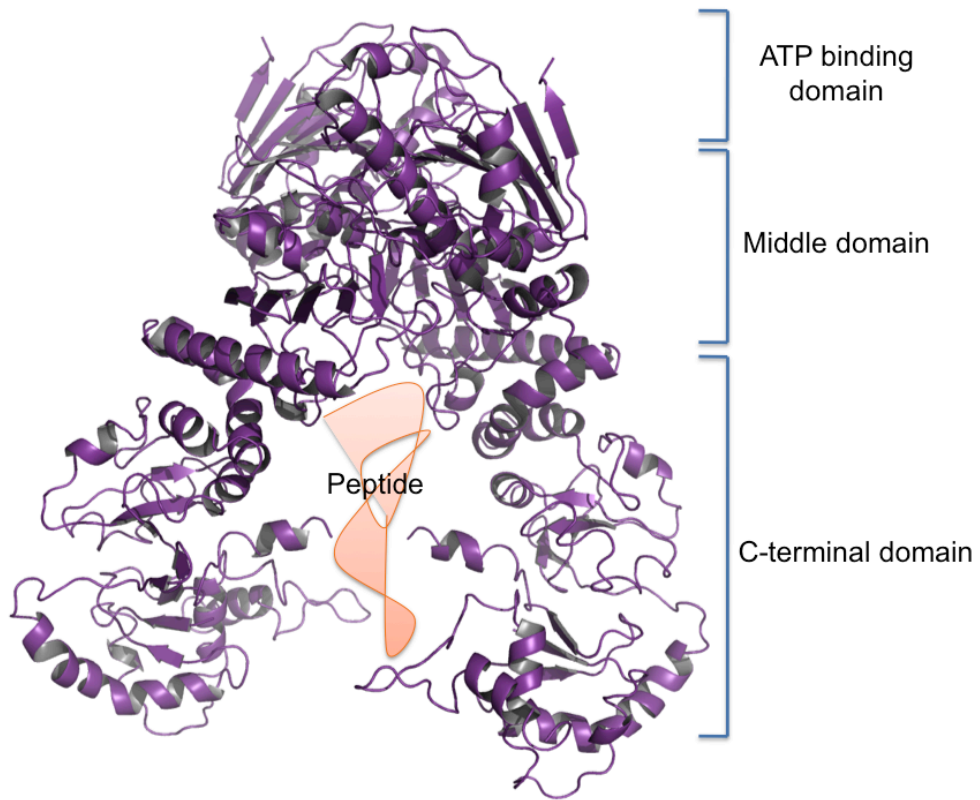


Figure 4-3: *Model of PfHsp90 dimerization.* The model coordinates were generated with Phyre (9) and SymmDock (10) using the structure template 2IOQ (Protein Databank). The cartoon illustration was generated with PyMOL (11).

The N-terminal ATP-binding domain is the most highly conserved domain of Hsp90 (4, 12-14). The N-terminal domain of PfHsp90 has 75% identity to that of HsHsp90 (4). Crystal structures of human and *P. falciparum* Hsp90 N-terminal domains (PDB ID: 2FWZ and 3K60, respectively) reveal that PfHsp90 Met84 adopts a different side-chain rotamer than human Met98, altering the shape of the “ceiling” of the binding pocket (15). Val186 of HsHsp90 is replaced by an isoleucine (Ile173) in PfHsp90, resulting in a slight constriction in the back of the pocket. The substitution of Ser52 (HsHsp90) with an alanine (Ala38) in the *P. falciparum* ortholog enlarges the posterior end of the pocket (15). The Lys112 to Arg98 substitution results in a much bulkier, basic residue (PDB ID: 3K60) (Figure 4-4). Even though this last substitution is not involved in ATP hydrolysis, in general, these differences in pocket architecture suggest that the PfHsp90 ATP-binding domain is slightly more hydrophobic, constricted, and basic relative to the human ortholog.

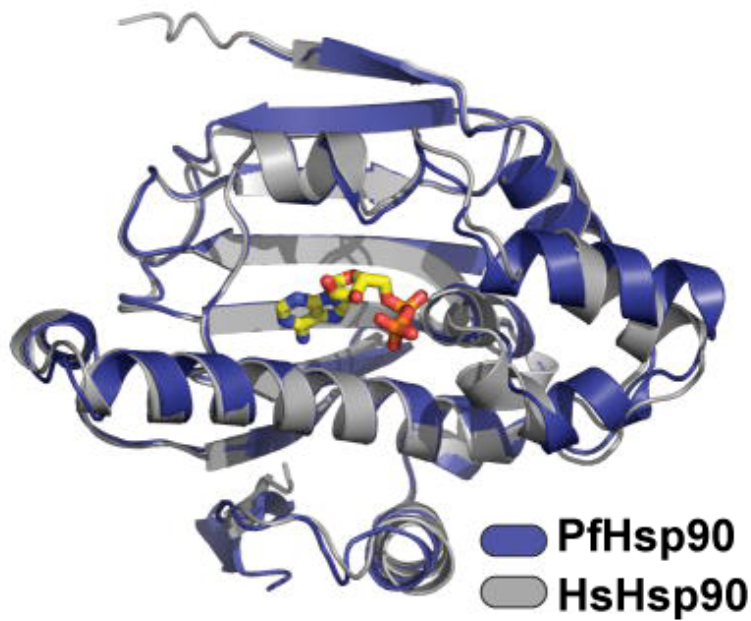


Figure 4-4: *Superposition of the human and P.falciparum Hsp90 ATP binding domains.* The domains show conservation of the domain architecture, but display some amino acid substitutions in the pocket where ATP binds (described in the text). ATP is colored yellow in this figure. This image has been reproduced from Corbett and Berger, 2010 (15).

The recent biochemical characterization of full-length PfHsp90 showed that it contains a hyperactive ATPase domain in comparison to HsHsp90 and that this domain can be inhibited successfully using the GA analog 17-AAG (16). To build on this biochemical characterization of PfHsp90, the objectives of the work presented in this chapter were:

1. To understand if there is any sequence variation at the ATP-binding site of PfHsp90 among different taxa as well as among different global isolates of malaria. Polymorphisms in the ligand-binding site would facilitate the development of resistance to inhibitors of this domain. Conversely, the presence of selection pressure to conserve the residues of the ligand-binding site would deter the development of drug resistance.
2. To repurpose an existing Hsp90 ATP-mimetic inhibitor, PU-H71, against PfHsp90 as an inhibitor of its N-terminal domain and as a molecular tool for understanding PfHsp90 biology.
3. Biochemical exploration of the selectivity of binding of the inhibitor analog to the PfHsp90 and HsHsp90 ATP-binding domains. From the natural product library screen presented in Chapter 3, harmine was found to be selective for binding to the PfHsp90 ATP-binding domain. Methoxy-6-harmalan (a related derivative of harmine) also competed for binding of the PfHsp90 ATP-binding domain, but unlike harmine, it did not show selectivity for PfHsp90 binding relative to the binding inhibition observed for the HsHsp90 ATP-binding domain. This result suggests that harmine derivatives display preferential binding of orthologous Hsp90 ATP-binding sites and can be screened for binding specificity. Therefore, to determine ligand binding specificity, harmine and its structural analog harmalol were used.
4. To determine if structural differences between PfHsp90 and HsHsp90 are sufficient to confer antigenic specificity. The rationale of this objective is that these 2 orthologous domains can mediate specific intermolecular interactions if structural differences can be distinguished by a species-specific Hsp90 antibody.

2 MATERIALS AND METHODS

2.1 Multiple sequence alignment

The multiple sequence alignment of the Hsp90 ATP binding domains from different taxa was generated using MUSCLE (17). MUSCLE was chosen due to the ability to handle a large number of sequences and to correct for gap penalties that are introduced in the initial round of progressive alignment.

2.2 Sequencing of the PfHsp90 ATP-Binding Domain

Genomic DNA was extracted from *P. falciparum* infected patient whole blood using the QiaAMP DNA Mini Kit (QIAGEN). The PfHsp90 ATP-binding domain was PCR amplified using the forward primer 5'-GAAATGCTCCACACAATTAA-3' and the reverse primer 5'-CACCAAATTGTCCGATAATA-3' at an annealing temperature of 56°C. DNA sequencing of this amplicon was performed using a standard capillary gene sequencer (3130xl genetic analyzer, Applied Biosystems) with the same primers. Homology modeling of the domain was done using Phyre (protein fold recognition server) (9, 18), and the structure alignment and substitution modeling were achieved using the Ccp4 suite of programs (19).

2.3 PU-H71 and Geldanamycin (GA) docking in the PfHsp90 GHKL domain structure

The GA and PU-H71 docking models were generated using the PfHsp90 crystal structure template (PDB ID: 3K60) and the HsHsp90 co-crystal structure with PU-H71 (PDB ID: 2FWZ). The docking was done using Coot 0.1 (20). Visualization of the model and preparation of the figures was performed with PyMOL 1.1 (11).

2.4 Cloning and Protein Purification

The cloning and protein purification was carried out as described in chapter 3. The same conditions were used for the expression and purification of the full length PfHsp90. The PfHsp90 full length construct was kindly made available from the labs of Dr. Didier Picard and Dr. Utpal Tatu.

2.5 Site-directed mutagenesis

The PfHsp90 and HsHsp90 ATP binding domains have been cloned in the pET28b and pET15b plasmids as mentioned in chapter 3 and as previously reported (21). The PfHsp90 Arg98Lys and HsHsp90 Lys112Arg mutants were generated using the site specific primers: PfHsp90 Arg98Lys forward 5'- GGT ACT ATT GCA AAA TCA GGA ACC AAA -3' reverse 5'- TTT GGT TCC TGA TTT TGC AAT AGT ACC -3' HsHsp90 Lys112Arg forward 5'- TTG ATT AGT AAT TCT AGT GAT GCC TTA -3' reverse 5'- TAA GGC ATC ACT AGA ATT ACT AAT CAA -3'. The site directed mutagenesis procedure was followed as per instructions of the QuickChange site-directed mutagenesis kit (Agilent Technologies, Santa Clara, CA) with some modifications. Briefly, the mutant plasmid was amplified using the proofreading enzyme *Pfx* (Invitrogen, Carlsbad, CA). Denaturation of the initial template was allowed to take place for 3 min at 95°C. After the initial denaturation, 14 cycles of denaturation (95°C), annealing (58°C) and elongation (68°C) took place. The nascent template was digested by the *DpnI* enzyme (37°C for 1 hour), which digests methylated DNA that has been replicated inside bacteria. The undigested plasmids were transformed in ultracompetent XL-Gold 10 cells (Agilent Technologies, Santa Clara, CA). The plasmids were purified using the Qiagen Miniprep kit (Qiagen, Germantown, MD). These plasmids were screened for the presence of the mutation using Sanger sequencing (Applied Biosystems 3130xl, Carlsbad, CA) after amplification of the Hsp90 ATP binding domain gene using standard T7 primers and annealing conditions (Novagen, Madison, WI).

2.6 Surface Plasmon Resonance (SPR) Measurements

All SPR measurements were conducted on a Biacore X instrument (GE Healthcare, Waukesha, WI) at 25°C. The recombinant PfHsp90 ATP binding domain was purified as previously described (21) and immobilized to one of two flow cells on a CM5 chip (GE Healthcare, Waukesha, WI) using an amine coupling kit (GE Healthcare, Waukesha, WI) as per manufacturer's protocol. The second flow cell was sham activated and deactivated and was used as a reference for the refractive index changes during the experiment. Immobilizations and binding observations were performed using a flow buffer that consisted of: 10 mM HEPES pH 7.5, 150 mM KCl, 3 mM EDTA, 0.005% P20 surfactant. 12000 response units (RU) of immobilized protein were obtained with a 30 μ L injection of 100 μ g/mL protein in 10 mM sodium acetate pH 4.0. For binding experiments with a range of ligand concentrations (5 μ M -

1.25 mM), the 5 mM ligand stock was diluted in the flow buffer and was run over the surface of the chip at a flow rate of 5 μ L/min with 40 μ L injections. When necessary, 2.0 M NaCl pH 5.0 was used to dissociate ligand and restore the baseline for the subsequent concentration of drug. The steady state responses were plotted against the ligand concentrations. To obtain the dissociation constant, these responses were fit to a 1:1 Langmuir binding model by nonlinear regression using the BiaEvaluation 4.1 software (GE Healthcare, Waukesha, WI).

2.7 ATPase Activity Assay

ATPase activity of full length Hsp90 was measured using the coupled LDH/NADH method as previously described (22). Briefly, the reaction mixture was set up in a final volume of 100 μ L containing 25 mM HEPES, 5 mM MgCl₂, 5 mM KCl, 3 μ M Hsp90, 5 mM ATP, 0.2 mM NADH, 3 mM phosphoenolpyruvate, 4.7 U pyruvate kinase, 7.4 U lactate dehydrogenase, 0.03% Tween 20, and 10% glycerol. The decrease in NADH absorbance at 340 nm was recorded continuously for 40 minutes using an EnSpire multimode reader (Perkin Elmer, Waltham, MA). The mixture without the ATPase was incubated at 37°C for 2 minutes and then NADH absorbance was recorded for 3 minutes and used as background to account for spontaneous ATP hydrolysis. The NADH absorbance was recorded for 20 minutes continuously at an acquisition rate of 3 readings per minute at the wavelength of 340 nm.

2.8 *P. falciparum* culture methods and preparation of protein extracts

The *P. falciparum* culture was grown in 5% hematocrit and RPMI 1640 medium supplemented with 0.25% Albumax II, 2 g/L sodium bicarbonate, 0.1 mM hypoxanthine, 25 mM HEPES (pH 7.5), 50 g/L gentamycin at 37°C, 5% O₂, and 6% CO₂. The parasite protein extraction protocol was kindly provided by Dr. Jerome Clain (personal communication). 800 mL of mixed stages of parasites at an average parasitemia of 9% was used for protein extraction. To purify the intact parasites, the red blood cells were lysed with 0.1% saponin and washed with PBS until the solution was translucent to eliminate most of the hemoglobin. The parasites were lysed on a nutator at 4°C for 1hr in 2 mL of: 10 mM Hepes pH 7.5, 1.5 mM MgCl₂, 10 mM KCl, 10 μ L benzonase, 10 μ L protease inhibitor cocktail, 10 μ L PMSF, 1% dodecylmaltoside (w/v). The denatured extracts were resolved with SDS-PAGE (12%). The gels were Western blotted using a dilution of 1:2000 for the PfHsp90 antibody (StressMarq Biosciences).

3 RESULTS

3.1 The PfHsp90 ATP binding domain is structurally conserved

Multiple sequence alignment revealed that the Hsp90 ATP binding domain is well conserved among the different taxa, particularly at positions that are required for the formation of secondary structures (Figure 4-5). The PfHsp90 ATP binding domain is most similar to the Hsp90 ATP binding domain of *P. berghei*. The ATP binding domain of HsHsp90 α is more divergent than observed with the Hsp90 ATP binding domain of the apicomplexan parasites. Several positions of polymorphisms in this domain among the different taxa suggest that the possibility for selective targeting exists.

3.2 Sequencing of the PfHsp90 ATP-Binding Domain from *P. falciparum* Malaria Patient Isolates

Patient isolates (n = 102) were selected from returning travelers to diverse geographic allocations for sequencing of the PfHsp90 ATP-binding domain. Three substitutions were identified at residue position 41 (Ile41Thr) and three substitutions at position 106 (Ser106Leu) (Figure 4-6a). Homology modeling of the PfHsp90 ATP-binding domain using the AMP-PNP bound crystal structure template (PDB ID: 3K60) revealed that Ile41 is outside the ATP-binding domain and Ser106 is located at the back of the helix facing away from the binding pocket (Figure 4-6b). Leucine substitution of this residue is not expected to affect ligand binding (Figure 4-6c).

Beta-sheet



Alpha-helix



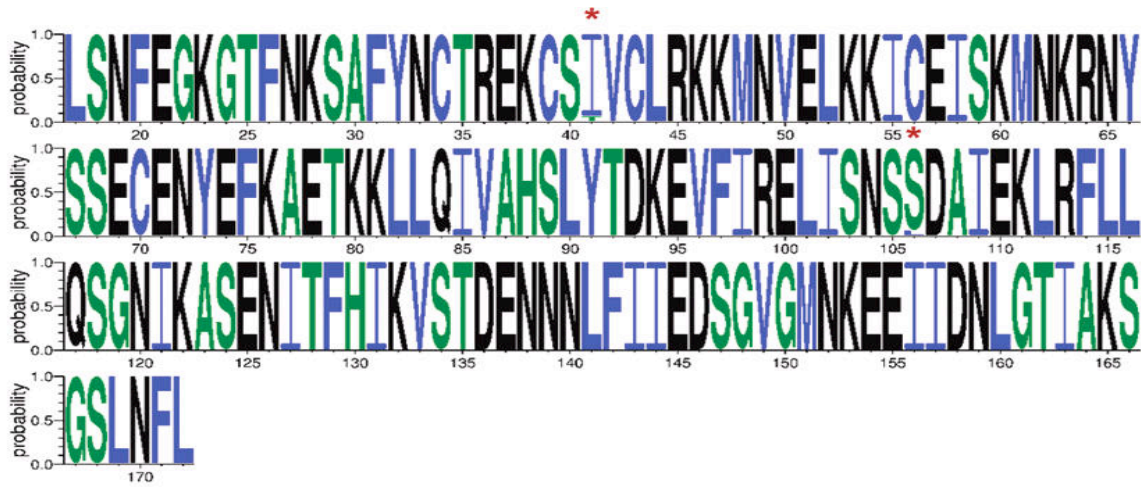
P. falciparum -MSTETFAFNADIRQ-LMSLIINTFYNSKEIFLRELISNASDALDKIRYESITDQKLSAEPEFFIRIIPDKTNNTLTIEDSGIGMTKNDLNNLGTIARSGTKAFMEAIQASG
P. berghei -MSKETFAFNADIRQ-LMSLIINTFYNSKEIFLRELISNASDALDKIRYESITDQKLSAEPEFFIRIIPDKTNNTLTIEDSGIGMTKNDLNNLGTIARSGTKAFMEAIQASG
P. vivax -MSKETFAFNADIRQ-LMSLIINTFYNSKEIFLRELISNASDALDKIRYEAITDQKLSAEPEFFIRIIPDKTNNTLTIEDSGIGMTKNDLNNLGTIARSGTKAFMEAIQASG
P. chaubadi -MSKETFAFNADIRQ-LMSLIINTFYNSKEIFLRELISNASDALDKIRYESITDQKLSAEPEFFIRIIPDKTNNTLTIEDSGIGMTKNDLNNLGTIARSGTKAFMEAIQASG
P. knowlesi -MSKETFAFNADIRQ-LMSLIINTFYNSKEIFLRELISNASDALDKIRYEAITDQKLSAEPEFFIRIIPDKTNNTLTIEDSGIGMTKNDLNNLGTIARSGTKAFMEAIQASG
P. yoelii -MSKETFAFNADIRQ-LMSLIINTFYNSKEIFLRELISNASDALDKIRYESITDQKLSAEPEFFIRIIPDKTNNTLTIEDSGIGMTKNDLNNLGTIARSGTKAFMEAIQASG
E. tenella MENKETFAFNADIQQ-LMSLIINTFYNSKEIFLRELISNASDALDKIRYEAITEPEKPKTKPELFIIRLIPDKANNTLTIEDSGIGMTKAEVNNLGTIARSGTKAFMEALQAGG
N. caninum MADTETFAFNADIQQ-LMSLIINTFYNSKEIFLRELISNASDALDKIRYEAITDPEKPKGAERLFIIRVFNKQNNLTIEDDGIKMTKAEVNNLGTIARSGTKAFMEALQAGG
T. gondii MADTETFAFNADIQQ-LMSLIINTFYNSKEIFLRELISNASDALDKIRYEAITDPEKPKGAERLFIIRVFNKQNNLTIEDDGIKMTKAEVNNLGTIARSGTKAFMEALQAGG
C. hominis --MVETFAFNADIQQ-LMSLIINTFYNSKEIFLRELISNASDALDKIRYESLTDPEQLKSNEEMHIRIIPDKVNNLTIEDSGIGMTKKNELNNLGTIARSGTKAFMEAIQAGG
C. parvum --MVETFAFNADIQQ-LMSLIINTFYNSKEIFLRELISNASDALDKIRYESLTDPEQLKSNEEMHIRIIPDKVNNLTIEDSGIGMTKKNELNNLGTIARSGTKAFMEAIQAGG
C. muris --MVETFAFNADIQQ-LMSLIINTFYNSKEIFLRELISNASDALDKIRYESLTDPEQLKSNEEMHIRIIPDKVNNLTIEDSGIGMTKKNELNNLGTIARSGTKAFMEAIQAGG
T. parva TPDQEVYAFNADISQ--LLSLIINAFYNSKEIFLRELISNASDALEKIRYEAIKDPKQIEDQPDYIRLYADKNNNTLTIEDSGIGMTKADLVNNLGTIARSGTRAFMEALQAGS
T. annulata TPDQEVYAFNADISQ--LLSLIINAFYNSKEIFLRELISNASDALEKIRYEAIKDPKQIEDQPDYIRLYADKNNNTLTIEDSGIGMTKADLVNNLGTIARSGTRAFMEALQAGS
H. sapiens EEEVETFAFQAEIAQ-LMSLIINTFYNSKEIFLRELISNASDALDKIRYESLTDPSKLDGSKELHINLIPNKQDRTLTIIVDTGIGMTKADLVNNLGTIARSGTKAFMEALQAGA
S. cerevisiae --MASETFFEQAEITQ-LMSLIINTFYNSKEIFLRELISNASDALDKIRYKSLDPKQLETEPDLFIIRIPKPEQKVLIRDSGIGMTKAEVNNLGTIARSGTKAFMEALSAGA
T. cruzi --MTETFAFQAEINQ-LMSLIINTFYNSKEIFLRELISNASDADCKIRYQSLTDPVGLGDEPHLRIRVIPDRVNTLTVEDTSGIGMTKADLVNNLGTIARSGTKAFMEALEAGG
T. brucei --MTETFAFQAEINQ-LMSLIINTFYNSKEIFLRELISNASDADCKIRYQSLTDPVGLGDEPHLRIRVIPDRVNTLTVEDTSGIGMTKADLVNNLGTIARSGTKAFMEALEAGG
L. infantum --MTETFAFQAEINQ-LMSLIINTFYNSKEIFLRELISNASDADCKIRYQSLTDPVGLGDEPHLRIRVIPDRVNTLTVEDTSGIGMTKADLVNNLGTIARSGTKAFMEALEAGG
L. major --MTETFAFQAEINQ-LMSLIINTFYNSKEIFLRELISNASDADCKIRYQSLTDPVGLGDEPHLRIRVIPDRVNTLTVEDTSGIGMTKADLVNNLGTIARSGTKAFMEALEAGG
E. histolytica E-MTETYQFQAEINQLL-SLIINAFYNSKIDFLRELISNASDALDKIRYQSLQDKSVLEAEPVIRITADKDNKQLIIEDTSGIGMTKADLVNNLGTIARSGTKAFMEALQAGG
E. dispar KEMTETYQFQAEINQLL-SLIINAFYNSKIDFLRELISNASDALDKIRYQSLQDKSVLEAEPVIRITADKDNKQLIIEDTSGIGMTKADLVNNLGTIARSGTKAFMEALQAGG



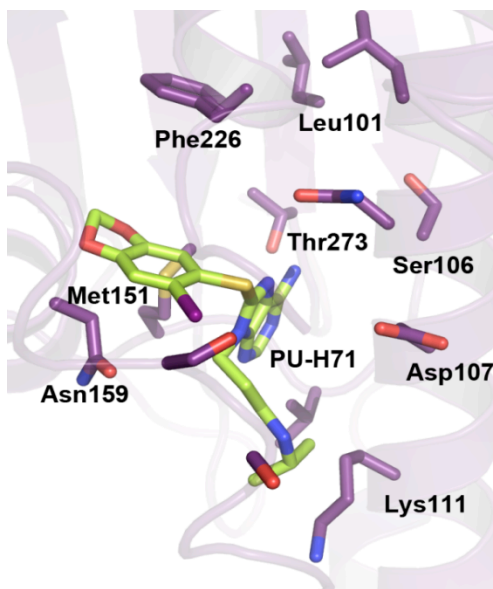
P. falciparum DISMIGQFGVGFYSA-YLVADHVVISKNNNDEQYVWESAAGGSFTVTKDETNEK-LGRGTKIILHLKEDQLEYLEEKRIKDLVKKHSEFISFPIKLYCERONEKEITASEEEEEGE
P. berghei DISMIGQFGVGFYSA-YLVADHVVISKNNNDEQYVWESAAGGSFTVTKDETNEK-IGRGTKIILHLKEDQLEYLEEKRIKDLVKKHSEFISFPIKLYCERONEKEITASEEEEEAQD
P. vivax DISMIGQFGVGFYSA-YLVADHVVISKNNNDEQYVWESAAGGSFTVTKDETNEK-MGRGTKIILHLKDDQLEYLEEKRIKDLVKKHSEFISFPIKLYCERONEKEITASEDEAAE
P. chaubadi DISMIGQFGVGFYSA-YLVADHVVISKNNNDEQYVWESAAGGSFTVTKDETNEK-IGRGTKIILHLKEDQLEYLEEKRIKDLVKKHSEFISFPIKLYCERONEKEITASEDEAAQ
P. knowlesi DISMLVNSSVPYSA-YLVADHVVISKNNNDEQYVWESAAGGSFTVTKDESNEK-IGRGTKIILHLKDDQLEYLEEKRIKDLVKKHSEFISFPIKLYCERONEKEITASEDEAAE
P. yoelii DISMIGQFGVGFYSA-YLVADHVVISKNNNDEQYVWESAAGGSFTVTKDETNEK-IGRGTKIILHLKEDQLEYLEEKRIKDLVKKHSEFISFPIKLYCERONEKEITASEDEAAQ
E. tenella DISMIGQFGVGFYSA-YLVADSVTVVSKNNNDEQYVWESAAGGSFTVQKDDKYEP-LGRGTKIILHLKEDQLEYLEERRIKDLVKKHSEFISFPIELAVEKTHEVTESEDEEEK
N. caninum DISMIGQFGVGFYSA-YLVADKVTVVTRHNDDEMYVWESAAGGSFTVSKAEGQYENIVRGTRILHMKEDQTEYLEDRRLKDLVKKHSEFISFPIELAVEKSVDKETDSEEEKEG
T. gondii DISMIGQFGVGFYSA-YLVADKVTVVSRHNDDEMYVWESAAGGSFTVSKAEGQFENIVRGTRILHMKEDQTEYLEDRRLKDLVKKHSEFISFPIELAVEKSVDKETDSEEEKEP
C. hominis DVSMIGQFGVGFYSA-YLVADKVTVITKHNDEQYIWESAGGSFTITNDTSDNK-LQRGTRILHLKEDQDLYLEERTLRDLVKKHSEFISFPIELAVEKTTTEKITDSDVDEEE
C. parvum DVSMIGQFGVGFYSA-YLVADKVTVITKHNDEQYIWESAGGSFTITNDTSDNK-LQRGTRILHLKEDQDLYLEERTLRDLVKKHSEFISFPIELAVEKTTTEKITDSDVDEEE
C. muris DISMIGQFGVGFYSA-YLVADKVTVITKHNDEQYIWESAGGSFTITDSDNS-LSRGTRIVLHLKEDQLEYLEERLRDLVKKHSEFISFPIQLSVEKTTTEKITDSDVDEEE
T. parva DVSMIGQFGVGFYSA-YLVADKVTVVSKNNADQYVWESASGHFTVKKDDSHPE-LKRGTRILHLKEDQTEYLEERRIKELVKKHSEFISFPIQLSVEKTTTEKITDSDVDEEE
T. annulata DVSMIGQFGVGFYSA-YLVADKVTVVSKNNADQYVWESASGHFTVKKDDSHPE-LKRGTRILHLKEDQTEYLEERRIKELVKKHSEFISFPIQLSVEKTTTEKITDSDVDEEE
H. sapiens DVSMIGQFGVGFYSA-YLVAEKVTVITKHNDEQYIWESAGGSFTITNDTSDNK-LQRGTRILHLKEDQTEYLEERRIKELVKKHSEFISFPIQLSVEKTTTEKITDSDVDEEE
S. cerevisiae DVSMIGQFGVGFYSL-FLVADRVQVVISKNNDEQYIWESNAGGSFTVTLDEVNER-IGRGTILRLFLKDDQLEYLEEKRIKEVIRKHSEFVAYPIQLVVTKEVEKEVPIPEEEKD
T. cruzi DVSMIGQFGVGFYSA-YLVADRVTVVSKNNDEQYIWESAGGSFTVTPTP-DCD-LKRGTRIVLHLKEDQTEYLEERRIKELVKKHSEFISFPIQLSVEKTTTEKITDSDVDEEE
T. brucei DVSMIGQFGVGFYSA-YLVADRVTVVSKNNDEQYIWESAGGSFTVTPTP-DCD-LKRGTRIVLHLKEDQTEYLEERRIKELVKKHSEFISFPIQLSVEKTTTEKITDSDVDEEE
L. infantum DVSMIGQFGVGFYSA-YLVADRVTVVSKNNDEQYIWESAGGSFTITSTP-ESD-LKRGTRIVLHLKEDQTEYLEERRIKELVKKHSEFISFPIQLSVEKTTTEKITDSDVDEEE
L. major DVSMIGQFGVGFYSA-YLVADRVTVVSKNNDEQYIWESAGGSFTITSTP-ESD-LKRGTRIVLHLKEDQTEYLEERRIKELVKKHSEFISFPIQLSVEKTTTEKITDSDVDEEE
E. histolytica ADVSMIGQFGVGFYSSYLVAEKVTVITKHNDEQYIWESAGGSFTITLDESGER-LKRGTKIILHLKEDQTEYLEERRIKELVKKHSEFISFPIQLSVEKTTTEKITDSDVDEEE
E. dispar ADVSMIGQFGVGFYSSYLVAEKVTVITKHNDEQYIWESAGGSFTITLDESGER-LKRGTKIILHLKEDQTEYLEERRIKELVKKHSEFISFPIQLSVEKTTTEKITDSDVDEEE

Figure 4-5: *Multiple sequence alignment of the ATP binding domains of Hsp90 orthologs in different taxa.* Positions of variation are highlighted in grey. The green arrow represents beta-sheets and the orange rectangle represents the positions of the alpha-helices. The multiple sequence alignment was generated using the MUSCLE algorithm (17).

(a)



(b)



(c)

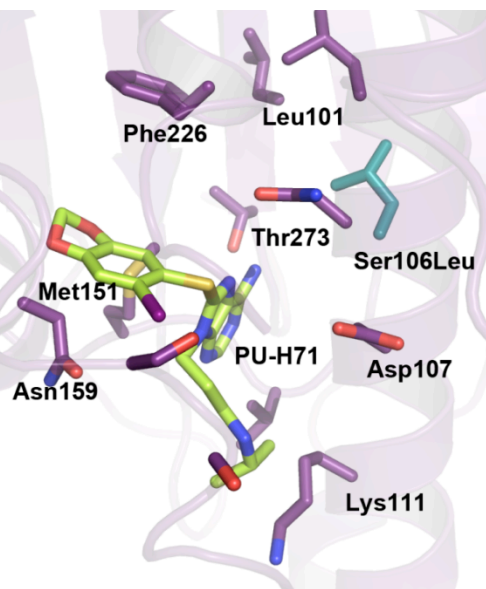


Figure 4-6: Sequencing of the PfHsp90 ATP-binding domain from 102 globally distributed patient isolates. (a) WebLogo representation of the multiple sequence alignment. Polar amino acids (G,S,T,Y,C,Q,N) are green, basic (K,R,H) blue, acidic (D,E) red and hydrophobic (A,V,L,I,P,W,F,M) amino acids are black. Asterisks indicate two low frequency mutations that were identified as Ile41Thr and Ser106Leu. The WebLogo representation was generated using version3 (23). (b) Homology modeling of the domain revealed that Ile41 is outside the ATP-binding domain. (c) Substitution of Ser106 by leucine (blue) does not affect substrate binding in the ATP-binding domain. The homology model diagrams were generated using PyMOL (11).

3.3 Homology modeling reveals that PU-H71 fits well in the PfHsp90 ATP binding domain

To understand whether PU-H71 fits into the PfHsp90 ATP-binding pocket, PU-H71 was docked in the crystal structure of the PfHsp90 ATP-binding domain (PDB ID: 3K60) (Figure 4-7a). The modeling suggests that PU-H71 likely employs ionic interactions with the guanidinium group of arginine 98 (Arg98). This group has the potential to confer tight interactions to the *Plasmodium* ATP-binding pocket. The generic Hsp90 inhibitor, geldanamycin (GA), was also modeled in the malaria Hsp90 binding pocket (Figure 4-7b). GA occupies a larger space of the pocket due to the ansamycin moiety and even though it has the chemical architecture to interact with Arg98, this drug is not as well suited to interact with Asp88 and Asp79 due to the absence of a basic purine scaffold.

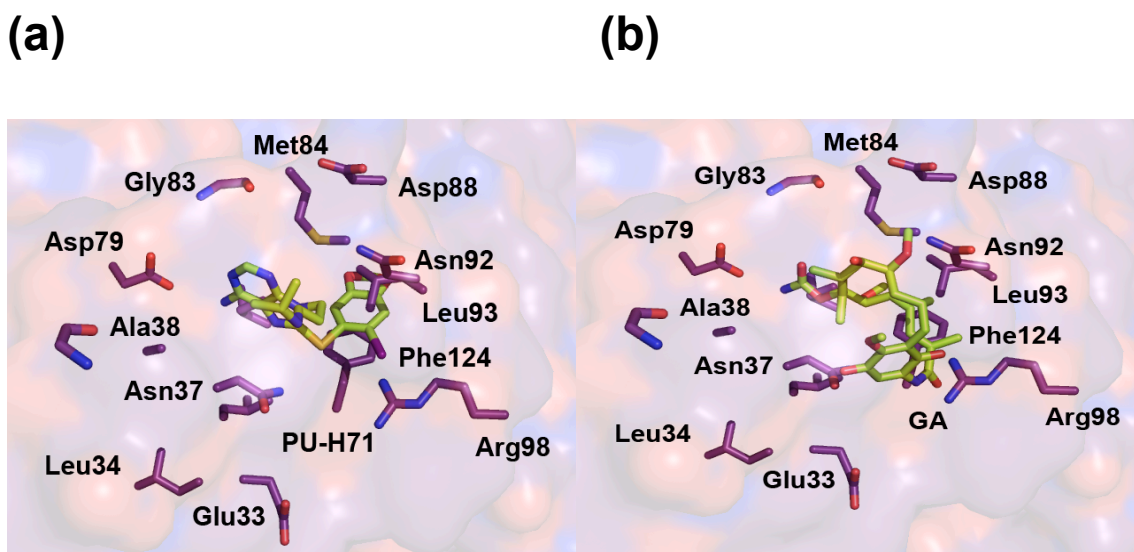
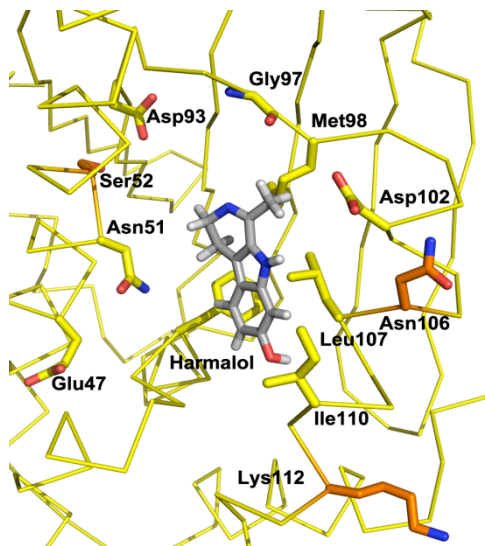


Figure 4-7: Illustration of docking PU-H71 (a) and geldanamycin (GA) (b) within the ATP-binding site of PfHsp90. The models were generated using the PfHsp90 crystal structure (PDB ID: 3K60). By convention, the electrostatic potential surface in the background denotes acidic residues in red and basic residues in blue. It has been included only in this figure to depict the architecture of the pocket.

3.4 Homology modeling reveals ortholog specific interactions with harmine and harmalol

Docking studies using the crystal structures of the PfHsp90 (PDB ID: 3K60) and HsHsp90 (2FWZ) ATP binding pockets suggest that the harmine methoxy group mediates interactions with the guanidinium group of arginine 98 (Arg98). This group has the potential to confer tight interactions to the *Plasmodium* ATP-binding pocket. Harmalol was successfully docked in the human Hsp90 binding pocket suggesting that Lys112 is mediating polar interactions with the harmalol hydroxyl group (Figure 4-8a). The planar conformation of these two molecules accommodates well in the hydrophobic and basic nature of the Hsp90 binding pocket. The absence of a polar hydroxyl group in harmine suggests that it mediates more specific interactions with the more constricted and hydrophobic ATP-binding pocket of PfHsp90 (Figure 4-8b).

(a)



(b)

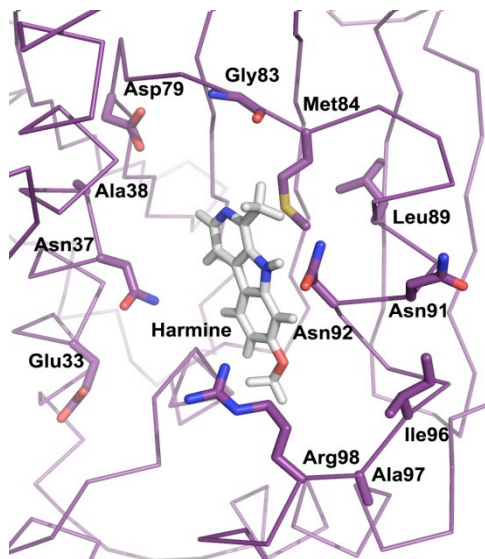
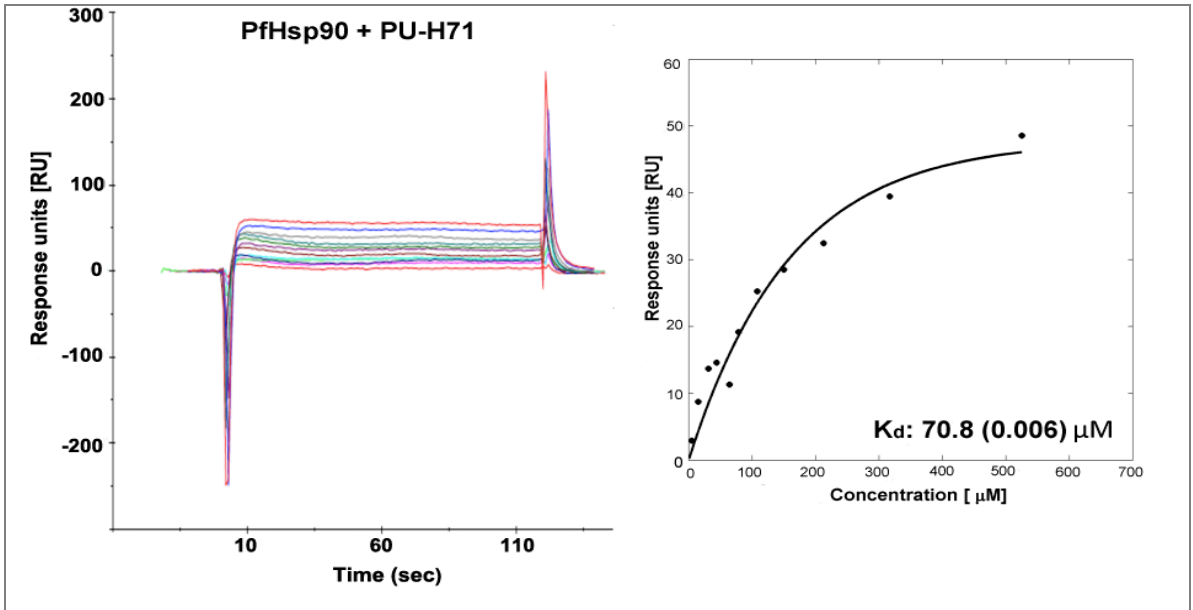


Figure 4-8: (a): Docking of harmalol in the ATP-binding site of HsHsp90 (PDB ID: 2FWZ). The residues highlighted in orange represent positions of variation among the Hsp90 ATP-binding pockets in different taxa. (b) Docking of harmine in the PfHsp90 crystal structure (PDB ID: 3K60).

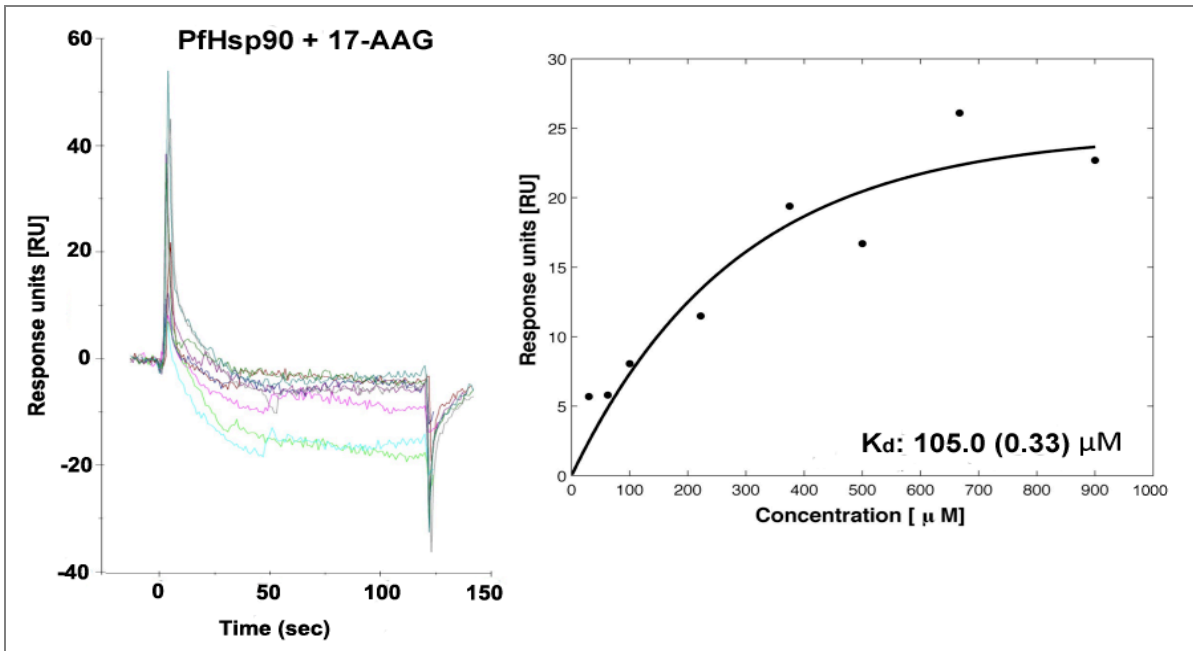
3.5 PU-H71 binds the PfHsp90 ATP-binding domain with high affinity

To quantify the affinity of PU-H71 for the PfHsp90 ATP-binding domain, surface plasmon resonance experiments were employed using a Biacore X system. Titration of the inhibitor on the surface-immobilized PfHsp90 ATP-binding domain reached saturation (Figure 4-9a). A titration dependent effect was observed for PU-H71 binding of the PfHsp90 ATP-binding domain with a dissociation constant (K_d) of $70.8 \pm 0.006 \mu\text{M}$ as compared to the positive control GA derivative 17AAG with a K_d of $105 \pm 0.33 \mu\text{M}$ (Figure 4-9b). To test the importance that the Arg98 guanidinium group plays in accommodating PU-H71 in the PfHsp90 ATP binding pocket, a R98K site directed mutant of PfHsp90 ATP binding domain was immobilized on the surface of a Biacore X chip. Analysis of the titration of PU-H71 on this immobilized R98K mutant PfHsp90 surface resulted in a K_d of $268 \pm 55.7 \mu\text{M}$ (Figure 4-9c).

(a)



(b)



(c)

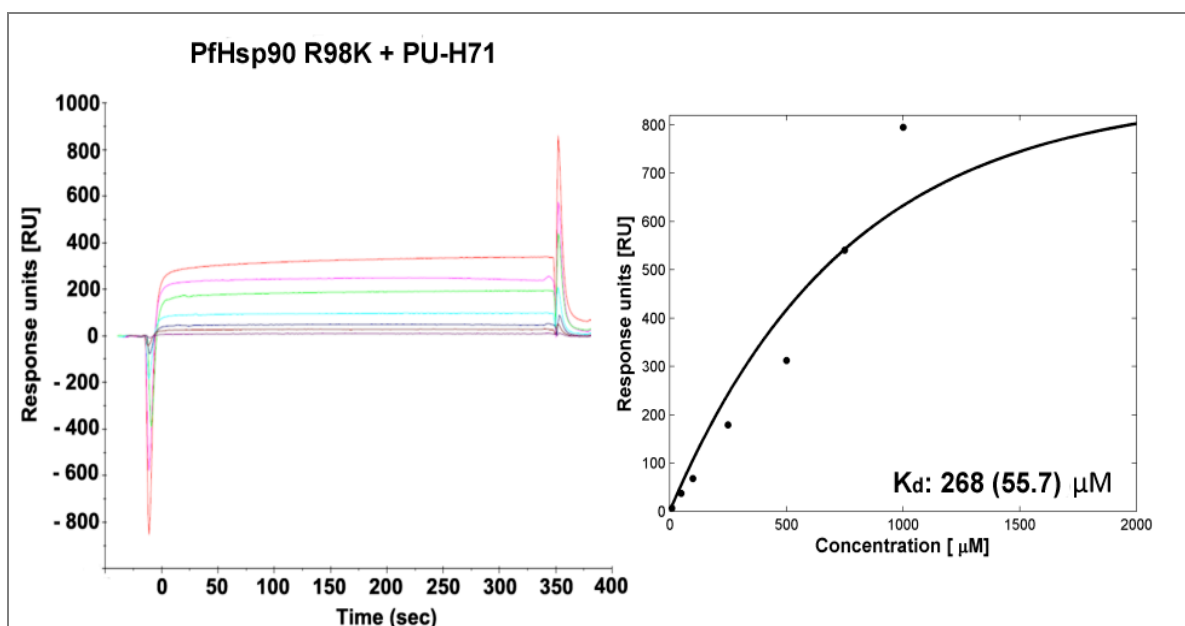


Figure 4-9: SPR measurements for PU-H71 binding of the ATP-binding domain of PfHsp90.

The colors on the sensorgrams represent varying concentrations of the respective drug injected over the surface with the immobilized PfHsp90. The steady state responses were fit using non-linear regression to a single class of binding site model (as shown on the right) to obtain the K_d value indicated. The number in parentheses represents standard error. (a) SPR measurements for PU-H71 binding of the ATP-binding domain of PfHsp90 (b) 17-AAG was used as a positive control drug. (c) SPR measurements for PU-H71 binding of the site directed R98K mutant ATP-binding domain of PfHsp90.

3.6 Harmine has affinity for the PfHsp90 ATP-binding domain

To quantify the affinity of harmine and harmalol for the PfHsp90 and HsHsp90 ATP-binding domain, surface plasmon resonance experiments were employed using a Biacore X system. Titration of harmine and harmalol on the surface-immobilized PfHsp90 ATP-binding domain reached saturation (Table 4-1). A titration dependent effect was observed for harmalol and harmine binding of the PfHsp90 ATP-binding domain with a dissociation constant $K_d = 7010 \pm 552 \mu\text{M}$ for harmalol and $K_d = 40 \pm 0.9 \mu\text{M}$ for harmine. The HsHsp90 ATP-binding domain was also immobilized on the surface of a Biacore X CM5 chip. Titration of harmalol on the surface of the HsHsp90 ATP binding domain chip reached saturation with $K_d = 224 \pm 20.6 \mu\text{M}$ (Table 4-1), but flowing of various concentrations of harmine on this surface did not reach saturation (Table 4-1).

To test the hypothesis that Arg98 plays an important role in accommodating harmine in the PfHsp90 ATP binding pocket and K112 plays an important role in accommodating harmalol in the HsHsp90 ATP binding pocket, an R98K site-directed mutant of PfHsp90 ATP binding domain was immobilized on the surface of a Biacore X chip. Reciprocally, a K112R site directed mutant of HsHsp90 was also immobilized on the surface of a Biacore X chip. The titration of harmine and harmalol on the immobilized R98K mutant surface reached saturation for harmalol binding, but not for harmine (Table 4-1). Analysis of the titration dependent effect observed for harmalol binding of the R98K mutant resulted in $K_d = 370 \pm 4.6 \mu\text{M}$. On the surface with the immobilized K112R (Table 4-1), titration of harmine reached saturation with $K_d = 74.7 \pm 3.3 \mu\text{M}$. A titration dependent effect was not observed for harmalol with this mutant.

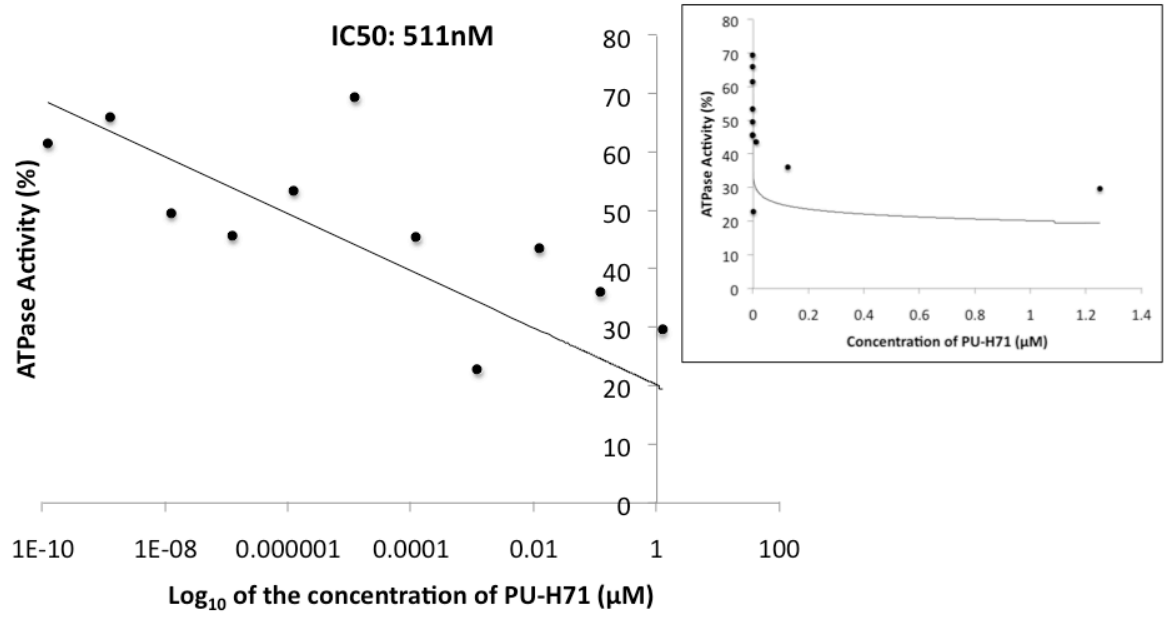
Table 4-1: Surface plasmon resonance (SPR) measurements for harmalol and harmine binding of the ATP-binding domains of PfHsp90 and HsHsp90. Where possible, the steady state responses were fit using non-linear regression to a single class of binding site model to obtain the K_d value indicated. The number in parentheses represents standard error.

Drug	HsHsp90	PfHsp90
PU-H71	$K_d=22(14.3)\mu\text{M}$	$K_d=70.8(0.006)\mu\text{M}$
17-AAG	$K_d=42.5(0.02)\mu\text{M}$	$K_d=105.0(0.33)\mu\text{M}$
Harmine	No fit	$K_d=40.0(0.9)\mu\text{M}$
Harmalol	$K_d=224(20.6)\mu\text{M}$	$K_d=7010(522)\mu\text{M}$
Harmane	No fit	No binding
Harmol	No fit	No binding
Methoxy-6-harmalan	Interference	Interference
Radicicol	No fit	No fit
Drug	HsHsp90 K112R	PfHsp90 R98K
17-AAG	No fit	No fit
Harmalol	No fit	$K_d=370(4.6)\mu\text{M}$
Harmine	$K_d=74.7(3.3)\mu\text{M}$	No fit
PU-H71	$K_d=153.0(0.7)\mu\text{M}$	$K_d=268(55.7)\mu\text{M}$
Radicicol	No fit	$K_d=386.7(9.12)\mu\text{M}$

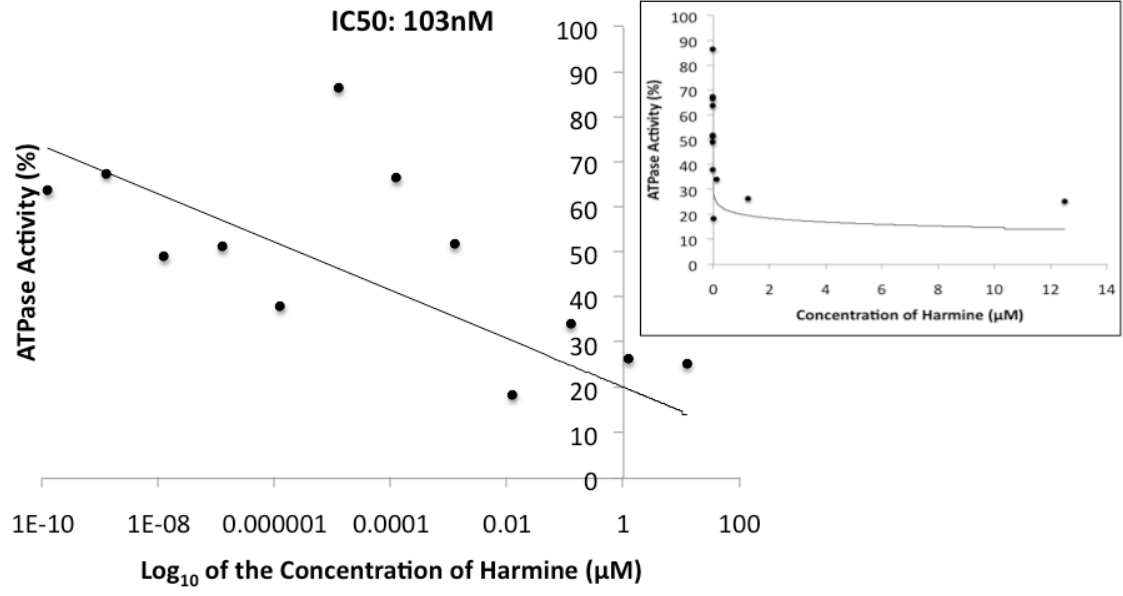
PU-H71 and harmine inhibit PfHsp90 ATPase activity

Full-length PfHsp90 was also expressed to test the ability of PU-H71 and harmine to inhibit the PfHsp90 ATPase activity. PU-H71 inhibited ATPase activity with an IC_{50} of 511 nM (Figure 4-10a), while harmine inhibited the ATPase activity with an IC_{50} of 103 nM (Figure 4-10b). Drug positive controls included radicicol (144 nM) (Figure 9c) and 17-AAG (146 nM) (Figure 4-10d). Previously published data with the same construct, but using a different approach, reported an IC_{50} of 207 nM for GA inhibition of PfHsp90 ATPase activity (16).

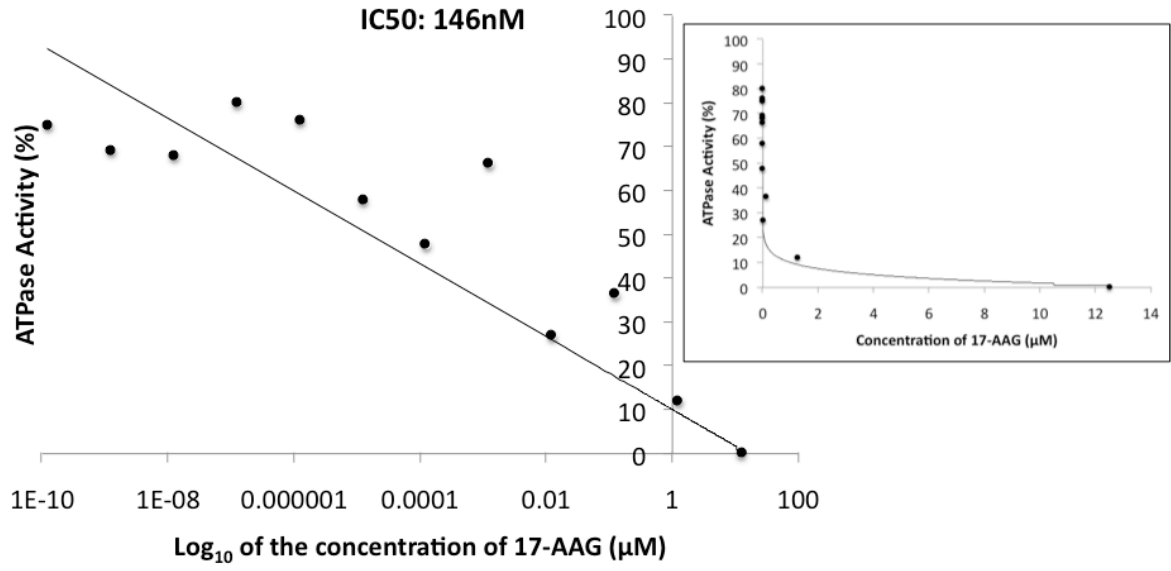
(a)



(b)



(c)



(d)

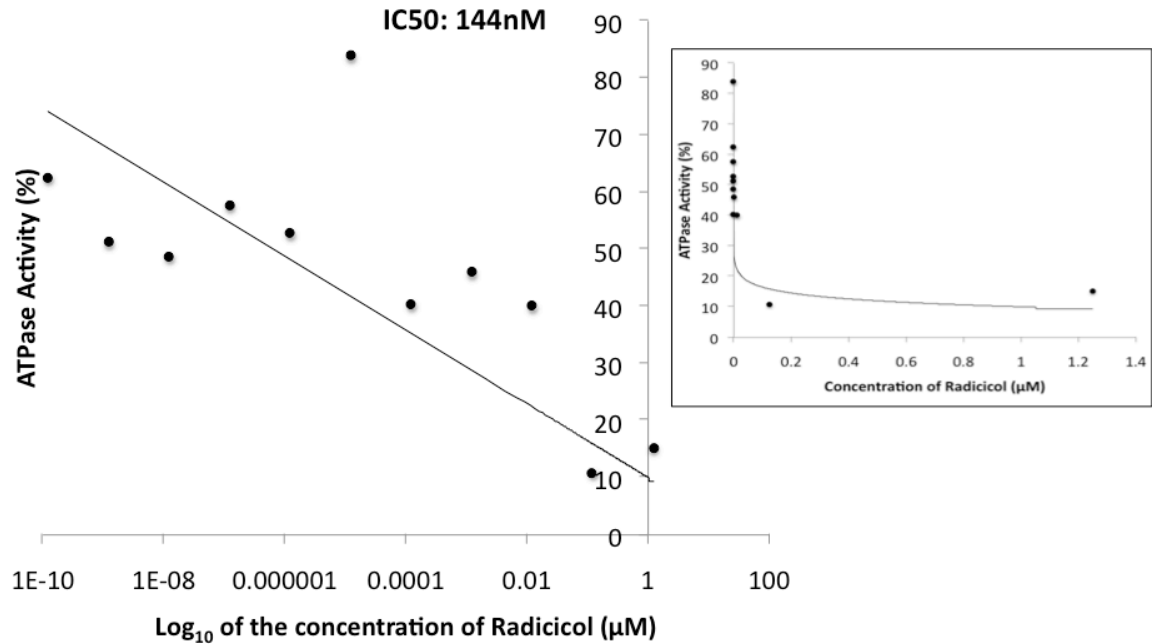


Figure 4-10: The effect of each of PU-H71 (a) and harmine (b) on the ATPase activity of full length recombinant PfHsp90. The positive control drugs 17-AAG (c) and radicicol (d) were also tested for inhibition of the activity. The IC₅₀ of PfHsp90 ATPase activity was determined by plotting percent activity remaining (relative to no drug control) versus inhibitor concentration (MATLAB R2009). The inset shows the logarithmic curve of the reduction of ATPase activity with increasing concentrations of each drug.

3.7 Anti-PfHsp90 antibody displays antigenic specificity against PfHsp90

A specific anti-PfHsp90 rabbit polyclonal antibody has been developed in the lab of Dr. Utpal Tatu (2, 3) and was obtained from StressMarq Biosciences. The recombinant ATP binding domain constructs of PfHsp90 and HsHsp90 were run on SDS-PAGE and subjected to Western blotting (Figure 4-11a). Both constructs were detected at the expected size (25 kDa) on the Coomassie stained gel, but only the PfHsp90 construct was detected on the film exposed to the anti-PfHsp90 Western blot. In addition, the anti-PfHsp90 antibody only recognized PfHsp90 in parasite extracts. No chemiluminescence signal was present in the lane with uninfected erythrocyte extracts (Figure 4-11b). A band corresponding to 25 kDa was observed in addition to the band expected at 81 kDa for PfHsp90 in the parasite extract lane. This band is quite likely a degradation product of full length PfHsp90 and may correspond to the ATP-binding domain of the protein, which is quite stable in comparison to the labile full length protein.

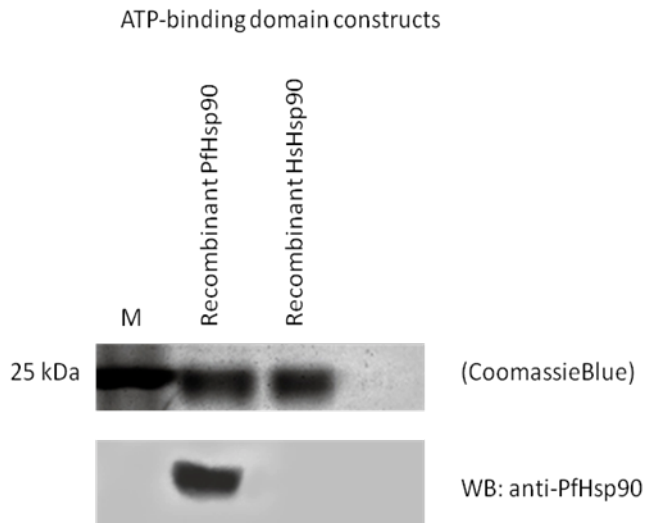
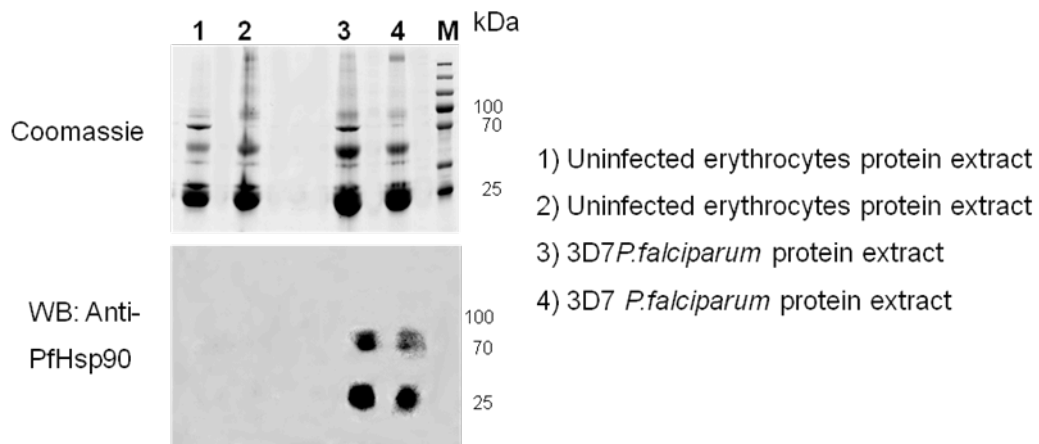
(a)**(b)**

Figure 4-11: *Anti-PfHsp90 antibody displays antigenic specificity.* Blotting with anti-PfHsp90 antibody shows that only the PfHsp90 N-terminal ATP binding domain can be recognized but not the HsHsp90 N-terminal ATP binding domain (a). This antigen specificity extends to recognition of the native protein from protein extracts (b). The chemiluminescence signal was only present in the lanes with the parasite protein extracts.

4 DISCUSSION

Hsp90 has a unique Bergerat fold at the N-terminal ATP-binding pocket that can be inhibited competitively by small molecules (7). Because Hsp90 regulates the cell cycle, potentiation of drug resistance, and buffering of phenotypic variation, many Hsp90 clients are essential proteins within abnormal cells (24-26). Each of the Hsp90 paralogs fold a distinct set of client proteins (14, 27). The central hypothesis of my thesis is that targeting of cytosolic-inducible PfHsp90 (PF07_0029) is a compelling strategy as this protein is upregulated in the early ring stage of the *P. falciparum* erythrocytic cycle and retains domains (such as the EEVD motif) consistent with its chaperone function (2, 3, 5, 6, 16). The aim of the results presented in this chapter is to establish PfHsp90 as a biochemical target and to assess the affinity of a few existing and novel Hsp90 inhibitors for the PfHsp90 ATP-binding domain.

Sequencing of the region of the PfHsp90 gene encoding the N-terminal part of the protein demonstrated that the PfHsp90 ATP-binding domain is highly conserved in clinical isolates from around the world. This finding suggests that this domain is under selection pressure to be conserved due to the essential function that it plays in empowering the protein with the energy needed to fold client proteins. Even though these isolates have not been under Hsp90 inhibitor pressure, the absence of any polymorphisms in the binding pocket, even at positions that are not directly involved in ATP binding or hydrolysis, is encouraging for pursuing this domain as a target for the development of antimalarial compounds.

Because of the toxicity associated with GA and its derivatives (25, 28, 29), the strategy here was to repurpose a novel purine scaffold inhibitor (PU-H71) that was selected on the basis of docking studies with the PfHsp90 crystal structure. PU-H71 is in phase I clinical trials against various neoplastic diseases and has shown no toxicity at therapeutic doses (28-32).

The assumptions derived from the docking studies were supported by the fact that PU-H71 has a high affinity for the PfHsp90 ATP-binding pocket, as demonstrated by the K_d constant and by the inhibition of ATPase activity to levels comparable to those seen with traditional Hsp90 inhibitors such as GA and its derivatives. The tight interaction of PU-H71 with the guanidinium group of R98 accounts, at least partially, for the affinity of PU-H71 for the PfHsp90 ATP-binding pocket because the K_d constant increased 3.8-fold with the R98K mutation.

Harmine also exhibits selectivity for PfHsp90, which is likely due to the Arg98 residue, setting it apart from Human Hsp90 (Lys112). On the basis of the biochemical approach taken here to understand the specificity of the derivatives, it was determined that the position corresponding to HsHsp90 Lys112 and PfHsp90 Arg98 is important in contributing to specific interactions with the harmine derivatives. Quantification of the binding of harmine derivatives to PfHsp90 and HsHsp90 using wild-type and site-directed mutant constructs of the PfHsp90 ATP-binding domain was achieved using surface plasmon resonance.

Harmine showed a high affinity for the PfHsp90 ATP-binding pocket and harmalol exhibited a high affinity for the HsHsp90 ATP-binding pocket, as demonstrated by the K_d constants obtained from the surface plasmon resonance studies. Arg98 plays a major role in the affinity of harmine for the PfHsp90 ATP-binding pocket because titration-dependent binding and saturation of the signal was not present on the chip with the Arg98Lys site-directed construct. In a similar way, with the replacement of Lys112 with arginine in the HsHsp90 ATP-binding domain construct, titration-dependent binding and saturation of the response were not observed for harmalol. This finding suggests that ortholog-specific binding was lost with the mutation. In fact, the switching of these residues altered the binding affinity. Harmalol showed higher affinity for PfHsp90 Arg98Lys, while harmine displayed higher affinity for HsHsp90 Lys112Arg. This position does not play an important role in the ATPase activity of this domain (15), but it is located inside the ATP-binding pocket and is well conserved among parasitic Hsp90 orthologs. Substitutions at this position were not observed among clinical isolates of *P. falciparum*. In addition to its ligand binding specificity, the anti-PfHsp90 antibody displayed antigenic recognition specificity, suggesting that topological differences exist at the N-terminal binding domain, even though it is functionally conserved. These topological differences account for specific intermolecular interactions and can be exploited for the identification of selective drugs.

PU-H71 and harmine showed ATPase inhibitory activity at levels comparable to the generic Hsp90 inhibitor GA, which is known to cause potent inhibition of PfHsp90. Relative to the radicicol and 17-AAG positive controls, harmine displayed the lowest PfHsp90 ATPase IC_{50} . On the basis of the biochemical characterization presented here, we cannot rule out non-specific targets for harmine, but the observation of the ortholog-specific affinity of harmine and harmalol is encouraging for future studies to explore the structure of harmine by synthetic chemistry in

order to increase its specificity. Modification of the structure of harmine would likely also stabilize the drug from metabolic breakdown.

References

1. Shonhai A (2010) Plasmodial heat shock proteins: targets for chemotherapy. *FEMS immunology and medical microbiology* 58(1):61-74.
2. Banumathy G, Singh V, Pavithra SR, & Tatu U (2003) Heat shock protein 90 function is essential for Plasmodium falciparum growth in human erythrocytes. *The Journal of biological chemistry* 278(20):18336-18345.
3. Pavithra SR, Banumathy G, Joy O, Singh V, & Tatu U (2004) Recurrent fever promotes Plasmodium falciparum development in human erythrocytes. *The Journal of biological chemistry* 279(45):46692-46699.
4. Kumar R, Pavithra SR, & Tatu U (2007) Three-dimensional structure of heat shock protein 90 from Plasmodium falciparum: molecular modelling approach to rational drug design against malaria. *Journal of biosciences* 32(3):531-536.
5. Pavithra SR, Kumar R, & Tatu U (2007) Systems analysis of chaperone networks in the malarial parasite Plasmodium falciparum. *PLoS computational biology* 3(9):1701-1715.
6. Acharya P, Kumar R, & Tatu U (2007) Chaperoning a cellular upheaval in malaria: heat shock proteins in Plasmodium falciparum. *Molecular and biochemical parasitology* 153(2):85-94.
7. Dutta R & Inouye M (2000) GHKL, an emergent ATPase/kinase superfamily. *Trends in biochemical sciences* 25(1):24-28.
8. Bergerat A, *et al.* (1997) An atypical topoisomerase II from Archaea with implications for meiotic recombination. *Nature* 386(6623):414-417.
9. Kelley LA & Sternberg MJ (2009) Protein structure prediction on the Web: a case study using the Phyre server. *Nature protocols* 4(3):363-371.
10. Schneidman-Duhovny D, Inbar Y, Nussinov R, & Wolfson HJ (2005) PatchDock and SymmDock: servers for rigid and symmetric docking. *Nucleic acids research* 33(Web Server issue):W363-367.
11. Lill MA & Danielson ML (2011) Computer-aided drug design platform using PyMOL. *Journal of computer-aided molecular design* 25(1):13-19.
12. Dollins DE, Immormino RM, & Gewirth DT (2005) Structure of unliganded GRP94, the endoplasmic reticulum Hsp90. Basis for nucleotide-induced conformational change. *The Journal of biological chemistry* 280(34):30438-30447.
13. Immormino RM, *et al.* (2004) Ligand-induced conformational shift in the N-terminal domain of GRP94, an Hsp90 chaperone. *The Journal of biological chemistry* 279(44):46162-46171.
14. Immormino RM, *et al.* (2009) Different poses for ligand and chaperone in inhibitor-bound Hsp90 and GRP94: implications for paralog-specific drug design. *Journal of molecular biology* 388(5):1033-1042.
15. Corbett KD & Berger JM (2010) Structure of the ATP-binding domain of Plasmodium falciparum Hsp90. *Proteins* 78(13):2738-2744.

16. Pallavi R, *et al.* (2010) Heat shock protein 90 as a drug target against protozoan infections: biochemical characterization of HSP90 from *Plasmodium falciparum* and *Trypanosoma evansi* and evaluation of its inhibitor as a candidate drug. *The Journal of biological chemistry* 285(49):37964-37975.
17. Edgar RC (2004) MUSCLE: a multiple sequence alignment method with reduced time and space complexity. *BMC bioinformatics* 5:113.
18. Bennett-Lovsey RM, Herbert AD, Sternberg MJ, & Kelley LA (2008) Exploring the extremes of sequence/structure space with ensemble fold recognition in the program Phyre. *Proteins* 70(3):611-625.
19. Anonymous (1994) The CCP4 suite: programs for protein crystallography. *Acta crystallographica. Section D, Biological crystallography* 50(Pt 5):760-763.
20. Emsley P, Lohkamp B, Scott WG, & Cowtan K (2010) Features and development of Coot. *Acta crystallographica. Section D, Biological crystallography* 66(Pt 4):486-501.
21. Shahinas D, Liang M, Datti A, & Pillai DR (2010) A repurposing strategy identifies novel synergistic inhibitors of *Plasmodium falciparum* heat shock protein 90. *Journal of medicinal chemistry* 53(9):3552-3557.
22. Norby JG (1988) Coupled assay of Na⁺,K⁺-ATPase activity. *Methods in enzymology* 156:116-119.
23. Crooks GE, Hon G, Chandonia JM, & Brenner SE (2004) WebLogo: a sequence logo generator. *Genome research* 14(6):1188-1190.
24. Rutherford SL & Lindquist S (1998) Hsp90 as a capacitor for morphological evolution. *Nature* 396(6709):336-342.
25. Chiosis G, Caldas Lopes E, & Solit D (2006) Heat shock protein-90 inhibitors: a chronicle from geldanamycin to today's agents. *Curr Opin Investig Drugs* 7(6):534-541.
26. Luo W, Sun W, Taldone T, Rodina A, & Chiosis G (2010) Heat shock protein 90 in neurodegenerative diseases. *Molecular neurodegeneration* 5:24.
27. Dollins DE, Warren JJ, Immormino RM, & Gewirth DT (2007) Structures of GRP94-nucleotide complexes reveal mechanistic differences between the hsp90 chaperones. *Molecular cell* 28(1):41-56.
28. Solit DB & Chiosis G (2008) Development and application of Hsp90 inhibitors. *Drug discovery today* 13(1-2):38-43.
29. Taldone T & Chiosis G (2009) Purine-scaffold Hsp90 inhibitors. *Current topics in medicinal chemistry* 9(15):1436-1446.
30. Cerchietti LC, *et al.* (2010) BCL6 repression of EP300 in human diffuse large B cell lymphoma cells provides a basis for rational combinatorial therapy. *The Journal of clinical investigation*.
31. Cerchietti LC, *et al.* (2009) A purine scaffold Hsp90 inhibitor destabilizes BCL-6 and has specific antitumor activity in BCL-6-dependent B cell lymphomas. *Nature medicine* 15(12):1369-1376.
32. Chiosis G, *et al.* (2003) Development of purine-scaffold small molecule inhibitors of Hsp90. *Current cancer drug targets* 3(5):371-376.

Chapter 5

THE ATP MIMETIC PU-H71 REVERSES ANTIMALARIAL RESISTANCE – INSIGHTS ON CELLULAR MECHANISMS

1 INTRODUCTION

As discussed so far, drug resistance is one of the major impediments to control *P. falciparum* malaria worldwide. Hsp90 is an essential component of the buffering capacity of eukaryotic cells in the event of stress. *P. falciparum* requires Hsp90 for cell cycle progression. The hypothesis here is that inhibition of PfHsp90 may be able to not only cripple the parasite but also serve as an adjunctive antimalarial by circumventing drug resistance. The reasoning is that this chaperone likely facilitates the proper expression of drug resistance factors such as efflux pumps. In the previous chapters, it was shown that Hsp90 inhibitors synergize with conventional antimicrobials such as CQ when used in combination. What remains unclear is the ability of PfHsp90 inhibitors to reverse antimalarial resistance and the mechanism of the synergistic phenotype.

To this end, the antimalarial activity of the purine analog PU-H71 was pursued as a potential antimalarial. Apart from its attractive pharmacokinetic profile and its potency (1-5), the use of an established and specific Hsp90 inhibitor facilitates the dissection of the role of Hsp90 in malaria. Given the success of PU-H71 in other diseases, the central hypothesis was that PU-H71 may serve well as an antimalarial with synergistic potential. In the experiments presented below, PU-H71 exhibited antimalarial activity in the nanomolar range, displayed synergistic activity with CQ, and was able to reverse CQ resistance in a cell-based assay using the CQR strain W2. PU-H71 is the first antimalarial that acts synergistically with an antimalarial in a drug-sensitive and drug-resistant background.

PU-H71 caused arrest at the ring stage during the intra-erythrocytic cycle. Co-immunoprecipitation analysis revealed that PfHsp90 interacts directly with the CQ resistance transporter (PfCRT). This finding suggests that the interaction of PfHsp90 with PfCRT underlies the synergistic phenotype and that PU-H71 may be an effective adjunctive antimalarial drug in combination therapies.

2 MATERIALS AND METHODS

2.1 *P. falciparum* Culture Methods and Antimalarial Cell Assay

The *P. falciparum* strains 3D7, W2 and Dd2 were grown in 5% hematocrit and RPMI 1640 medium supplemented with 0.25% Albumax II, 2 g/L sodium bicarbonate, 0.1 mM hypoxanthine, 25 mM HEPES (pH 7.5), 50 g/L gentamycin at 37°C, 5% O₂, and 6% CO₂. Growth inhibition of *P. falciparum* cultures was quantified using a flow cytometric assay(6). The cultures were synchronized with 5% sorbitol and grown for 48 hours. They were diluted to 1.0% rings and 0.5% hematocrit and cultured in the presence of each of the drugs or their combinations for 72 hours. The cultures were stained for 1 h at room temperature (RT) with 1× SYBR Green in phosphate buffered saline (PBS) pH 7.4 solution. Samples were analyzed with a Cytomics FC-500 MPL flow cytometer, (Beckman Coulter, Miami, FL). Inhibition of parasite growth in each sample was evaluated relative to infected erythrocytes without drug treatment (PBS alone). To establish the rings and mature flow cytometry gates, the parasites were sampled at the time points of 0, 6, 12, 24, 36 and 48 h. To test the heat shock response, the experimental schema was adapted from Pavithra *et al* (7). The parasites were heat shocked for 2 hours at 40°C. The temperature was restored to 37°C for 10 hours and parasites were then heat shocked for another 10 hours at 40°C. Rings and trophozoites were distinguished based on the gating established for the different points of the *P. falciparum* intra-erythrocytic cycle described above.

2.2 In vitro PU-H71 and chloroquine drug interactions.

In vitro drug interactions were defined as previously published antimalarial combinations (8-10). IC₅₀s and fractional IC₅₀s (FIC₅₀) were derived by dose-response curve fitting of the data from duplicate 72-hr assays. FIC₅₀ was determined using the formula $IC_{50}(A + \text{fixed } [B]) / IC_{50} \text{ of A alone}$. Average sum FIC₅₀ was determined by the sum of the ratio of the IC₅₀ of each drug in combination treatments over the IC₅₀ of each of the drug administered alone (i.e. $IC_{50}(A + \text{fixed } [B]) / IC_{50} \text{ of A alone} + IC_{50}(B + \text{fixed } [A]) / IC_{50} \text{ of B alone}$). Synergistic activity was defined by a sum FIC ratio ≤ 0.5 . In addition, the FIC₅₀ values were used to plot isobolograms, which display synergistic activity of the drugs if the points lie below the diagonal line that joins the FIC₅₀ points of 1 on each of the axes.

To determine the CQ potentiation effect of PU-H71 in both the CQ sensitive parasite line 3D7 and the CQ resistant line W2, the response modification index (RMI) was calculated using the formula $IC_{50}(CQ+PU-H71)/IC_{50}(CQ)$. An RMI of ≈ 1 denotes no change in antimalarial activity, whereas an RMI $\ll 1$ represents potentiation of antimalarial activity (i.e. synergistic activity) and an RMI $\gg 1$ is a sign of antagonistic activity (9, 10).

2.3 Parasite protein extraction

Plasmodium falciparum W2 culture (800 mL, mixed stages of parasites) at an average parasitemia of 9% was used for protein extraction. To purify the intact parasites, the red blood cells were lysed with 0.1% saponin and washed with PBS until the solution was translucent to eliminate most of the hemoglobin. The parasites were lysed on a nutator at 4°C for 1 hr in 2 mL of: 10 mM HEPES pH 7.5, 1.5 mM MgCl₂, 10 mM KCl, 10 μL benzamide hydrochloride, 10 μL protease inhibitor cocktail, 10 μL PMSF, 1% dodecylmaltoside (w/v). The lysed parasites were spun down at 14000 rpm for 30 minutes and the supernatant containing the soluble protein extract was used for co-immunoprecipitation.

2.4 Co-immunoprecipitation of PfHsp90 and PfCRT

The rabbit anti-PfHsp90 antibody was obtained from StressMarq Biosciences (Victoria, BC) and the rabbit anti-PfCRT antibody was obtained from the malaria resource centre (MR4). The corresponding (PfHsp90 or PfCRT) antibody (16 μg) was conjugated to 200 μL of protein A/G/L sepharose beads slurry (BioVision, Mountain View, CA) by incubation for 2 hr at room temperature on a rotator. After washing the unbound antibody with 0.1 M sodium borate pH 9.0, the antibody was conjugated to the beads with 20 mM dimethyl pimelimidate (DMP) in borate solution twice for 30 minutes. The beads were washed with 50 mM glycine at pH 2.5 and were further washed with PBS pH 7.4.

The conjugated antibody bead slurry as well as unbound beads (control) was incubated with 100 μg of the parasite protein extract for 4 h under rotation at 4°C. After centrifugation, the unbound protein solution was removed and the beads were washed 2× with 1% SDS, 5 mM EDTA pH 8.0 solution (denaturing conditions). The beads were boiled in this solution at 95°C for 5 minutes and were further analyzed with SDS-PAGE (12%) and Western blotting using a dilution of 1:2000 for the PfHsp90 antibody and 1:1000 for the PfCRT antibody. For the non-

denaturing condition elution, proteins bound to the beads were eluted with 0.1 M glycine, pH 2.5, and the samples were neutralized by adding 1 M Tris-HCl pH 9.0, and analyzed by native PAGE.

For the recombinant PfHsp90-interactor pulldown experiment, 50 µg of histidine-tagged full length PfHsp90 was incubated overnight at 4°C with 500 µL of Ni-NTA Superflow (Qiagen, Germantown, MD) bead slurry equilibrated in binding buffer (50 mM Tris-HCl pH 7.5, 150 mM NaCl, 10% glycerol, 10 mM imidazole). The next day, the PfHsp90 bound bead slurry was incubated with 100 µg of the parasite protein extract for 2 h under rotation at 4°C. The beads were washed twice with 1% SDS, 5 mM EDTA pH 8.0. The beads were boiled in this solution at 95°C for 5 minutes and the supernatant was further analyzed with SDS-PAGE (12%) and Western blotting using a dilution of 1:1000 for the PfCRT antibody.

2.5 LC-MS/MS Analysis

Bands from silver-stained and Coomassie stained gels of the denatured reciprocal immunoprecipitation supernatants were cut and submitted for in-gel trypsin digestion and LC-MS/MS analysis at the Advanced Protein Technology Centre at the Hospital for Sick Children (Dr. Li Zhang, Toronto, ON). The following report was generated from Scaffold v3.2 to report the protocol followed during the analysis: MS/MS samples were analyzed using Mascot (Matrix Science, London, UK; version Mascot). Mascot was set up to search the NCBI nr_20110813 database (selected for *Plasmodium falciparum*, 18091 entries) with the digestion enzyme trypsin. Mascot was searched with a fragment ion mass tolerance of 0.40 Da and a parent ion tolerance of 20 PPM. Iodoacetamide derivative of cysteine was specified in Mascot as a fixed modification. Pyro-glu from E of the N-terminus, s-carbamoyl methyl cysteine cyclization (N-terminus) of the N-terminus, deamidation of asparagine and glutamine, oxidation of methionine and acetylation of the N-terminus were specified in Mascot as variable modifications. Scaffold (version Scaffold_3.2.0, Proteome Software Inc., Portland, OR) was used to validate MS/MS based peptide and protein identifications. Peptide identifications were accepted if they could be established at greater than 50 % probability as specified by the Peptide Prophet algorithm (11). Protein identifications were accepted if they could be established at greater than 80 % probability and contained at least 1 identified peptide. Proteins that contained similar peptides and could not be differentiated based on MS/MS analysis alone were grouped to satisfy the principles of

parsimony. The proteins identified were cross-referenced to PlasmoDB (12) and the protein-protein interaction network was generated using Cytoscape v2.8 (13).

3 RESULTS

3.1 PU-H71 exhibits anti-malarial activity in *P.falciparum* cell culture, acts synergistically with chloroquine, and can reverse chloroquine resistance.

To determine the antimalarial potency of PU-H71, a cell-based anti-malarial assay was performed based on flow cytometric measurements of SYBR Green staining of *P. falciparum*-infected red blood cells. PU-H71 demonstrated a 50% inhibitory concentration (IC₅₀) of 111nM ± 8 nM (Figure 5-1) in the CQ-sensitive strain 3D7. PU-H71 was evaluated for synergy and resistance reversal in combination with the antimalarial chloroquine (CQ). Isobolograms were generated for the synergistic combination of each drug in the parasite strain 3D7 (Figure 5-2a) and in the CQ-resistant strain W2 (Figure 5-2b). Fractional inhibitory concentration (FIC) ratios were calculated as previously described (8-10), with synergy defined by an average sum FIC ratio for both drugs of ≤0.5. The axes of an isobologram are the ratios of the IC₅₀ of each of the drugs. An iso-effect curve in an isobologram, also known as an isobole, joins the points representing the iso-effective doses (doses corresponding to a constant effect level) of drug combinations in various combination mixtures. When the combination is additive, the isobole (i.e. line joining the points that represent all combinations with the same effect, including the equally effective concentrations of drug used alone) is a straight line. Synergistic combinations give concave isoboles and antagonistic combinations give convex isoboles. The degree of potentiation can be deduced by the extent of the curvature of the isobole towards the origin (10, 14).

Reversal of resistance in this study was defined by the ability to restore CQ susceptibility to the IC₅₀ range typically seen with the susceptible strain *P. falciparum* strain (3D7) and by a response modification index (RMI) << 1 to represent potentiation of CQ antimalarial activity (defined in Materials and Methods). A range between 0.4-0.5 sum FIC ratios was observed for 3D7 in the concentration range 1.25×10⁻¹¹ M to 1.25×10⁻⁷ M for each of the drugs (Figure 5-2a). With the CQ-resistant line W2, a sum FIC ratio range between 0.2-1.0 in the concentration range 1.25×10⁻¹¹ M to 1.25×10⁻⁷ M (Figure 5-2b). The RMI for CQ using the above drug combinations was in the range of 0.007-0.08 for 3D7 and 0.002-0.11 for W2 (Figure 5-3). This index

represents the extent to which PU-H71 modifies the CQ IC_{50} . PU-H71 strongly potentiates CQ both in the CQ-sensitive background (3D7) and in the CQ-resistant background (W2).

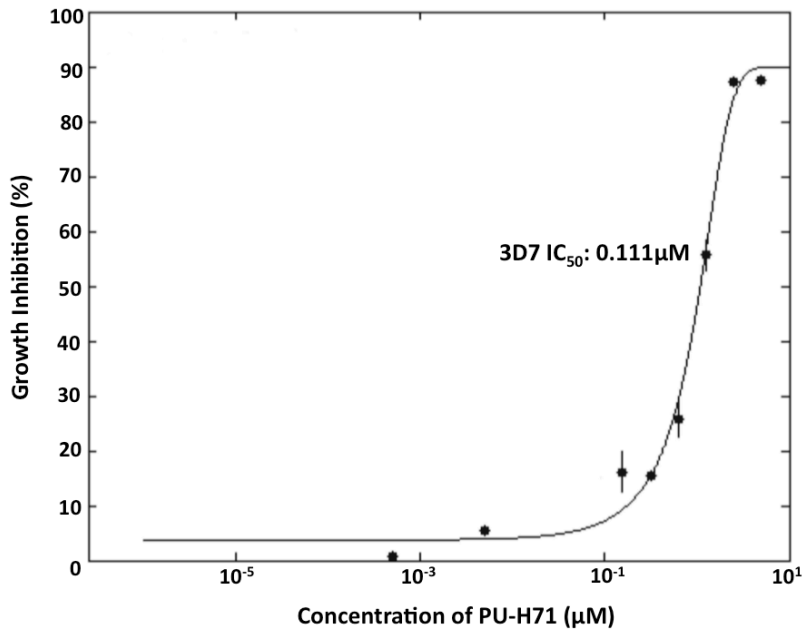


Figure 5-1: Antimalarial activity of PU-H71 using a standard SYBR Green cell based flow cytometry assay. The activity was tested in the laboratory strain 3D7 obtaining an IC₅₀ of 111 ± 8 nM (single experiment performed in duplicate).

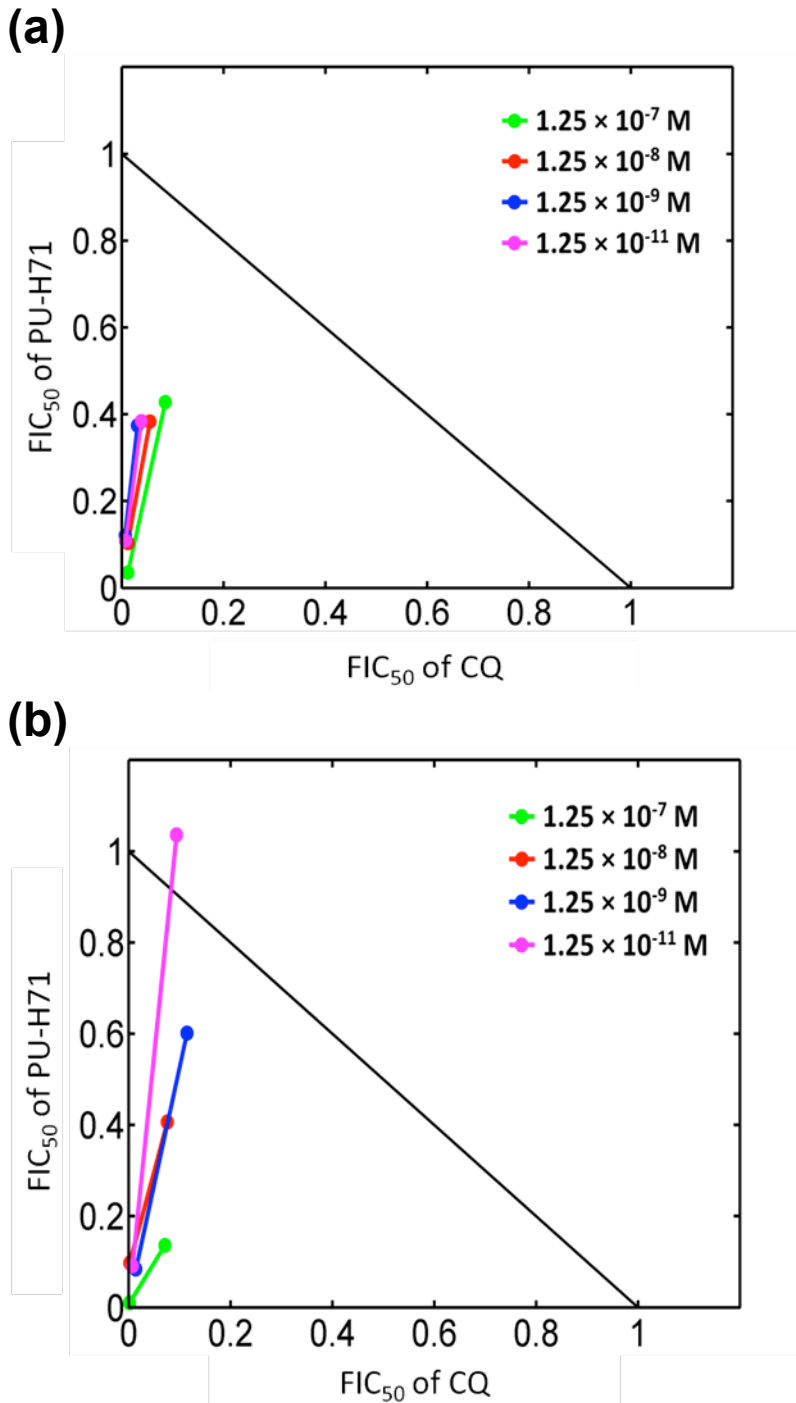


Figure 5-2: PU-H71 acts synergistically with chloroquine (CQ) in the laboratory *P. falciparum* 3D7 strain (a) and can reverse CQ resistance in the resistant strain W2 (b). Synergistic activity was defined by calculations of the average sum fractional inhibitory concentration ratio FIC₅₀ and by the FIC₅₀ ratios lying under the line of additivity in the diagrams shown here. The lines joining the points in the isobologram denote replicates. (a) Mean Σ FIC₅₀: 0.27 ± 0.19 (b) Mean Σ FIC₅₀: 0.40 ± 0.36

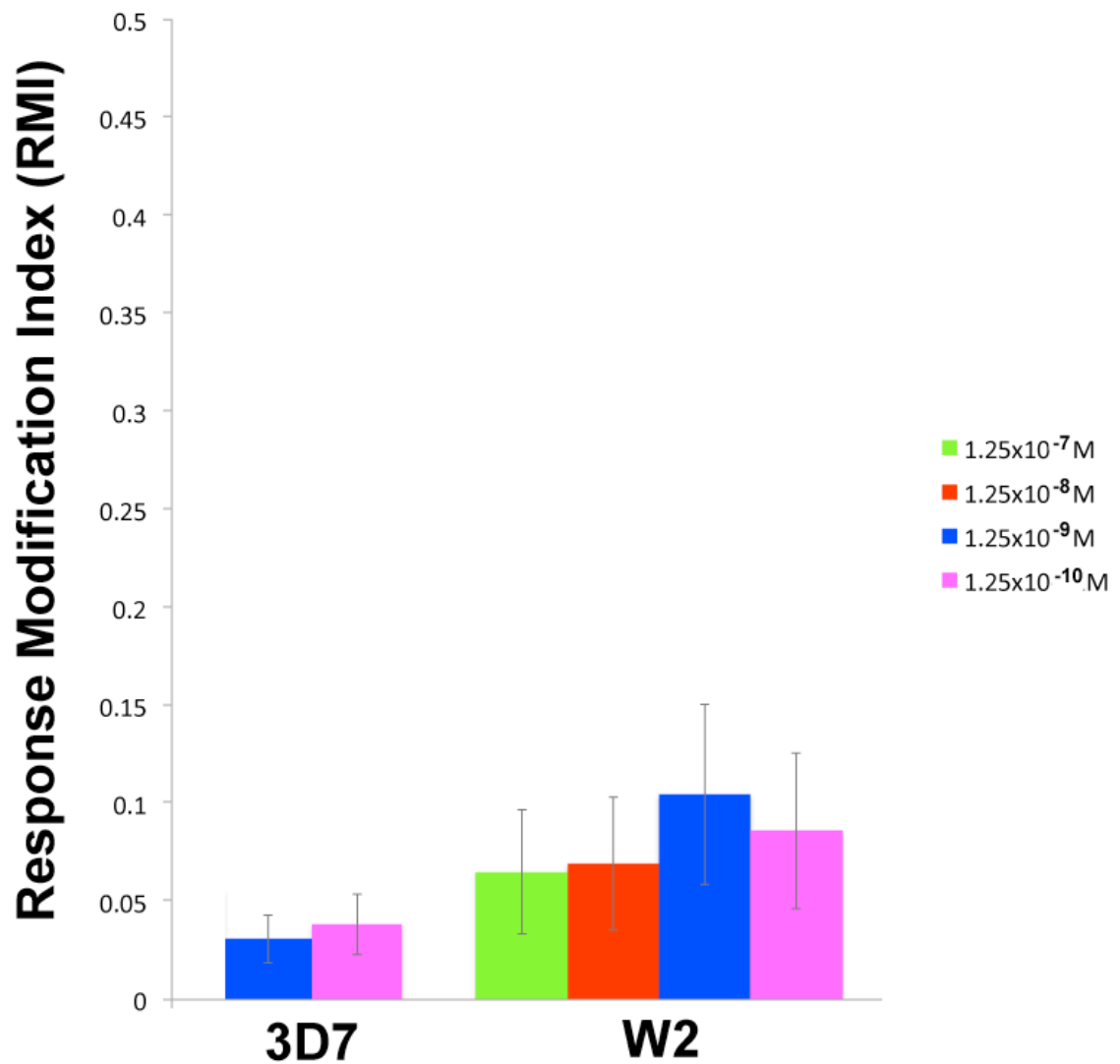


Figure 5-3: *PU-H71 potentiates chloroquine and reverses chloroquine resistance.* The PU-H71 resistance reversal and CQ potentiation activity was determined by a response modification index (RMI) $\ll 1$ (9, 10). The corresponding RMI is shown for each of the doses tested in both the CQ sensitive parasite line 3D7 and the CQ resistant line W2.

3.2 Immunoprecipitation studies demonstrate a direct association between PfHsp90 and PfCRT

To determine whether the mechanism of synergism with CQ and of CQ resistance reversal might be related to a direct interaction between PfCRT and PfHsp90, we performed co-immunoprecipitation of W2 parasite protein extracts with antibodies specific to PfHsp90 or PfCRT. Immunodetection of PfCRT was observed following anti-PfHsp90 immunoprecipitation under both non-denaturing (Figure 5-4) and denaturing conditions (Figure 5-5a). In the reciprocal experiment, PfHsp90 was immunodetected following immunoprecipitation when anti-PfCRT conjugated to sepharose beads was used with malaria extracts under both non-denaturing (Figure 5-4) and denaturing conditions (Figure 5-5a). Under denaturing conditions, a secondary band was present at ~60 kDa in addition to the expected bands for PfHsp90 (81 kDa) and PfCRT (50 kDa). Western blots of the parasite extracts confirmed the presence of PfHsp90 and PfCRT in the extracts (Figure 5-5b). It was hypothesized that the secondary band was remnant hemoglobin in the parasite extracts. Stripping of the blots and re-blotting confirmed the presence of hemoglobin at the observed size (Figure 5-5c).

In order to further confirm the direct association between PfCRT and PfHsp90, histidine tagged full length PfHsp90 was bound to Ni-NTA Superflow beads (Qiagen, Germantown, MD) and the bound beads were incubated with W2 parasite extracts. PfCRT was immunodetected from the denatured pulled down proteins (Figure 5-5d).

Additionally, it was shown that inhibition of PfHsp90 by PU-H71 for 24 h in cell culture resulted in loss of PfCRT protein, as would be expected based on Hsp90 client proteins being targeted for degradation upon its inhibition (15, 16) (Figure 5-6). In addition, a marked increase in the level of PfHsp90 protein is observed in the presence of PU-H71 inhibition.

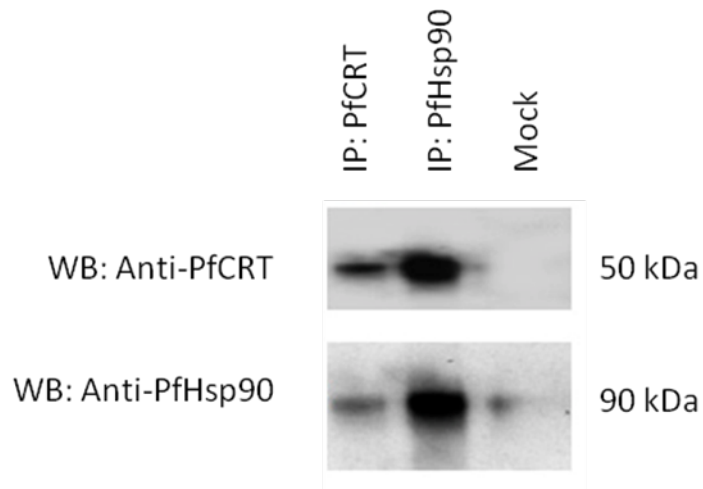
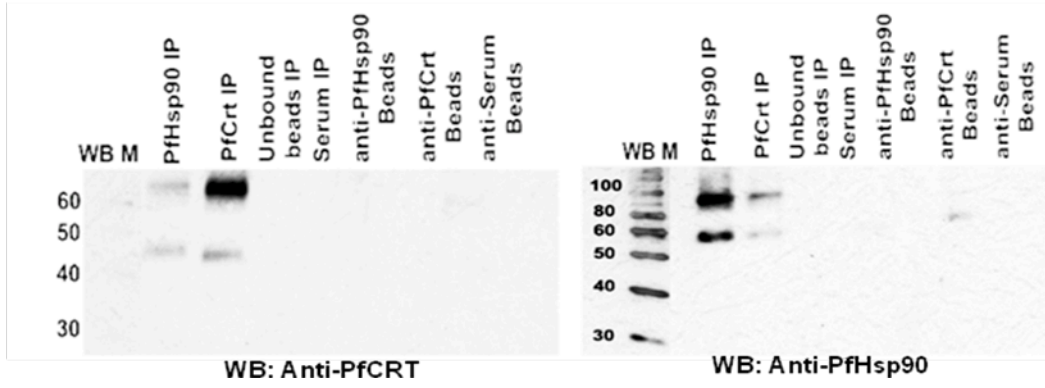
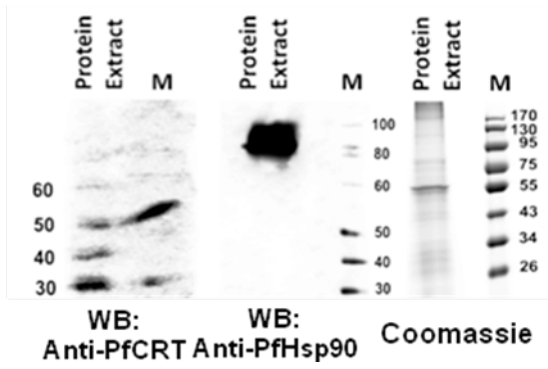


Figure 5-4: *PfHsp90* interacts with *PfCRT* based on co-immunoprecipitation studies. (A) Under non-denaturing conditions, immunoprecipitation with anti-PfHsp90 pulled down both itself and the *P. falciparum* Chloroquine resistance transporter (PfCRT), and the converse experiment with anti-PfCRT resulted in both itself and PfHsp90 being pulled down as compared to mock (beads alone plus extract).

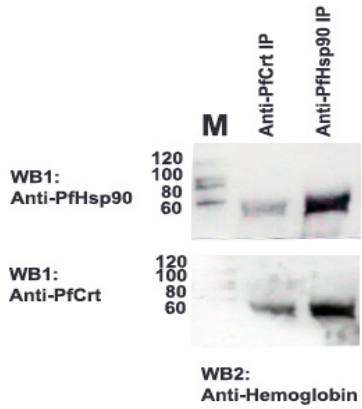
(a)



(b)



(c)



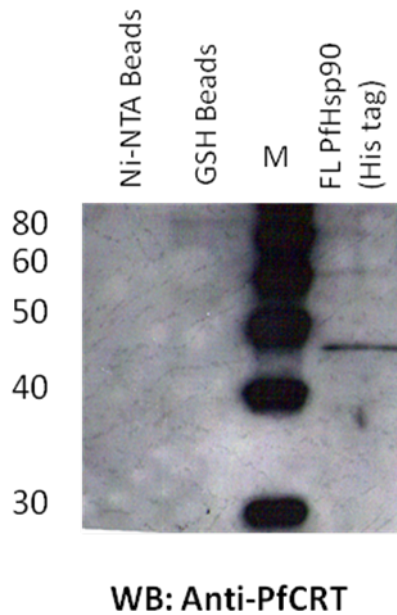
(d)

Figure 5-5: Co-immunoprecipitation of PfHsp90 and PfCRT under denaturing conditions. (a) Anti-PfCRT and Anti-PfHsp90 western blots of the immunoprecipitation proteins. Controls include from left to right: empty beads incubated with the extract, rabbit antiserum conjugated beads incubated with extract, denatured anti-PfHsp90 beads with no extract, denatured anti-PfCRT beads with no extract and denatured antiserum beads with no extract. (b) PfHsp90 and PfCRT are present in *P. falciparum* culture extracts. (c) Anti-hemoglobin western blot of stripped blots from (a) to determine the identity of the secondary band. (d) Anti-PfCRT western blot of pulled down proteins from histidine tagged full length PfHsp90 bound Ni-NTA beads. GSH Beads: Glutathione beads.

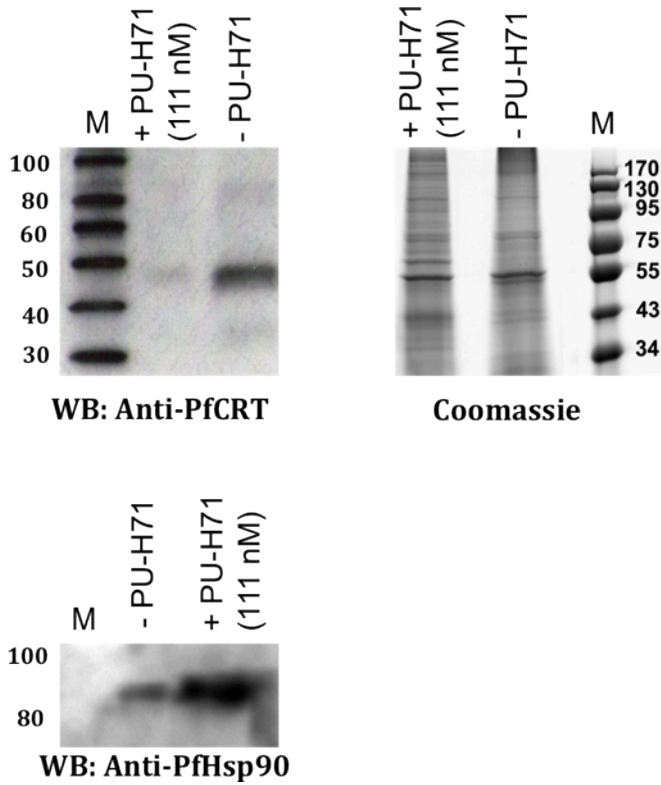


Figure 5-6: Treatment with PU-H71 lowers the level of PfCRT protein. Extracts from *P. falciparum* strain W2 treated and untreated with 111 nM PU-H71 (24 h) and immunoblotted with anti-PfCRT and anti-PfHsp90 antibody to determine the level of PfCRT. The Coomassie stained gel has been included to show equal loading (24 μ g/lane).

LC-MS/MS analysis of co-immunoprecipitated proteins confirms the association of PfCRT and PfHsp90

Analysis by LC-MS/MS of co-immunoprecipitation gel bands subjected to tryptic digestion identified a total of 148 proteins from the anti-PfCRT pulldown and 187 proteins from the anti-PfCRT pulldown (Appendix 3). Apart from confirming the association between PfHsp90 and PfCRT, several of the identified proteins were known interactors of PfHsp90 and PfCRT based on previous protein-protein interaction studies, key among which are the association of PfHsp90 with PfHsp70, PfHsp60, cyclophilin, Hsp70/Hsp90 organizing protein (HOP) (17, 18). The protein interactions were visualized and clustered by molecular function using Cytoscape (13) and Gene Ontology (GO) (Figure 5-7). As expected, apart from a major cell signalling cluster (28.1% of all proteins identified) consisting of protein kinases and transcription factors, a virulence cluster (16.7%) including major factors such as erythrocyte membrane protein 1 (EMP1), apical membrane antigen 1 (AMA1), erythrocyte binding antigen 165 (EBA-165), merozoite surface protein 1 and 7 (MSP1, MSP7) and other drug resistance associated proteins apart from PfCRT were part of the constructed network such as: multidrug resistance transporter 1 (MDR1) and Cg4. Of particular interest in this analysis was the protein degradation cluster consisting of proteasome subunits, ubiquitin ligase, ubiquitin hydrolase and peptidases because it is consistent with previous association of this machinery with Hsp90 in other eukaryotes for the targeting of misfolded client proteins for degradation (19, 20). In accordance with the role of PfHsp90 in chaperoning stress-induced proteins as opposed to primary protein folding, the identified clusters of proteins participating in metabolism and translation were relatively small. A reconstruction of the PfHsp90 interactome model with previously known interactors that were present in this LC-MS/MS analysis is shown in Figure 5-8.

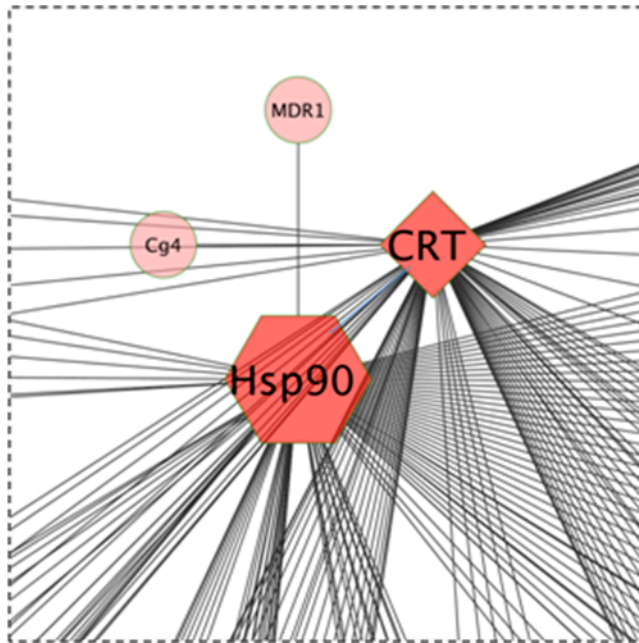
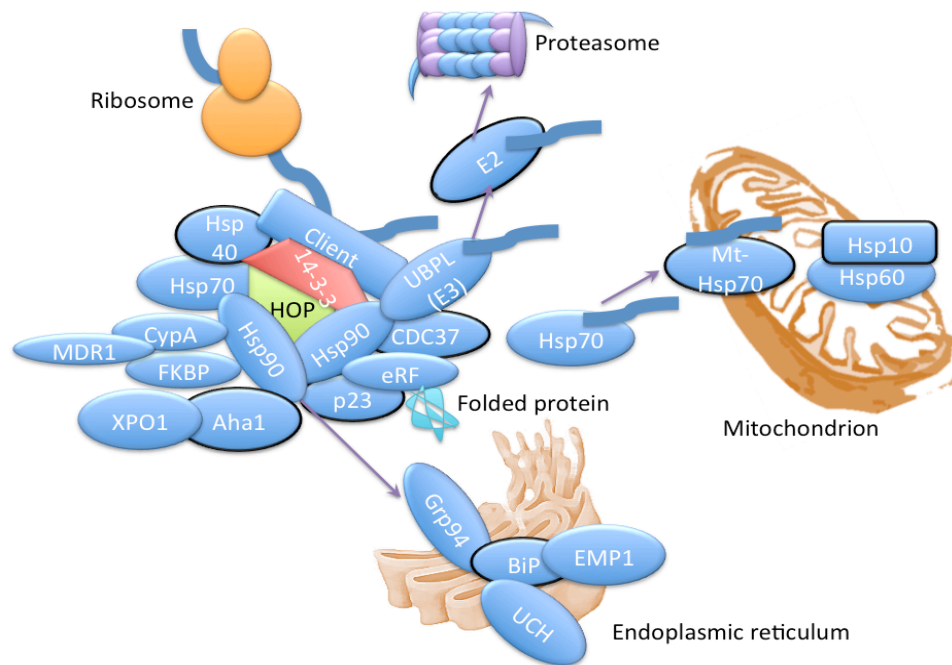
(b)

Figure 5-7: Unweighted protein-protein interaction network of LC-MS/MS analyzed PfHsp90 and PfCRT co-immunoprecipitated proteins. (a) The image was generated using Cytoscape v2.8. For the list of the members of each cluster, please see Appendix 3. (b) An enlarged excerpt of the interaction network that depicts the interaction between PfHsp90 and PfCRT.



Client

DNA helicase

Lactate dehydrogenase

Triosephosphate isomerase

Fructose-bisphosphate aldolase A

Glyceraldehyde 3-phosphate dehydrogenase

Phosphatidylinositol 3-and 4-kinase

Proliferating cell nuclear antigen

Chloroquine resistance factor Cg4

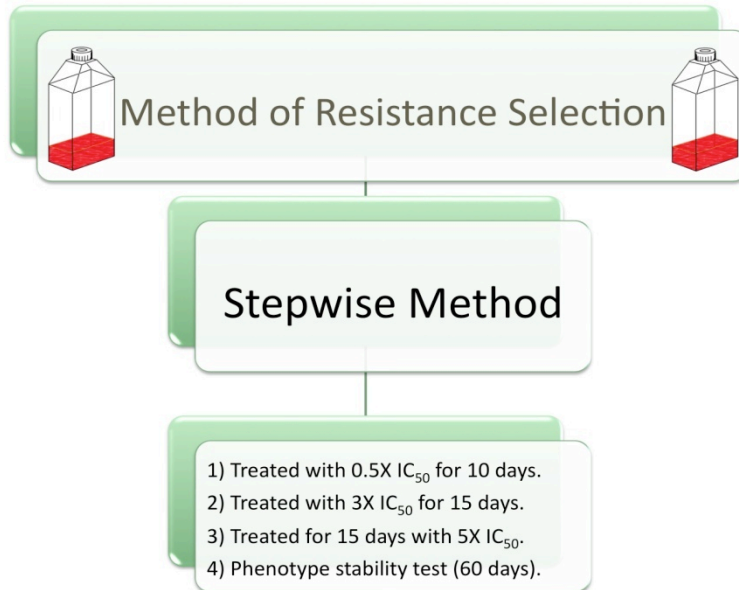
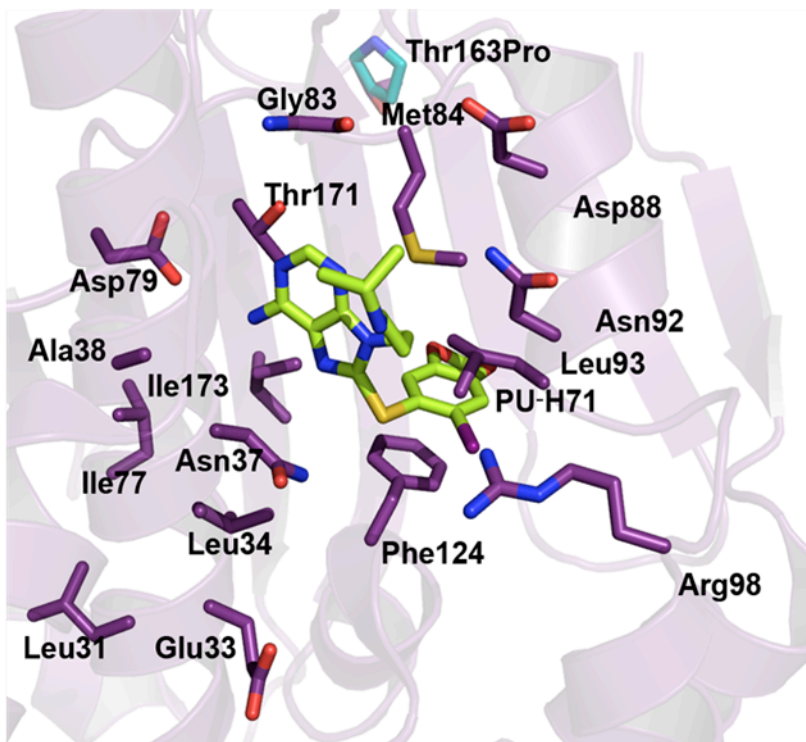
Chloroquine resistance transporter (CRT)

Multidrug resistance transporter 1 (MDR1)

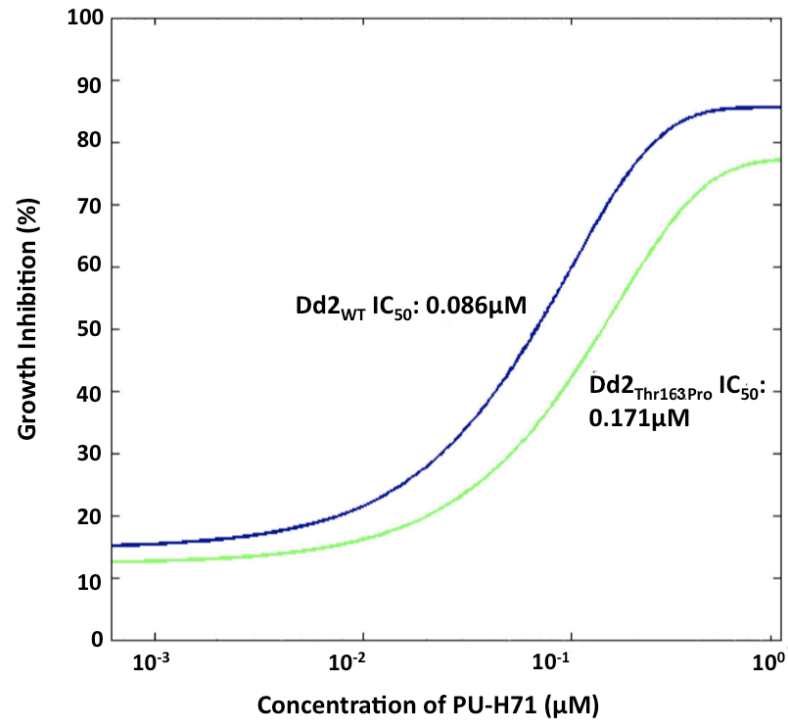
Figure 5-8: A simplified model of the PfHsp90 interactome as witnessed from the LC-MS/MS analysis and verified by published literature. The interactors shown with a black outline have been included for completion. They were not present in the list of identified interactors from the LC-MS/MS analysis. Client refers to any protein that requires the chaperone activity of PfHsp90 for folding. CRT and MDR1 are introduced in this study as novel clients.

3.3 Resistance selection results in an ATP binding domain mutant with elevated PU-H71 IC₅₀

In order to test the hypothesis that the PfHsp90 ATP-binding domain is the specific target of PU-H71, a step-wise resistance selection method was implemented (based on the work of Sidhu *et al.* (21)). Using this method, 1.25×10^8 parasites underwent selection with increasing concentrations of compound ranging from $0.5 \times$ to $5 \times$ IC₅₀ concentrations in a step-wise fashion (Figure 5-9a). After several months, a single strain was identified in the presence of Hsp90 inhibitor APPA (22). DNA sequencing analysis of the Hsp90 ATP-binding domain showed that this mutant line contains a Thr163Pro mutation. This mutation was located close to the ATP-binding pocket as shown by homology modeling (Figure 5-9b). The IC₅₀ of PU-H71 was elevated from 86 nM in the unselected Dd2 strain to 171 nM in the mutant Dd2^{T163P} strain (Figure 5-9c). Despite the elevation in the IC₅₀ of PU-H71, synergy, as defined by the calculated FIC and isobologram analysis, was still observed between CQ and PU-H71 (Figure 5-9).

(a)**(b)**

(c)



(d)

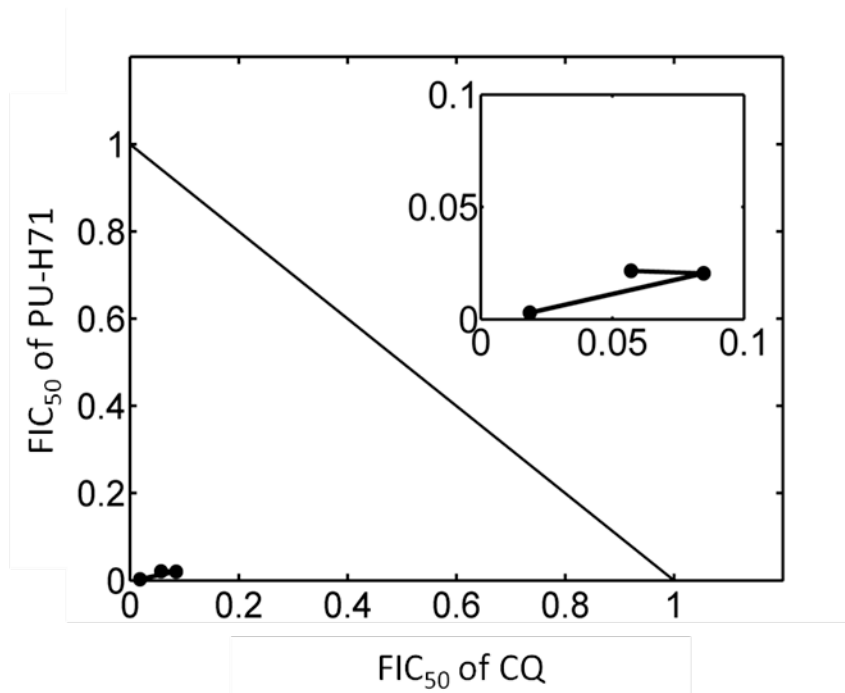
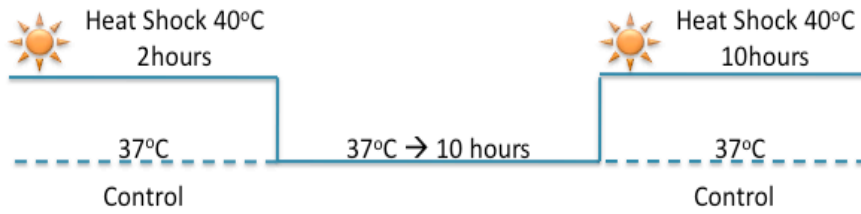


Figure 5-9: *A step-wise selection method was used to generate the PfHsp90 Thr163Pro mutant in strain Dd2. (a) An illustration of the selection method. (b) The mutation is depicted in the model structure of the ATP-binding domain. (c) The presence of this mutation resulted in doubling of the PU-H71 IC₅₀ in the cell-based assay. (d) Synergy between PU-H71 and CQ in the Thr163Pro mutant was observed. The inset provides a magnified view of the FIC₅₀ ratios for the different PU-H71 and CQ drug combinations.*

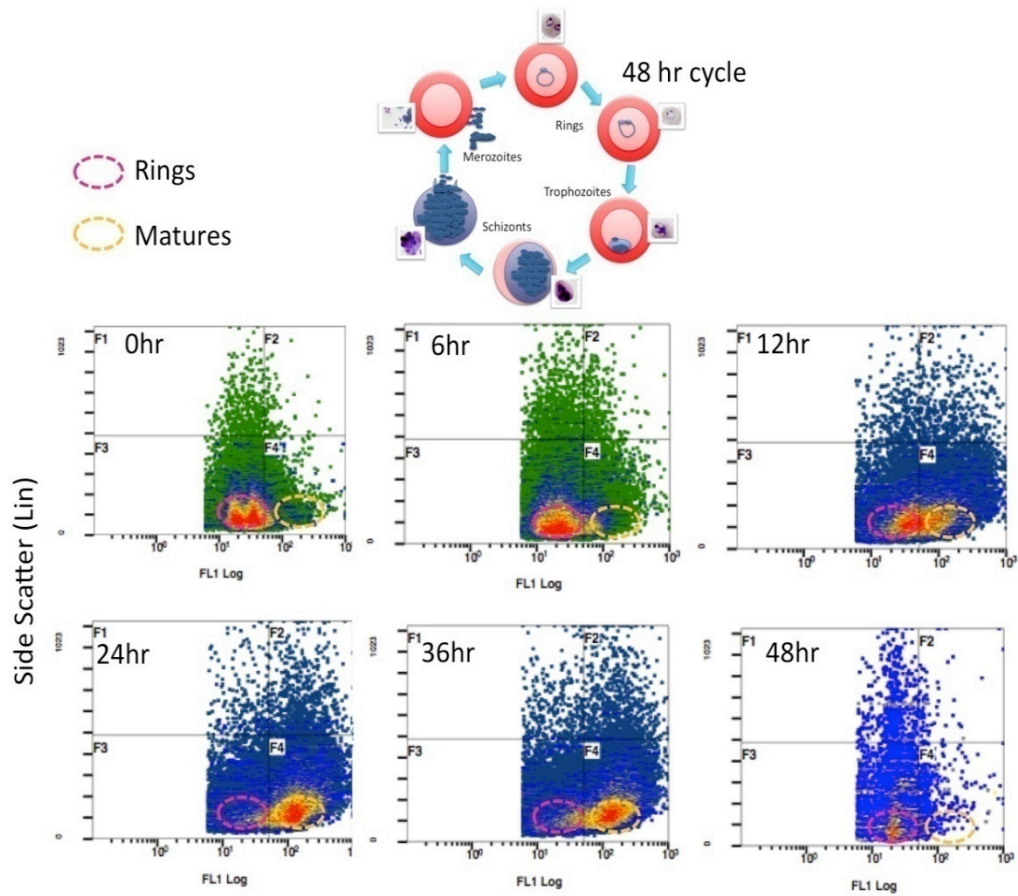
3.4 PU-H71 arrests growth at the ring stage in the erythrocytic cycle

The activity of PU-H71 was tested in a heat shock assay to determine its ability to arrest the transition of early ring-stage parasites to more mature trophozoite stages during the intra-erythrocytic lifecycle, a phenotype observed with other Hsp90 inhibitors (7). Using a heat shock experimental schema adapted from Pavithra *et al.* (7) (Figure 5-10a), parasites were heat shocked for 2 hours at 40°C. The temperature was restored to 37°C for 10 hours and parasites were then heat shocked for another 10 hours at 40°C. Rings and trophozoites were distinguished based on a SYBR green fluorescence assay using flow cytometry, which detects the higher DNA content in mature stage parasites (Figure 5-10b). Gating of the ring and mature stage parasites based on SYBR Green fluorescence shifts is shown in Figure 5-10b. Counts in each stage-specific gate were used to quantify populations in the presence and absence of heat shock and in the presence and absence of PU-H71 as shown in Figure 5-10c. In the presence of heat shock stress, a significant increase in mature stage parasite progression was observed. Treatment with PU-H71 was marked by a significant reduction of progression to the mature stage under normal conditions (Unpaired two-tailed Student's t-Test $p < 0.05$). Following heat shock stress, PU-H71 was able to reduce progression to the mature stage but to a lesser degree. Similar experiments were conducted with CQ, which did not exhibit this phenotype.

(a)



(b)



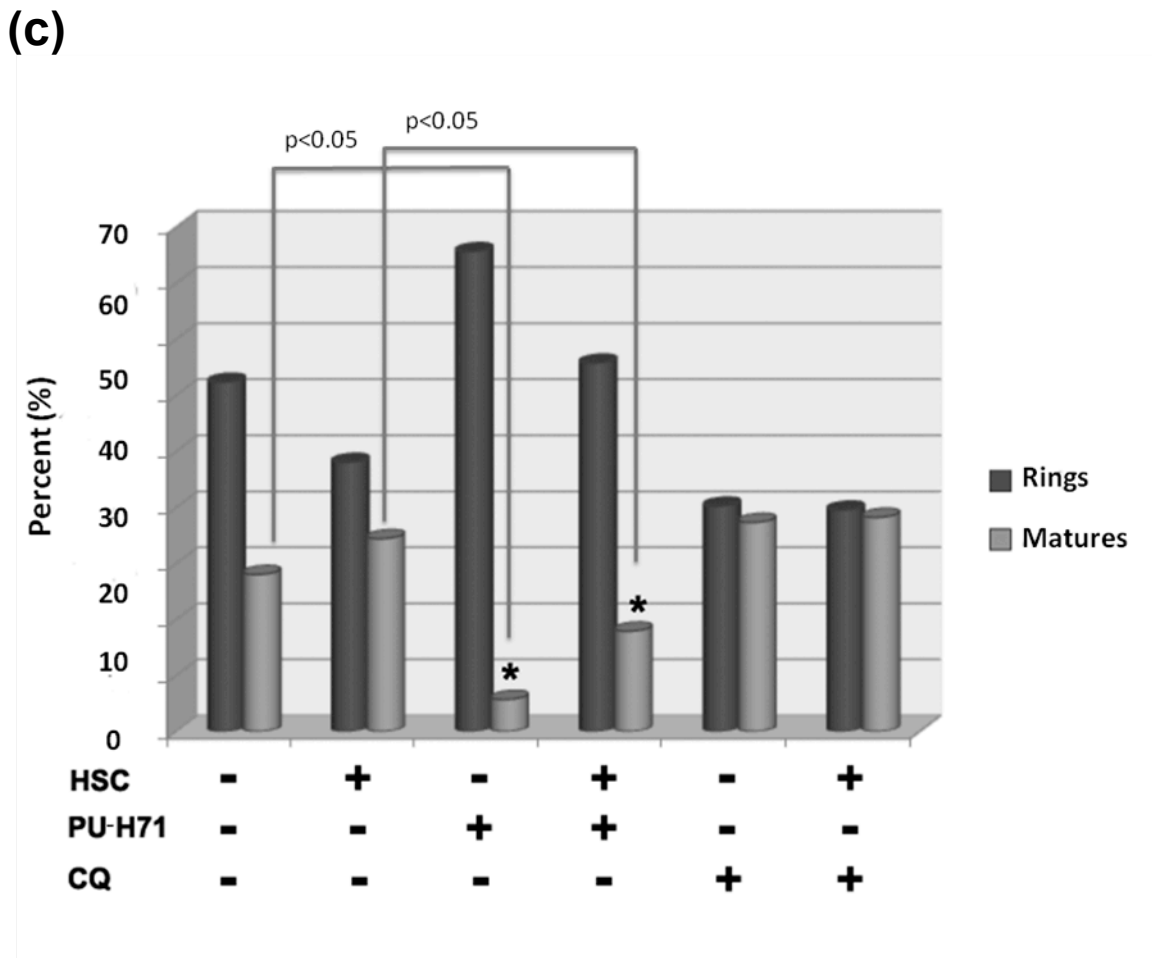


Figure 5-10: *PU-H71 slows down transition of rings to matures: a feature of Hsp90 inhibitors in malaria.* (a) Scheme of heat shock stress (HSC) was followed as previously published to simulate malaria febrile episodes. (b) This sample experiment depicts separation of rings and mature parasites using flow cytometry during a normal 48 hour life cycle of *P. falciparum* in culture. The red circle gate captures rings and the yellow circle, the mature parasites. The gradient of green-blue-yellow-red of the dots in the background represents the intensity of counted events in that particular area of the plot. (c) Quantification of rings and matures in the presence and absence of HSC or drug (after the full 22 hr period shown in (a) using flow cytometry. *Significance relative to no drug controls. (Unpaired two-tailed Student's t-test $p < 0.05$) $n = 2$. A representative replicate is shown in (c). No significant difference was observed with CQ in the progression of rings to matures.

4 DISCUSSION

P. falciparum causes the most severe form of human malaria (17, 23). Eradication of malaria has been precluded in part by the development of drug resistance to several classes of antimalarials. Evolution of resistance to artemisinins (24, 25), the mainstay of current treatment for malaria, bodes poorly for this class of drugs as with previously recommended agents. Combination therapies appear less prone to resistance, but the pharmacodynamic approach of synergistic agents has not been explored fully and mechanistically in malaria. We and others have previously shown that targeting Hsp90, a central chaperone that serves as a buffer under stress conditions, e.g., heat shock, can be potentially synergistic in various diseases (26-31). The fact that malaria parasites have a life cycle that occurs in two physiologically diverse habitats (cold-blooded mosquito and warm-blooded human hosts) suggests that a robust adaptation mechanism must exist to manage the heat shock caused by the change of host as well as by intense febrile episodes in the human host during severe infection. Therefore crippling Hsp90, a central player in this response, is likely inimical to the health of the parasite.

While others have demonstrated the antimalarial properties of inhibiting Hsp90 using a GA derivative (32), our focus was on the synergistic potential of this molecule in recovering the activity of CQ. Additionally, because of the toxicity associated with GA and its derivatives, our strategy was to repurpose a novel purine scaffold inhibitor (PU-H71) (33) that was selected on the basis of docking studies with the PfHsp90 crystal structure (Chapter 4). PU-H71 is in phase I clinical trials against various neoplastic diseases and has shown no toxicity at therapeutic doses (33).

PU-H71 is an effective killer of *P. falciparum* *in vitro* with an IC_{50} in the nanomolar range. In keeping with our hypothesis and previous studies in *C. albicans* (34-37) that inhibiting Hsp90 should recoup the activity of other key antimalarials, PU-H71 is synergistic with CQ and was able to reverse CQ resistance in the resistant strain W2, suggesting that PfHsp90 may be an important hub molecule for CQ resistance-associated pathways in malaria, as seen also with the LC-MS/MS analysis of co-immunoprecipitated proteins. This is akin to the phenotype observed in *C. albicans* by Cowen et al. where reversal of azole and echinocandin resistance was achieved using Hsp90 inhibitors *in vitro* (34-37). In order to determine whether the synergistic phenotype and resistance reversal by PfHsp90 inhibitors are based on direct or indirect physical interactions

with putative resistance factors, co-immunoprecipitation studies were carried out. These data demonstrate that a direct physical interaction occurs between the CQ transporter PfCRT and PfHsp90. We speculate that disrupting this interaction would lead to the early degradation of PfCRT, which would reduce the levels of PfCRT at the digestive vacuole membrane. The identification of protein degradation machinery proteins as one of the major clusters of the LC-MS/MS analysis from the co-immunoprecipitation hits is consistent with the hypothesis that inhibition of PfHsp90 by PU-H71 would target misfolded PfCRT for degradation. The caveat in this case is the arrest of the parasites in the ring stage and being able to delineate the effect of this arrest on the rate of PfCRT protein translation. Future studies will focus on fully elaborating this interaction and further dissecting the pathway between PfHsp90 and PfCRT expression. Co-localization studies may provide more insight in this association.

In vitro, PU-H71 inhibition was seen to arrest parasites at the ring stage, a phenotype reported previously for Hsp90 inhibitors by Pavithra *et al.* (7). The elevated PU-H71 IC₅₀ in the selected Dd2^{T163P} mutant further suggests the specificity of this purine analog in targeting PfHsp90. We suspect that the essential nature of Hsp90 precludes the facile generation of mutants in the critical ATP-binding domain. The marginal lowering of the IC₅₀ may be explained by the fact that this mutant Hsp90 molecule is still able to bind ATP for cell survival. The reduced number of mature parasites following heat shock suggests that this strain may have a defect in early stage progression, suggesting that the mutation alters the normal stress response (7, 38). A null mutant is almost certainly lethal as observed in other eukaryotic systems (39). An Hsp90 knockdown strategy has been unsuccessful, likely because attempts in every system to date have resulted in non-viability (40, 41). Of concern was the previous observation that although inhibition of *Leishmania donovani* by GA was effective, some mutants survived, presumably through episomal amplification of the Hsp90 gene (42). Gene amplification has been previously reported for *P. falciparum* (43), and is therefore a possible mechanism of resistance to Hsp90 inhibitors. From a therapeutic standpoint, despite the elevated IC₅₀ in response to resistance selection in this study, we still observed the synergistic activity of PU-H71 with CQ.

PU-H71 strongly potentiates CQ against the CQS line 3D7 and the CQR line W2. This response is unlike previously known CQ resistance reversal agents such as the calcium channel blockers verapamil, amlodipine, and diltiazem, which only potentiate CQ against a CQR background, but not a CQS background (9, 44). As described in chapter 3, harmine also synergized with

chloroquine both in the CQS line 3D7 and the CQR line W2. This finding with two PfHsp90 inhibitors may represent a unique feature of PfHsp90 inhibitors as adjunctive, synergistic agents with CQ. Even though the direct association of PfHsp90 with PfCRT may explain the synergistic activity of PfHsp90 inhibitors with CQ in a CQR background, it is more difficult to rationalize this chemical interaction in a CQS background. Previous evidence suggests that up regulation of PfCRT levels is not required for resistance. In addition, Sidhu *et al.* conducted allelic exchange experiments that replaced endogenous *pfcr*t alleles of a CQS line with *pfcr*t alleles of CQR lines from Asia, Africa and South America. They concluded that mutations of the *pfcr*t gene may be sufficient to explain the full phenotype of CQR and provide chemosensitization to verapamil. Therefore, the folding of the PfCRT protein by PfHsp90 may not be sufficient to explain the synergistic activity.

In yeast, pharmacological stress by the quinoline ring containing antimalarials such as CQ, mefloquine and quinidine activated the Hsp90-STI1 complex. Cross resistance assays in yeast determined that the Hsp90 co-chaperone STI1 conferred resistance to mefloquine (3.4-fold) (45). This finding suggests that in the case of malaria, treatment of infected red blood cells with chloroquine may trigger the activation of the PfHsp90 chaperone activity both in CQS and CQR strains. Inhibition of the PfHsp90 activity may hinder the folding of client proteins that are involved in mounting a response to pharmacological stress in the cell, leading to collateral arrest of the infected cell activities. In addition, the mass spec analysis of the PfHsp90 interactors revealed association of PfHsp90 with hemoglobin degradation proteases such as plasmepsins. Increased CQ sensitivity was also observed with genetic ablation of plasmepsins (46), potentially due to the additive formation of toxic byproducts in the absence of hemozoin formation. Therefore, inhibition of PfHsp90 may contribute to reduced levels of plasmepsins leading to hemozoin accumulation, which is further bound by CQ and cannot be incorporated into the inert hemozoin crystal.

References

1. Cerchietti LC, *et al.* (2009) A purine scaffold Hsp90 inhibitor destabilizes BCL-6 and has specific antitumor activity in BCL-6-dependent B cell lymphomas. *Nature medicine* 15(12):1369-1376.
2. Solit DB & Chiosis G (2008) Development and application of Hsp90 inhibitors. *Drug discovery today* 13(1-2):38-43.
3. Taldone T & Chiosis G (2009) Purine-scaffold Hsp90 inhibitors. *Current topics in medicinal chemistry* 9(15):1436-1446.
4. Usmani SZ, Bona RD, Chiosis G, & Li Z (2010) The anti-myeloma activity of a novel purine scaffold HSP90 inhibitor PU-H71 is via inhibition of both HSP90A and HSP90B1. *Journal of hematology & oncology* 3:40.
5. Usmani SZ & Chiosis G (2011) HSP90 inhibitors as therapy for multiple myeloma. *Clinical lymphoma, myeloma & leukemia* 11 Suppl 1:S77-81.
6. Johnson JD, *et al.* (2007) Assessment and continued validation of the malaria SYBR green I-based fluorescence assay for use in malaria drug screening. *Antimicrobial agents and chemotherapy* 51(6):1926-1933.
7. Pavithra SR, Banumathy G, Joy O, Singh V, & Tatu U (2004) Recurrent fever promotes Plasmodium falciparum development in human erythrocytes. *The Journal of biological chemistry* 279(45):46692-46699.
8. Mishra LC, Bhattacharya A, & Bhasin VK (2007) Antiplasmodial interactions between artemisinin and triclosan or ketoconazole combinations against blood stages of Plasmodium falciparum in vitro. *The American journal of tropical medicine and hygiene* 76(3):497-501.
9. Pereira MR, *et al.* (2011) In vivo and in vitro antimalarial properties of azithromycin-chloroquine combinations that include the resistance reversal agent amlodipine. *Antimicrobial agents and chemotherapy* 55(7):3115-3124.
10. Bell A (2005) Antimalarial drug synergism and antagonism: mechanistic and clinical significance. *FEMS microbiology letters* 253(2):171-184.
11. Keller A, Nesvizhskii AI, Kolker E, & Aebersold R (2002) Empirical statistical model to estimate the accuracy of peptide identifications made by MS/MS and database search. *Analytical chemistry* 74(20):5383-5392.
12. Aurecochea C, *et al.* (2009) PlasmoDB: a functional genomic database for malaria parasites. *Nucleic acids research* 37(Database issue):D539-543.
13. Smoot ME, Ono K, Ruscheinski J, Wang PL, & Ideker T (2011) Cytoscape 2.8: new features for data integration and network visualization. *Bioinformatics* 27(3):431-432.
14. Fidock DA, Rosenthal PJ, Croft SL, Brun R, & Nwaka S (2004) Antimalarial drug discovery: efficacy models for compound screening. *Nature reviews. Drug discovery* 3(6):509-520.

15. da Rocha Dias S, *et al.* (2005) Activated B-RAF is an Hsp90 client protein that is targeted by the anticancer drug 17-allylamino-17-demethoxygeldanamycin. *Cancer research* 65(23):10686-10691.
16. Workman P (2004) Combinatorial attack on multistep oncogenesis by inhibiting the Hsp90 molecular chaperone. *Cancer letters* 206(2):149-157.
17. Shonhai A (2010) Plasmodial heat shock proteins: targets for chemotherapy. *FEMS immunology and medical microbiology* 58(1):61-74.
18. Pavithra SR, Kumar R, & Tatu U (2007) Systems analysis of chaperone networks in the malarial parasite *Plasmodium falciparum*. *PLoS computational biology* 3(9):1701-1715.
19. Blagg BS & Kerr TD (2006) Hsp90 inhibitors: small molecules that transform the Hsp90 protein folding machinery into a catalyst for protein degradation. *Medicinal research reviews* 26(3):310-338.
20. Galigniana MD, *et al.* (2004) Retrograde transport of the glucocorticoid receptor in neurites requires dynamic assembly of complexes with the protein chaperone hsp90 and is linked to the CHIP component of the machinery for proteasomal degradation. *Brain research. Molecular brain research* 123(1-2):27-36.
21. Sidhu AB, *et al.* (2007) In vitro efficacy, resistance selection, and structural modeling studies implicate the malarial parasite apicoplast as the target of azithromycin. *The Journal of biological chemistry* 282(4):2494-2504.
22. Shahinas D, Liang M, Datti A, & Pillai DR (2010) A repurposing strategy identifies novel synergistic inhibitors of *Plasmodium falciparum* heat shock protein 90. *Journal of medicinal chemistry* 53(9):3552-3557.
23. Wellems TE & Miller LH (2003) Two worlds of malaria. *N Engl J Med* 349(16):1496-1498.
24. Noedl H, Socheat D, & Satimai W (2009) Artemisinin-resistant malaria in Asia. *The New England journal of medicine* 361(5):540-541.
25. Noedl H, *et al.* (2008) Evidence of artemisinin-resistant malaria in western Cambodia. *The New England journal of medicine* 359(24):2619-2620.
26. Chiosis G (2006) Targeting chaperones in transformed systems--a focus on Hsp90 and cancer. *Expert Opin Ther Targets* 10(1):37-50.
27. Chiosis G, Caldas Lopes E, & Solit D (2006) Heat shock protein-90 inhibitors: a chronicle from geldanamycin to today's agents. *Curr Opin Investig Drugs* 7(6):534-541.
28. Chiosis G, Lucas B, Shtil A, Huezio H, & Rosen N (2002) Development of a purine-scaffold novel class of Hsp90 binders that inhibit the proliferation of cancer cells and induce the degradation of Her2 tyrosine kinase. *Bioorg Med Chem* 10(11):3555-3564.
29. Luo W, Sun W, Taldone T, Rodina A, & Chiosis G (Heat shock protein 90 in neurodegenerative diseases. *Mol Neurodegener* 5:24.
30. Luo W, *et al.* (2007) Roles of heat-shock protein 90 in maintaining and facilitating the neurodegenerative phenotype in tauopathies. *Proc Natl Acad Sci U S A* 104(22):9511-9516.

31. Taldone T, *et al.* (Assay strategies for the discovery and validation of therapeutics targeting *Brugia pahangi* Hsp90. *PLoS Negl Trop Dis* 4(6):e714.
32. Pallavi R, *et al.* (2010) Heat shock protein 90 as a drug target against protozoan infections: biochemical characterization of HSP90 from *Plasmodium falciparum* and *Trypanosoma evansi* and evaluation of its inhibitor as a candidate drug. *The Journal of biological chemistry* 285(49):37964-37975.
33. Caldas-Lopes E, *et al.* (2009) Hsp90 inhibitor PU-H71, a multimodal inhibitor of malignancy, induces complete responses in triple-negative breast cancer models. *Proc Natl Acad Sci U S A* 106(20):8368-8373.
34. Cowen LE, Carpenter AE, Matangkasombut O, Fink GR, & Lindquist S (2006) Genetic architecture of Hsp90-dependent drug resistance. *Eukaryot Cell* 5(12):2184-2188.
35. Cowen LE & Lindquist S (2005) Hsp90 potentiates the rapid evolution of new traits: drug resistance in diverse fungi. *Science* 309(5744):2185-2189.
36. Cowen LE, *et al.* (2009) Harnessing Hsp90 function as a powerful, broadly effective therapeutic strategy for fungal infectious disease. *Proceedings of the National Academy of Sciences of the United States of America* 106(8):2818-2823.
37. Singh SD, *et al.* (2009) Hsp90 governs echinocandin resistance in the pathogenic yeast *Candida albicans* via calcineurin. *PLoS pathogens* 5(7):e1000532.
38. Acharya P, Kumar R, & Tatu U (2007) Chaperoning a cellular upheaval in malaria: heat shock proteins in *Plasmodium falciparum*. *Molecular and biochemical parasitology* 153(2):85-94.
39. Rutherford SL & Lindquist S (1998) Hsp90 as a capacitor for morphological evolution. *Nature* 396(6709):336-342.
40. Birnby DA, *et al.* (2000) A transmembrane guanylyl cyclase (DAF-11) and Hsp90 (DAF-21) regulate a common set of chemosensory behaviors in *Caenorhabditis elegans*. *Genetics* 155(1):85-104.
41. Borkovich KA, Farrelly FW, Finkelstein DB, Taulien J, & Lindquist S (1989) hsp82 is an essential protein that is required in higher concentrations for growth of cells at higher temperatures. *Molecular and cellular biology* 9(9):3919-3930.
42. Wiesgigl M & Clos J (2001) Heat shock protein 90 homeostasis controls stage differentiation in *Leishmania donovani*. *Mol Biol Cell* 12(11):3307-3316.
43. Kadekoppala M, *et al.* (2001) Rapid recombination among transfected plasmids, chimeric episome formation and trans gene expression in *Plasmodium falciparum*. *Mol Biochem Parasitol* 112(2):211-218.
44. Martin SK, Oduola AM, & Milhous WK (1987) Reversal of chloroquine resistance in *Plasmodium falciparum* by verapamil. *Science* 235(4791):899-901.
45. Delling U, Raymond M, & Schurr E (1998) Identification of *Saccharomyces cerevisiae* genes conferring resistance to quinoline ring-containing antimalarial drugs. *Antimicrobial agents and chemotherapy* 42(5):1034-1041.

46. Moura PA, Dame JB, & Fidock DA (2009) Role of Plasmodium falciparum digestive vacuole plasmepsins in the specificity and antimalarial mode of action of cysteine and aspartic protease inhibitors. *Antimicrobial agents and chemotherapy* 53(12):4968-4978.

Chapter 6

THE *PLASMODIUM FALCIPARUM* HEAT SHOCK PROTEIN 90 INHIBITORS HARMINE AND PU-H71 ARE SYNERGISTIC *IN VIVO* – The *P.berghei* model

1 INTRODUCTION

Animal models remain indispensable for the evaluation of antimalarials and vaccines. Until World War II, antimalarial studies and research on the mode of action of drugs, such as quinine, as well as the search for new drugs were carried out in birds infected with various *Plasmodium* species (1). A few studies were conducted in rhesus monkeys. The World War II program was coordinated by the US Public Health Service in which over 4000 compounds were examined, with the majority of studies performed in chicks infected with *P. gallinaceum* or ducklings infected with *P. lophurae* (1).

Plasmodium species that cause human disease cannot infect non-primate animal models (with the exception of a laboratory immunocompromised mouse model that has been developed to sustain *P. falciparum*-parasitized human erythrocytes *in vivo* and is daily transfused with human blood) (2). Nowadays, the *in vivo* evaluation of candidate antimalarials begins with the use of the rodent malaria parasites *P. berghei*, *P. yoelii*, *P. chabaudi*, and *P. vinckei* (3). Evaluation of the antimalarials mefloquine, halofantrine, and artemisinin derivatives was carried out in rodent models. As such, these *in vivo* rodent models have been validated as an essential part of the antimalarial discovery process (3, 4).

P. berghei is the mouse parasite that most closely resembles *P. falciparum* in terms of its symptoms and life cycle (2). Just like *P. falciparum*, *P. berghei* differs from *P. vivax* and *P. ovale* in that it does not have a hypnozoite stage in the liver (1, 2). For the great majority of experimental therapies using murine malaria, different strains of albino laboratory mice have been employed. Because the *in vitro* techniques used to maintain mouse parasites are impractical, cryopreservation or *in vivo* blood passaging for murine malaria is performed (1, 2).

The two routes for infecting mice with donor blood are intraperitoneal (i.p.) and intravenous (i.v.) (2). The i.p. route was chosen for practical reasons in this preliminary drug evaluation. A wide range of parasitemia levels is found in animals inoculated i.p. The resulting infection in any group of recipient animals shows less variation with the i.v. route, but these injections are difficult and time-consuming to perform at the initial stages of drug evaluation (2). The focus on this initial *in vivo* study was the evaluation of the antimalarial effect and the doses required for a significant effect. The effect of PU-H71 and harmine in these models was evaluated alone and in combination with CQ.

In vivo assays to evaluate drug combinations are more complex than *in vitro* studies due to compound parameters, e.g. route of administration, number of applications, and the half-life of the drugs. A drug interaction can be defined as the observed fraction of the effective dose at 50% inhibition of parasite load (ED₅₀) or 90% inhibition of parasite load (ED₉₀). However, an accurate evaluation of ED₅₀ or ED₉₀ is difficult for low-activity compounds, as has been observed for antibiotics and sulphonamides. The combination effect in this study has been evaluated using previously published definitions (3, 5, 6) of drug interactions *in vivo* as defined in the Materials and Methods section. The main goal of the work presented in this chapter was to establish the potential synergistic effect of PU-H71 and harmine with existing antimalarials *in vivo* using mouse models of malaria. In the *P. berghei* mouse model of malaria, PU-H71 and harmine synergized with CQ to reduce parasite load and increase survival.

2 MATERIALS AND METHODS

2.1 *Plasmodium berghei* mouse model studies and drug administration

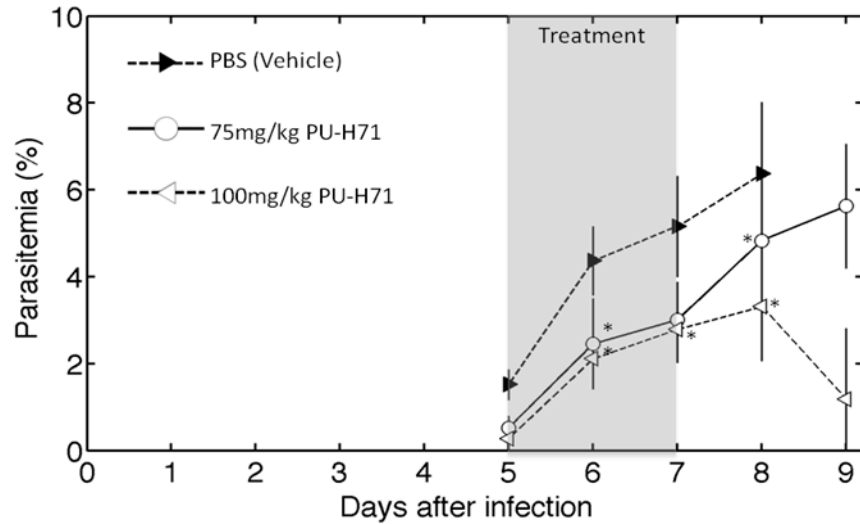
All the *in vivo* experiments were performed together with Dr. Ian Crandall. BALB/c mice were ordered from the Jackson Laboratories (Bar Harbor, ME). The mice were housed and fed by the staff at the Division of Comparative Medicine at the University of Toronto according to the guidelines of the Canadian Council on Animal Care. Blood was collected from a donor animal that had a parasitaemia of approximately 20% in a 10 ml heparinized syringe. Mice were infected intra-peritoneally (i.p.) with 10^6 *Plasmodium berghei* ANKA strain parasites passaged in the laboratory of Dr. Ian Crandall and Dr. Kevin Kain. This mouse model of malaria was chosen because upon infection with this especially virulent ANKA strain, the mice can be monitored for signs of severe disease such as lethargy, ruffled fur and sunken eyes. In addition, the trajectory of the parasitemia changes in these models is predictable with the mice reaching a parasitemia of 1% 5 days after infection and cerebral malaria at day 13. As such, any changes in response to drug treatment may be monitored accordingly. Following infection, mouse weight and parasitemia were monitored daily. The PU-H71, harmine and CQ solutions were prepared fresh daily in PBS. Injections were performed intra-peritoneally (i.p.) for 3 days in a row after the parasitemia level reached 1%. Untreated control animals were treated with PBS alone. Synergistic drug interactions were determined using previously published definitions of antimalarial drug synergy *in vivo*, which postulate that two drugs are synergistic if the treatment with a combination of less or equal to half the ED_{50} for each drug results in parasitemia inhibition of $\approx 50\%$ or more (6, 7). Another published definition of drug synergism *in vivo* suggests that the percent inhibition of parasitemia by the combination treatment is 10% higher than the sum of the inhibition observed by each of the treatments alone at the same doses (i.e. $\%inhibition (A+B) > \%inhibition (A) + \%inhibition (B) + 10\%$ (5).

3 RESULTS

3.1 PU-H71 shows a significant antimalarial effect in mouse models of malaria without significant toxicity

To evaluate the antimalarial effect of PU-H71 in animals, *Plasmodium berghei* ANKA (10^6 parasites) infected BALB/c mice were used. Daily intraperitoneal injections with PU-H71 were commenced once the parasitemia (i.e. the percent infected red blood cells) reached ~1% (Day 5). Parasitemia was monitored by microscopic examination of Giemsa-stained thin blood smears prepared daily throughout the experiment. CQ (30 mg/kg) was used as the positive control and PBS was used as a vehicle control. Treatment of mice with 75 mg/kg and 100 mg/kg PU-H71 showed a significant protective effect ($p \leq 0.05$, unpaired t-test) in terms of reduced parasite burden and increased host survival relative to the PBS control group, respectively (Figure 6-1a,b). The highest reduction in parasitemia was observed with three daily intraperitoneal injections of 100 mg/kg PU-H71. At day 8 (one day after the complete treatment was over), the group treated with 100mg/kg was marked by an average of $46.3 \pm 10.8\%$ inhibition of parasitemia relative to the vehicle. The combination of 25 mg/kg PU-H71 with 0.25 mg/kg CQ resulted in a significant ($p \leq 0.05$, parametric unpaired t-test) average parasitemia reduction of $42.6 \pm 9.4\%$ and improved survival by 3 days (Figure 6-2a,b) compared to 0.25 mg/kg CQ treatment alone. Using published definitions of synergism *in vivo* (described in Materials and Methods), the combination of 25 mg/kg PU-H71 ($\sim 4\times$ less than ED_{50}) and 0.25 mg/kg CQ ($\sim 5\times$ lower than ED_{50}) are the lowest doses at which synergistic activity was achieved. Other combinations were also able to achieve synergy (Table 6-1, Figure 6-3, 6-4). Treatment with 2.5, 25, 75 and 100 mg/kg PU-H71 alone resulted in 15.8%, 11.7%, 24.2% and 46.3% inhibition of parasitemia on day 8, respectively. Combination treatments 0.25 mg/kg CQ + 2.5 mg/kg PU-H71 and 0.25 mg/kg CQ + 25 mg/kg PU-H71 resulted in 30.6% and 42.6% inhibition of parasitemia on day 8, respectively. Complete parasitological cure was not observed with any of those treatments. There was no significant toxic effect observed with any of the treatment regimens using PU-H71 both in infected mice and uninfected controls as evaluated by weight, cage activity and grooming behavior. Mice receiving both PU-H71 and CQ showed fewer symptoms of disease (ruffled fur, lethargy, sunken eyes) and better survival than mice treated with each of the drugs at the same doses.

(a)



(b)

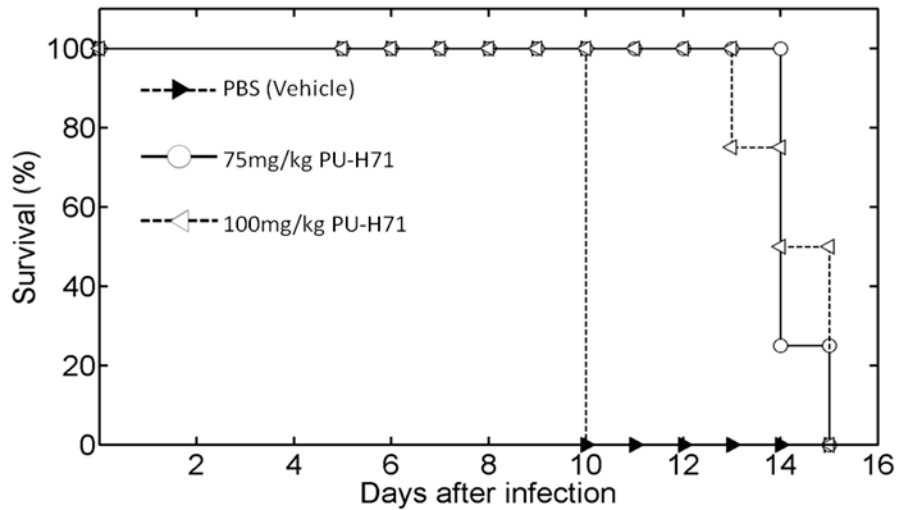
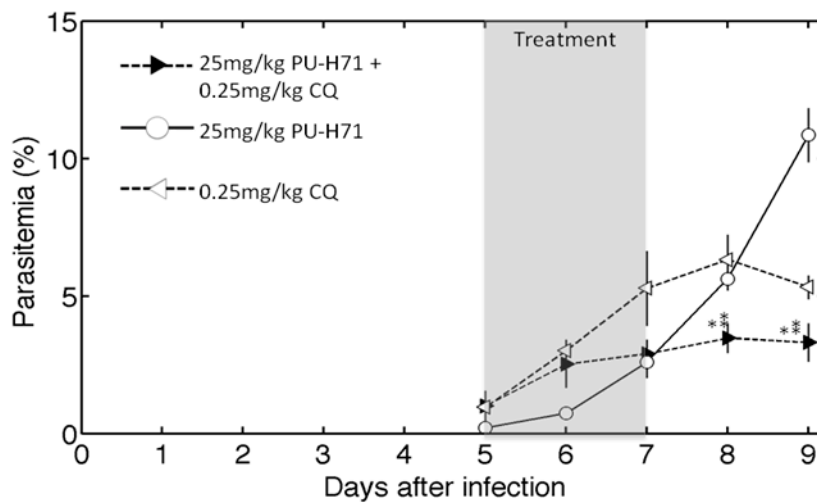


Figure 6-1: *Plasmodium berghei* mouse model results of intra-peritoneal injection treatment with PU-H71. Mice were infected on day 0 and treatment was started on day 5 at parasitemia of 1%. (a) Average parasitemia levels in response to drug treatments alone as indicated (n = 4). * denotes significant differences in parasitemia relative to the vehicle control (Student's t-test $p \leq 0.05$). (b) Kaplan-Meier survival plot for PU-H71 alone versus placebo.

(a)



(b)

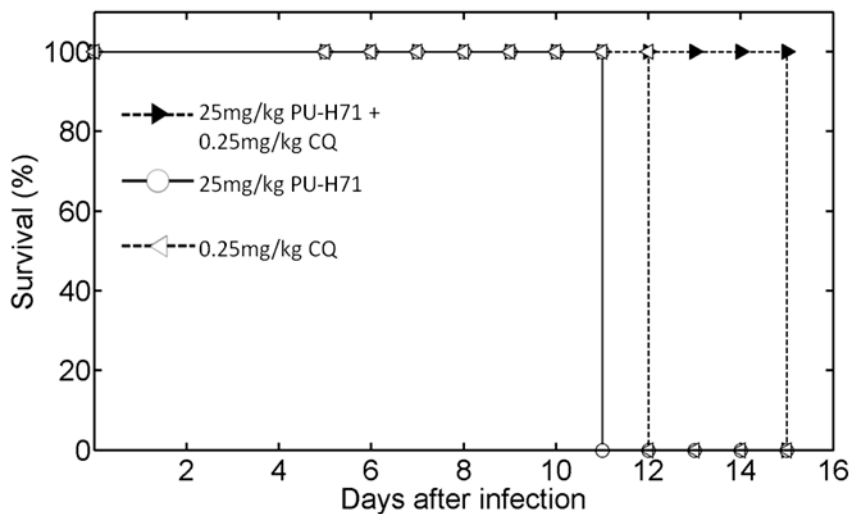
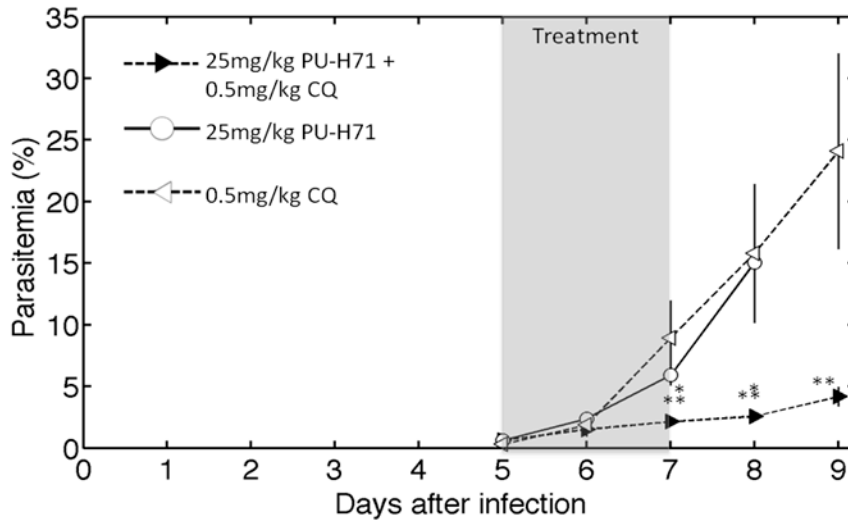


Figure 6-2: *Plasmodium berghei* mouse model results of intra-peritoneal injection treatment with 25 mg/kg PU-H71 and 0.25 mg/kg CQ. Mice were infected on day 0 and treatment was started on day 5 at parasitemia of 1%. (a) Average parasitemia levels in response to drug treatments as indicated (n = 4). * denotes significant differences in parasitemia relative to PU-H71 treatment alone. ** denotes significant differences in parasitemia relative to the CQ treatment alone (Student's t-test $p \leq 0.05$). (b) Kaplan-Meier survival plot for this combination treatment.

(a)



(b)

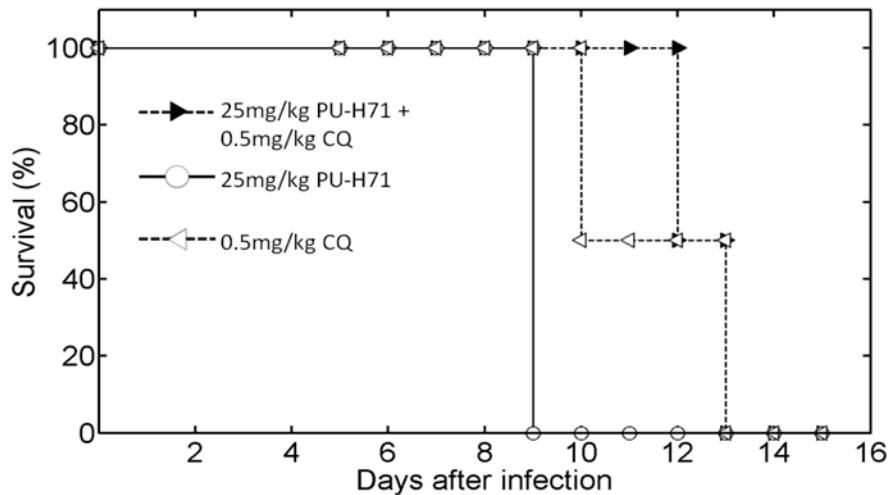
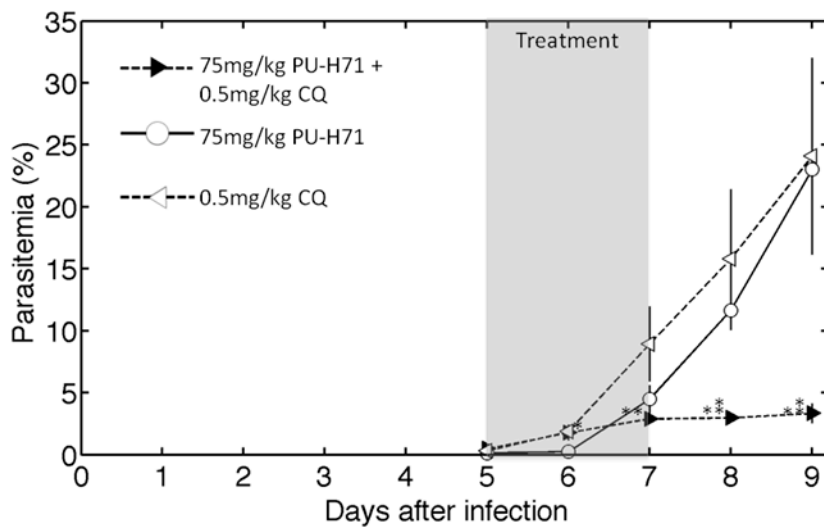


Figure 6-3: *Plasmodium berghei* mouse model results of intra-peritoneal injection treatment with 25 mg/kg PU-H71 and 0.5 mg/kg CQ. Mice were infected on day 0 and treatment was started on day 5 at parasitemia of 1%. (a) Average parasitemia levels in response to drug treatments as indicated (n = 4). * denotes significant differences in parasitemia relative to PU-H71 treatment alone. ** denotes significant differences in parasitemia relative to the CQ treatment alone (Student's t-test $p \leq 0.05$). (b) Kaplan-Meier survival plot for this combination treatment.

(a)



(b)

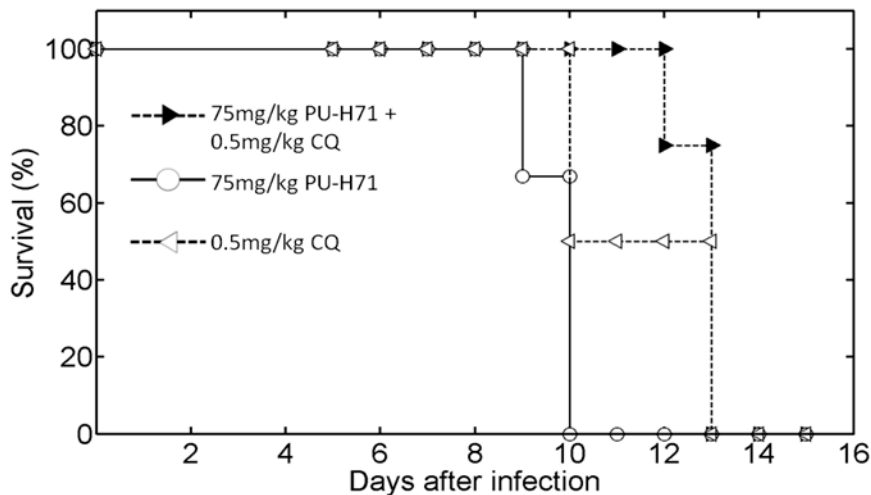


Figure 6-4: *Plasmodium berghei* mouse model results of intra-peritoneal injection treatment with 75 mg/kg PU-H71 and 0.5 mg/kg CQ. Mice were infected on day 0 and treatment was started on day 5 at parasitemia of 1%. (a) Average parasitemia levels in response to drug treatments as indicated (n = 4). * denotes significant differences in parasitemia relative to PU-H71 treatment alone. ** denotes significant differences in parasitemia relative to the CQ treatment alone (Student's t-test $p \leq 0.05$). (b) Kaplan-Meier survival plot for this combination treatment.

Table 6-1: Summary of the drug combinations tested in the *Plasmodium berghei* mouse model trials.

Combinations tested	Synergy Observed (Yes/No)
2.5 mg/kg PU-H71 + 0.25 mg/kg CQ	No
25 mg/kg PU-H71 + 0.25 mg/kg CQ	Yes
25 mg/kg PU-H71 + 0.5 mg/kg CQ	Yes
75 mg/kg PU-H71 + 0.5 mg/kg CQ	Yes
25 mg/kg PU-H71 + 5 mg/kg CQ	No
75 mg/kg PU-H71 + 5 mg/kg CQ	No
25 mg/kg PU-H71 + 12.5 mg/kg CQ	No
75 mg/kg PU-H71 + 12.5 mg/kg CQ	No

3.2 Harmine potentiated chloroquine in mouse models of malaria without significant toxicity

Plasmodium berghei ANKA (10^6 parasites) infected BALB/c mice were used to determine the antimalarial effect of harmine *in vivo*. Daily intraperitoneal injections with harmine were commenced once the parasitemia (i.e. the percent infected red blood cells) reached ~1% (Day 3) for 3 days consecutively. Parasitemia was evaluated daily by the use of Giemsa-stained thin blood smears throughout the experiment. CQ (30 mg/kg) was used as the positive control and PBS was used as a vehicle control. Treatment of mice with 100 mg/kg harmine reduced parasite burden significantly on day 8 ($p \leq 0.05$, unpaired t-test) relative to the PBS control group (Figure 6-5). Combination treatments consisting of harmine and chloroquine had the highest protective effect on parasite load.

The combination of 75 mg/kg harmine with 5 mg/kg CQ resulted in a significant ($p < 0.05$, parametric unpaired t-test) average parasitemia reduction of $96.4 \pm 1.5\%$ (Figure 6-5). Other combinations of 75 mg/kg harmine and 100 mg/kg harmine with 0.5 mg/kg CQ were also tested for synergistic activity. Using published definitions of drug synergism *in vivo* (5, 6) (described in Materials and Methods), the combination of 75 mg/kg harmine and 5 mg/kg chloroquine represents the lowest doses at which synergistic activity was achieved. The synergistic combination of 100 mg/kg harmine and 5 mg/kg chloroquine resulted in an average of $97.8 \pm 1.5\%$ inhibition of parasitemia (Figure 6-5). Complete parasitological cure was not observed with any of those treatments, but no parasites were present on the Giemsa stained microscope slides from the cage of mice treated with 100 mg/kg harmine and 5 mg/kg chloroquine on day 6 (24 h after treatment completion). Unlike PU-H71 that has been evaluated in mouse models for several diseases, this is the first *in vivo* evaluation of harmine. No significant toxic effect was observed with any of the treatment regimens using harmine both in infected mice and uninfected controls as evaluated by weight (Figure 6-6), cage activity and grooming behavior. Mice receiving both harmine and CQ showed fewer symptoms of disease (ruffled fur, lethargy, sunken eyes) in comparison with the administration of each of the drugs alone. No survival benefit was observed with any of the harmine treatments.

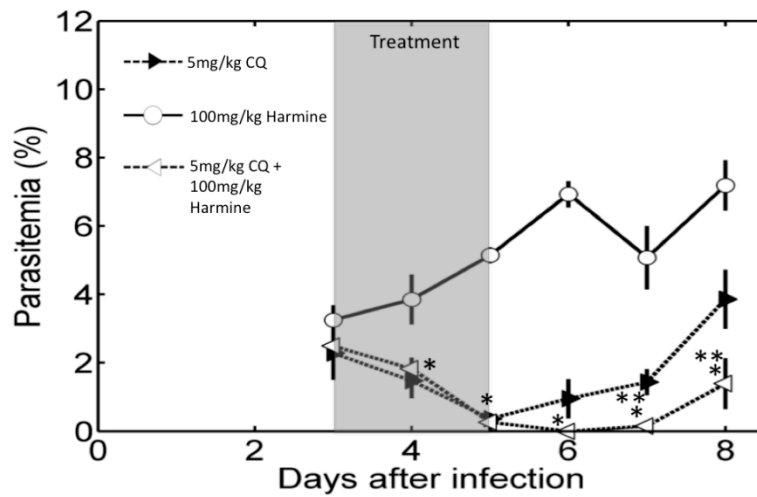
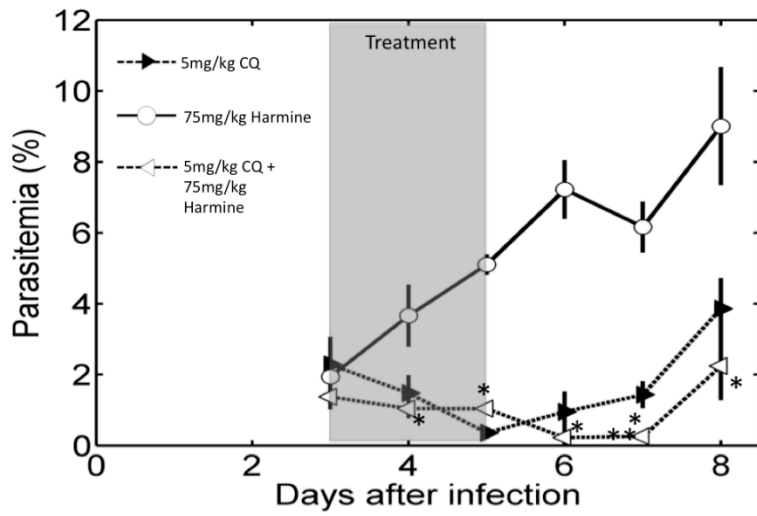
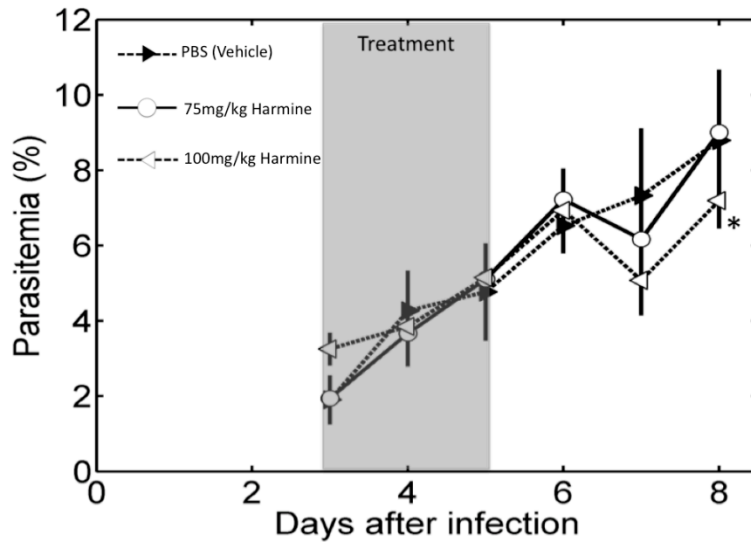


Figure 6-5: *Plasmodium berghei* parasitemia changes in response to intra-peritoneal injection treatment with harmine and its combinations. Mice were infected on day 0 and treatment was started on day 3 at parasitemia of 1%. The first graph shows average parasitemia levels in response to drug treatments alone (n = 4). * denotes significant differences in parasitemia relative to the vehicle control (Student's t-test $p \leq 0.05$). In the combination treatment graphs, * denotes significant differences in parasitemia relative to harmine treatment alone. ** denotes significant differences in parasitemia relative to the CQ treatment alone (n = 4) (Student's t-test $p \leq 0.05$).

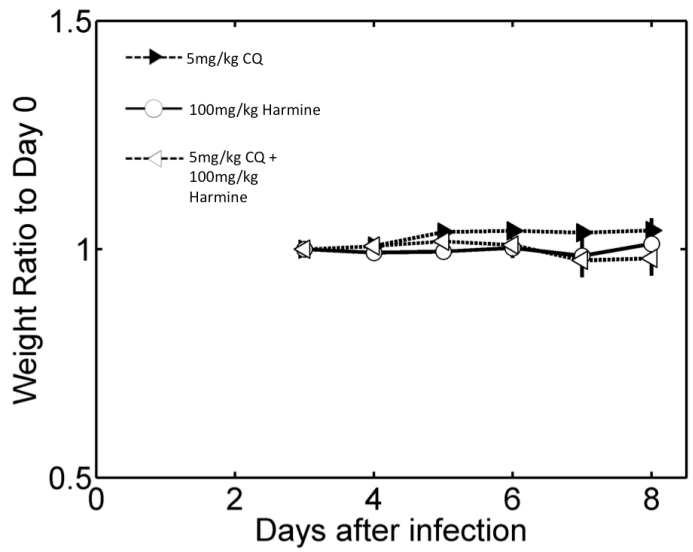
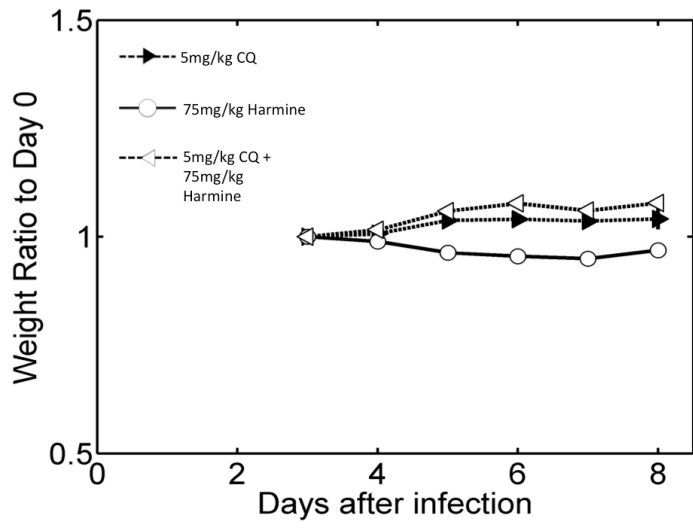
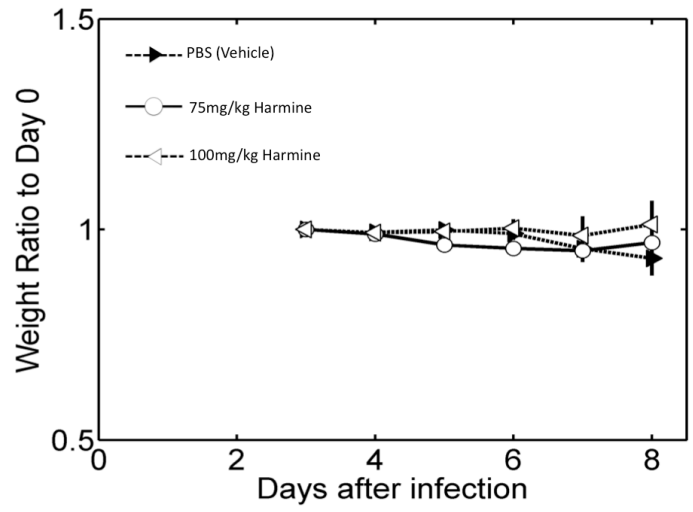


Figure 6-6: *Plasmodium berghei* mouse model weight changes in response to intra-peritoneal injection treatment with harmine. No significant changes in weight were observed (Student's t-test $p \leq 0.05$).

4 DISCUSSION

Using an *in vivo* mouse model of infection with *P. berghei*, we found a significant effect of PU-H71 in reducing parasitemia and improving survival. Importantly, PU-H71 showed synergistic activity at 25 mg/kg and 75 mg/kg with sub-therapeutic concentrations of CQ (0.25 mg/kg and 0.5 mg/kg) *in vivo*. As expected, the concentration of PU-H71 required to treat the rodent infections was significantly higher than the IC_{50} calculated from cell culture inhibition. This discrepancy reflects the constraints on the bioavailability of the drug due to the pharmacokinetic parameters in the host infected. However, the lack of any significant toxicity effects by the doses used for treatment is encouraging for the therapeutic potential of this inhibitor and for continuing the evaluation of this drug at the higher doses necessary to clear the infection.

In cancer models, all 12 Hsp90 inhibitors in clinical trials have been consistently given at high doses (50–100 mg/kg) in order to achieve efficacy (8). The use of PU-H71 over several weeks in mice suggests the safety of this drug (9-11). Future studies also need to evaluate the combination of PU-H71 with other antimalarials such as amodiaquine and to see whether PfHsp90 is an essential chaperone that potentiates the expression of other resistance determinants. It would be of particular interest to determine the role of PfCRT in altering susceptibility to lumefantrine, since wild-type PfCRT is associated with diminished lumefantrine susceptibility (12).

The administration of harmine alone (75 mg/kg and 100 mg/kg daily) resulted in a modest effect on parasitemia *in vivo*. Reasons that may explain the modest response *in vivo* relative to that observed *in vitro* may be the short half-life of harmine in plasma and the effects of metabolism on this drug. For example, harman is commonly metabolized into 3- and 6-hydroxy harman and displays a short half-life in plasma (13).

The significance of this study lies in the combination of harmine with CQ and the CQ potentiation efficacy that harmine exhibits. This type of synergy, which is known as potentiation, occurs when a compound possesses little or no activity on its own, but it enhances the activity of another active compound (14). This effect is what we observed with harmine (75 mg/kg and 100 mg/kg) and CQ (5 mg/kg) combinations in mice.

In future studies, it would be interesting to evaluate the suppressive activity of PU-H71 and harmine for further development in prophylactic combinations. An established test exists for

testing antimalarial suppressive activity, i.e., Peter's 4-day test (15). The animals are infected and given a fixed dose of the candidate drug (30 mg/kg) once daily for 4 consecutive days, starting on the day of the infection. Parasitemia is evaluated on the day following the last treatment to determine the presence and degree of suppressive activity at the screening dose (2, 15).

The synergistic activity of these Hsp90 inhibitors *in vivo* is encouraging for circumventing antimalarial resistance. Previous reports have suggested the existence of CQR rodent parasites *P. yoelii* N67 and *P. berghei* RC (2). A recent investigation of the *P. yoelii* N67 strain suggests that this strain is CQS (7). *P. berghei* RC is reportedly highly CQR, but the mice do not reach parasitemia levels higher than 2%, which hinders the assessment of drug efficacy (7). However, it is possible to attempt to select for resistance *in vivo* over a long period of time (2, 16). A range of single doses of the drug are given an hour following the infection of groups of mice and the development of parasitemia is followed with daily blood films. That dose that prolongs the attainment of 2% parasitemia for a period of 7-10 days is administered at the time of each passage. Comparison of the time taken to reach a 2% parasitemia in the treated group versus the untreated control is used to calculate the "2% delay time". Each successive passage is treated with the same, single, fixed dose to extend the delay time as much as possible and therefore, to reduce susceptibility (2).

References

1. Sherman IW (2005) The life of Plasmodium: an overview. *Molecular approaches to malaria*, ed Sherman IW (ASM Press, Washington, D.C), pp 3-23.
2. Robinson WPaBL (1999) Malaria. *Handbook of mouse models of infection*, ed M.Sandy OZa (Academic, London), pp 757-773.
3. Fidock DA, Rosenthal PJ, Croft SL, Brun R, & Nwaka S (2004) Antimalarial drug discovery: efficacy models for compound screening. *Nature reviews. Drug discovery* 3(6):509-520.
4. Fidock DA (2010) Drug discovery: Priming the antimalarial pipeline. *Nature* 465(7296):297-298.
5. Min-Oo G, Fortin A, Poulin JF, & Gros P (2010) Cysteamine, the molecule used to treat cystinosis, potentiates the antimalarial efficacy of artemisinin. *Antimicrobial agents and chemotherapy* 54(8):3262-3270.
6. Bell A (2005) Antimalarial drug synergism and antagonism: mechanistic and clinical significance. *FEMS microbiology letters* 253(2):171-184.
7. Pereira MR, *et al.* (2011) In vivo and in vitro antimalarial properties of azithromycin-chloroquine combinations that include the resistance reversal agent amlodipine. *Antimicrobial agents and chemotherapy* 55(7):3115-3124.
8. Biamonte MA, *et al.* (2010) Heat shock protein 90: inhibitors in clinical trials. *J Med Chem* 53(1):3-17.
9. Taldone T & Chiosis G (2009) Purine-scaffold Hsp90 inhibitors. *Current topics in medicinal chemistry* 9(15):1436-1446.
10. Usmani SZ, Bona RD, Chiosis G, & Li Z (2010) The anti-myeloma activity of a novel purine scaffold HSP90 inhibitor PU-H71 is via inhibition of both HSP90A and HSP90B1. *Journal of hematology & oncology* 3:40.
11. Usmani SZ & Chiosis G (2011) HSP90 inhibitors as therapy for multiple myeloma. *Clinical lymphoma, myeloma & leukemia* 11 Suppl 1:S77-81.
12. Mwai L, *et al.* (2009) In vitro activities of piperazine, lumefantrine, and dihydroartemisinin in Kenyan Plasmodium falciparum isolates and polymorphisms in pfcrt and pfmdr1. *Antimicrobial agents and chemotherapy* 53(12):5069-5073.
13. Pfau W & Skog K (2004) Exposure to beta-carbolines norharman and harman. *Journal of chromatography. B, Analytical technologies in the biomedical and life sciences* 802(1):115-126.
14. Berenbaum MC (1989) What is synergy? *Pharmacological reviews* 41(2):93-141.
15. Peters W, Davies EE, & Robinson BL (1975) The chemotherapy of rodent malaria, XXIII Causal prophylaxis, part II: Practical experience with Plasmodium yoelii nigeriensis in drug screening. *Annals of tropical medicine and parasitology* 69(3):311-328.

16. Peters W, Bafort J, & Ramkaran AE (1970) The chemotherapy of rodent malaria. XI. Cyclically transmitted, chloroquine-resistant variants of the Keyberg 173 strain of *Plasmodium berghei*. *Annals of tropical medicine and parasitology* 64(1):41-51.

Chapter 7

DISCUSSION AND CONCLUSIONS

P. falciparum is a protozoan parasite that causes the most severe form of human malaria and is responsible for a majority of global morbidity and mortality (1, 2). The complexity of the parasite's life cycle is partially responsible for the lack of an effective vaccine. The impact of malaria is exacerbated by the emergence of resistance to antimalarials, which is facilitated by the unknown mechanism of drug action and solicitation of fraudulent drugs in endemic countries. An urgent need exists to develop novel drugs that can be used in combination to circumvent resistance (3-5).

Ideally, combination regimens incorporate two novel agents with potent efficacy and similar pharmacokinetic profiles; however, this is not met by any existing combination in use or in development (4, 5). The most successful current combination is ACT, but even patients treated with ACT suffer occasionally from late recrudescences due to the short half-lives of artemisinin derivatives (4, 5). Combination with longer acting drugs is employed with the hope that the potent action of artemisinin will prevent resistance selection to the longer-acting drug. The risk of a single long-acting agent using combination therapy with the PfHsp90 inhibitors PU-H71 and harmine also exists because both of these drugs have short half-lives. However, the ability of these two drugs to potentiate CQ activity provides strong motivation for their further development.

Drug development is a laborious and time-consuming process. It is important to start with drugs that have already been investigated for absorption, distribution, and excretion in rodents and humans. Successful candidate drugs need to be easy to manufacture, stable, readily formulated, bioavailable, have an acceptable half-life, and should be safe to administer (6). For antimalarials, transmission-blocking activity is also a desirable property (4, 5). In the future, the transmission-blocking activity of the PfHsp90 inhibitors and their combinations can be evaluated with *P. falciparum* gametocytes produced *in vitro* (7, 8). The preliminary findings of my thesis suggest that the PfHsp90 inhibitors PU-H71 and harmine are attractive candidates to enable successful drug development due to their promising potency, pharmacological characteristics, and lack of

toxic effects. These results support the use of PfHsp90 as an antimalarial drug target with the potential of circumventing drug resistance. A drug discovery platform for rational drug combinations in the clinic can be built by integrating proteomic and genomic approaches.

One limitation of preliminary antimalarial evaluations in general is the use of *in vitro* screens and culturing methods that select for the fittest isolate under laboratory conditions. Multiple drug-resistant and drug-sensitive isolates from around the world have now been culture-adapted and can be obtained from the Malaria Research and Reference Reagent Resource Center. However, all of these isolates have been passaged in multiple laboratories over many years. As such, the biology of these strains has changed and adapted to laboratory life. Therefore, the evaluation of compound activity in these strains can only be predictive. The evaluation of the PfHsp90 inhibitors PU-H71 and harmine *in vivo* is encouraging in potentiating the effect of CQ, but their assessment in an endemic malaria site would be paramount for their further clinical evaluation. The attractive research interface with these inhibitors will provide the motivation for their further development.

In summary, malaria prophylaxis and treatment is challenged by a plastic parasite that is able to generate drug resistance in a short time. The treatment options are limited and novel therapeutic strategies are required. The *in vitro* and *in vivo* data support the role for the Hsp90 inhibitors PU-H71 and harmine, which have a high affinity for the PfHsp90 ATP-binding domain, as being able to act synergistically with CQ in an animal model of malaria. PU-H71 recoups CQ activity in a CQR strain *in vitro*.

From the study of the PfHsp90 inhibitors synergistic activity with CQ, a complex putative model emerges for both CQS and CQR *P.falciparum* (Figure 7-1). Under pharmacological stress, the PfHsp90 chaperone machinery is activated. PfHsp90 activity is required for the folding of drug-resistance and virulence associated proteins in the infected cell. Inhibition of PfHsp90 activity hinders trafficking of parasitic proteins to the erythrocyte surface (9), folding of PfCRT and PfMDR1 and hemoglobin byproduct detoxification in both CQS and CQR states.

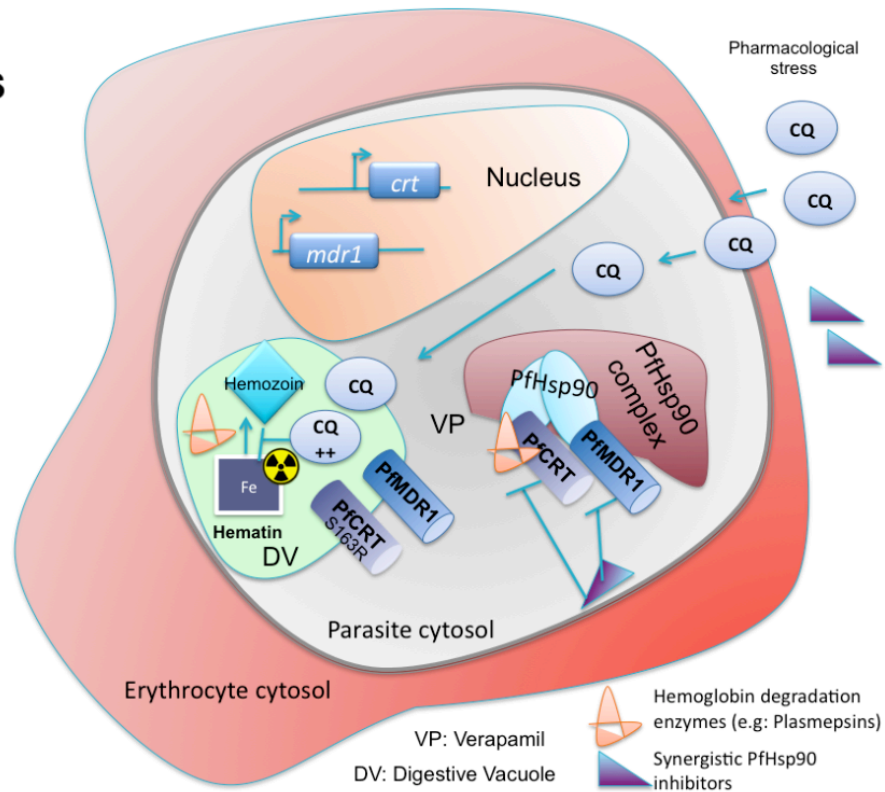
In CQR parasites, less CQ accumulates in the digestive vacuole due to a critical charge loss mutation of PfCRT (K76T) that permits the transport of charged CQ molecules to the cytosol (10-12). The single amino acid change S163R is thought to block the leak of charged CQ by reintroducing a positive charge to PfCRT, thus restoring CQ sensitivity (12-14). CQR has also

been associated with polymorphisms of PfHsp90 that result in the expansion of a pentaglutamate region in the acidic linker domain of the protein (15). Indeed, another study showed that the region of chromosome 7 of the *P.falciparum* genome that contains both the *pfert* and *pfhsp90* genes displays reduced recombination activity, but is flanked by recombination hotspots (16), suggesting a recent selective sweep potentially due to extensive CQ pressure in the field. These two independent results attest to selection pressure in conserving these two genes and their association, but simultaneously introducing polymorphisms that are able to confer a fitness advantage due to recombination events in flanking regions.

However, with this caveat in mind, there are significant implications for the synergistic activity of Hsp90 inhibitors with conventional antimicrobials when used in combination. Targeting PfHsp90 affords the possibility of developing a synergistic adjunctive therapy with the potential of reversing resistance to existing antimalarials such as CQ. One could envision the development of a chemical genomic catalog of PfHsp90 interactions weighted by the average FIC ratios of the dual targets. The broad spectrum of Hsp90 interactions provides extensive possibilities for adjunctive therapies that decrease the likelihood of developing resistance. A catalog of these interactions will allow for rational selection and circulation of alternative combinations to avoid the prolonged exposure of the parasites to a single therapy.

The monumental achievements of malaria research in the previous century have laid the groundwork for reaching the milestones of malaria treatment and control. Even though we are far from the eradication of malaria, a lot of progress is being made in establishing targets for rational antimalarial therapy and discovering the steps involved in parasite invasion, host immunity, and parasite egress. These findings are essential for predicting protective immunity, reversing antimalarial resistance, and blocking the transmission of malaria.

CQS



CQR

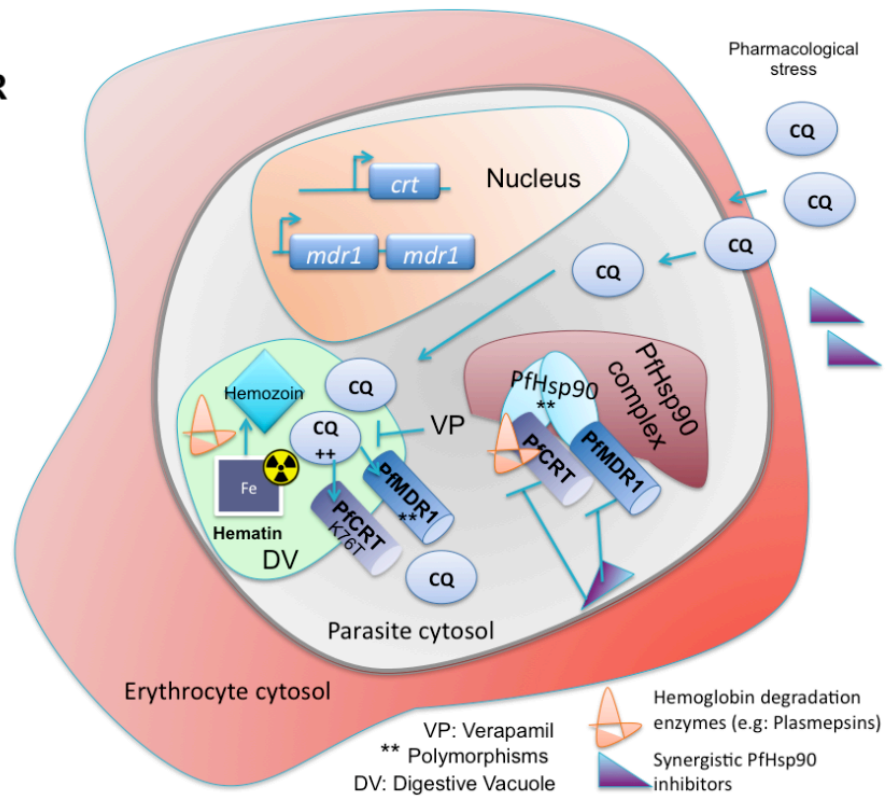


Figure 7-1: *Illustration of the emerging cellular model of PfHsp90 inhibitors and CQ in CQS and CQR P.falciparum infected RBCs.* Drug application introduces pharmacological stress which may result in activation of the PfHsp90 chaperone machinery. CQ accumulation in the digestive vacuole inhibits the detoxification of hemoglobin byproducts in CQS, but not CQR parasites. Inhibition of PfHsp90 chemosensitizes the cells by an arrest of folding clients involved in detoxification, multiple drug resistance and virulence factors. CQS: CQ sensitive CQR: CQ resistant.

References

1. White NJ, *et al.* (1999) Averting a malaria disaster. *Lancet* 353(9168):1965-1967.
2. Sachs J & Malaney P (2002) The economic and social burden of malaria. *Nature* 415(6872):680-685.
3. Price RN & Douglas NM (2009) Artemisinin combination therapy for malaria: beyond good efficacy. *Clinical infectious diseases : an official publication of the Infectious Diseases Society of America* 49(11):1638-1640.
4. Fidock DA (2010) Drug discovery: Priming the antimalarial pipeline. *Nature* 465(7296):297-298.
5. Fidock DA, Rosenthal PJ, Croft SL, Brun R, & Nwaka S (2004) Antimalarial drug discovery: efficacy models for compound screening. *Nature reviews. Drug discovery* 3(6):509-520.
6. Leeson PD & St-Gallay SA (2011) The influence of the 'organizational factor' on compound quality in drug discovery. *Nature reviews. Drug discovery* 10(10):749-765.
7. Robinson WPaBL (1999) Malaria. *Handbook of mouse models of infection*, ed M.Sandy OZa (Academic, London), pp 757-773.
8. Sherman IW (2005) The life of Plasmodium: an overview. *Molecular approaches to malaria*, ed Sherman IW (ASM Press, Washington, D.C), pp 3-23.
9. Shonhai A (2010) Plasmodial heat shock proteins: targets for chemotherapy. *FEMS immunology and medical microbiology* 58(1):61-74.
10. Cooper RA, Hartwig CL, & Ferdig MT (2005) pfcrt is more than the Plasmodium falciparum chloroquine resistance gene: a functional and evolutionary perspective. *Acta tropica* 94(3):170-180.
11. Cooper RA, *et al.* (2002) Alternative mutations at position 76 of the vacuolar transmembrane protein PfCRT are associated with chloroquine resistance and unique stereospecific quinine and quinidine responses in Plasmodium falciparum. *Molecular pharmacology* 61(1):35-42.
12. Chinappi M, Via A, Marcatili P, & Tramontano A (2010) On the mechanism of chloroquine resistance in Plasmodium falciparum. *PloS one* 5(11):e14064.
13. Johnson DJ, *et al.* (2004) Evidence for a central role for PfCRT in conferring Plasmodium falciparum resistance to diverse antimalarial agents. *Molecular cell* 15(6):867-877.
14. Wellems TE (2004) Transporter of a malaria catastrophe. *Nature medicine* 10(11):1169-1171.
15. Su XZ & Wellems TE (1994) Sequence, transcript characterization and polymorphisms of a Plasmodium falciparum gene belonging to the heat-shock protein (HSP) 90 family. *Gene* 151(1-2):225-230.

16. Mu J, *et al.* (2010) Plasmodium falciparum genome-wide scans for positive selection, recombination hot spots and resistance to antimalarial drugs. *Nature genetics* 42(3):268-271.

Appendices

APPENDIX 1: LIST OF THE WIDE RANGE OF HSP90 TARGETING PROJECTS

PRIMARY AUTHOR	SENIOR AUTHOR	YEAR	APPLICATION
Wang G	Tangpisuthipongsa D	2011	Neurodegenerative Disease and Stroke
Ju HQ	Xing GW	2011	Anti HSV-1& HSV-2
Roe ND	Ren J	2011	Myocardial Contractile Dysfunction
Yun TJ	Kehry MR	2011	Inflammation and Autoimmune Diseases
Luo W	Chiosis G	2008, 2010	Neurodegenerative Disease
Watanabe T	Tobinai K	2010	Bortezomib-induced Peripheral Neuropathy
Pallavi R	Tatu U	2010	Protozoan Infections
Reidy M	Masison DC	2010	<i>Saccharomyces cerevisiae</i> [PSI+] prions
Qin Z	Parsons C	2010	Kaposi's sarcoma-associated herpesvirus (KSHV)
Taldone T	Chiosis G, Devaney E	2010	<i>Brugia pahangi</i>

Moleda L	Wiest R	2010	Portal Hypertension
Ujino S	Takaku H	2009, 2010	Hepatitis C Virus
Zheng ZZ	Xia NS	2010	Hepatitis E Virus
Chen YM	Chen TY	2010	Nodavirus
Singh S	Cowen LE	2009	<i>Candida albicans</i>
Li Q	Qiao Z	2009	<i>Leishmania donovani</i>
Taguwa S	Matsuura Y	2009	Hepatitis C Virus
Dutta D	Chawla-Sarkar M	2009	Rotavirus
Suzuki K, <u>Tokui K</u>	Sobue G	2009, 2009	Spinal and Bulbar Muscular Atrophy (SBMA)
Prodromou C	Piper P	2009	Fungal Infections
Cowen LE	Lindquist S	2009	Fungal Infections
Nguyen N	Boulay G	2009	Diabetes
Rice JW	Hall SE	2008	Rheumatoid Arthritis
Yang B	Verkman AS	2008	Nephrogenic Diabetes Insipidus
Zhang X	Zhang J	2008	Acute Pulmonary Thromboembolism
Liu C	Galanis E	2008	Measles
McLellan CA	Gunatilaka AA	2007	Arabidopsis Thermotolerance
Roviezzo F	Cirino G	2007	Splanchnic Artery Occlusion Shock
Ansar S	Blagg BS	2007	Alzheimer's Disease

Dello Russo C	Feinstein DL	2006	Autoimmune Encephalomyelitis
Okamoto T	Matsuura Y	2006	Hepatitis C Virus
Batulan Z	Durham HD	2006	Familial Amyotrophic Lateral Sclerosis
Waza M	Sobue G	2006	Neurodegenerative Disorders
Romanello M	Tell G	2006	Osteoporosis
Cid C	Alcazar A	2006	Multiple Sclerosis
Cowen LE	Lindquist S	2005	<i>Candida albicans</i>
Basha W	Tanaka J	2005	Human Cytomegalovirus
Devaney E	Kinnaird JH	2005	<i>Brugia pahangi</i>
Kumar R	Barik S	2005	<i>Plasmodium falciparum</i>
Kupatt C	Feron O	2004	Myocardial Dysfunction
Ai JH	Zhu T	2003	Hypertension
Takahashi A	Shirasu K	2003	Plant Disease Resistance
Konduri GG	Pritchard KA Jr.	2003	Pulmonary Hypertension
Graefe SE	Clos J	2002	<i>Trypanosoma cruzi</i>
Wiesgigl M	Clos J	2001	<i>Leishmania donovani</i>
Dhillon VB	Isenberg DA	1994	<i>Lupus Erythematosus</i>

APPENDIX 2: SAFETY AND TOLERABILITY OF AVAILABLE ANTIMALARIAL DRUGS

DRUG	ADVERSE EFFECTS	CONTRAINDICATIONS
Chloroquine	GI upset, itching, dizziness	Epilepsy
Sulfadoxine-pyrimethamine	None	Pregnancy, renal disease
Quinine	Tinnitus, vertigo, headache, fever, syncope, delirium, nausea	G6PD deficiency, pregnancy, optic neuritis, tinnitus, thrombocytopenic purpura, blackwater fever
Mefloquine	Vomiting, headache, insomnia, vivid dreams, anxiety, dizziness	Depression, schizophrenia, anxiety disorder, psychosis, irregular heartbeat
Atovaquone-chloroguanide	GI upset, stomatitis, headache	Children <11kg, pregnancy, breast-feeding, renal disease
Artemether-lumefantrine	Dizziness, palpitations	Pregnancy, severe malaria
Artesunate-mefloquine	Vomiting, anorexia, diarrhea	Depression, schizophrenia, anxiety disorder, psychosis, irregular heartbeat
Halofantrine	GI upset, slow heart rate	Conduction abnormalities, pregnancy, breast-feeding, infancy, use of mefloquine
Primaquine	GI upset, elevated levels of methemoglobin	Pregnancy, G6PD deficiency, breast-feeding

This summary has been adapted from:

Baird JK. New England Journal of Medicine, 2005 Apr 14;352(15):1565-77.

APPENDIX 3: A DETAILED OVERVIEW OF THE INTERACTORS IDENTIFIED THROUGH CO-IMMUNOPRECIPITATION AND LC-MS/MS ANALYSIS

Anti-PfCRT Pulldown

Identified Proteins (147)	Short form	PlasmoDB ID
Heat shock protein 70 (HSP70) homologue [Plasmodium falciparum 3D7], gi 23505079 emb CAD51861.1 Heat shock protein 70 (HSP70) homologue [Plasmodium falciparum 3D7]	Hsp70	MAL13P1.540
RecName: Full=Heat shock 70 kDa protein; Short=HSP70; AltName: Full=74.3 kDa protein; AltName: Full=Cytoplasmic antigen, gi 309690 gb AAA29626.1 heat shock protein 70 [Plasmodium falciparum]	Hsp70	MAL13P1.540
enolase [Plasmodium falciparum 3D7], gi 50400239 sp Q8IJN7.1 ENO_PLAF7 RecName: Full=Enolase; AltName: Full=2-phospho-D-glycerate hydro-lyase; AltName: Full=2-phosphoglycerate dehydratase, gi 23495020 gb AAN35353.1 AE014831_29 enolase [Plasmodium falciparum 3D7]	ENO	PF10_0155
protein disulfide isomerase [Plasmodium falciparum 3D7], gi 225632282 emb CAX64161.1 protein disulfide isomerase [Plasmodium falciparum 3D7]	PDI	MAL8P1.17

<p>fructose-bisphosphate aldolase [Plasmodium falciparum 3D7], gi 113623 sp P14223.1 ALF_PLAFA RecName: Full=Fructose-bisphosphate aldolase; AltName: Full=41 kDa antigen, gi 74920225 sp Q7KQL9.1 ALF_PLAF7 RecName: Full=Fructose-bisphosphate aldolase, gi 146386478 pdb 2EPH A Chain A, Crystal Structure Of Fructose-Bisphosphate Aldolase From Plasmodium Falciparum In Complex With Trap-Tail Determined At 2.7 Angstrom Resolution, gi 146386479 pdb 2EPH B Chain B, Crystal Structure Of Fructose-Bisphosphate Aldolase From Plasmodium Falciparum In Complex With Trap-Tail Determined At 2.7 Angstrom Resolution, gi 146386480 pdb 2EPH C Chain C, Crystal Structure Of Fructose-Bisphosphate Aldolase From Plasmodium Falciparum In Complex With Trap-Tail Determined At 2.7 Angstrom Resolution, gi 146386481 pdb 2EPH D Chain D, Crystal Structure Of Fructose-Bisphosphate Aldolase From Plasmodium Falciparum In Complex With Trap-Tail Determined At 2.7 Angstrom Resolution, gi 146386682 pdb 2PC4 A Chain A, Crystal Structure Of Fructose-Bisphosphate Aldolase From Plasmodium Falciparum In Complex With Trap-Tail Determined At 2.4 Angstrom Resolution, gi 146386683 pdb 2PC4 B Chain B, Crystal Structure Of Fructose-Bisphosphate Aldolase From Plasmodium Falciparum In Complex With Trap-Tail Determined At 2.4 Angstrom Resolution,</p>	<p>FBPA</p>	<p>PF14_0425</p>
---	-------------	------------------

<p>gi 146386684 pdb 2PC4 C Chain C, Crystal Structure Of Fructose-Bisphosphate Aldolase From Plasmodium Falciparum In Complex With Trap-Tail Determined At 2.4 Angstrom Resolution,</p> <p>gi 146386685 pdb 2PC4 D Chain D, Crystal Structure Of Fructose-Bisphosphate Aldolase From Plasmodium Falciparum In Complex With Trap-Tail Determined At 2.4 Angstrom Resolution,</p> <p>gi 23497496 gb AAN37038.1 AE014823_18 fructose-bisphosphate aldolase [Plasmodium falciparum 3D7], gi 160067 gb AAA29473.1 aldolase [Plasmodium falciparum]</p>		
<p>heat shock protein 86 [Plasmodium falciparum 3D7], gi 505338 gb AAA66178.1 heat shock protein 86 [Plasmodium falciparum], gi 2642495 gb AAC47837.1 heat shock protein 86 [Plasmodium falciparum], gi 23498766 emb CAD50836.1 heat shock protein 86 [Plasmodium falciparum 3D7]</p>	Hsp90	PF07_0029
<p>Chain A, Structure Of Plasmodium Falciparum Ornithine Delta-Aminotransferase, gi 302148759 pdb 3LG0 B Chain B, Structure Of Plasmodium Falciparum Ornithine Delta-Aminotransferase, gi 302148760 pdb 3LG0 C Chain C, Structure Of Plasmodium Falciparum Ornithine Delta-Aminotransferase, gi 302148761 pdb 3LG0 D Chain D, Structure Of Plasmodium Falciparum Ornithine Delta-Aminotransferase, gi 302148879 pdb 3NTJ A Chain A, Redox Regulation Of Plasmodium Falciparum Ornithine Delta- Aminotransferase, gi 302148880 pdb 3NTJ B</p>	OAT	PFF0435w

Chain B, Redox Regulation Of Plasmodium Falciparum Ornithine Delta- Aminotransferase, gi 302148881 pdb 3NTJ C Chain C, Redox Regulation Of Plasmodium Falciparum Ornithine Delta- Aminotransferase, gi 302148882 pdb 3NTJ D Chain D, Redox Regulation Of Plasmodium Falciparum Ornithine Delta- Aminotransferase		
merozoite surface protein-1 [Plasmodium falciparum]	MSP-1	PFI1475w
phosphoglycerate kinase [Plasmodium falciparum 3D7], gi 129926 sp P27362.1 PGK_PLAF7 RecName: Full=Phosphoglycerate kinase, gi 160592 gb AAA29727.1 3-phosphoglycerate kinase [Plasmodium falciparum], gi 23505125 emb CAD51907.1 phosphoglycerate kinase [Plasmodium falciparum 3D7]	PGK	PFI1105w
falcilysin [Plasmodium falciparum 3D7], gi 6249557 gb AAF06062.1 AF123458_1 falcilysin [Plasmodium falciparum], gi 23615736 emb CAD52728.1 falcilysin [Plasmodium falciparum 3D7]	FLN	PF13_0322
endoplasmin homolog precursor, putative [Plasmodium falciparum 3D7], gi 23496745 gb AAN36300.1 AE014847_27 endoplasmin homolog precursor, putative [Plasmodium falciparum 3D7]	Grp94	PFL1070c
conserved Plasmodium protein [Plasmodium falciparum 3D7], gi 74862993 sp Q8I659.1 YPF11_PLAF7 RecName: Full=Uncharacterized protein PFB0765w, gi 23503419 gb AAN37613.1 conserved Plasmodium	UNK	PFB0765w

protein [Plasmodium falciparum 3D7]		
S-adenosylmethionine synthetase [Plasmodium falciparum 3D7], gi 9927542 gb AAG02013.1 AF180426_1 methionine adenosyltransferase [Plasmodium falciparum], gi 10129955 gb AAG13449.1 S-adenosylmethionine synthetase [Plasmodium falciparum], gi 23505122 emb CAD51904.1 S-adenosylmethionine synthetase [Plasmodium falciparum 3D7]	SAMS	PFI1090w
integral membrane protein, putative [Plasmodium falciparum 3D7], gi 225631735 emb CAG25372.2 integral membrane protein, putative [Plasmodium falciparum 3D7]	ITM	PFL1140w
Pyruvate kinase: Chain A, Crystal Structure Of Pff1300w., gi 284055701 pdb 3KHD B Chain B, Crystal Structure Of Pff1300w., gi 284055702 pdb 3KHD C Chain C, Crystal Structure Of Pff1300w., gi 284055703 pdb 3KHD D Chain D, Crystal Structure Of Pff1300w	PK	Pff1300w
reticulocyte binding protein-like protein 4 [Plasmodium falciparum]	RH4	PFD1150c
putative erythrocyte membrane protein [Plasmodium falciparum]	EMP1	PFD0655w
reticulocyte-binding protein 3 homologue [Plasmodium falciparum 3D7], gi 74862587 sp Q8I4R2.1 RBP3_PLAF7 RecName: Full=Reticulocyte-binding protein 3; Flags: Precursor, gi 23497036 gb AAN36586.1 reticulocyte-binding protein 3 homologue [Plasmodium	RBP3	PFL2520w

falciparum 3D7]		
N6-adenine-specific methylase, putative [Plasmodium falciparum 3D7], gi 225632021 emb CAX64358.1 N6-adenine-specific methylase, putative [Plasmodium falciparum 3D7]	N6-DAM	MAL13P1.255
m1-family aminopeptidase [Plasmodium falciparum 3D7], gi 31340516 sp O96935.2 AMP1_PLAFQ RecName: Full=M1 family aminopeptidase; AltName: Full=Pfa-M1, gi 23615263 emb CAD52253.1 m1-family aminopeptidase [Plasmodium falciparum 3D7], gi 24744851 emb CAA70301.2 zinc-aminopeptidase [Plasmodium falciparum]	AMP1	MAL13P1.56
RhopH2 [Plasmodium falciparum]	RhoPH2	PFI1445w
conserved Plasmodium protein, unknown function [Plasmodium falciparum 3D7], gi 23498933 emb CAD51011.1 conserved Plasmodium protein, unknown function [Plasmodium falciparum 3D7]	UNK	
myo-inositol 1-phosphate synthase, putative [Plasmodium falciparum 3D7], gi 23504603 emb CAD51482.1 myo-inositol 1- phosphate synthase, putative [Plasmodium falciparum 3D7]	MIPS	PFE0585c
elongation factor-1 alpha [Plasmodium falciparum 3D7], gi 124513852 ref XP_001350282.1 elongation factor-1 alpha [Plasmodium falciparum 3D7], gi 23615698 emb CAD52690.1 elongation factor-1 alpha [Plasmodium falciparum 3D7], gi 23615699 emb CAD52691.1 elongation factor-1	EF1-a	PF13_0305

alpha [Plasmodium falciparum 3D7]		
heat shock protein 70 (hsp70), putative [Plasmodium falciparum 3D7], gi 225632011 emb CAX64348.1 heat shock protein 70 (hsp70), putative [Plasmodium falciparum 3D7]	Hsp70	
conserved Plasmodium protein [Plasmodium falciparum 3D7], gi 254688478 gb AAC71923.3 conserved Plasmodium protein [Plasmodium falciparum 3D7]	UNK	
conserved Plasmodium protein, unknown function [Plasmodium falciparum 3D7], gi 225631665 emb CAX63951.1 conserved Plasmodium protein, unknown function [Plasmodium falciparum 3D7]	UNK	
elongation factor 2 [Plasmodium falciparum 3D7], gi 23497558 gb AAN37099.1 AE014824_18 elongation factor 2 [Plasmodium falciparum 3D7]	EF2	PF14_0486
serine hydroxymethyltransferase [Plasmodium falciparum 3D7], gi 6319183 gb AAF07198.1 AF195023_1 SHMT [Plasmodium falciparum], gi 23496877 gb AAN36430.1 serine hydroxymethyltransferase [Plasmodium falciparum 3D7]	SHMT	PFL1720w
erythrocyte membrane protein 1, PfEMP1 [Plasmodium falciparum 3D7], gi 23499282 emb CAD51362.1 erythrocyte membrane protein 1, PfEMP1 [Plasmodium falciparum 3D7]	EMP1	

erythrocyte membrane protein 1, PfEMP1 [Plasmodium falciparum 3D7], gi 23498273 emb CAD49244.1 erythrocyte membrane protein 1, PfEMP1 [Plasmodium falciparum 3D7]	EMP1	
peptidase, putative [Plasmodium falciparum 3D7], gi 23497589 gb AAN37130.1 AE014824_49 peptidase, putative [Plasmodium falciparum 3D7]	PEP	PF14_0382
ubiquitin carboxyl-terminal hydrolase, putative [Plasmodium falciparum 3D7], gi 224591368 emb CAD49004.2 ubiquitin carboxyl- terminal hydrolase, putative [Plasmodium falciparum 3D7]	UCH	PF13_0096
conserved Plasmodium protein [Plasmodium falciparum 3D7], gi 23495200 gb AAN35530.1 conserved Plasmodium protein [Plasmodium falciparum 3D7]	UNK	
M17 leucyl aminopeptidase [Plasmodium falciparum 3D7], gi 23497510 gb AAN37052.1 M17 leucyl aminopeptidase [Plasmodium falciparum 3D7]	LAP	PF14_0439
PfEMP1 variant 2 of strain MC [Plasmodium falciparum]	EMP1-2	PFA0075w
adenosine deaminase, putative [Plasmodium falciparum 3D7], gi 23495155 gb AAN35486.1 AE014833_57 adenosine deaminase, putative [Plasmodium falciparum 3D7], gi 28974401 gb AAO61667.1 adenosine deaminase [Plasmodium falciparum]	ADA	PF10_0289
Hsp70/Hsp90 organizing protein, putative	HOP	PF14_0324

[Plasmodium falciparum 3D7], gi 75016029 sp Q8ILC1.1 STI1L_PLAF7 RecName: Full=STI1-like protein, gi 23497393 gb AAN36937.1 Hsp70/Hsp90 organizing protein, putative [Plasmodium falciparum 3D7]		
NOT family protein, putative [Plasmodium falciparum 3D7], gi 23495975 gb AAN35638.1 NOT family protein, putative [Plasmodium falciparum 3D7]	NOT	PF11_0049
Myb-like DNA-binding domain, putative [Plasmodium falciparum 3D7], gi 23496165 gb AAN35825.1 Myb-like DNA- binding domain, putative [Plasmodium falciparum 3D7]	Myb-L	PF13_0088
erythrocyte membrane protein 1 [Plasmodium falciparum]	EMP1	
hexokinase [Plasmodium falciparum 3D7], gi 46361188 emb CAG25052.1 hexokinase [Plasmodium falciparum 3D7]	HK	PF11_155w
endoplasmic reticulum-resident calcium binding protein [Plasmodium falciparum 3D7], gi 23496024 gb AAN35686.1 AE014837_28 endoplasmic reticulum-resident calcium binding protein [Plasmodium falciparum 3D7], gi 1899003 gb AAB49899.1 membrane-associated calcum-binding protein [Plasmodium falciparum]	ER-CBP	PF11_0098
heat shock protein 60 [Plasmodium falciparum 3D7], gi 23495018 gb AAN35351.1 heat shock protein 60 [Plasmodium falciparum 3D7]	Hsp60	PF10_0153

cytoadherence linked asexual protein [Plasmodium falciparum]	CLAP	MAL7P1.229
conserved Plasmodium protein, unknown function [Plasmodium falciparum 3D7], gi 23615490 emb CAD52481.1 conserved Plasmodium protein, unknown function [Plasmodium falciparum 3D7]	UNK	
conserved Plasmodium protein, unknown function [Plasmodium falciparum 3D7], gi 23615642 emb CAD52634.1 conserved Plasmodium protein, unknown function [Plasmodium falciparum 3D7]	UNK	
pantothenate kinase, putative [Plasmodium falciparum 3D7], gi 255528797 gb AAN36812.2 pantothenate kinase, putative [Plasmodium falciparum 3D7]	PANK	PF14_0200
conserved Plasmodium protein, unknown function [Plasmodium falciparum 3D7], gi 23504686 emb CAD51564.1 conserved Plasmodium protein, unknown function [Plasmodium falciparum 3D7]	UNK	
NOT family protein, putative [Plasmodium falciparum 3D7], gi 23497235 gb AAN36782.1 NOT family protein, putative [Plasmodium falciparum 3D7]	NOT	
structural maintenance of chromosome protein, putative [Plasmodium falciparum 3D7], gi 23496242 gb AAN35901.1 AE014840_49 structural maintenance of chromosome protein,	SMC	PF11_0317

putative [Plasmodium falciparum 3D7]		
structure specific recognition protein [Plasmodium falciparum 3D7], gi 23497463 gb AAN37006.1 structure specific recognition protein [Plasmodium falciparum 3D7]	SSRP	PF14_0393
erythrocyte membrane protein [Plasmodium falciparum]		
erythrocyte membrane protein [Plasmodium falciparum], gi 78039805 emb CAJ39083.1 erythrocyte membrane protein [Plasmodium falciparum]		
apicoplast RNA methyltransferase precursor, putative [Plasmodium falciparum 3D7], gi 254688488 gb AAC71960.3 apicoplast RNA methyltransferase precursor, putative [Plasmodium falciparum 3D7]	ARMT	PFB0855c
serine/threonine protein kinase, putative [Plasmodium falciparum 3D7], gi 23497479 gb AAN37021.1 serine/threonine protein kinase, putative [Plasmodium falciparum 3D7]	STPK	PF14_0516
conserved Plasmodium protein [Plasmodium falciparum 3D7], gi 23496920 gb AAN36472.1 conserved Plasmodium protein [Plasmodium falciparum 3D7]	UNK	
RNA pseudouridylate synthase, putative [Plasmodium falciparum 3D7], gi 74862473 sp Q8I3Z1.1 MLRR1_PLAF7 RecName: Full=MATH and LRR domain-containing	RUSD	PFE0570w

protein PFE0570w, gi 23504600 emb CAD51479.1 RNA pseudouridylate synthase, putative [Plasmodium falciparum 3D7]		
erythrocyte membrane protein 1 [Plasmodium falciparum]	EMP1	
conserved protein [Plasmodium falciparum 3D7], gi 23496728 gb AAN36283.1 conserved protein [Plasmodium falciparum 3D7]	UNK	
RhopH1/Clag3.1 [Plasmodium falciparum]	RhopH1/Cla g3.1	PFC0110w
conserved Plasmodium protein, unknown function [Plasmodium falciparum 3D7], gi 255528861 gb AAN37032.2 conserved Plasmodium protein, unknown function [Plasmodium falciparum 3D7]	UNK	
rhoptry-associated protein 2, RAP2 [Plasmodium falciparum 3D7], gi 6683933 gb AAF23400.1 rhoptry-associated protein 2 [Plasmodium falciparum], gi 23504502 emb CAD51382.1 rhoptry- associated protein 2, RAP2 [Plasmodium falciparum 3D7]	RAP2	PFE0080c
conserved Plasmodium protein [Plasmodium falciparum 3D7], gi 23496796 gb AAN36350.1 conserved Plasmodium protein [Plasmodium falciparum 3D7]	UNK	
protein kinase, putative [Plasmodium falciparum 3D7], gi 46361186 emb CAG25050.1 protein kinase, putative [Plasmodium falciparum 3D7]	PK	
6-phosphogluconate dehydrogenase, decarboxylating,	6PGDH	PF14_0520

putative [Plasmodium falciparum 3D7], gi 23497592 gb AAN37133.1 AE014824_52 6- phosphogluconate dehydrogenase, decarboxylating, putative [Plasmodium falciparum 3D7]		
conserved Plasmodium protein [Plasmodium falciparum 3D7], gi 254922452 gb AAN35426.2 conserved Plasmodium protein [Plasmodium falciparum 3D7]	UNK	
conserved Plasmodium protein [Plasmodium falciparum 3D7], gi 3845221 gb AAC71904.1 conserved Plasmodium protein [Plasmodium falciparum 3D7]	UNK	
pseudouridylate synthase, putative [Plasmodium falciparum 3D7], gi 225632204 emb CAX64089.1 pseudouridylate synthase, putative [Plasmodium falciparum 3D7]	USD2	
erythrocyte membrane protein 1, PfEMP1 [Plasmodium falciparum 3D7], gi 46361274 emb CAG25137.1 erythrocyte membrane protein 1, PfEMP1 [Plasmodium falciparum 3D7]	PfEMP1	
origin recognition complex subunit 2, putative [Plasmodium falciparum 3D7], gi 23498754 emb CAD50824.1 origin recognition complex subunit 2, putative [Plasmodium falciparum 3D7]	ORC-S2	MAL7P1.21
conserved Plasmodium protein, unknown function [Plasmodium falciparum 3D7], gi 23497758 gb AAN37296.1 conserved Plasmodium protein, unknown function [Plasmodium falciparum	UNK	

3D7]		
<p>helicase 45 [Plasmodium falciparum 3D7], gi 23497730 gb AAN37268.1 helicase 45 [Plasmodium falciparum 3D7], gi 83272531 gb ABC00776.1 eIF4A-like [Plasmodium falciparum], gi 112434012 gb ABI18354.1 eIF4A-like [Plasmodium falciparum]</p>	CDC45	PF14_0655
<p>conserved Plasmodium protein, unknown function [Plasmodium falciparum 3D7], gi 225631752 emb CAG25008.2 conserved Plasmodium protein, unknown function [Plasmodium falciparum 3D7]</p>	UNK	
<p>rhopty associated protein 1 (rop1) precursor [Plasmodium falciparum]</p>	RAP1	PF14_0102
<p>mitogen-activated protein kinase 1 [Plasmodium falciparum 3D7], gi 23497362 gb AAN36907.1 AE014820_57 mitogen-activated protein kinase 1 [Plasmodium falciparum 3D7]</p>	MAPK1	PF14_0294
<p>ran binding protein 1, putative [Plasmodium falciparum 3D7], gi 17148533 emb CAD12772.1 Ran-binding protein [Plasmodium falciparum 3D7], gi 23498262 emb CAD49233.1 ran binding protein 1, putative [Plasmodium falciparum 3D7]</p>	RANBP1	PFD0950w
<p>conserved Plasmodium protein, unknown function [Plasmodium falciparum 3D7], gi 23499086 emb CAD51166.1 conserved Plasmodium protein, unknown function [Plasmodium falciparum 3D7]</p>	UNK	

Plasmodium exported protein (PHISTc), unknown function [Plasmodium falciparum 3D7], gi 23499274 emb CAD51354.1 Plasmodium exported protein (PHISTc), unknown function [Plasmodium falciparum 3D7]	PHISTc	PFB0105c
phosphatidylinositol 4-kinase, putative [Plasmodium falciparum 3D7], gi 225631648 emb CAX51867.1 phosphatidylinositol 4-kinase, putative [Plasmodium falciparum 3D7]	PI4K	PFE0485w
conserved Plasmodium protein, unknown function [Plasmodium falciparum 3D7], gi 23497661 gb AAN37201.1 conserved Plasmodium protein, unknown function [Plasmodium falciparum 3D7]	UNK	
Malaria Parasite Nucleosome Assembly Protein (Nap)	NAP	PFI0930c
elongation factor 1-beta [Plasmodium falciparum 3D7], gi 6740011 gb AAF27524.1 AF217234_1 translation elongation factor 1 beta [Plasmodium falciparum], gi 23505032 emb CAD51815.1 elongation factor 1-beta [Plasmodium falciparum 3D7]	EF1-b	PFI0645w
splicing factor 3b, subunit 3, 130kD, putative [Plasmodium falciparum 3D7], gi 23496869 gb AAN36422.1 AE014849_41 splicing factor 3b, subunit 3, 130kD, putative [Plasmodium falciparum 3D7]	SF3b	PFL1680w
tRNA pseudouridine synthase, putative [Plasmodium falciparum 3D7],	PSUI	PFI0420c

gi 23495040 gb AAN35373.1 AE014831_49 tRNA pseudouridine synthase, putative [Plasmodium falciparum 3D7]		
RIFIN [Plasmodium falciparum]	RIFIN	PFA0010c
Rrp6 homologue, putative [Plasmodium falciparum 3D7], gi 23497545 gb AAN37086.1 Rrp6 homologue, putative [Plasmodium falciparum 3D7]	RRP6	PF14_0473
conserved Plasmodium protein [Plasmodium falciparum 3D7], gi 23496929 gb AAN36481.1 conserved Plasmodium protein [Plasmodium falciparum 3D7]	UNK	
Plasmodium exported protein (hyp17), unknown function [Plasmodium falciparum 3D7], gi 23497816 gb AAN37353.1 Plasmodium exported protein (hyp17), unknown function [Plasmodium falciparum 3D7]	HYP17	PF14_0740
Plasmodium Purine Nucleoside Phosphorylase V66i-V73i-Y160f Mutant, gi 282403625 pdb 3FOW B Chain B, Plasmodium Purine Nucleoside Phosphorylase V66i-V73i-Y160f Mutant	PNPase	PFE0660c
protein kinase, putative [Plasmodium falciparum 3D7], gi 23497389 gb AAN36933.1 protein kinase, putative [Plasmodium falciparum 3D7]	PK	
P-type calcium transporting ATPase [Plasmodium falciparum], gi 301599379 dbj BAJ12383.1 P-type calcium transporting ATPase [Plasmodium falciparum], gi 301599417 dbj BAJ12402.1 P-type calcium transporting ATPase [Plasmodium falciparum], gi 301601420 dbj BAJ12242.1 P-type	P-CAT	PFA0310c

calcium transporting ATPase [Plasmodium falciparum]		
conserved Plasmodium protein, unknown function [Plasmodium falciparum 3D7], gi 225631834 emb CAX64229.1 conserved Plasmodium protein, unknown function [Plasmodium falciparum 3D7]	UNK	
SET domain protein, putative [Plasmodium falciparum 3D7], gi 263429753 sp C6KTD2.1 HKNMT_PLAF7 RecName: Full=Putative histone-lysine N-methyltransferase PFF1440w, gi 225631776 emb CAG25109.2 SET domain protein, putative [Plasmodium falciparum 3D7]	SET	PFD0190w
conserved Plasmodium protein, unknown function [Plasmodium falciparum 3D7], gi 23497609 gb AAN37149.1 conserved Plasmodium protein, unknown function [Plasmodium falciparum 3D7]	UNK	
conserved Plasmodium protein, unknown function [Plasmodium falciparum 3D7], gi 23497287 gb AAN36833.1 conserved Plasmodium protein, unknown function [Plasmodium falciparum 3D7]	UNK	
Pfs77 protein [Plasmodium falciparum 3D7], gi 994809 emb CAA85779.1 Pfs77 [Plasmodium falciparum], gi 46361164 emb CAG25028.1 Pfs77 protein [Plasmodium falciparum 3D7]	Pfs77	PFF1035w
conserved Plasmodium protein, unknown function [Plasmodium falciparum 3D7],	UNK	

gi 23498849 emb CAD50926.1 conserved Plasmodium protein, unknown function [Plasmodium falciparum 3D7]		
conserved Plasmodium protein [Plasmodium falciparum 3D7], gi 23495036 gb AAN35369.1 conserved Plasmodium protein [Plasmodium falciparum 3D7]	UNK	
SET domain protein, putative [Plasmodium falciparum 3D7], gi 23615377 emb CAD52368.1 SET domain protein, putative [Plasmodium falciparum 3D7]	SET	
conserved Plasmodium membrane protein, unknown function [Plasmodium falciparum 3D7], gi 23615400 emb CAD52391.1 conserved Plasmodium membrane protein, unknown function [Plasmodium falciparum 3D7]	UNK	
conserved Plasmodium protein, unknown function [Plasmodium falciparum 3D7], gi 46361048 emb CAG25335.1 conserved Plasmodium protein, unknown function [Plasmodium falciparum 3D7]	UNK	
elongation factor 1-gamma, putative [Plasmodium falciparum 3D7], gi 225631998 emb CAD52519.2 elongation factor 1-gamma, putative [Plasmodium falciparum 3D7]	EF1-c	PF13_0214
conserved Plasmodium protein, unknown function [Plasmodium falciparum 3D7], gi 23615606 emb CAD52598.1 conserved Plasmodium protein, unknown function [Plasmodium falciparum 3D7]	UNK	

ubiquitin-activating enzyme E1, putative [Plasmodium falciparum 3D7], gi 23496781 gb AAN36335.1 ubiquitin-activating enzyme E1, putative [Plasmodium falciparum 3D7]	UBE1	PFL1245w
rhopty-associated protein 3, RAP3 [Plasmodium falciparum 3D7], gi 23504501 emb CAD51381.1 rhopty-associated protein 3, RAP3 [Plasmodium falciparum 3D7]	RAP3	PFE0075c
conserved Plasmodium protein, unknown function [Plasmodium falciparum 3D7], gi 255528747 gb AAN36641.2 conserved Plasmodium protein, unknown function [Plasmodium falciparum 3D7]	UNK	
proliferation-associated protein 2g4, putative [Plasmodium falciparum 3D7], gi 23497329 gb AAN36874.1 AE014820_24 proliferation-associated protein 2g4, putative [Plasmodium falciparum 3D7]	P38-2G4	PF14_0261
splicing factor, putative [Plasmodium falciparum 3D7], gi 23615373 emb CAD52364.1 splicing factor, putative [Plasmodium falciparum 3D7]	SF	PFE0865c
mismatch repair protein pms1 homologue, putative [Plasmodium falciparum 3D7], gi 23498929 emb CAD51007.1 mismatch repair protein pms1 homologue, putative [Plasmodium falciparum 3D7]	PMS1	MAL7P1.145
myosin D [Plasmodium falciparum 3D7], gi 14194222 gb AAK56302.1 AF376800_1 myosin D [Plasmodium falciparum],	MyD	PFL1435c

gi 23496819 gb AAN36373.1 myosin D [Plasmodium falciparum 3D7]		
conserved Plasmodium protein [Plasmodium falciparum 3D7], gi 23495153 gb AAN35484.1 conserved Plasmodium protein [Plasmodium falciparum 3D7]	UNK	
ADP-ribosylation factor, putative [Plasmodium falciparum 3D7], gi 23615316 emb CAD52307.1 ADP-ribosylation factor, putative [Plasmodium falciparum 3D7]	ARF-a	PFE1305c-a
RecName: Full=S-antigen protein; Flags: Precursor, gi 160671 gb AAA29758.1 S antigen precursor [Plasmodium falciparum]	PMMSA	
vacuolar ATP synthase, catalytic subunit a [Plasmodium falciparum 3D7], gi 418177 sp Q03498.1 VATA_PLAFA RecName: Full=V-type proton ATPase catalytic subunit A; Short=V-ATPase subunit A; AltName: Full=V- ATPase 69 kDa subunit; AltName: Full=Vacuolar proton pump subunit alpha, gi 50401476 sp Q76NM6.1 VATA_PLAF7 RecName: Full=V-type proton ATPase catalytic subunit A; Short=V-ATPase subunit A; AltName: Full=V-ATPase 69 kDa subunit; AltName: Full=Vacuolar proton pump subunit alpha, gi 160736 gb AAA29782.1 vacuolar ATPase [Plasmodium falciparum], gi 23615264 emb CAD52254.1 vacuolar ATP synthase, catalytic subunit a [Plasmodium falciparum 3D7]	V-ATPase	PFE0965c

erythrocyte membrane protein 1 [Plasmodium falciparum]		
erythrocyte membrane protein pfemp3, putative [Plasmodium falciparum 3D7], gi 23496775 gb AAN36329.1 erythrocyte membrane protein pfemp3, putative [Plasmodium falciparum 3D7]	EMP3	PFB0095c
histone binding protein, putative [Plasmodium falciparum 3D7], gi 23496587 gb AAN36145.1 histone binding protein, putative [Plasmodium falciparum 3D7]	HBP	PFL0280c
conserved Plasmodium protein [Plasmodium falciparum 3D7], gi 23495038 gb AAN35371.1 conserved Plasmodium protein [Plasmodium falciparum 3D7]	UNK	
Tetratricopeptide repeat family protein, putative [Plasmodium falciparum 3D7], gi 23615561 emb CAD52553.1 Tetratricopeptide repeat family protein, putative [Plasmodium falciparum 3D7]	TTPR	PFI1060w
ATP synthase (C/AC39) subunit, putative [Plasmodium falciparum 3D7], gi 23497689 gb AAN37228.1 AE014826_27 ATP synthase (C/AC39) subunit, putative [Plasmodium falciparum 3D7]	C/AC39	PF14_0615
conserved Plasmodium protein, unknown function [Plasmodium falciparum 3D7], gi 74873275 sp O97239.1 DOP1_PLAF7 RecName: Full=Protein dopey homolog PFC0245c,	UNK	

gi 4493896 emb CAB39005.1 conserved Plasmodium protein, unknown function [Plasmodium falciparum 3D7]		
methionine-tRNA ligase, putative [Plasmodium falciparum 3D7], gi 23495207 gb AAN35537.1 methionine-tRNA ligase, putative [Plasmodium falciparum 3D7]	MetRS	PF10_0053
ribosomal protein l7ae, putative [Plasmodium falciparum 3D7], gi 3649767 emb CAB11116.1 ribosomal protein l7ae, putative [Plasmodium falciparum 3D7]	l7ae	PFC0405c
serine/threonine protein kinase, putative [Plasmodium falciparum 3D7], gi 255528876 gb AAN37089.2 serine/threonine protein kinase, putative [Plasmodium falciparum 3D7]	STPK	
caspase, putative [Plasmodium falciparum 3D7], gi 23615677 emb CAD52669.1 caspase, putative [Plasmodium falciparum 3D7], gi 85822147 gb ABC84559.1 metacaspase precursor [Plasmodium falciparum]	CASP	PF13_0289
conserved Plasmodium protein, unknown function [Plasmodium falciparum 3D7], gi 23615336 emb CAD52327.1 conserved Plasmodium protein, unknown function [Plasmodium falciparum 3D7]	UNK	
DNA repair endonuclease, putative [Plasmodium falciparum 3D7], gi 23615815 emb CAD52807.1 DNA repair endonuclease, putative [Plasmodium falciparum 3D7]	DRE	MAL13P1.346

apical membrane antigen 1 [Plasmodium falciparum]	AMA1	PF11_0486
conserved Plasmodium protein [Plasmodium falciparum 3D7], gi 254945426 gb AAN36521.2 conserved Plasmodium protein [Plasmodium falciparum 3D7]	UNK	
RecName: Full=Glucose-6-phosphate isomerase; Short=GPI; AltName: Full=Phosphoglucose isomerase; Short=PGI; AltName: Full=Phosphohexose isomerase; Short=PHI, gi 160310 gb AAA29610.1 glucosephosphate isomerase [Plasmodium falciparum]	G6PI	PF14_0341
cell division cycle protein 48 homologue, putative [Plasmodium falciparum 3D7], gi 225631753 emb CAG25009.2 cell division cycle protein 48 homologue, putative [Plasmodium falciparum 3D7]	CDC48	PFF0940c
conserved Plasmodium protein, unknown function [Plasmodium falciparum 3D7], gi 23504695 emb CAD51573.1 conserved Plasmodium protein, unknown function [Plasmodium falciparum 3D7]	UNK	
adenosylhomocysteinase(S-adenosyl-L-homocysteine hydrolase) [Plasmodium falciparum 3D7], gi 78099800 sp P50250.2 SAHH_PLAF7 RecName: Full=Adenosylhomocysteinase; Short=AdoHcyase; AltName: Full=PfSAHH; AltName: Full=S-adenosyl-L-homocysteine hydrolase, gi 56554255 pdb 1V8B A Chain A, Crystal Structure Of A Hydrolase, gi 56554256 pdb 1V8B B Chain B, Crystal Structure Of A Hydrolase,	AdoHcyase	PFE1050w

<p>gi 56554257 pdb 1V8B C Chain C, Crystal Structure Of A Hydrolase, gi 56554258 pdb 1V8B D Chain D, Crystal Structure Of A Hydrolase, gi 22087607 gb AAM90981.1 AF525293_1 S-adenosyl-L-homocysteine hydrolase [Plasmodium falciparum], gi 23504696 emb CAD51574.1 adenosylhomocysteinase(S-adenosyl-L-homocysteine hydrolase) [Plasmodium falciparum 3D7]</p>		
<p>ATP synthase beta chain, mitochondrial precursor, putative [Plasmodium falciparum 3D7], gi 23496878 gb AAN36431.1 AE014849_50 ATP synthase beta chain, mitochondrial precursor, putative [Plasmodium falciparum 3D7]</p>	M-AS	
<p>conserved Plasmodium protein [Plasmodium falciparum 3D7], gi 23494928 gb AAN35262.1 conserved Plasmodium protein [Plasmodium falciparum 3D7]</p>	UNK	
<p>conserved Plasmodium protein [Plasmodium falciparum 3D7], gi 23496623 gb AAN36180.1 conserved Plasmodium protein [Plasmodium falciparum 3D7]</p>	UNK	
<p>conserved Plasmodium protein, unknown function [Plasmodium falciparum 3D7], gi 23615772 emb CAD52764.1 conserved Plasmodium protein, unknown function [Plasmodium falciparum 3D7]</p>	UNK	
<p>peptide chain release factor, putative [Plasmodium falciparum 3D7], gi 23498750 emb CAD50820.1 peptide chain release factor, putative [Plasmodium falciparum 3D7]</p>	eRF	MAL7P1.20

Cg4 protein [Plasmodium falciparum 3D7], gi 23498770 emb CAD50840.1 Cg4 protein [Plasmodium falciparum 3D7]	Cg4	PF07_0033
conserved Plasmodium protein, unknown function [Plasmodium falciparum 3D7], gi 23504575 emb CAD51454.1 conserved Plasmodium protein, unknown function [Plasmodium falciparum 3D7]	UNK	
conserved Plasmodium membrane protein, unknown function [Plasmodium falciparum 3D7], gi 255528911 gb AAN37226.2 conserved Plasmodium membrane protein, unknown function [Plasmodium falciparum 3D7]	UNK	
erythrocyte membrane protein [Plasmodium falciparum], gi 78042161 emb CAJ40261.1 erythrocyte membrane protein [Plasmodium falciparum], gi 78042163 emb CAJ40262.1 erythrocyte membrane protein [Plasmodium falciparum]	EMP	
conserved Plasmodium protein, unknown function [Plasmodium falciparum 3D7], gi 225631871 emb CAX64265.1 conserved Plasmodium protein, unknown function [Plasmodium falciparum 3D7]	UNK	
conserved Plasmodium protein, unknown function [Plasmodium falciparum 3D7], gi 23505026 emb CAD51809.1 conserved Plasmodium protein, unknown function [Plasmodium falciparum 3D7]	UNK	

rabGDI [Plasmodium falciparum 3D7]	rabGD1	PFL2060c
Ankyrin, putative [Plasmodium falciparum 3D7], gi 23497289 gb AAN36835.1 Ankyrin, putative [Plasmodium falciparum 3D7]	ANK	PF10_0102

Anti-PfHsp90 Pulldown

Identified Proteins (188)	Short form	PlasmoDB ID
14-3-3 protein, putative [Plasmodium falciparum 3D7], gi 225632253 emb CAX64133.1 14-3-3 protein, putative [Plasmodium falciparum 3D7]	14-3-3	MAL8P1.69
conserved Plasmodium protein [Plasmodium falciparum 3D7], gi 74862993 sp Q8I659.1 YPF11_PLAF7 RecName: Full=Uncharacterized protein PFB0765w, gi 23503419 gb AAN37613.1 conserved Plasmodium protein [Plasmodium falciparum 3D7]	UNK	
integral membrane protein, putative [Plasmodium falciparum 3D7], gi 225631735 emb CAG25372.2 integral membrane protein, putative [Plasmodium falciparum 3D7]	ITM	
conserved Plasmodium protein, unknown function [Plasmodium falciparum 3D7], gi 23498933 emb CAD51011.1 conserved Plasmodium protein, unknown function [Plasmodium falciparum 3D7]	UNK	
phosphoethanolamine N-methyltransferase [Plasmodium falciparum 3D7], gi 23615568 emb CAD52560.1 phosphoethanolamine N-methyltransferase [Plasmodium falciparum 3D7], gi 38018254 gb AAR08195.1 phosphoethanolamine N-methyltransferase [Plasmodium falciparum]	PEAMT	MAL13P1.214
Plasmodium Purine Nucleoside Phosphorylase V66i-V73i-Y160f Mutant, gi 282403625 pdb 3FOW B	PNPase	PFE0660c

Chain B, Plasmodium Purine Nucleoside Phosphorylase V66i-V73i-Y160f Mutant		
RecName: Full=Elongation factor 1-alpha; Short=EF-1-alpha, gi 9887 emb CAA43018.1 EF-1 alpha [Plasmodium falciparum]	EF1-a	PF13_0305
conserved Plasmodium protein, unknown function [Plasmodium falciparum 3D7], gi 225631665 emb CAX63951.1 conserved Plasmodium protein, unknown function [Plasmodium falciparum 3D7]	UNK	
putative erythrocyte membrane protein [Plasmodium falciparum]	EMP	
reticulocyte binding protein-like protein 4 [Plasmodium falciparum]	RH4	PFD1150c
lactate dehydrogenase [Plasmodium falciparum]	LDH	PF13_0141
NOT family protein, putative [Plasmodium falciparum 3D7], gi 23495975 gb AAN35638.1 NOT family protein, putative [Plasmodium falciparum 3D7]	NOT	PF11_0049
serine esterase, putative [Plasmodium falciparum 3D7], gi 254832630 gb ACT82972.1 serine esterase, putative [Plasmodium falciparum 3D7]	SE	PF11_0168a
erythrocyte membrane protein 1, PfEMP1 [Plasmodium falciparum 3D7], gi 23498273 emb CAD49244.1 erythrocyte membrane protein 1, PfEMP1 [Plasmodium falciparum 3D7]	EMP1	PFD0655w
heat shock protein hsp70 homologue Pfhsp70-3 [Plasmodium falciparum 3D7]	Hsp70-3	PF11_0351

erythrocyte membrane protein [Plasmodium falciparum]	EMP	
conserved Plasmodium protein, unknown function [Plasmodium falciparum 3D7], gi 23615363 emb CAD52354.1 conserved Plasmodium protein, unknown function [Plasmodium falciparum 3D7]	UNK	
triosephosphate isomerase [Plasmodium falciparum 3D7], gi 586112 sp Q07412.1 TPIS_PLAFA RecName: Full=Triosephosphate isomerase; Short=TIM; AltName: Full=Triose-phosphate isomerase, gi 75009812 sp Q7KQM0.1 TPIS_PLAF7 RecName: Full=Triosephosphate isomerase; Short=TIM; AltName: Full=Triose-phosphate isomerase, gi 160706 gb AAA18799.1 triosephosphate isomerase [Plasmodium falciparum], gi 23497448 gb AAN36991.1 triosephosphate isomerase [Plasmodium falciparum 3D7]	TPI	PF14_0378
peptidyl-prolyl cis-trans isomerase [Plasmodium falciparum 3D7], gi 23496087 gb AAN35748.1 AE014838_26 peptidyl-prolyl cis-trans isomerase [Plasmodium falciparum 3D7], gi 758222 emb CAA59933.1 peptidylprolyl isomerase [Plasmodium falciparum]	PPI	PFC0975c
serine/threonine protein kinase, putative [Plasmodium falciparum 3D7], gi 23497479 gb AAN37021.1 serine/threonine protein kinase, putative [Plasmodium falciparum 3D7]	STPK	PF14_0516
conserved Plasmodium protein [Plasmodium	UNK	

falciparum 3D7], gi 254688478 gb AAC71923.3 conserved Plasmodium protein [Plasmodium falciparum 3D7]		
erythrocyte membrane protein 1 [Plasmodium falciparum]	EMP1	
conserved Plasmodium protein [Plasmodium falciparum 3D7], gi 3845274 gb AAC71944.1 conserved Plasmodium protein [Plasmodium falciparum 3D7]	UNK	
RNA pseudouridylate synthase, putative [Plasmodium falciparum 3D7], gi 74862473 sp Q8I3Z1.1 MLRR1_PLAF7 RecName: Full=MATH and LRR domain-containing protein PFE0570w, gi 23504600 emb CAD51479.1 RNA pseudouridylate synthase, putative [Plasmodium falciparum 3D7]	RUSD	PFE0570w
spindle pole body protein, putative [Plasmodium falciparum 3D7], gi 23477022 emb CAB38989.3 spindle pole body protein, putative [Plasmodium falciparum 3D7]	SPB	PFC0165w
erythrocyte membrane protein [Plasmodium falciparum], gi 78039805 emb CAJ39083.1 erythrocyte membrane protein [Plasmodium falciparum]	EMP	
conserved Plasmodium protein [Plasmodium falciparum 3D7], gi 23494996 gb AAN35329.1 conserved Plasmodium protein [Plasmodium falciparum 3D7]	UNK	
conserved Plasmodium protein, unknown function	UNK	

<p>[Plasmodium falciparum 3D7], gi 23499086 emb CAD51166.1 conserved Plasmodium protein, unknown function [Plasmodium falciparum 3D7]</p>		
<p>conserved Plasmodium protein, unknown function [Plasmodium falciparum 3D7], gi 23615490 emb CAD52481.1 conserved Plasmodium protein, unknown function [Plasmodium falciparum 3D7]</p>	UNK	
<p>cof-like hydrolase, had-superfamily, subfamily iib [Plasmodium falciparum 3D7], gi 23496786 gb AAN36340.1 cof-like hydrolase, had-superfamily, subfamily iib [Plasmodium falciparum 3D7]</p>	COF-HAD	PFL1270w
<p>conserved Plasmodium protein [Plasmodium falciparum 3D7], gi 23496796 gb AAN36350.1 conserved Plasmodium protein [Plasmodium falciparum 3D7]</p>	UNK	
<p>glyceraldehyde-3-phosphate dehydrogenase [Plasmodium falciparum 3D7], gi 83753748 pdb 1YWG O Chain O, The Structure Of Glyceraldehyde-3-Phosphate Dehydrogenase From Plasmodium Falciparum, gi 83753749 pdb 1YWG P Chain P, The Structure Of Glyceraldehyde-3- Phosphate Dehydrogenase From Plasmodium Falciparum, gi 83753750 pdb 1YWG Q Chain Q, The Structure Of Glyceraldehyde-3-Phosphate Dehydrogenase From Plasmodium Falciparum, gi 83753751 pdb 1YWG R Chain R, The Structure Of Glyceraldehyde-3-Phosphate Dehydrogenase From</p>	G3PD	PF14_0598

<p>Plasmodium Falciparum, gi 23497672 gb AAN37211.1 AE014826_10 glyceraldehyde-3-phosphate dehydrogenase [Plasmodium falciparum 3D7], gi 19401842 gb AAL87686.1 glyceraldehyde-3- phosphate dehydrogenase [Plasmodium falciparum]</p>		
<p>serine/threonine protein kinase, putative [Plasmodium falciparum 3D7], gi 23510651 emb CAD49036.1 serine/threonine protein kinase, putative [Plasmodium falciparum 3D7]</p>	STPK	
<p>ubiquitin carboxyl-terminal hydrolase, putative [Plasmodium falciparum 3D7], gi 224591368 emb CAD49004.2 ubiquitin carboxyl- terminal hydrolase, putative [Plasmodium falciparum 3D7]</p>	UCHL	PF13_0096
<p>phosphoglycerate kinase [Plasmodium falciparum 3D7], gi 129926 sp P27362.1 PGK_PLAF7 RecName: Full=Phosphoglycerate kinase, gi 160592 gb AAA29727.1 3-phosphoglycerate kinase [Plasmodium falciparum], gi 23505125 emb CAD51907.1 phosphoglycerate kinase [Plasmodium falciparum 3D7]</p>	PGK	PF11105w
<p>peptide chain release factor, putative [Plasmodium falciparum 3D7], gi 23498750 emb CAD50820.1 peptide chain release factor, putative [Plasmodium falciparum 3D7]</p>	eRF	MAL7P1.20
<p>conserved Plasmodium protein [Plasmodium falciparum 3D7], gi 23496590 gb AAN36147.1 conserved Plasmodium protein [Plasmodium</p>	UNK	

falciparum 3D7]		
conserved Plasmodium protein, unknown function [Plasmodium falciparum 3D7], gi 225631834 emb CAX64229.1 conserved Plasmodium protein, unknown function [Plasmodium falciparum 3D7]	UNK	
erythrocyte membrane protein 1 [Plasmodium falciparum]	EMP1	
metal-dependent hydrolase, putative [Plasmodium falciparum 3D7], gi 23497694 gb AAN37233.1 metal-dependent hydrolase, putative [Plasmodium falciparum 3D7]	HDOD	PF14_0620
proliferating cell nuclear antigen [Plasmodium falciparum 3D7], gi 400740 sp P31008.1 PCNA_PLAFK RecName: Full=Proliferating cell nuclear antigen; Short=PCNA; AltName: Full=Cyclin, gi 46576879 sp P61074.1 PCNA_PLAF7 RecName: Full=Proliferating cell nuclear antigen; Short=PCNA; AltName: Full=Cyclin, gi 9932 emb CAA48673.1 proliferating cell nuclear antigen [Plasmodium falciparum], gi 23615747 emb CAD52739.1 proliferating cell nuclear antigen [Plasmodium falciparum 3D7]	PCNA	PF13_0328
plasmodium falciparum gamete antigen 27/25 [Plasmodium falciparum 3D7], gi 5911418 gb AAD55784.1 AF179422_1 antigen Pfg27/25 [Plasmodium falciparum], gi 160295 gb AAA63424.1 gametocytogenesis onset- specific protein [Plasmodium falciparum],	Pfg27/25	PF13_0011

<p>gi 1340126 emb CAA59328.1 Pfg27/25 [Plasmodium falciparum], gi 23615166 emb CAD52156.1 plasmodium falciparum gamete antigen 27/25 [Plasmodium falciparum 3D7]</p>		
<p>fructose-bisphosphate aldolase [Plasmodium falciparum 3D7], gi 113623 sp P14223.1 ALF_PLAFA RecName: Full=Fructose-bisphosphate aldolase; AltName: Full=41 kDa antigen, gi 74920225 sp Q7KQL9.1 ALF_PLAF7 RecName: Full=Fructose-bisphosphate aldolase, gi 146386478 pdb 2EPH A Chain A, Crystal Structure Of Fructose-Bisphosphate Aldolase From Plasmodium Falciparum In Complex With Trap-Tail Determined At 2.7 Angstrom Resolution, gi 146386479 pdb 2EPH B Chain B, Crystal Structure Of Fructose-Bisphosphate Aldolase From Plasmodium Falciparum In Complex With Trap-Tail Determined At 2.7 Angstrom Resolution, gi 146386480 pdb 2EPH C Chain C, Crystal Structure Of Fructose-Bisphosphate Aldolase From Plasmodium Falciparum In Complex With Trap-Tail Determined At 2.7 Angstrom Resolution, gi 146386481 pdb 2EPH D Chain D, Crystal Structure Of Fructose-Bisphosphate Aldolase From Plasmodium Falciparum In Complex With Trap-Tail Determined At 2.7 Angstrom Resolution, gi 146386682 pdb 2PC4 A Chain A, Crystal Structure Of Fructose-Bisphosphate Aldolase From Plasmodium Falciparum In Complex With Trap-Tail</p>	<p>FBPA</p>	<p>PF14_0425</p>

<p>Determined At 2.4 Angstrom Resolution, gi 146386683 pdb 2PC4 B Chain B, Crystal Structure Of Fructose-Bisphosphate Aldolase From Plasmodium Falciparum In Complex With Trap-Tail</p> <p>Determined At 2.4 Angstrom Resolution, gi 146386684 pdb 2PC4 C Chain C, Crystal Structure Of Fructose-Bisphosphate Aldolase From Plasmodium Falciparum In Complex With Trap-Tail</p> <p>Determined At 2.4 Angstrom Resolution, gi 146386685 pdb 2PC4 D Chain D, Crystal Structure Of Fructose-Bisphosphate Aldolase From Plasmodium Falciparum In Complex With Trap-Tail</p> <p>Determined At 2.4 Angstrom Resolution, gi 23497496 gb AAN37038.1 AE014823_18 fructose-bisphosphate aldolase [Plasmodium falciparum 3D7], gi 160067 gb AAA29473.1 aldolase [Plasmodium falciparum]</p>		
<p>SET domain protein, putative [Plasmodium falciparum 3D7], gi 263429753 sp C6KTD2.1 HKNMT_PLAF7 RecName: Full=Putative histone-lysine N- methyltransferase PFF1440w, gi 225631776 emb CAG25109.2 SET domain protein, putative [Plasmodium falciparum 3D7]</p>	SET	PFD0190w
<p>malaria antigen [Plasmodium falciparum 3D7], gi 74842607 sp Q8ID94.1 YPF12_PLAF7 RecName: Full=Uncharacterized protein MAL13P1.304, gi 23615740 emb CAD52732.1 malaria antigen [Plasmodium falciparum 3D7]</p>	MA	MAL13P1.304
VAR2CSA [Plasmodium falciparum]	PfEMP1	PFL0030c

<p>RecName: Full=Heat shock 70 kDa protein; Short=HSP70; AltName: Full=74.3 kDa protein; AltName: Full=Cytoplasmic antigen, gi 309690 gb AAA29626.1 heat shock protein 70 [Plasmodium falciparum]</p>	Hsp70	MAL13P1.540
<p>reticulocyte-binding protein 3 homologue [Plasmodium falciparum 3D7], gi 74862587 sp Q8I4R2.1 RBP3_PLAF7 RecName: Full=Reticulocyte-binding protein 3; Flags: Precursor, gi 23497036 gb AAN36586.1 reticulocyte- binding protein 3 homologue [Plasmodium falciparum 3D7]</p>	RBP3	PFL2520w
<p>dcp1 homologue, putative [Plasmodium falciparum 3D7], gi 23495181 gb AAN35511.1 dcp1 homologue, putative [Plasmodium falciparum 3D7]</p>	DCP1	PF10_0314
<p>erythrocyte membrane protein 1 [Plasmodium falciparum]</p>	EMP1	
<p>cytoadherence linked asexual protein [Plasmodium falciparum]</p>	CLAP	MAL7P1.229
<p>conserved Plasmodium protein, unknown function [Plasmodium falciparum 3D7], gi 255528861 gb AAN37032.2 conserved Plasmodium protein, unknown function [Plasmodium falciparum 3D7]</p>	UNK	
<p>conserved Plasmodium protein, unknown function [Plasmodium falciparum 3D7], gi 23510657 emb CAD49042.1 conserved Plasmodium protein, unknown function [Plasmodium falciparum 3D7]</p>	UNK	

conserved Plasmodium protein [Plasmodium falciparum 3D7], gi 254832643 gb AAN35797.2 conserved Plasmodium protein [Plasmodium falciparum 3D7]	UNK	
nucleolar preribosomal GTPase, putative [Plasmodium falciparum 3D7], gi 23504868 emb CAD51649.1 nucleolar preribosomal GTPase, putative [Plasmodium falciparum 3D7]	NPR-GTPase	PF14_0072
erythrocyte membrane protein 1, PfEMP1 [Plasmodium falciparum 3D7], gi 23498322 emb CAD49295.1 erythrocyte membrane protein 1, PfEMP1 [Plasmodium falciparum 3D7]	EMP1	
conserved protein, unknown function [Plasmodium falciparum 3D7], gi 255528785 gb AAN36773.2 conserved protein, unknown function [Plasmodium falciparum 3D7]	UNK	
TatD-like deoxyribonuclease, putative [Plasmodium falciparum 3D7], gi 23477010 emb CAD49076.1 TatD-like deoxyribonuclease, putative [Plasmodium falciparum 3D7]	TatD-Dnase	PFA0580c
merozoite surface protein-1 [Plasmodium falciparum]	MSP1	PFI1475w
merozoite surface protein 7 [Plasmodium falciparum], gi 237665244 gb ACR10051.1 merozoite surface protein 7 [Plasmodium falciparum]	MSP7	PF13_0197
conserved protein [Plasmodium falciparum 3D7], gi 23495981 gb AAN35644.1 conserved protein [Plasmodium falciparum 3D7]	UNK	

1-cys peroxiredoxin [Plasmodium falciparum 3D7], gi 4996210 dbj BAA78369.1 1-cys peroxidoxin [Plasmodium falciparum], gi 23499261 emb CAD51341.1 1-cys peroxiredoxin [Plasmodium falciparum 3D7]	1CYS-PRX	MAL7P1.159
RecName: Full=Hypoxanthine-guanine-xanthine phosphoribosyltransferase; Short=HGPRP; Short=HGXPRT; Short=HGXPRTase, gi 5821998 pdb 1CJB A Chain A, Malarial Purine Phosphoribosyltransferase, gi 5821999 pdb 1CJB B Chain B, Malarial Purine Phosphoribosyltransferase, gi 5822000 pdb 1CJB C Chain C, Malarial Purine Phosphoribosyltransferase, gi 5822001 pdb 1CJB D Chain D, Malarial Purine Phosphoribosyltransferase, gi 9914 emb CAA34355.1 unnamed protein product [Plasmodium falciparum]	HGXPRT	PF10_0121
conserved Plasmodium protein [Plasmodium falciparum 3D7], gi 23496564 gb AAN36122.1 conserved Plasmodium protein [Plasmodium falciparum 3D7]	UNK	
conserved Plasmodium protein, unknown function [Plasmodium falciparum 3D7], gi 23499104 emb CAD51184.1 conserved Plasmodium protein, unknown function [Plasmodium falciparum 3D7]	UNK	
erythrocyte membrane protein one [Plasmodium falciparum]	EMP1	
ornithine aminotransferase [Plasmodium falciparum]	OAT	PFF0435w
conserved Plasmodium protein, unknown function	UNK	

<p>[Plasmodium falciparum 3D7], gi 23505159 emb CAD51940.1 conserved Plasmodium protein, unknown function [Plasmodium falciparum 3D7]</p>		
<p>pyridoxine/pyridoxal 5-phosphate biosynthesis enzyme [Plasmodium falciparum 3D7], gi 46361162 emb CAG25026.1 pyridoxine/pyridoxal 5-phosphate biosynthesis enzyme [Plasmodium falciparum 3D7]</p>	PLP	PFI0965w
<p>GTP-binding nuclear protein ran/tc4 [Plasmodium falciparum 3D7], gi 156098524 ref XP_001615294.1 GTP-binding nuclear protein Ran [Plasmodium vivax SaI-1], gi 585782 sp P38545.1 RAN_PLAFA RecName: Full=GTP-binding nuclear protein Ran; AltName: Full=GTPase Ran; AltName: Full=Ras-like protein TC4, gi 23496106 gb AAN35767.1 AE014838_45 GTP- binding nuclear protein ran/tc4 [Plasmodium falciparum 3D7], gi 476130 gb AAA19587.1 homologue to human Ran/TC4 nuclear GTP-binding protein, PIR Accession Number A44393 [Plasmodium falciparum], gi 15072338 gb AAG12165.1 Ras-related nuclear protein Ran/TC4 [Plasmodium berghei], gi 148804168 gb EDL45567.1 GTP-binding nuclear protein Ran, putative [Plasmodium vivax]</p>	RAN/TC4	PF11_0183
<p>plasmepsin I [Plasmodium falciparum 3D7], gi 1172529 sp P39898.2 PLM1_PLAFA RecName: Full=Plasmepsin-1; AltName: Full=Aspartic hemoglobinase I; AltName: Full=PfAPG; Flags: Precursor, gi 75009813 sp Q7KQM4.1 PLM1_PLAF7</p>	PLM1	PF14_0076

<p>RecName: Full=Plasmepsin-1; AltName: Full=Aspartic hemoglobinase I; AltName: Full=PfAPG; Flags: Precursor, gi 482941 emb CAA53432.1 aspartic hemoglobinase [Plasmodium falciparum], gi 23497140 gb AAN36688.1 plasmepsin I [Plasmodium falciparum 3D7], gi 58372401 gb AAW71444.1 plasmepsin 1 [Plasmodium falciparum], gi 58372403 gb AAW71445.1 plasmepsin 1 [Plasmodium falciparum], gi 58372405 gb AAW71446.1 plasmepsin 1 [Plasmodium falciparum], gi 58372407 gb AAW71447.1 plasmepsin 1 [Plasmodium falciparum], gi 58372409 gb AAW71448.1 plasmepsin 1 [Plasmodium falciparum]</p>		
<p>eukaryotic initiation factor 5a, putative [Plasmodium falciparum 3D7], gi 21310117 gb AAM46152.1 AF382208_1 eukaryotic translation initiation factor 5A [Plasmodium falciparum], gi 23496573 gb AAN36131.1 AE014844_42 eukaryotic initiation factor 5a, putative [Plasmodium falciparum 3D7]</p>	EIF-5a	PFL0210c
<p>Rrp6 homologue, putative [Plasmodium falciparum 3D7], gi 23497545 gb AAN37086.1 Rrp6 homologue, putative [Plasmodium falciparum 3D7]</p>	RRP6	PF14_0473
<p>Chain A, Crystal Structure Of Pff1300w., gi 284055701 pdb 3KHD B Chain B, Crystal Structure Of Pff1300w., gi 284055702 pdb 3KHD C</p>	PK	Pff1300w

Chain C, Crystal Structure Of Pff1300w., gi 284055703 pdb 3KHD D Chain D, Crystal Structure Of Pff1300w		
HAP protein [Plasmodium falciparum 3D7], gi 23497142 gb AAN36690.1 AE014817_13 HAP protein [Plasmodium falciparum 3D7], gi 4584228 emb CAB40630.1 HAP protein [Plasmodium falciparum], gi 58372421 gb AAW71454.1 histo-aspartic protease [Plasmodium falciparum], gi 58372423 gb AAW71455.1 histo-aspartic protease [Plasmodium falciparum], gi 58372425 gb AAW71456.1 histo-aspartic protease [Plasmodium falciparum], gi 58372427 gb AAW71457.1 histo-aspartic protease [Plasmodium falciparum], gi 58372429 gb AAW71458.1 histo-aspartic protease [Plasmodium falciparum]	HAP	PF14_0078
conserved Plasmodium protein, unknown function [Plasmodium falciparum 3D7], gi 225632147 emb CAX64036.1 conserved Plasmodium protein, unknown function [Plasmodium falciparum 3D7]	UNK	
zinc finger protein, putative [Plasmodium falciparum 3D7], gi 23615713 emb CAD52705.1 zinc finger protein, putative [Plasmodium falciparum 3D7]	UNK	
dynein-related AAA-type ATPase [Plasmodium falciparum 3D7], gi 255528838 gb AAN36939.2 dynein-related AAA-type ATPase [Plasmodium falciparum 3D7]	AAA_5	PF07728

conserved Plasmodium protein [Plasmodium falciparum 3D7], gi 23496920 gb AAN36472.1 conserved Plasmodium protein [Plasmodium falciparum 3D7]	UNK	
conserved Plasmodium protein, unknown function [Plasmodium falciparum 3D7], gi 225631807 emb CAX64204.1 conserved Plasmodium protein, unknown function [Plasmodium falciparum 3D7]	UNK	
conserved Plasmodium protein, unknown function [Plasmodium falciparum 3D7], gi 255528828 gb AAN36917.2 conserved Plasmodium protein, unknown function [Plasmodium falciparum 3D7]	UNK	
TRAP-like protein [Plasmodium falciparum 3D7], gi 46361116 emb CAG25403.1 TRAP-like protein [Plasmodium falciparum 3D7]	MTRAP	PF10_0281
ribosomal protein I7ae, putative [Plasmodium falciparum 3D7], gi 3649767 emb CAB11116.1 ribosomal protein I7ae, putative [Plasmodium falciparum 3D7]	I7ae	PFC0405c
adapter-related protein, putative [Plasmodium falciparum 3D7], gi 225631797 emb CAD51726.2 adapter-related protein, putative [Plasmodium falciparum 3D7]	AP2	PFF0655c
RIFIN [Plasmodium falciparum]	RIFIN	PFA0010c
apicoplast RNA methyltransferase precursor, putative [Plasmodium falciparum 3D7], gi 254688488 gb AAC71960.3 apicoplast RNA	ARMT	PFB0855c

methyltransferase precursor, putative [Plasmodium falciparum 3D7]		
ATP-dependent helicase, putative [Plasmodium falciparum 3D7], gi 263429743 sp C0H4W3.1 HEPF1_PLAF7 RecName: Full=Probable ATP-dependent helicase PF08_0048, gi 225632260 emb CAX64141.1 ATP-dependent helicase, putative [Plasmodium falciparum 3D7]	HX	PF08_0048
tRNA pseudouridine synthase, putative [Plasmodium falciparum 3D7], gi 23495040 gb AAN35373.1 AE014831_49 tRNA pseudouridine synthase, putative [Plasmodium falciparum 3D7]	PSUI	PFI0420c
erythrocyte membrane protein 1 [Plasmodium falciparum]	EMP1	
Plasmodium exported protein (PHISTb), unknown function [Plasmodium falciparum 3D7], gi 23504928 emb CAD51712.1 Plasmodium exported protein (PHISTb), unknown function [Plasmodium falciparum 3D7]	PHISTb	PFB0080c
conserved Plasmodium protein, unknown function [Plasmodium falciparum 3D7], gi 23498834 emb CAD50911.1 conserved Plasmodium protein, unknown function [Plasmodium falciparum 3D7]	UNK	
dihydrolipoamide acyltransferase, putative [Plasmodium falciparum 3D7], gi 4493882 emb CAB38991.1 dihydrolipoamide acyltransferase, putative [Plasmodium falciparum	DlaT	PFC0170c

3D7]		
DNA-directed RNA polymerase 3 largest subunit [Plasmodium falciparum 3D7], gi 23615426 emb CAD52417.1 DNA-directed RNA polymerase 3 largest subunit [Plasmodium falciparum 3D7]	RNAPIII	PF13_0150
conserved Plasmodium protein, unknown function [Plasmodium falciparum 3D7], gi 23615806 emb CAD52798.1 conserved Plasmodium protein, unknown function [Plasmodium falciparum 3D7]	UNK	
conserved Plasmodium protein, unknown function [Plasmodium falciparum 3D7], gi 23497527 gb AAN37069.1 conserved Plasmodium protein, unknown function [Plasmodium falciparum 3D7]	UNK	
ATP-dependent phosphofructokinase, putative [Plasmodium falciparum 3D7], gi 23496219 gb AAN35878.1 AE014840_26 ATP-dependent phosphofructokinase, putative [Plasmodium falciparum 3D7]	PFK	PFI0755c
3D7Surf4.2; surface-associated interspersed gene 4.2, (SURFIN4.2) [Plasmodium falciparum 3D7], gi 23498306 emb CAD49278.1 3D7Surf4.2 [Plasmodium falciparum 3D7]	SURFIN4.2	PFD1160w
conserved Plasmodium protein, unknown function [Plasmodium falciparum 3D7], gi 6562728 emb CAB62867.1 conserved Plasmodium protein, unknown function [Plasmodium falciparum 3D7]	UNK	

phosphoglycerate mutase, putative [Plasmodium falciparum 3D7], gi 23496132 gb AAN35792.1 AE014839_1 phosphoglycerate mutase, putative [Plasmodium falciparum 3D7]	PGM	PFD0660w
Chain A, Plasmodium Falciparum Cyclophilin Complexed With Cyclosporin A	CyP	PFE0505w
ADP-ribosylation factor [Plasmodium falciparum 3D7], gi 3182916 sp Q94650.3 ARF1_PLAFA RecName: Full=ADP-ribosylation factor 1, gi 311772094 pdb 3LRP A Chain A, Crystal Structure Of Plasmodium Falciparum Adp-Ribosylation Factor 1, gi 23495068 gb AAN35400.1 AE014832_22 ADP-ribosylation factor [Plasmodium falciparum 3D7], gi 1565278 emb CAB02498.1 ADP-ribosylation factor [Plasmodium falciparum], gi 1932731 gb AAB63304.1 ADP-ribosylation factor [Plasmodium falciparum]	ARF-a	PFE1305c-a
conserved Plasmodium protein, unknown function [Plasmodium falciparum 3D7], gi 46361054 emb CAG25341.1 conserved Plasmodium protein, unknown function [Plasmodium falciparum 3D7]	UNK	
multi-drug resistance 1 [Plasmodium falciparum]	MDR1	PFE1150w
MIF4G domain containing protein [Plasmodium falciparum 3D7], gi 23496012 gb AAN35674.1 MIF4G domain containing protein [Plasmodium falciparum 3D7]	MIF4G	PF11_0086
exonuclease, putative [Plasmodium falciparum 3D7],	exo-Dnase	

gi 23615753 emb CAD52745.1 exonuclease, putative [Plasmodium falciparum 3D7]		
conserved Plasmodium protein [Plasmodium falciparum 3D7], gi 23496227 gb AAN35886.1 conserved Plasmodium protein [Plasmodium falciparum 3D7]	UNK	
conserved Plasmodium protein [Plasmodium falciparum 3D7], gi 23495983 gb AAN35646.1 conserved Plasmodium protein [Plasmodium falciparum 3D7]	UNK	
signal recognition particle receptor alpha subunit, putative [Plasmodium falciparum 3D7], gi 23615794 emb CAD52786.1 signal recognition particle receptor alpha subunit, putative [Plasmodium falciparum 3D7]	SRPR-a	PF13_0350
conserved Plasmodium protein, unknown function [Plasmodium falciparum 3D7], gi 23498735 emb CAD50805.1 conserved Plasmodium protein, unknown function [Plasmodium falciparum 3D7]	UNK	
nuclear transport factor 2, putative [Plasmodium falciparum 3D7], gi 255528775 gb AAN36734.2 nuclear transport factor 2, putative [Plasmodium falciparum 3D7]	NTF2	PF14_0122
Zinc finger, C3HC4 type, putative [Plasmodium falciparum 3D7], gi 23498950 emb CAD51028.1 Zinc finger, C3HC4 type, putative [Plasmodium falciparum 3D7]	UNK	
conserved Plasmodium protein [Plasmodium	UNK	

falciparum 3D7], gi 3845221 gb AAC71904.1 conserved Plasmodium protein [Plasmodium falciparum 3D7]		
mitochondrial ACP precursor [Plasmodium falciparum 3D7], gi 23496615 gb AAN36172.1 mitochondrial ACP precursor [Plasmodium falciparum 3D7]	MACP	PFL0415w
conserved Plasmodium membrane protein, unknown function [Plasmodium falciparum 3D7], gi 23497265 gb AAN36811.1 conserved Plasmodium membrane protein, unknown function [Plasmodium falciparum 3D7]	UNK	
conserved Plasmodium protein, unknown function [Plasmodium falciparum 3D7], gi 3764010 emb CAA15603.1 conserved Plasmodium protein, unknown function [Plasmodium falciparum 3D7]	UNK	
stevor, putative [Plasmodium falciparum 3D7], gi 23497842 gb AAN37379.1 AE014828_58 stevor, putative [Plasmodium falciparum 3D7]	STEVOR	
conserved Plasmodium protein, unknown function [Plasmodium falciparum 3D7], gi 46361071 emb CAG25358.1 conserved Plasmodium protein, unknown function [Plasmodium falciparum 3D7]	UNK	
conserved Plasmodium protein, unknown function [Plasmodium falciparum 3D7], gi 23497159 gb AAN36707.1 conserved Plasmodium protein, unknown function [Plasmodium falciparum 3D7]	UNK	

vacuolar ATP synthase subunit D, putative [Plasmodium falciparum 3D7], gi 23615557 emb CAD52549.1 vacuolar ATP synthase subunit D, putative [Plasmodium falciparum 3D7]	V-ATPase	PFE0965c
Plasmodium exported protein (PHISTc) [Plasmodium falciparum 3D7], gi 254688492 gb AAC71970.2 Plasmodium exported protein (PHISTc) [Plasmodium falciparum 3D7]	PHISTc	PFB0105c
Fe-S-cluster redox enzyme, putative [Plasmodium falciparum 3D7], gi 23505114 emb CAD51896.1 Fe-S-cluster redox enzyme, putative [Plasmodium falciparum 3D7]	Fe4S4	PFI1050c
conserved Plasmodium protein, unknown function [Plasmodium falciparum 3D7], gi 46362277 emb CAG25215.1 conserved Plasmodium protein, unknown function [Plasmodium falciparum 3D7]	UNK	
conserved Plasmodium protein, unknown function [Plasmodium falciparum 3D7], gi 23615306 emb CAD52297.1 conserved Plasmodium protein, unknown function [Plasmodium falciparum 3D7]	UNK	
BRIX domain, putative [Plasmodium falciparum 3D7], gi 23499103 emb CAD51183.1 BRIX domain, putative [Plasmodium falciparum 3D7]	BRIX	PF07_0122
zinc finger protein, putative [Plasmodium falciparum 3D7], gi 23496283 gb AAN35941.1 zinc finger protein, putative [Plasmodium falciparum 3D7]	UNK	

conserved Plasmodium protein, unknown function [Plasmodium falciparum 3D7], gi 23615336 emb CAD52327.1 conserved Plasmodium protein, unknown function [Plasmodium falciparum 3D7]	UNK	
conserved Plasmodium membrane protein, unknown function [Plasmodium falciparum 3D7], gi 225631981 emb CAX64320.1 conserved Plasmodium membrane protein, unknown function [Plasmodium falciparum 3D7]	UNK	
conserved Plasmodium protein [Plasmodium falciparum 3D7], gi 23495152 gb AAN35483.1 conserved Plasmodium protein [Plasmodium falciparum 3D7]	UNK	
erythrocyte membrane protein 1 [Plasmodium falciparum]	EMP1	
conserved Plasmodium protein [Plasmodium falciparum 3D7], gi 254922398 gb AAN35297.2 conserved Plasmodium protein [Plasmodium falciparum 3D7]	UNK	
conserved Plasmodium protein, unknown function [Plasmodium falciparum 3D7], gi 259495129 sp C6KSS5.1 LRR2_PLAF7 RecName: Full=Protein PFF0380w, gi 46362309 emb CAG25247.1 conserved Plasmodium protein, unknown function [Plasmodium falciparum 3D7]	Unk	
Cu ²⁺ -transporting ATPase, Cu ²⁺ transporter [Plasmodium falciparum 3D7],	Cu ²⁺ ATPase	PFI0240c

gi 23504950 emb CAD51734.1 Cu ²⁺ -transporting ATPase, Cu ²⁺ transporter [Plasmodium falciparum 3D7]		
Plasmodium exported protein [Plasmodium falciparum 3D7], gi 254945434 gb AAN36594.2 Plasmodium exported protein [Plasmodium falciparum 3D7]	UNK	
erythrocyte membrane-associated antigen, putative [Plasmodium falciparum 3D7], gi 23498284 emb CAD49256.1 erythrocyte membrane-associated antigen, putative [Plasmodium falciparum 3D7]	EMAA	MAL7P1.12
valine-tRNA ligase, putative [Plasmodium falciparum 3D7], gi 3764016 emb CAA15609.1 valine-tRNA ligase, putative [Plasmodium falciparum 3D7]	ValRS	PFC0470w
conserved Plasmodium protein [Plasmodium falciparum 3D7], gi 254945380 gb AAN36319.2 conserved Plasmodium protein [Plasmodium falciparum 3D7]	UNK	
proteasome subunit alpha type 2, putative [Plasmodium falciparum 3D7], gi 46361040 emb CAG25327.1 proteasome subunit alpha type 2, putative [Plasmodium falciparum 3D7]	PSA2	PFF0420c
conserved Plasmodium protein, unknown function [Plasmodium falciparum 3D7], gi 23504832 emb CAD51613.1 conserved Plasmodium protein, unknown function [Plasmodium falciparum 3D7]	UNK	

conserved Plasmodium protein, unknown function [Plasmodium falciparum 3D7], gi 23615630 emb CAD52622.1 conserved Plasmodium protein, unknown function [Plasmodium falciparum 3D7]	UNK	
proteasome regulatory subunit, putative [Plasmodium falciparum 3D7], gi 23615808 emb CAD52800.1 proteasome regulatory subunit, putative [Plasmodium falciparum 3D7]	PRS	PFI0630w
conserved Plasmodium protein, unknown function [Plasmodium falciparum 3D7], gi 255528848 gb AAN36985.2 conserved Plasmodium protein, unknown function [Plasmodium falciparum 3D7]	UNK	
conserved Plasmodium protein, unknown function [Plasmodium falciparum 3D7], gi 225632030 emb CAX64366.1 conserved Plasmodium protein, unknown function [Plasmodium falciparum 3D7]	UNK	
probable protein, unknown function [Plasmodium falciparum 3D7], gi 23497783 gb AAN37321.1 probable protein, unknown function [Plasmodium falciparum 3D7]	UNK	
phosphatidylinositol 3-and 4-kinase, putative [Plasmodium falciparum 3D7], gi 7672216 emb CAA15608.2 phosphatidylinositol 3-and 4-kinase, putative [Plasmodium falciparum 3D7]	PI3+4K	PFC0475c
10b antigen, putative [Plasmodium falciparum 3D7],	10b	PF10_0213

gi 23495078 gb AAN35410.1 AE014832_32 10b antigen, putative [Plasmodium falciparum 3D7]		
Sec1 family protein, putative [Plasmodium falciparum 3D7], gi 254922486 gb AAN35528.2 Sec1 family protein, putative [Plasmodium falciparum 3D7]	SEC1	PF10_0331
conserved Plasmodium protein, unknown function [Plasmodium falciparum 3D7], gi 4493979 emb CAB39038.1 conserved Plasmodium protein, unknown function [Plasmodium falciparum 3D7]	UNK	
CCAAT-box DNA binding protein subunit B [Plasmodium falciparum 3D7], gi 23496401 gb AAN36057.1 AE014843_21 CCAAT-box DNA binding protein subunit B [Plasmodium falciparum 3D7]	CBF-B	PF11_0477
conserved protein [Plasmodium falciparum 3D7], gi 23496728 gb AAN36283.1 conserved protein [Plasmodium falciparum 3D7]	UNK	
conserved Plasmodium protein, unknown function [Plasmodium falciparum 3D7], gi 23504695 emb CAD51573.1 conserved Plasmodium protein, unknown function [Plasmodium falciparum 3D7]	UNK	
conserved protein, unknown function [Plasmodium falciparum 3D7], gi 75016040 sp Q8ILI6.1 AN32_PLAF7 RecName: Full=Acidic leucine-rich nuclear phosphoprotein 32-related protein; AltName: Full=ANP32/acidic nuclear phosphoprotein-like protein,	UNK	

gi 23497325 gb AAN36870.1 conserved protein, unknown function [Plasmodium falciparum 3D7]		
conserved Plasmodium protein, unknown function [Plasmodium falciparum 3D7], gi 46361228 emb CAG25089.1 conserved Plasmodium protein, unknown function [Plasmodium falciparum 3D7]	UNK	
proteasome subunit alpha, putative [Plasmodium falciparum 3D7], gi 225632219 emb CAD51297.2 proteasome subunit alpha, putative [Plasmodium falciparum 3D7]	PSA	MAL8P1.128
transcription factor with AP2 domain(s), putative [Plasmodium falciparum 3D7], gi 23496748 gb AAN36303.1 transcription factor with AP2 domain(s), putative [Plasmodium falciparum 3D7]	AP2-TF	PFD0200c
RNA helicase, putative [Plasmodium falciparum 3D7], gi 23499189 emb CAD51269.1 RNA helicase, putative [Plasmodium falciparum 3D7], gi 156072132 gb ABU45417.1 DEAD-box helicase 11 [Plasmodium falciparum]	RNA-HX	PF08_0111
conserved Plasmodium membrane protein, unknown function [Plasmodium falciparum 3D7], gi 23615400 emb CAD52391.1 conserved Plasmodium membrane protein, unknown function [Plasmodium falciparum 3D7]	UNK	
ubiquitin-protein ligase, putative [Plasmodium falciparum 3D7], gi 7768298 emb CAB11123.3 ubiquitin-protein ligase, putative [Plasmodium falciparum 3D7]	UBPL	PFC0550w

histamine-releasing factor, putative [Plasmodium falciparum 3D7], gi 62901380 sp Q8I3Z5.1 TCTP_PLAF7 RecName: Full=Translationally-controlled tumor protein homolog; Short=TCTP, gi 23504595 emb CAD51474.1 histamine-releasing factor, putative [Plasmodium falciparum 3D7]	HRF	PFE0545c
erythrocyte binding antigen-165 [Plasmodium falciparum 3D7], gi 23498305 emb CAD49277.1 erythrocyte binding antigen-165 [Plasmodium falciparum 3D7]	EBA-165	PFD1155w
conserved Plasmodium protein, unknown function [Plasmodium falciparum 3D7], gi 225631977 emb CAX64316.1 conserved Plasmodium protein, unknown function [Plasmodium falciparum 3D7]	UNK	
conserved Plasmodium protein, unknown function [Plasmodium falciparum 3D7], gi 23497359 gb AAN36904.1 conserved Plasmodium protein, unknown function [Plasmodium falciparum 3D7]	UNK	
eukaryotic translation initiation factor 5, putative [Plasmodium falciparum 3D7], gi 23496599 gb AAN36156.1 AE014845_11 eukaryotic translation initiation factor 5, putative [Plasmodium falciparum 3D7]	EIF-5	PFL0335c
40S ribosomal protein S25, putative [Plasmodium falciparum 3D7], gi 255528798 gb AAN36818.2 40S ribosomal protein S25, putative [Plasmodium falciparum 3D7]	RPS25	PF14_0205

conserved Plasmodium protein, unknown function [Plasmodium falciparum 3D7], gi 225631941 emb CAX64285.1 conserved Plasmodium protein, unknown function [Plasmodium falciparum 3D7]	UNK	
conserved Plasmodium protein, unknown function [Plasmodium falciparum 3D7], gi 23615272 emb CAD52262.1 conserved Plasmodium protein, unknown function [Plasmodium falciparum 3D7]	UNK	
RRM containing cyclophilin [Plasmodium falciparum 3D7], gi 225631965 emb CAX64305.1 RRM containing cyclophilin [Plasmodium falciparum 3D7]	RRM-CyP	PF13_0122
glutamyl-tRNA(Gln) amidotransferase subunit A, putative [Plasmodium falciparum 3D7], gi 23498227 emb CAD49198.1 glutamyl-tRNA(Gln) amidotransferase subunit A, putative [Plasmodium falciparum 3D7]	Glu-ADT	PFD0780w
conserved Plasmodium protein, unknown function [Plasmodium falciparum 3D7], gi 23498781 emb CAD50851.1 conserved Plasmodium protein, unknown function [Plasmodium falciparum 3D7]	UNK	
asparagine-rich protein, putative [Plasmodium falciparum 3D7], gi 23496839 gb AAN36392.1 AE014849_11 asparagine-rich protein, putative [Plasmodium falciparum 3D7]	UNK	
conserved Plasmodium protein [Plasmodium	UNK	

falciparum 3D7], gi 23496960 gb AAN36511.1 conserved Plasmodium protein [Plasmodium falciparum 3D7]		
conserved Plasmodium membrane protein, unknown function [Plasmodium falciparum 3D7], gi 23498166 emb CAD49138.1 conserved Plasmodium membrane protein, unknown function [Plasmodium falciparum 3D7]	UNK	
conserved Plasmodium protein [Plasmodium falciparum 3D7], gi 23496379 gb AAN36036.1 conserved Plasmodium protein [Plasmodium falciparum 3D7]	UNK	
GTPase activator, putative [Plasmodium falciparum 3D7], gi 23504972 emb CAD51755.1 GTPase activator, putative [Plasmodium falciparum 3D7]	GAP	PF08_0120
exportin 1, putative [Plasmodium falciparum 3D7], gi 4725981 emb CAB10574.2 exportin 1, putative [Plasmodium falciparum 3D7]	XPO1	PFC0135c
erythrocyte membrane protein 1 [Plasmodium falciparum]	EMP1	
conserved Plasmodium membrane protein [Plasmodium falciparum 3D7], gi 23503393 gb AAC71900.2 conserved Plasmodium membrane protein [Plasmodium falciparum 3D7]	UNK	
conserved Plasmodium protein, unknown function [Plasmodium falciparum 3D7], gi 23615393 emb CAD52384.1 conserved Plasmodium protein, unknown function [Plasmodium falciparum 3D7]	UNK	

conserved Plasmodium protein, unknown function [Plasmodium falciparum 3D7], gi 23505158 emb CAD51939.1 conserved Plasmodium protein, unknown function [Plasmodium falciparum 3D7]	UNK	
erythrocyte membrane protein [Plasmodium falciparum]	EMP1	
conserved Plasmodium protein, unknown function [Plasmodium falciparum 3D7], gi 23499014 emb CAD51094.1 conserved Plasmodium protein, unknown function [Plasmodium falciparum 3D7]	UNK	
conserved Plasmodium protein [Plasmodium falciparum 3D7], gi 3845193 gb AAC71883.1 conserved Plasmodium protein [Plasmodium falciparum 3D7]	UNK	
DNA helicase, putative [Plasmodium falciparum 3D7], gi 46362278 emb CAG25216.1 DNA helicase, putative [Plasmodium falciparum 3D7]	DNA-HX	PFF0225w
conserved Plasmodium protein [Plasmodium falciparum 3D7], gi 23496901 gb AAN36453.1 conserved Plasmodium protein [Plasmodium falciparum 3D7]	UNK	
pantothenate kinase, putative [Plasmodium falciparum 3D7], gi 255528797 gb AAN36812.2 pantothenate kinase, putative [Plasmodium falciparum 3D7]	PANK	PF14_0200
conserved Plasmodium protein, unknown function [Plasmodium falciparum 3D7],	UNK	

gi 6562704 emb CAB62843.1 conserved Plasmodium protein, unknown function [Plasmodium falciparum 3D7]		
conserved Plasmodium protein, unknown function [Plasmodium falciparum 3D7], gi 23497261 gb AAN36807.1 conserved Plasmodium protein, unknown function [Plasmodium falciparum 3D7]	UNK	